Report No. FHWA/RD-81/001

FIELD STUDY OF PILE GROUP ACTION

INTERIM REPORT

March 1981

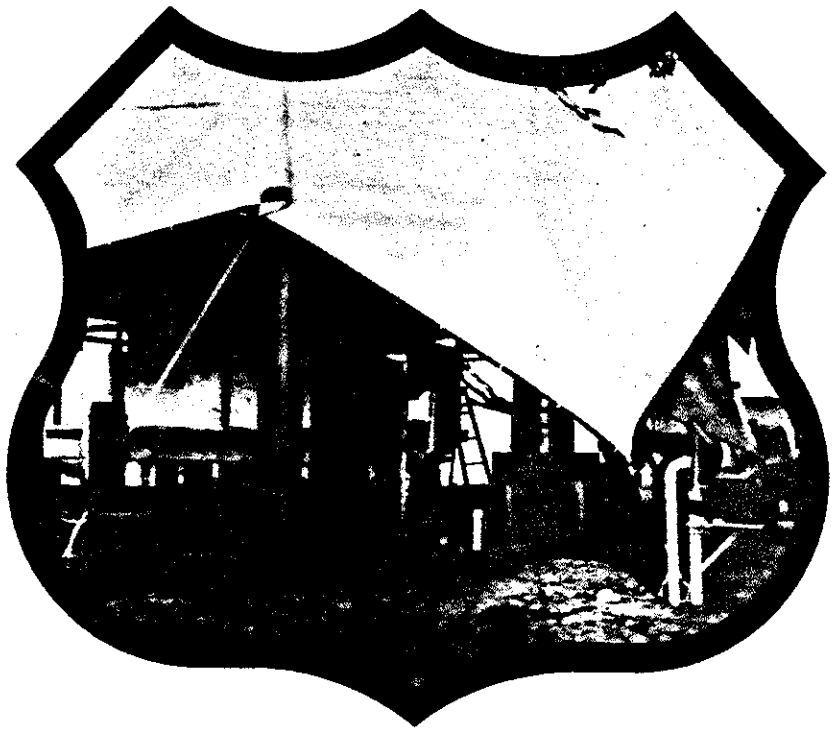

Document is available to the public through the National Technical Information Service, Springfield, Virginia 22161

Prepared for
FEDERAL HIGHWAY ADMINISTRATION
Offices of Research & Development
Materials Division
Washington, D.C. 20590

Preface

This is the first report for a project entitled "Field Study of Pile Group Action." The Final Report will follow this report. This Interim Report describes several mathematical models for pile groups, presents an analysis of a proposed field experiment using one of the models, and describes details of instrumentation and procedures for that experiment. The Final Report report will describe the results of the field experiment, which will involve the load testing to failure of an instrumented, full-scale 9-pile group and two control (reference) piles at several times after installation. Two tests will also be performed on subgroups of piles within the main 9-pile group, and uplift tests of six individual piles will also be conducted.

The Final Report will be divided into a main text and six separately bound appendices, labeled A-F. The main text will summarize the prominent results of the study. Appendix A is to be a user's guide for Program PILGP1, a mathematical pile group model; Appendix B will contain documentation for PILGP1; Appendix C will contain detailed geotechnical data for the test site; Appendix D will contain selected load-settlement, load distribution, and load transfer plots; Appendix E will be an evaluation of instrument performance; and Appendix F will consist of graphs and tables that support the main text but that are not essential to the integrity of the main text.

The project is sponsored by the Offices of Research and Development, Federal Highway Administration, U.S. Department of Transportation. Raymond Internationl Builders, Inc., is the prime research contractor. The University of Houston Central Campus (UHCC) is a subcontractor responsible for mathematical modeling, pile instrumentation, electronic data acquisition, analysis of results, and report preparation. Fugro Gulf, Inc., is also a subcontractor, responsible for the geotechnical study and for the ground instrumentation systems. Farmer Foundation Company was retained to design and install the uplift anchors that are described in the text.

TABLE OF CONTENTS

Chapter 1. Mathematical Models for Pile Groups

Objectives

The process of designing a pile group to resist a given set of loads involves a number of elements, including the use of semi-empirical rules to size the group and estimate pile forces for a trial design, the application of codes and specifications, application of the experience of the design team, mathematical modeling, load testing of piles, and cost analyses. Mathematical modeling of a pile group may be employed in the design process as an analytical tool to predict or verify some aspect of constructability or performance of a trial deisgn that has been developed at some other point in the design process. Mathematical modeling may be employed repeatedly on trial designs until a tentative final design is reached. In this phase of design, it is often desirable to use a very simple model or design charts developed from some model. The tentative final deisgn may then be analyzed more rigorously by direct use of a resonably comprehensive mathematical model, especially when the loading, structural, or stratigraphic conditions are outside the direct experience of the design team or when the performance requirements for the group are different from those with which the design team are familiar.

A mathematical model is a vehicle whose practical purpose may be said to be that of the transfer of the experiences of one set of analysts to another in the most basic terms possible, so that those experiences can be applied to new situations. In terms of the pile group problem, the transferred experiences are the observed behavior of single piles and pile groups, and the mathematical model is a computational scheme that predicts the physical behavior of a pile group in terms of soil properties, structural properties, and loadings.

A number of mathematical models for pile groups have been developed in recent years. The predictive capability of each model is largely untested, however, because few adequate observations of the behavior of single piles and pile groups have been made. Because of this lack of data against which to judge models, a comprehensive series

of static load tests on single piles and an instrumented pile group will be conducted as a part of this project.

The objectives of Chapters 1 - 5 of this report are to

a. Evaluate several existing pile group models with respect to their accuracy of prediction of behavior and adaptability to design office use.

b. Select the most promising of the models and analyse a proposed full-scale pile group load test to be conducted in Houston, Texas, as a test of the model and to aid in designing the instrumentation system for the test.

c. Present a detailed design of the full-scale load test.

The results for the full-scale test and analyses are given in the remaining chapters. Further details are presented in Appendixes A - G.

General

The primary purpose of any computational procedure for analyzing the behavior of pile foundation systems is to determine the deformation of the foundation-superstructure interface, usually a pile cap, as a function of the load applied to the interface. Additionally, the stresses and deformations within the piles themselves are required so that the piles can be designed structurally. In order to be complete, any mathematical model which describes the behavior of loaded pile groups should consider the following effects:

a. Properties of the structural elements; for example,
   (1) Structural details of the piles and variations thereof
   (2) Details of the pile cap
   (3) Details of the cap-pile connections

b. Nature of the loading; for example,
   (1) The effect of vertical loads, moments, lateral shears, and eccentric loads applied to the cap
   (2) The effect of long-term loading
   (3) The effect of dynamic loading

c. Properties of the supporting soil and details of the soil profile, including
   (1) Stress-deformation characteristics of the soil

(2) The effect of slippage between piles and soil as the piles approach failure and other nonlinear effects

(3) The effect of negative skin friction

d. The effect of installation, including

(1) Changes in stress-deformation properties of the soil within and around the group, which may be time-dependent

(2) Residual stresses within the piles following driving, which are functions of soil stratigraphy, details of the pile driving equipment, and possibly the size of the group and sequence of installation

(3) The effects of construction aids such as jetting on the state of stress in the soil, stress-deformation properties of the soil and residual stresses within the piles

(4) The effect of variable pile penetration for piles driven to a blow count criterion rather than to uniform penetration

e. The geometry of the group, including

(1) Correct three-dimensional geometry of the piles, as many groups are installed with piles having various attitudes in space

(2) Geometric details of the piles, such as taper

f. Interaction among elements of the group, such as

(1) The influence of cap-soil contact

(2) The mechanical influence of soil reactions from a generic pile on the physical behavior of other piles in the group ("pile-soil-pile interaction")

Consideration will be limited here primarily to groups of vertical piles that are loaded vertically and statically, although some models that will be described permit general geometry and loading. For the case of vertical groups, a desirable set of outputs from the complete mathematical model, from a designer's point of view, might be:

a. Ultimate bearing capacity of the group

b. Settlement under a prescribed load

c. Distribution of load among piles to assess the structural adequacy of piles and cap

d. Pattern of load transfer from piles to soil

e. Group efficiency

f. Stresses produced in the soil mass (for possible long-term settlement analysis)

The present state of the art on the subject of vertically loaded pile groups is covered broadly in Refs. 10, 43, and 44.

A potential ideal model would conceivably be a finite element model which could consider the effects enumerated and the output items just listed and which would also consider problems of constructability. Unfortunately, no ideal model currently exists that is capable of considering all of these effects or producing all of the outputs. Even if such a model did exist, the expense of making an analysis, including the expense of determining inputs, would be unquestionably exorbitant. Analysts therefore must resort to making simplifying assumptions in modeling pile groups.

Existing Analytical Techniques

Existing analytical models for pile groups can be placed into five general categories, as described below. Models that address only the problem of constructability, such as the wave equation model, have been omitted from further discussion.

a. Simple Finite Element Models. These models typically consider linearly elastic, weightless soil, special cases of pile geometry such as all vertical piles or all piles lying in a plane, and pile-cap-soil interaction (5,53). Attempts have been made to include nonlinearity, particularly the inability of soil to resist tensile stresses, in the case of a single pile (e.g., 20) and in the case of pile groups by simplifying the problem through assumption of plane strain behavior (19). The details of the mechanics of the finite element method are well-known and will not be described here. This class of models suffers from the difficulty that, at present, the effect of pile installation on the stress-deformation behavior of the soil, particularly at the pile-soil interface, cannot be included directly without prior knowledge of this effect. Interface behavior includes not only the limiting adhesion between the pile and soil but also stress-deformation properties of the soil in the immediate vicinity of the interface. Regarding the latter consideration,

Cooke and Price (14) have used the linear finite element model to compute displacements in the soil mass around a single pile in stiff clay under a loading of much less than ultimate. In order that the computed soil displacements approximately equal those measured in the vicinity of a pile being loaded, they found it necessary to vary the Young's modulus of the soil as follows: Within one radius of the side of the pile the Young's modulus of the soil varied from $120c_u$ (where c_u = undrained cohesion) at the surface to the $240c_u$ at the pile tip to $2300c_u$ 10 diameters beneath the tip. Greater than one radius from the pile the corresponding values were $1100c_u$, $2300c_u$, and $2300c_u$. The generality by which these variations can be extended to other cases is not known.

The practical problem also exists that execution of one analysis, involving only one system of loads applied to the pile cap, can be extremely time consuming on a digital computer. Ottaviani (53) cites execution times of 200 minutes for a single load applied to a symmetric group of nine vertical piles in an elastic soil modeled with a moderate number of elements using a version of the program "Solid Sap" on a Univac 1108 computer. This time problem has been diminished in some cases by resorting to partial boundary element formulation and can be partially overcome in practice by developing parametric solutions for conditions of simple geometry and the assumption of simple soil properties. However, this parametric approach is difficult to implement using the finite element model if one wishes to vary such parameters as attitude of the piles, the effects of varying degrees of load eccentricity, nonlinear soil properties, layered soil, and depth-variable structural properties of the piles.

Finally, the finite element model as applied to piles, as well as the elastic halfspace models described later, have no provision for a failure mechanism within the soil mass and therefore cannot be used to compute ultimate capacity or efficiency of pile groups. The finite element model is capable of considering cap-soil interaction and computing stresses in the soil mass, but such stresses may not be accurate in forms of the model available for three-dimensional pile group analysis since tension usually exists in some elements representing the soil, leading to inadmissible stress patterns in real soil, which cannot resist tension.

It may be concluded therefore that this class of models, while potentially powerful, does not at present properly consider all of the effects required of a complete model.

b. Elastic Solid Model. Poulos and his associates (18, 42, 55, 56, 57, 58, 59, 60), and Banerjee and his associates (6, 12, 13), among others, have developed a model that utilizes the well-known Mindlin equations for point loads in the interior of an elastic halfspace in combination with simple load-deformation equations for beams and columns (piles). In this model the piles are discretized, as illustrated in Fig. 1.1, and simultaneous, linear equations are developed that relate thrusts and moments at each node on each pile to corresponding deformations. This is accomplished by computing a vector of loads at the various nodes that connect the discrete elements, in which compatability between the displacements computed through the column or beam equations and those computed through the halfspace equations is achieved.

Mathematically, the basic elastic solid model, involving only vertical forces and pile displacements, can be described as follows. Referring to Fig. 1.1,

$$[C_{ij}]\ \{\bar{Q}_{ij}\} = \{\delta_{ij}\} \tag{1.1}$$

where $[C_{ij}]$ is a fully populated matrix of coefficients derived from Mindlin's elasticity equations (57) for an elastic halfspace, and $\{\bar{Q}_{ij}\}$ is a matrix of loads transferred from the piles to the halfspace at the various nodes, which can be related to the thrusts in the piles $\{Q_{ij}\}$ by simple finite difference procedures. Further,

$$[D_{ij}]\ \ \{Q_{ij}\} = \{\delta_{ij}\} \tag{1.2}$$

where $[D_{ij}]$ is a banded matrix containing simple elastic flexibility terms for the various pile elements of the type L/AE_{pile}.

Unlike the finite element model, the elastic solid model does not explictly consider the effects of the presence of piles and their reinforcing effect on the halfspace when accounting for pile-soil-pile interaction. Specifically, the application of Eq. (1.1) does not depend on the properties of the piles inserted into the halfspace.

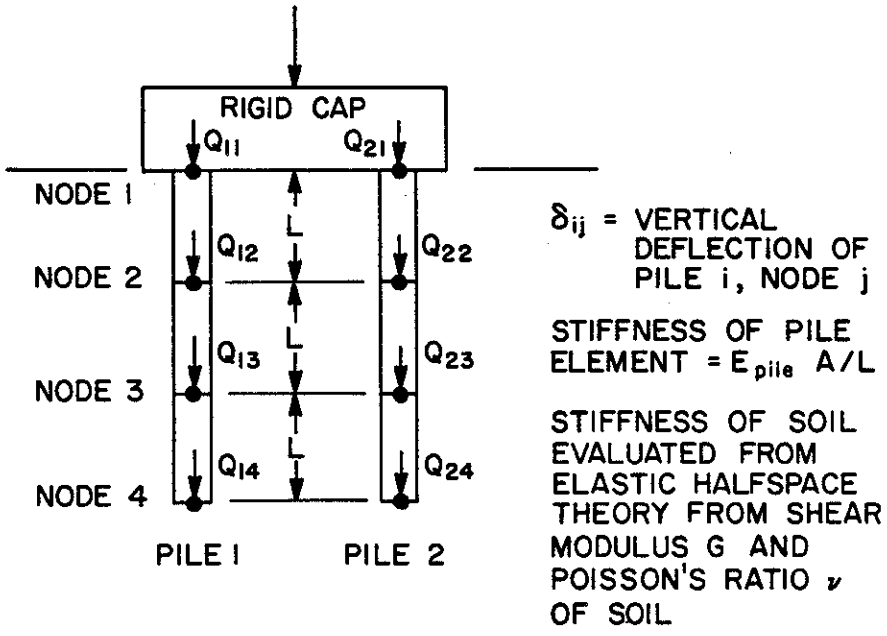

FIGURE 1.1. SIMPLE PILE GROUP AND NOTATION FOR ELASTIC SOLID MODEL

The boundary conditions vary. For the simple case depicted in Fig. 1.1, the boundary conditions are that $Q_{11} + Q_{21}$ = applied load and that $\delta_{11} = \delta_{21}$. After applying these boundary conditions, Eqs. (1.1) and (1.2) are in essence solved simultaneously to obtain the deflection at the pile head and thrust and deflection at each node.

Use of the elastic halfspace equations allows for complete coupled behavior between all nodes in the system but suffers from the restrictive necessity to describe the soil as linear elastic medium capable of resisting tensile stresses and from an inability to include the effects of body weight of the soil (factors that in principle can be overcome in finite element models). Since the soil must possess radially symmetric properties, the elastic halfspace assumption makes it impossible to describe directly the effects that pile installation has on the stress-deformation behavior in the vicinity of the piles as was crudely demonstrated by Cooke and Price with the finite element model. Such effects result from changes in density and effective stresses around the piles, arching in granular soils, changes in the direction of principal stresses, remolding, and residual stresses in the pile and soil. Once the pile group is loaded, loads transferred from the piles to the soil are likely to change the stress-deformation properties of the soil further, through changes in the magnitudes and direction of principal effective stresses, dilatancy, and degradation at the pile-soil contact if loading is cyclic.

With regard to the generation of tensile stresses within the halfspace representing the soil, deformations computed at a generic node due to loads transferred from the pile to the soil at or near that node and at nearby nodes will be in error, compared with those deformations that must exist in the real soil, if there is net tension within the soil mass. Net tension occurs most predominantly when piles have a significant end load, as exists when piles are driven into a deposit of sand. Because the tensile stresses are greatest nearest the point of applied load, the error in computed nodal deflection is diminished with increasing distance between the point at which load is transferred to the soil and the point which deformation is computed, due to St. Venant's principle.

The elastic solid model in its basic form is much more efficient to execute on a digital computer than is the finite element model. Variations of the basic model described here include provisions for pile-soil slip by inputting a value of limiting stress between piles and soil, a stiffer layer at or below the tips of the piles, and cap-soil interaction. Numerous parametric studies have been made and published, although little information regarding stress distribution in the piles or soil has been made available. However, since, among other things, the soil is treated as an elastic medium, this model cannot be considered complete with regard to the requirements presented previously.

c. Load Transfer Function Model. The load transfer function model (4, 9, 11) provides a means to circumvent the assumptions of linearly elastic, weightless soil found in the elastic solid model and to some extent accounts for the effects of installation on the stress-deformation behavior of the soil near the piles. The load transfer function model uses only the second of the equations of the elastic solid model (Eq. (1.2)) but uses a modified formulation as illustrated in Fig. 1.2 (modified after Ref. 16). This model uses characteristic nonlinear load transfer functions to relate local pile movement (δ_{ij}) to the shearing reaction of the soil over the peripheral area of the discretized element (F_{ij}), and, in the case of the last element, the end or tip reaction (Q_{ib}). The graphical relationships of F_{ij} to δ_{ij} and Q_{iB} to δ_{iB} are often termed "f-z" and "Q-z" curves.

The load transfer functions could be formulated through off-line finite element modeling, but knowledge concerning the slippage characteristics of the pile-soil interface is not sufficient to permit this without including empirical inputs based on pile load test results. Practical formulations are therefore presently used that were derived directly from analysis of full-scale load tests of instrumented piles in various types of soil. These formulations represent the current state of the art (80). The f-z and Q-z curves depicted in Fig. 1.2 can be developed in two ways. First, the effects of the existence of post-installation residual stresses at the pile shaft-soil interface and pile tip can be considered explitly if they are known. In such a case the pile is also in a state of known compressive stress (that is the pile springs

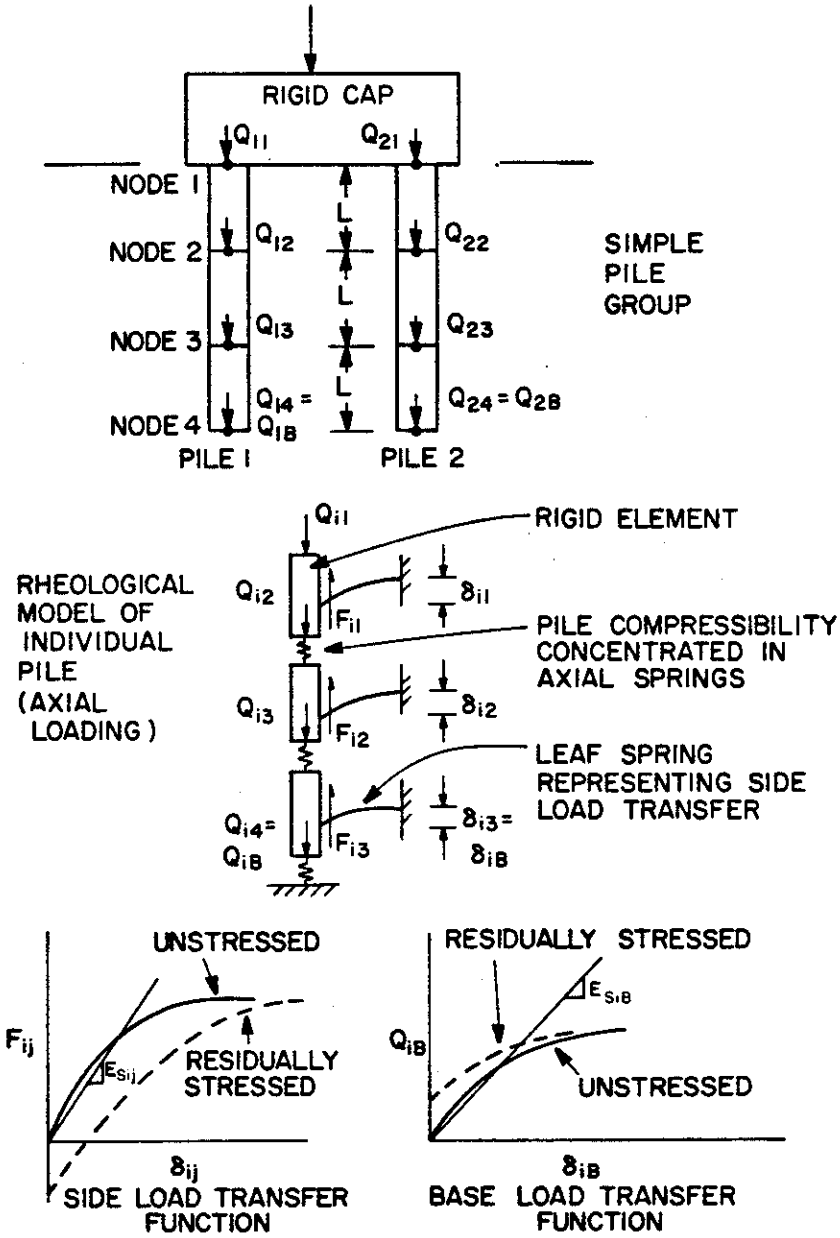

FIGURE 1.2. SIMPLE PILE GROUP, RHEOLOGICAL MODEL, AND AXIAL LOAD TRANSFER FUNCTIONS FOR LOAD TRANSFER FUNCTION MODEL

are compressed) and the analysis proceeds from that point. Second, the effects of post-installation residual stresses, if any, may be considered implicitly, producing the curves shown in solid lines. When this is done the pile is assumed to be unstressed (that is, the pile springs are not compressed), and the analysis proceeds from that point. To date, insufficient data have been obtained from tests on residually stressed piles to permit formulation of explicit load transfer functions for residually stressed piles (32), although Holloway, et al. (29) have used a one-dimensional wave equation algorithm to predict, in effect, the offsets in the curves in Fig. 1.2. Baseline formulations for shaft load transfer functions where residual stresses are considered implicitly are given by Vijayvergiya (80):

$$f_{ij} = f_{ij\ max}\ [2(\delta_{ij}/\delta_{ijc})^{1/2} - \delta_{ij}/\delta_{ijc}]\ ;\ \delta_{ij}/\delta_{ijc}<1 \qquad (1.3)$$

and $F_{ij} = f_{ij}$ x (peripheral area of element).

In Eq. (1.3), $f_{ij\ max}$ is the ultimate local unit side resistance, which may be determined in several ways. For illustrative purposes two simple procedures are suggested below.

For driven piles in clay: $f_{ij\ max} = \alpha c_u$ (1.4)

where $\alpha = 1$ if $c_u \leq 500$ psf (24 kN/m^2)

$\alpha = 0.5$ if $c_u \geq 1500$ psf (72 kN/m^2)

and α varies linearly from 1 to 0.5 for $500<c_u<1500$ psf (1). Tomlinson (72) suggests that α might be increased by 20% if the piles are tapered.

For driven piles in sand: $f_{ij\ max} = K\ \bar{\sigma}_v \tan \phi_{PS}$

$$\leq 0.12\ (10)^{1.5D_r^4}\ (\text{tsf}) \qquad (1.5)$$

The upper limit in Eq. (1.5) is an average value quoted by Vesić (79) and is a function of the relative density of the sand, D_r. The parameter K is an earth pressure coefficient, often taken as 1.25 for a pile in compression and 0.8 in tension; $\bar{\sigma}_v$ is the vertical effective stress in the sand; and ϕ_{PS} is the angle of pile-soil friction, which can be taken to be approximately five degrees less than the angle of internal friction of the sand (80).

A proposed relationship for load transfer at a pile tip (80) is

$$Q_{iB} = Q_{iB\ max}\ (\delta_{iB}/\delta_{iBc})^{1/3}\ ;\ \delta_{iB}/\delta_{iBc} < 1 \qquad (1.6)$$

in which $Q_{iB\ max}$ is the bearing capacity of the tip as calculated from bearing capacity theory for deep foundations.

In Eqs. (1.3) and (1.6), δ_{ijc} and δ_{iBc} are relative local deflections between the pile and soil at which the maximum load transfer is achieved in an isolated pile. Values for δ_{ijc} may be taken in the range 0.2 to 0.4 in. (the upper value being more appropriate in sands), and δ_{iBc} may be taken as approximately two to five percent of the diameter of the pile tip (80).

Since the unit load transfer functions (Eqs. (1.3) and (1.6)) were developed from correlations with load tests, some departure from true behavior at a specific site is probable. For this reason it is desirable to obtain improved functions at the site of a pile group to be modeled by conducting load tests on single piles that are instrumented to discriminate end bearing from side resistance. Further specific discussion of axial load transfer functions may be found in Refs. 16, 17, 30, 51, and 52.

Mathematically, the load transfer function model requires solution of the following set of equations for each ith pile in the group:

$$Q_{iB} = E_{siB}\ \delta_{iB} \qquad (1.7)$$

$$Q_{ij} = Q_{i,j+1} - F_{ij} \qquad (1.8)$$

$$F_{ij} = E_{sij}\ \delta_{ij} \qquad (1.9)$$

$$Q_{ij} = \frac{AE}{L}\ (\delta_{ij} - \delta_{i,j+1}),\ \text{where AE = pile stiffness} \qquad (1.10)$$

Equation (1.7) is applicable only for the bottom node and Eqs. (1.8)-(1.10) are applicable for the remaining nodes. The various terms are defined in Fig. 1.2. A final requirement is that the ordered pair of values for δ_{ij} and F_{ij} (or Q_{iB}) computed lie on the load transfer function curve for location ij. This requirement creates the necessity for the solution to be obtained iteratively since the load transfer functions are typically nonlinear. The boundary condition is specified load or displacement at the top of the pile. Closure is achieved at the

time the computed F_{ij}, Q_{iB}, and δ_{ij} values fall within a specified tolerance of each load transfer curve.

In preparation for group analysis the top axial load or displacement is varied and a nonlinear load-displacement curve, or "mode" curve is established for each pile head in the system. Nonlinear algorithms similar to the axial load-displacement algorithm just described can be used to develop lateral load-deformation mode curves about two lateral orthogonal axes through the pile heads, denoted v and w (49). Assuming that the pile is attached to the cap through a rotational elastic restraint spring (whose stiffness is infinite if the pile head is rigidly built into the cap), four pile-head lateral load relationships ("modes") relating shear, moment, displacement, and rotation are obtained for pile-head motion normal to or about the w-axis and four more are obtained for pile-head motion normal to or about the w-axis. These lateral load modes are indentical for the v and w axes if the pile is symmetric. A similar mode curve is obtainable for torsion (49). These various pile-head mode curves are depicted in Fig. 1.3.

In Fig. 1.3, α is used to denote rotation, Q denotes force, and M denotes moment. The subscripts u, v, w refer to a local coordinate system, also defined in Fig. 1.3, whose coordinates are X_i, Y_i, Z_i with respect to a global system defined for the group as a whole. If a given set of deformations for the pile heads is assumed, secant moduli can be drawn to the various mode curves in Fig. 1.3, as shown, and the pile-head loads and deformations for Pile i in its local coordinate system can be written as:

$$\begin{bmatrix} C_5 & 0 & 0 & 0 & 0 & 0 \\ 0 & C_{1v} & 0 & 0 & 0 & C_{2v} \\ 0 & 0 & C_{1w} & 0 & -C_{2w} & 0 \\ 0 & 0 & 0 & C_6 & 0 & 0 \\ 0 & 0 & -C_{3w} & 0 & C_{4w} & 0 \\ 0 & C_{3v} & 0 & 0 & 0 & C_{4v} \end{bmatrix} \begin{bmatrix} \delta_u \\ \delta_v \\ \delta_w \\ \alpha_u \\ \alpha_v \\ \alpha_w \end{bmatrix} = \begin{bmatrix} Q_u \\ Q_v \\ Q_w \\ M_u \\ M_v \\ M_w \end{bmatrix}_i \qquad (1.11)$$

where δ_{ui} is δ_{1i} from Fig. 1.2, etc. In simpler representation,

$$[S]_i \{\delta\}_i = \{F_i\} \qquad (1.12)$$

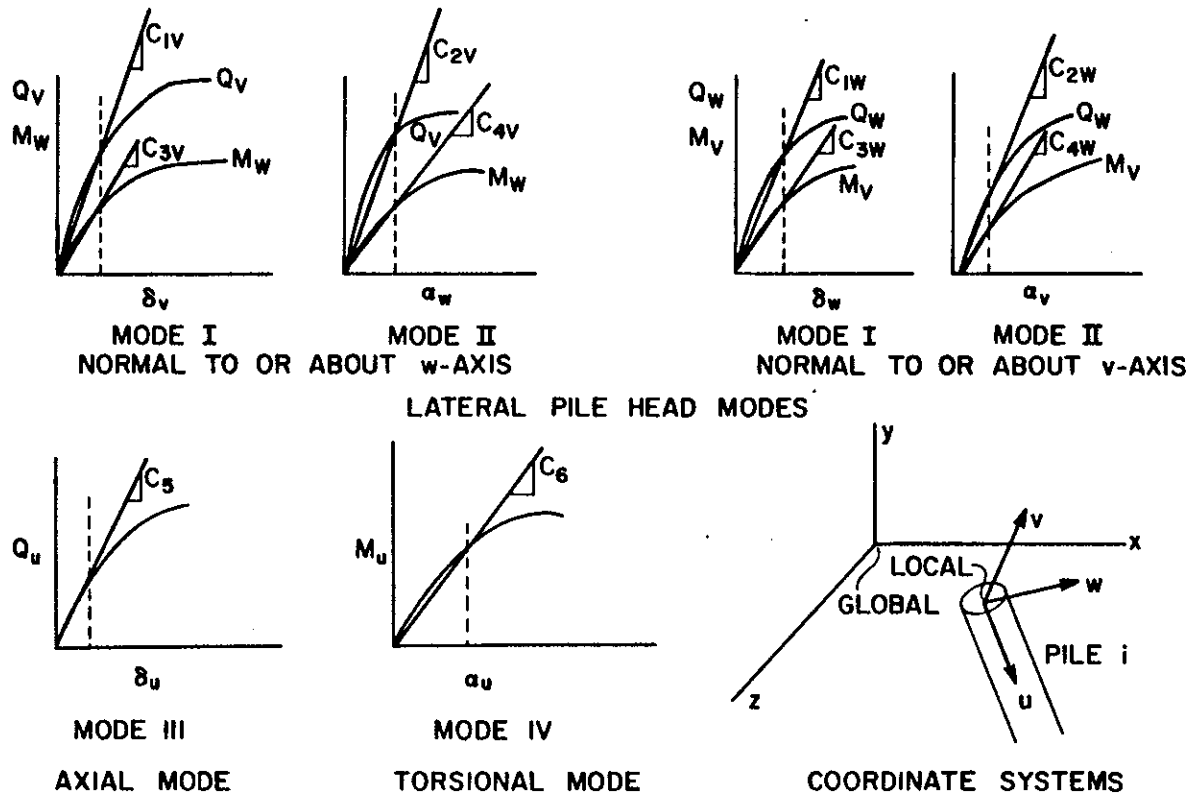

FIGURE 1.3. MODE CURVES FOR LOAD TRANSFER FUNCTION MODEL

The stiffness matrix $[S]_i$ is referred to global coordinates, and three dimensional pile and load vector orientation is introduced through a geometric transformation as follows, it the cap is assumed rigid:

$$[R]_i = [U]_i \; [S]_i \; [U]_i^T \tag{1.13}$$

where $[U]_i$ is a matrix for the pile defined in Ref. 49. The global stiffness matrix $[R]_i$ is obtained by summing $[R]_i$ for all pile heads. If the pile cap is not in contact with the ground then, $\{\Delta A\}$, the deformation vector at the global origin due to an incremental load vector $\{\Delta F\}$ applied at the global origin is given by

$$\{\Delta A\} = [R]^{-1} \; \{\Delta F\} \tag{1.14}$$

The corresponding pile-head deformation vector $\{\delta\}_i$ and pile-head load vector $\{F\}_i$ are given by

$$\{\delta\}_i = [U]_i^T \; \{\Delta A\} \tag{1.15}$$

$$\{F\}_i = [S]_i \; \{\delta\}_i \tag{1.16}$$

At this point compatibility is checked between load and deformation on each pile-head mode curve (Fig. 1.3). If load and deformation are not compatible, the secant modulus is adjusted such that it passes through the mode curve at the computed value of deformation, and the procedure is repeated iteratively until compatibility is achieved in all modes for every pile. The algorithms used to obtain the mode curves are then entered with computed pile-head deformation as boundary conditions to compute the distribution of soil reactions, moments, thrusts, and displacements along each pile.

The lateral pile-head reactions and deformations are compatible in this model in the v and w directions but may not be compatible in the direction of resultant lateral motion in the v-w plane. An error is also introduced by superimposing loads from Modes I and II (rows 2, 3, 5, and 6 of Eq. (1.11)) when the lateral deformations are in the nonlinear range. Errors of this type are minor except when lateral deformations of the pile heads are very large, as may occur near failure under high lateral loads or under high vertical loads when piles are battered to an extreme inclination.

The assumptions involved in the load transfer function model are as follows:

(1). The pile cap is rigid.

(2). The pile-head mode relationships are complete and independent of one another.

(3). The cap either does not contact the ground or the ground contact has a minimal influence on the behavior of the group. Experimental evidence indicates the latter condition may be true for most cases.

(4). The piles are elastic, although their structural properties can vary arbitrarily along their length, and each pile can be of a different length.

(5). The axial soil reaction against the piles can be expressed through the f-z and Q-z (load transfer function) relationships, and related functions can be used for lateral and torsional response. The axial, lateral, and torsional load transfer functions are not coupled.

(6). There is no effect of the loading of one pile on the load-deformation response of other piles in the group (i.e., no "pile-soil-pile interaction").

(7). Soil conditions, including in-situ stresses before installation, soil and water table profile, relative pile-soil flexibility, pile size, and installation technique, especially as related to the driving hammer and cushion, were similar in pile tests used to derive any parametric inputs f_{max} and δ_{ijc} to the load transfer functions to the corresponding parameters for the case being modeled. For example, f-z curves for long, flexible piles in stiff, overconsolidated clay will not necessarily be similar to f-z curves for short, rigid piles in normally consolidated clay.

(8). The installation of adjoining piles in the group causes no changes in these functions.

The success to which this model can be applied is directly dependent on how closely these assumptions are approached in the group being modeled.

Assumption 1 has been relaxed by recent extensions of the model (9,11). Assumption 6 limits the application of the model to cases where accurate settlements are not required (e.g., where distributions of

loads to pile heads may be the only concern), or to groups in which piles are widely spaced, such as offshore drilling platforms.

Assumptions 5, 7, and 8 require further elaboration. With respect to Assumption 5, the case has been made that significant difficulties exist in prediction of stress-deformation behavior of soils in the vicinity of a pile after installation. In general it is beyond the present state of the geotechnical art to make such predictions on a completely mathematical basis. Therefore, the load transfer functions are derived empirically from instrumented load tests on individual piles conducted in one mode (axial, lateral, or torsional). The uncoupling of the modes can be argued from the point that the primary modes, axial and lateral, produce predominant load transfer at different locations along the pile, with the greatest lateral load transfer occurring near the ground surface. If Assumptions 7 and 8 are fully realized, the model considers the effects of stress-deformation changes in the soil after installation, soil tension, residual stresses in the piles, body weight of the soil, arching, and the coupling that occurs between axial load transfer at one level and another in a single pile.

d. Subgrade Reaction Model. The subgrade reaction model, sometimes called the Reaction Coefficient Model is an antecedent to the load transfer function model (31). It is capable of handling three-dimensional geometry in its most advanced forms (3, 46, 63). The principal difference in the subgrade reaction and load transfer function models is that lateral response of a pile in the subgrade reaction model is modeled by using a modulus of subgrade reaction (26) or elastic beam on foundation theory, and axial response is modeled by a column of some characteristic length, instead of representing the soil-pile interaction through load transfer functions, to produce the coefficients in Eq. (1.11). This model has been extended into the nonlinear range for both piles and soil using elastic-plastic representations for the soil and pile material (48, 62). It suffers from the distinct disadvantage that pile-soil-pile interaction is not considered; however, it is easier to use directly by a practitioner than any of the other models described.

e. Hybrid Model. The finite element model, although theoretically suited to model the pile group problem, has not been developed sufficiently to combine the effects of such important

parameters as three-dimensional pile attitude, pile-soil slip, and the effect of pile installation on soil properties. It presently has undesirable computational speed characteristics, sufficient to make it impractical for all but the simplest parameter studies. A rational model combining the strong features of the elastic solid model and the load transfer function model, herein termed the "hybrid model," is therefore proposed as a practical tool for investigating the behavior of pile groups pending further advances in finite element modeling. The hybrid model is similar to the load transfer function model, except that the ability to handle the effect of load transfer from one pile on the load-deformation behavior of another pile is included by using that portion of the elastic solid model which calculates displacements at points in the halfspace that coincide with pile nodes due to load transferred from neighboring piles. In essence, a portion of the elastic solid model is used to correct the load transfer functions to account for the mechanical component pile-soil-pile interaction, which eliminates Assumption f of the load transfer function model.

The hybrid concept was first proposed for the special case of groups of laterally loaded vertical piles by Focht and Koch (25) and later extended to three-dimensional pile groups subjected to a general system of loads on the cap (49). The following assumptions, in addition to the assumptions for the Load Transfer Function Model, are employed in the hybrid model:

(1) The axial, lateral, and torsional modes of behavior of a single pile within the group are influenced mainly by the soil properties in the immediate vicinity of the pile after installation, which can best be modeled using the load transfer function model.

(2) Installation of other piles in the group either do not effect the load transfer functions, or effect them in a way that is predictable before an analysis is conducted.

(3) Loading of surrounding piles effects the load transfer functions only by making them softer or stiffer and has no effect on the maximum unit shaft resistance or end bearing. This modified stiffness effect can be accounted for by using the component of the elastic solid model that computes additional movements at the location of a node on one pile due to reactions against the soil at all nodes on all

other piles. In this way the objection of using Mindlin's equations (development of zones of tension in the soil immediately surrounding a loaded node) is minimized, because calculations are accomplished only for interaction of nodes on separate piles, which are typically spaced more widely than nodes on a single pile, and not for closely spaced nodes on a single pile where the problem of tension is most pronounced.

(4) The soil between and surrounding the piles is assumed to be weightless and elastic for purposes of considering the effect of loading of adjacent piles on the load transfer functions of a given pile. The reinforcing effects of the piles themselves (i.e., the fact that the pile-soil system is not a true homogeneous halfspace) are accounted for by using elastic constants for the elastic halfspace that are slightly higher than those for the soil.

The implied use of two independent soil regimes, one close to the pile that has been greatly influenced by installation, which is modeled mainly by f-z and Q-z curves, and one farther from the pile that is less influenced by pile installation, which is assumed to transmit stresses between piles in a group, is at least partly justified for piles in insensitive clay by the study of Cooke and Price reported earlier in which two separate soil regimes were identified.

The algorithmic approach to the hybrid model is to use the load transfer function model as the primary computational tool and to use the elastic solid model to correct the load transfer functions in the manner described below.

(a) The load transfer function portion of the model is used to analyze the pile group once, assuming that no pile-soil-pile interaction exists. The resulting solution includes the loads, axial and lateral, that are transferred from the piles to the soil and corresponding three-dimensional deflections (parallel to the u, v, and w axes) at every node in every pile.

(b) The displacement in the soil at the location of every Node i on every Pile I due to the effect of the load computed to be transferred in (a), above, from the pile to the soil at every Node j on every other Pile J is computed by

$$d_{XIi} = \sum_{\substack{J=1 \\ J\neq I}}^{N} \sum_{j=1}^{K} d_{XIi}^{Jj} \qquad (1.17)$$

$$d_{YIi} = \sum_{\substack{J=1 \\ J\neq I}}^{N} \sum_{j=1}^{K} d_{YIi}^{Jj} \qquad (1.18)$$

$$d_{ZIi} = \sum_{\substack{J=1 \\ J\neq I}}^{N} \sum_{j=1}^{K} d_{ZIi}^{Jj} \qquad (1.19)$$

where N and K are the number of piles and number of nodes per pile, respectively, d_{XIi} is the displacement in the soil mass in the X direction at Node i on Pile I due to the vector of soil reactions at every jth Node on every Jth pile, and d_{XIi}^{Jj} is the displacement due only to the vector of soil reactions on one jth Node on one Jth pile. The quantities d_{YIi}, d_{ZIi}, d_{YIi}^{Jj}, and d_{ZIi}^{Jj} are similarly defined, and all of these displacements are calculated by using the following relationships, in which G is the soil's shear modulus and v is the soil's Poisson's ratio. Figure 1.4 defines other symbols.

$$d_{XIi}^{Jj} = \frac{Q_{XJj}}{16\pi G(1-v)} \left\{ \frac{3-4v}{R_1} + \frac{1}{R_2} + \frac{(X_j^i)^2}{R_1^3} + \frac{(3-4v)(X_j^i)^2}{R_2^3} \right.$$

$$\left. + \frac{2C\zeta}{R_2^3}\left[1 - \frac{3(X_j^i)^2}{R_2^2}\right]\right\} + \frac{Q_{YJj}(X_j^i)(Y_j^i)}{16\pi G(1-v)} \left\{ \frac{1}{R_1^3} \right.$$

$$\left. + \frac{(3-4v)}{R_2^3} - \frac{6C\zeta}{R_2^5} - \frac{4(1-v)(1-2v)}{R_2(R_2+\zeta+C)^2}\right\} \qquad (1.20)$$

$$d_{YIi}^{Jj} = \frac{Q_{YJj}}{16\pi G(1-v)} \left\{ \frac{3-4v}{R_1} + \frac{1}{R_2} + \frac{(Y_j^i)^2}{R_1^3} + \frac{(3-4v)(Y_j^i)^2}{R_2^3} \right.$$

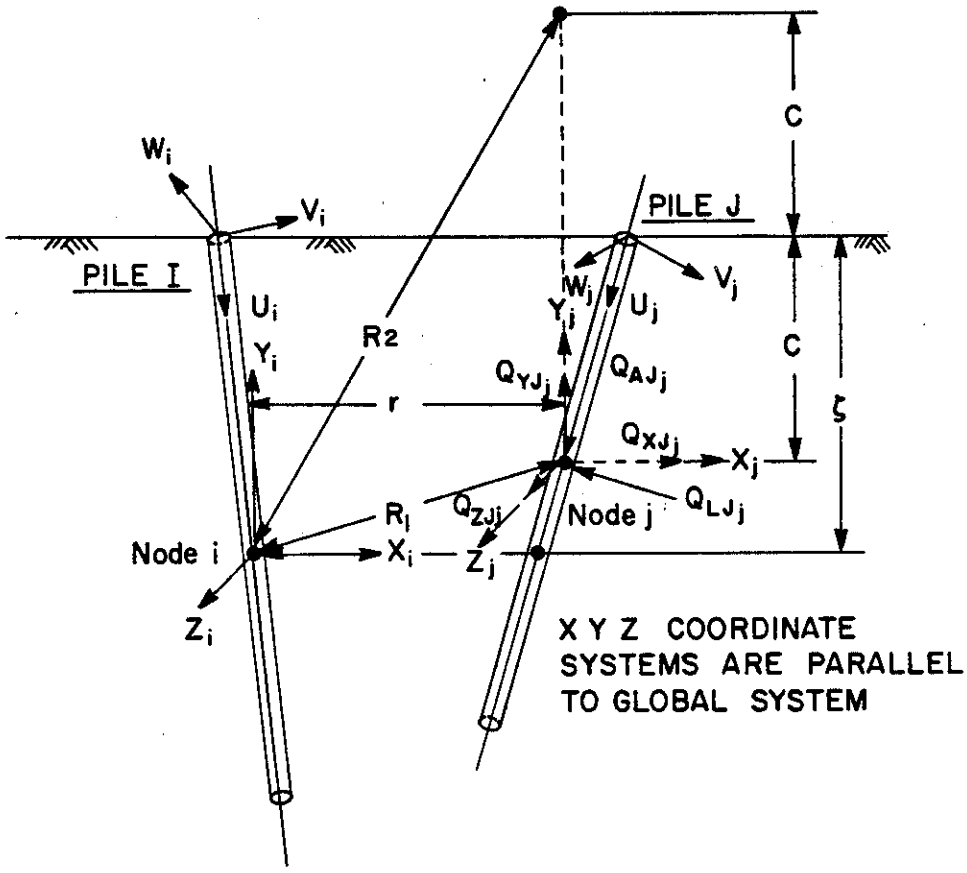

FIGURE 1.4. NOTATION AND COORDINATE SYSTEMS USED FOR COMPUTING ADDITIONAL DISPLACEMENTS FOR HYBRID MODEL

$$+ \frac{2C\zeta}{R_2^3}\left[1 - \frac{3(Y_j^i)^2}{R_2^2}\right]\} + \frac{Q_{XJj}^{i}(X_j^i)(Y_j)}{16\pi G(1-\nu)}\left\{\frac{1}{R_1^3}\right.$$

$$\left. + \frac{(3-4\nu)}{R_2^3} - \frac{6C\zeta}{R_2^5} - \frac{4(1-\nu)(1-2\nu)}{R_2(R_2+\zeta+C)^2}\right\} \quad \ldots\ldots\ldots(1.21)$$

$$d_{ZIi}^{Jj} = \frac{Q_{ZJj}}{16\pi G(1-\nu)}\left\{\frac{3-4\nu}{R_1} + \frac{8(1-\nu)^2 - (3-4\nu)}{R_2} + \frac{(\zeta-C)^2}{R_1^3}\right.$$

$$+ \frac{(3-4\nu)(Z+C)^2 - 2C\zeta}{R_2^3} + \frac{6C\zeta(\zeta+C)^2}{R_2^5}\}$$

$$+ \frac{Q_{XJj}(X_j^i) + Q_{YJj}(Y_j^i)}{16\pi G(1-\nu)}\left\{\frac{\zeta-C}{R_1^3} + \frac{(3-4\nu)(\zeta-C)}{R_2^3}\right.$$

$$\left. + \frac{6CZ(\zeta+C)}{R_2^5} + \frac{4(1-\nu)(1-2\nu)}{R_2(R_2+\zeta+C)}\right\} \quad \ldots\ldots\ldots(1.22)$$

In Eqs. (1.20), (1.21), and (1.22) (Mindlin's equations), X_j^i, Y_j^i, and Z_j^i are the coordinates of Node i on Pile I with respect to a local coordinate system that has its origin at Node j, Pile J (the loaded node) and is parallel to the global system. The parameters G and v can be constants or, as an approximation in a soil of varying stiffness, the average values that exist between the two nodes. In Fig. 1.4, Q_{AJj} is the axial load transferred from the pile to the soil at Node j, Pile J, and Q_{LJj} is the resultant lateral load transferred at that node, whose direction is obtained in the load transfer model. Q_{XJj}, Q_{YJj}, and Q_{ZJj} are these loads resolved to the local coordinate system at Node j. Additional deformations due to the transfer of torsional moments have been neglected in this algorithm, but they could be included with moderate effort. Elastic displacements transverse to the line of action of a force have been excluded since they are small relative to displacements parallel to the line of action.

(c) The displacements computed above are resolved into coordinate directions at Node i, Pile I, that are parallel to the u, v, w, (pile head) local coordinate system. The pile displacements computed neglecting pile-soil-pile interaction in those directions have been retained from Step (a).

(d) The axial (u-direction) load transfer curve at each node is then modified as illustrated in Fig. 1.5, which depicts an axial load transfer function where no residual stress exists in the pile. It is assumed that the soil deformation in the u direction produces a translation of the curve such that there is compatibility between the axial load transfer computed for the node in Step (a) and the sum of the axial (u) deflections computed in Steps (a) and (b). If lateral loading occurs on any pile in the system, similar modifications are made in the lateral load transfer curves independently in the v and w directions, so that it is not necessary to assume a resultant direction of lateral displacement along a pile. At this time it is appropriate to note that there is coupling between lateral (v- or w- direction) loads transferred to the soil from Pile J and the axial (u-direction) displacements on Pile I if the piles are not parallel. Hence, in such a case, the modified axial load transfer function is influenced by lateral loads on other piles in the group.

(e) The pile-head mode curves (Fig. 1.3) are redeveloped using the load transfer function model and the modified load transfer curves as inputs, and a new set of pile head loads and loads and deformations along each pile is computed.

(f) The deformations computed in Step (e) are compared with the combined deformations from Step (d). If they differ by a prescribed tolerance, the control returns to Step (b), using the computed transferred loads from Step (e), and the solution continues in an iterative fashion until closure is achieved.

The above algorithm has been programmed for the digital computer. Experience with the hybrid model indicates that one set of corrections of the load transfer functions is usually sufficient. Computation time has been reduced by computing deflections in Steps (a) and (e) at 50 nodes along each pile but limiting the computation of additional deflections, Step (b), to eleven nodes on each pile. The additional displacements at the remaining 39 nodes are determined by fitting the discrete displacement at the eleven nodes for which additional displacements were computed by cubic splines and then computing the displacement from the spline functions.

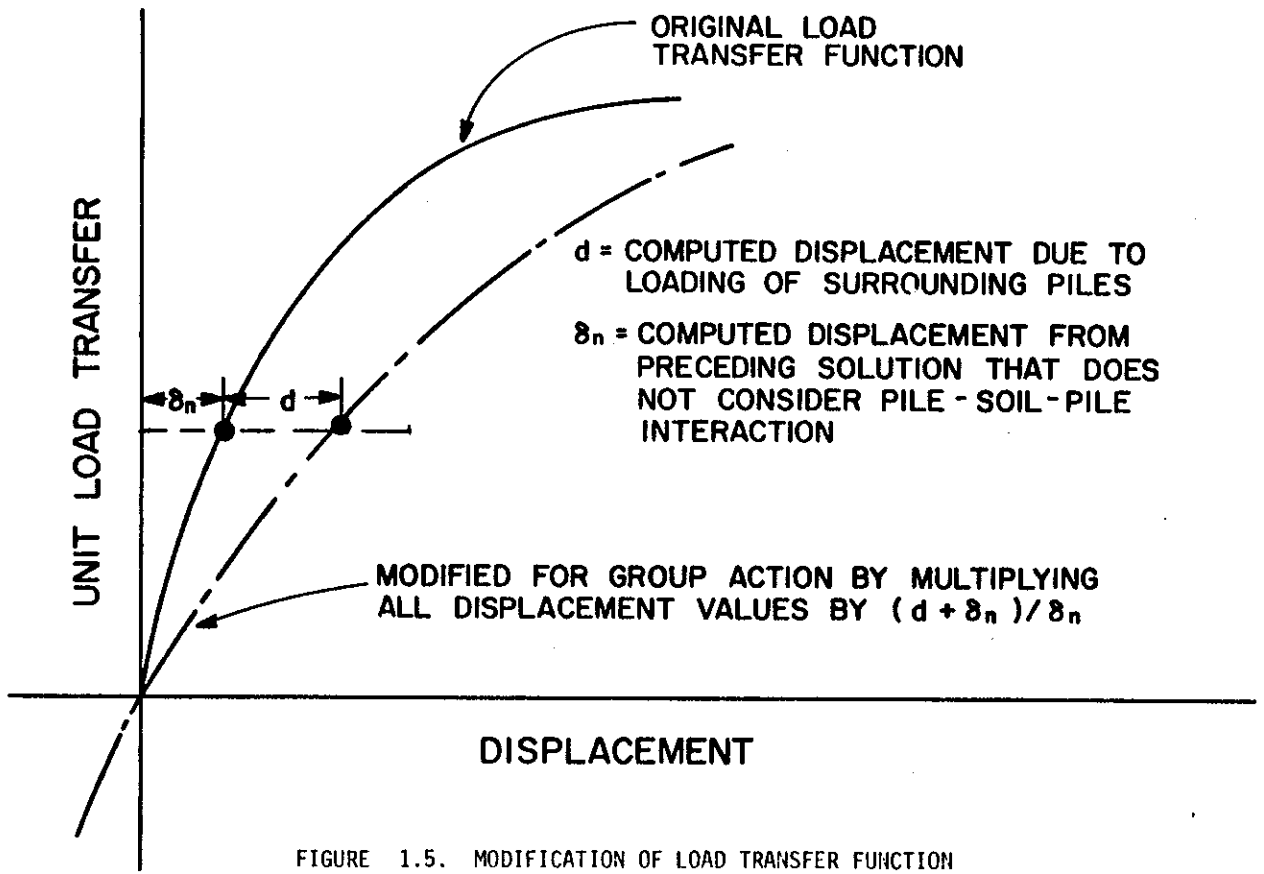

FIGURE 1.5. MODIFICATION OF LOAD TRANSFER FUNCTION FOR PILE-SOIL-PILE INTERACTION, HYBRID MODEL

Empirical evidence exists (69, 81) that whenever r (Fig. 1.4) exceeds about 0.2 times the length of Pile J, pile-soil-pile interaction is insignificant in relatively uniform soils. This observation has been used to further reduce computation time by including an option to exclude pile-soil-pile interaction calculations between piles that exceed this spacing everywhere along their lengths. With this option, the average execution time is about 10 seconds per pile per load on a Univac 1108 machine.

The choice of values for G and v in Step (b) is presently the most difficult aspect of applying the hybrid model. This problem will be addressed in Chapter 2, although preliminary analytical studies (50) with short term loading of groups of axially and laterally loaded piles in clay, both vertical and battered (34, 35, 36, 64, 65), indicate that in the absence of high quality stress-strain data G for short term horizontal or vertical loading on the cap is in the range of 170-270 times the undrained cohesion of the undisturbed soil. This range is consistent with values for undisturbed soils reported in the technical literature (39, 40), suggesting that the stress-deformation properties of the less disturbed soil beneath the pile tips and at some distance laterally from the group influences the behavior of a group of piles in clay more significantly than that of the more highly disturbed soil immediately adjacent to the piles or that disturbance is a short-lived phenomenon.

Long-term (consolidation) settlements in groups in uniform clays can be calculated in the hybrid, elastic solid, and finite element models by substituting the appropriate values and variation of drained elastic modulus and Poisson's ratio for the undrained values. When the consolidating soil lies entirely beneath the pile tips, it is most advantageous to use a version of the elastic solid model that permits distinctly different moduli to be input beneath the pile tips or the finite element model. In order to compute long-term settlements from the hybrid model in such a case, the computed tip and shaft loads on each pile from a short-term analysis can be used to compute consolidation settlement off line by using Boussinesq or Mindlin stress distribution charts. Charts based on Boussinesq theory are advisable since Boussinesq theory does not permit tension in the soil.

Miscellaneous Models

A number of models have been developed to yield distribution of loads among pile heads without regard for load-displacement behavior of the piles or capacity. These models are useful only where inclined and eccentric loads are applied to the cap and will therefore not be enumerated here.

Vesić (78) has described a simplified elastic solid model currently under development which shows promise primarily in its ease of use. He has also proposed the development of a new model based on the finite element method, perhaps coupled with the wave equation, to assess the effects of pile installation on group behavior. While such a model would be of great benefit, no version is known to yet exist.

The dynamic response of pile groups may in the future become a concern to transportation engineers. Several models for predicting such response to load applied at the pile cap have been proposed and have been used with varying degrees of success (46, 47, 63, 66, 70, 82). The basis of most of these models is elastic halfspace theory or replacement of piles by equivalent structural elements having damping and stiffness equivalent to values estimated for the real piles through the use of various techniques. Further consideration of dynamic group models is beyond the scope of this report.

Efficiency Models

The analytical models described in the preceding sections may be described as load-displacement models. As such, none is capable of computing the correct ultimate capacity of a single pile or pile group. The elastic solid, load transfer function, and hybrid models can yield a plunging failure load, but in the case of the elastic solid model, this load must be known in advance. In the load transfer function and hybrid models the plunging failure load in the group is always the sum of the individual plunging failure loads of the piles. Existing three-dimensional finite element models for pile groups are linear and hence do not permit calculation of ultimate capacity. A similar statement is true of the subgrade reaction model, although it is possible to calculate an ultimate load in one version (62).

On the other hand, several well-known methods exist for calculating, in an approximate manner, the ultimate capacity and efficiency of pile groups but which are incapable of predicting load-deformation characteristics. The Converse-Labarre formula (45) and Feld's rule (22) are examples of such methods, and the block failure model of Terzaghi and Peck (71) may be viewed as an efficiency model. No rational basis is known for the Converse-Labarre formula; however, the block failure model is rational and Feld's rule has a rational basis. It is significant to point out that these methods are only intended for application to friction pile groups in soft clay.

Group efficiency is normally defined as the ratio of the ultimate bearing capacity of a group of piles to the ultimate bearing capacity of an isolated pile times the number of piles in the group. As demonstrated by Whitaker (81) and Sowers, et al. (69), the efficiency can be less than unity for closely spaced groups of long friction piles in soft clay. However, when pile groups are installed in sand or are driven through clay or sand to rock, the efficiency is likely to be very near or possibly greater than unity. In these cases, efficiency models are not valid and are probably unnecessary for design purposes. For example, Vesić (75,76) has demonstrated that the average tip capacity of a pile in a group in sand is equal to that of an isolated pile and that the shaft resistance is greater within the group than for the isolated pile.

The problems of efficiency of friction pile groups in stiff overconsolidated clays or groups driven through stiff, overconsolidated clay to a firm bearing stratum other than rock is not well-understood, although the efficiency is not expected to be significantly less than unity for relatively small groups in these stratigraphic situations.

The analyst or designer is obviously faced with the problem that no single existing model can predict both the load-deformation and efficiency characteristics of a pile group. It is suggested, however, that the greatest concern of the designer is in most cases the settlement that occurs in the group under a given load rather than the efficiency of the group and that a load-deformation model is most appropriate for investigation of that phenomenon. Group settlement can be characterized by a settlement ratio, or ratio of group settlement

TABLE 1.1. GENERAL CHARACTERISTICS OF EXISTING MATHEMATICAL MODELS FOR PILE GROUPS

Characteristic	MODEL					
	Finite Element *	Elastic Solid	Load Transfer Function	Subgrade Reaction	Hybrid	Typical Efficiency Models
Factors Considered						
Changes in soil properties due to installation	C	C	B	B	B	C
3-D geometry and variable pile penetration	A	A	A	A	A	C
Variable structural and geometric details in piles	A	B	A	B	A	C
Nonlinearity of soil	C	C	A	B	A	C
Residual stresses	C	C	D	D	D	C
Characteristics of installation equipment (explicitly)	C	C	C	C	C	C
Sequence of pile installation	C	C	C	C	C	C
Pile-soil-pile interaction	A	A	C	C	A	A
Cap-soil interaction	A	A	C	C	C	B

TABLE 1.1 GENERAL CHARACTERISTICS OF EXISTING MATHEMATICAL MODELS FOR PILE GROUPS (CONT'D)

Characteristic	MODEL					
	Finite Element *	Elastic Solid	Load Transfer Function	Subgrade Reaction	Hybrid	Typical Efficiency Models
Factors Considered						
Cap flexibility	A	C	C	C	C	C
Applied eccentric loads and moments	A	B	A	A	A	C
Settlement under long-term loading	B	B	C	C	B	B

TABLE 1.1. GENERAL CHARACTERISTICS OF EXISTING MATHEMATICAL MODELS FOR PILE GROUPS (CONT'D)

Characteristic	MODEL					
	Finite Element*	Elastic Solid	Load Transfer Function	Subgrade Reaction	Hybrid	Efficiency Models
Outputs						
Ultimate bearing capacity	C	D	D	D	D	A
Settlement under a prescribed load	A	A	A	A	A	C**
Distribution of loads to piles	A	A	A	A	A	C
Pattern of load transfer	A	B	A	C	A	C
Stresses in soil mass	A***	B***	C	C	C	C**
Efficiency	C	C	D	D	D	A

*Three-dimensional algorithm without slip elements
**Block model can be easily adapted to give consolidation settlement and approximate stress distribution beneath an equivalent pier (44)
***Validity has not been established

to settlement of an isolated pile loaded to the average of the loads on the piles in the group.

When efficiency is a concern, as in the case of groups of friction piles in soft clay, one of the efficiency models (preferably the block failure model or Feld's rule) should be used as a supplementary tool to insure the desired factor of safety against plunging failure. This report will employ this philosophy.

General Comparison of Models

The five models described earlier in some detail are compared in tabular form in Table 1.1 according to the factors of soil-structure interaction each considers and according to the useful information output. Typical characteristics of the efficiency models are also indicated. The designations used in Table 1.1 are:

A: Characteristic of the model
B: Characteristic of special versions or considered partially
C: Not a characteristic of the model
D: Considered or output only if estimated before making the analysis and/or requires empirical interpretation of results.

The key to assigning designations, which was accomplished somewhat subjectively based on experience and literature review, was whether existing algorithms actually have the ability to consider or output the indicated items and not whether the theory on which algorithms were based have the capability for such considerations. The designations B for settlement under long-term loading and settlement under a prescribed load refers to the fact that linear theory must be used. Assignment of a designation A to a model does not necessarily mean that the model considers the item correctly, but only that it is considered in some rational manner.

Table 1.2 compares the load-deformation models in order of ease of usage, both in terms of direct use of specific algorithms (digital computer codes) and in terms of design aids that have been developed from the models. In evaluating the ease of direct use, the primary criterion was the time required by an engineer familiar with input methods to prepare input and interpret output. Secondarily, execution

TABLE 1.2. RANK OF LOAD-DEFORMATION MODELS FOR DESIGN USE ADAPTABILITY

Ease Of Direct Use Of Existing Algorithm

Rank	Model	Specific Algorithm Considered
1	Subgrade Reaction	Various
2	Elastic Solid	DEFPIG
	Load Transfer Function	BENT 151
	Hybrid	GP3B
5	Finite Element	Solid Sap

Availability of Parametric Design Aids

Rank	Model	Aids Available In References
1	Elastic Solid	6, 12, 13, 18, 54, 57, 58, 60
2	Finite Element	53
3	Hybrid Load Transfer Function Subgrade Reaction	None

time on the computer was considered. Specific algorithms evaluated and authors were DEFPIG (H. G. Poulos-presently in proprietary use of McClelland Engineers), Elastic Solid; BENT 151 (L. C. Reese), Load Transfer Function; GP3B (H. B. Ha), Hybrid; and Solid Sap (E. L. Wilson), Finite Element. The finite element model was rated hardest to use because of the extreme length of time that is required to input a three-dimensional mesh, to interpret results, and to execute the program. The hybrid, elastic solid, and load transfer function algorithms require approximately the same amount of effort by the user, although the hybrid and load transfer function methods require that the user be familiar with load transfer function formulations.

No design aids are known to have been developed for the hybrid, load transfer function, and subgrade reaction models because their use in the past has been principally in analyzing unique problems, such as foundations for offshore drilling platforms, that usually involve multi-directional loading and batter pile configurations.

Selection of Models for Further Study

None of the models described meets all of the requirements enumerated at the beginning of this chapter. However, the load transfer function and subgrade reaction models appear particularly deficient because they fail to take pile-soil-pile interaction into account, and they will be eliminated from further consideration as viable group models because of this fact. The finite element model meets three of the output requirements enumerated in Table 1.1, and partially meets a fourth. The hybrid model meets three, and the elastic solid model meets two and partially meets a third. The finite element method in its present form is not appropriate for direct design office use, and the hybrid and elastic solid models could successfully be used directly in a design office only for major foundation studies. All of the latter three models are adaptable, however, to the production of design aids that could be used in simple cases of routine foundation design. Of these three remaining models, the hybrid is the most readily adaptable to design problems involving batter piles and lateral loads and moments applied to the group.

On the basis of the preceding comments it was decided to study the finite element, elastic solid, and hybrid models in further detail by using each model to predict various aspects of the performance of several full-scale and large-scale model groups that have been tested in the past and that have been described in the technical literature. At the end of this detailed study a single model will be selected for modeling a proposed full-scale pile group to be load tested during Phase II of this project.

Chapter 2. Comparative Study of Prediction Capabilities of Finite Element, Elastic Solid, and Hybrid Models

General

The three remaining models were evaluated according to their ability to predict the performance of five different groups of vertical piles that had been tested under vertical load and reported in the literature. The models were studied in relation to their ability to replicate measured load-settlement behavior, load transfer patterns, load distribution among piles, and surface settlements, as the method permitted. An attempt was also made to obtain semi-empirically values of group capacity and efficiency from the load-settlement curves and to evaluate whether the models could be used approximately to obtain efficiency.

The tests chosen for this study were selected on the basis of several criteria described in Table 2.1.

The tests selected were:

a. A full-scale test of a nine-pile group of monotube piles in soft to medium stiff clay on Cortableau Bayou at the N.O.T. and M. railway crossing in Louisiana by the American Railway Engineering Association (2), hereafter referred to as the AREA test.

b. A large model test of a closely-spaced, nine-pile group of cylindrical aluminum tube piles in medium dense sand at Georgia Tech University (74, 75, 76), hereafter referred to as the Vesić test. (One group test, designated P-93, of a series of tests was modeled. One single pile test, designated P-13, was used as the reference pile test.)

c. A full-scale test of a nine-pile group of monotube piles driven through medium stiff clay into stiff clay in Omaha, Nebraska (64, 65), hereafter referred to as the Schlitt test.

d. A full-scale test of a nine-pile group of cylindrical steel piles driven into very sensitive, medium stiff clay in Japan (38), denoted the Koizumi and Ito test.

TABLE 2.1. CRITERIA FOR SELECTION OF TESTS

Importance	Criterion	Remarks
Primary	Tests should encompass a variety of soil conditions	
Primary	Single pile, identical to group piles, should have been tested at the site	Reference pile needed for assessment of pile-soil-pile interaction predictions and efficiency
Primary	Piles should be instrumented for load transfer measurement	Provides a more positive check on the model than modeling only load-settlement behavior
Primary	Quantitative measurement soil shear strength or density and angle of friction should be available	
Primary	Group should be at or near full scale	Many phenomena cannot be successfully modeled physically
Primary	Number of piles and pile spacing should be typical of pile configurations for highway structures	
Secondary	Surface movement records should be available	Provides further check on model
Secondary	Test should be carried to ultimate failure	

e. A full-scale test of a linear three-pile group of cylindrical steel piles driven into stiff, overconsolidated clay in London, England (15, 61), denoted the BRE test.

All of these tests meet all of the criteria listed in Table 2.1, with the following exceptions: The Schlitt and AREA tests were not conducted to complete failure, the Vesić test was not full-scale, and surface movements were not reported for the AREA and Schlitt tests. Pile penetration varied from five feet (Vesić test) to approximately sixty feet (AREA test), and pile spacing varied from two butt diameters (Vesić test) to 4.5 butt diameters (Schlitt test).

There exists a notable lack of well-documented, instrumented load tests on pile groups in sand, which was the primary reason for the choice of the large scale model test as an appropriate test to model mathematically. No appropriate tests meeting the criteria of Table 2.1 could be found with between three and nine piles, except for additional large-scale model tests reported by Vesić. Numerous other tests have been described in the literature that describe various aspects of load-settlement behavior (e.g. 7, 8, 33, 35, 37, 41), but these descriptions lack adequate data concerning either load transfer patterns, load distribution among piles, soil characteristics, surface settlements, or behavior under purely vertical loads which are essential to the investigation of the mathematical models. They were therefore not considered in this study.

Methodology of Comparative Study

The principal purpose of the comparative study was to determine how well each model predicted the behavior of a group of piles, rather than that of a single pile. Therefore, the first task performed in modeling each group test was to arrive at the inputs that would yield good replication of individual reference pile behavior at each site for each of the three models. These inputs were then used in the group model. In this way, the effects of any inappropriate choice of values for input parameters (such as Young's modulus of the soil and pile-soil slip value in the elastic solid model and f-z relationships for the hybrid model) on the predicted response of the group would be minimized,

making the comparative results for the group tests more indicative of the abilities of each model. In the reference pile, load-settlement behavior was investigated for each model. Load transfer behavior was investigated for the finite element model and hybrid models. Charts and/or algorithms to yield load transfer characteristics in the elastic solid model have been developed only for special cases that could not be applied to the tests being modeled.

The inputs for each model were adjusted in modeling of the behavior of reference piles as follows:

a. Hybrid. A direct computer solution was used (Program GP3B). The geometric and structural properties of the pile were input. The pile dimensions are shown in the figures describing the tests later in this chapter. In each of the tests the piles were hollow steel or aluminum piles. Only in Piles 7 and 9 in Schlitt's test were the piles filled with concrete. For purposes of modeling, the Young's moduli for the various pile materials were taken as follows:

Steel .....3.0 x 10^7psi = 20.7 x 10^7 kN/m^2
Aluminum.....1.01 x 10^7psi = 6.96 x 10^7 kN/m^2
Concrete.....2.5 x 10^6psi = 17.2 x 10^6 kN/m^2

Step variations in section properties were used where the pile was tapered. Baseline f-z and Q-z curves were first used to obtain load-settlement curves and load transfer patterns in the reference piles. The curves were those of Vijayvergiya (80) described analytically in Eqs. (1.3) and (1.6). For purposes of describing f_{max}, Eq. (1.4) was used for the clay tests, except for the Schlitt test, where the λ factor (80) was used arbitrarily. Equation (1.5) was used for the sand test, with K taken as 0.7. Q_{max} for the sand test was evaluated from the product of the base area, the vertical effective stress, and a bearing capacity factor N_q^* taken initially as 40 according to Ref. 80. In the clay tests, Q_{max} was taken as the product of the base area, the undrained cohesion of the soil at the tips of the piles and a bearing capacity factor N_c, taken to be 9. No residual stresses were assumed to exist. The f-z curves were varied with depth as soil properties changed.

All solutions were then repeated with adjusted f-z and Q-z curves as necessary to affect reasonable agreement between measured and

computed results, and the adjusted load transfer functions were then used for the later analysis of group behavior.

b. Elastic solid. The elastic solid model was studied using graphs developed from parametric studies. The solutions obtained from these graphs were checked using a direct computer solution (Program DEFPIG) for the AREA and Vesić tests. The specific procedure for using the charts to obtain load-settlement response is described by Poulos in Ref. 55. For the test in sand, a special "boundary element" formulation proposed by Banerjee and Davies (5) was also used. This formulation permits a uniformly increasing modulus with depth which the method proposed in Ref. 55 does not. In both methods the structural and geometric properties of the piles were modeled using average properties and by treating each pile as if it were prismatic, since the procedure does not contain provisions for explicitly handling tapered piles. The soil in the Poulos model was treated in the most general manner permitted by the model, which is a two layer system in which the soil along the shafts and beneath the base may have different elastic properties. For the clay tests, the elastic modulus of the soil was taken to be constant with depth and was estimated from the reported undrained cohesion c_u since reliable stress-strain data were generally unavailable. The elastic modulus E was taken initially to be in the range of 400-1000 c_u, as suggested in the literature for undisturbed soils (39, 40) and varied until reasonable agreement was reached. In the test in sand it was deemed appropriate to define separate soil moduli at and below the pile tips (E_{BASE}) and above the pile tips (E_s). Initially, as a baseline, E_{BASE} was set equal to E_B, evaluated from Eq. (2.1), which is an expression proposed by Vesić (73) for the elastic modulus of sand directly beneath the tips of driven piles. It includes the effects of compaction and confinement produced by installing the pile.

$$E_B = 25(1-\nu^2)\bar{\gamma}z\, N_q^* (1 + D_r^2) \qquad (2.1)$$

where

ν = Poisson's ratio of the soil, taken as 0.5 since the soil was near critical density

$\bar{\gamma}$ = Effective unit weight of the soil

z = Tip depth

N_q^* = Bearing capacity factor

D_r = Relative density

In order to obtain a baseline value for E_B, N_q^* was calculated from the measured tip capacity of the pile. The modulus of the soil above the pile tip E_s was taken initially as 0.1 E_{BASE} in accordance with recommendations made by Poulos. In the Banerjee and Davies version E_{BASE} was similarly defined, and the modulus along the shaft was then fixed by the linear variation provided in their version of the model.

The analytical procedure employed permits nonlinearity in the load-settlement relationship to be included if the ultimate or maximum shaft and tip loads are known and input. Since they were known in each test, they were input, and complete load-settlement curves were replicated.

Finally, the moduli were varied until reasonable agreement between measured and predicted load-settlement behavior was achieved.

c. Finite element. Solutions were obtained by using graphs obtained from parametric studies by Ottaviani (53) for an elastically "uniform" soil (i.e., the tests in clay). The Ottaviani study assumed a uniform elastic soil. The baseline moduli were chosen and then varied as in the elastic solid model. Poisson's ratio was taken as 0.45 for clay (the only value available from Ottaviani's graphs).

The second task in the study was to use adjusted inputs from the replication of reference pile behavior directly as input in analysis of the associated group. In modeling the groups by the hybrid method, it was necessary to choose a modulus of elasticity for the ambient soil, a variation thereof, and a value for Poisson's ratio. Poisson's ratio was taken to be 0.5 in each case. Several different group solutions in each case were obtained by varying the soil modulus. In clay, E was assumed constant with respect to depth and was varied as a function of

the reported value of undisturbed undrained cohesion in a manner similar to that employed in the single pile analyses with the elastic solid model. In sand, E was varied with depth in a manner similar to the ambient modulus variation in the boundary element model. The value of E_{BASE} was also varied.

The most appropriate value for the modulus of the ambient soil was observed from the various group solutions, enabling the input value for the ambient soil modulus to be evaluated. The hybrid model is the only model of the three that presently permits input of independent values of soil modulus to account for pile-soil-pile interaction once the behavior of a reference pile has been established.

The elastic solid and finite element group solutions proceeded directly with the use of parameters evaluated by modeling the reference piles. The elastic solid model requires establishment of ratios of settlement of the pile group to that of the reference pile. These ratios are computed by solving systems of simultaneous algebraic equations that employ pile-soil-pile interaction factors (54) that were obtained from Refs. 54, 57, and 60. Solution of these equations, which was accomplished using a hand calculator, also yields distribution of loads to the piles, but not load transfer patterns.

The elastic solid model also permits calculations of surface settlements (5,59) which were also obtained in this phase of the study for those group tests where surface movements were monitored.

The tedious process of solving simultaneous equations that is necessary with the elastic solid model can be circumvented in some special cases by using tabular settlement ratio values (57). A proprietary computer program, DEFPIG, also calculates interaction factors and solves equations. That program, which handles pile-soil-slip in a somewhat more appropriate manner than can be accomplished in the hand-graph solution, was used to check the load-settlement curves from hand solutions for the AREA and Vesić tests.

Efficiency

It has already been stated that the three models being considered do not yield either ultimate capacity of the group or group efficiency.

An attempt was made in studying the output from modeling the pile group tests to investigate whether capacity and efficiency could be computed in an approximate fashion by determining the "failure" load corresponding to a "failure settlement" or to a rate of settlement that might be considered to represent failure.

Two procedures were employed to thus estimate failure load from the computed and measured load-settlement curves.

a. Modified Davisson Failure Load (MDFL). Fellenius (23) has analyzed a number of methods for predicting the failure load of piles that have been tested to a load that does not produce plunging failure and has recommended adoption of a technique proposed by Davisson for computing failure load. In that method

$$S_f = \left(\frac{L}{AE}\right) Q_f + 0.15 + \frac{B}{120} \quad \text{(inches)} \tag{2.2}$$

for a single pile, where S_f = settlement corresponding to failure load, Q_f, L is the length of the pile, AE is the elastic stiffness of the pile, and B = diameter of pile tip, in inches. The first term represents elastic foreshortening of the pile, and the second and third represent tip quake, or displacement necessary to attain irrecoverable tip deformation.

Since most piles have some load transferred between the butt and the tip, the failure settlement computed by Eq. (2.2) has been modified for this study to reduce somewhat the elastic foreshortening term by using an average value of load in the pile at failure rather than the value at the butt, so that the modified form of Eq. (2.2) becomes

$$S_f = \left(\frac{0.6L}{AE}\right) Q_f + 0.15 + \frac{B}{120} \quad \text{(inches)} \tag{2.3}$$

For a pile group a further modification is made:

$$S_{fg} = \left(\frac{0.6L}{AE}\right) \frac{Q_{fg}}{N} + 0.15 + \frac{\sqrt{N}\,B}{120} \quad \text{(inches)} \tag{2.4}$$

where the subscript g pertains to the group and N = number of piles in the group. The use of the square root term is partly justified on the basis that observations have indicated that settlement in a pile group is approximately proportional to the square root of the width of the group

(79) and the fact that most of the increase in settlement that occurs in a group in excess of that in a single pile occurs as a result of added displacement of the pile tip. Equation (2.4) is basically an assumption and is probably not valid for nonsquare groups.

Using Eq. (2.3) for the reference pile and (2.4) for the group, "failure" loads were determined from the measured and computed load-settlement curves for both the single pile and the group and the efficiency obtained as

$$\text{Efficiency} = \frac{\text{Indicated group failure load}}{N \times (\text{Indicated reference pile failure load})} \qquad (2.5)$$

b. Slope Method. Fuller and Hoy (27), among others, have indicated that failure of a single pile may be said to occur arbitrarily when the slope of the gross load-settlement curve reaches 0.05 in./ton (0.014 cm/kN). The failure load for reference piles was therefore also obtained from the load-settlement curve using this criterion. It is assumed that this criterion can be applied to groups by stating that group failure occurs when the slope of the gross load-settlement curve for the group reaches 0.05 in./$\sqrt{N}$ per ton (0.014 cm/$\sqrt{N}$ per kN). This criterion was used to compute the group failure load, and the group efficiency was computed as indicated for the MDFL method.

It should be mentioned here that these methods, especially the latter method, are tenuous at best, because they both depend on the shape of the measured or computed load-settlement curve, which is dependent on many factors. For example, the shape of the measured curve depends strongly on the type of test conducted, such as slow maintained load, quick maintained load, cyclic, or constant rate of penetration (23), while the ultimate load may be relatively independent of these effects (27).

Efficiency was also computed for each test from Feld's rule and from the block failure mechanism.

Results of Comparative Study

The results of the comparative study are presented in Figures 2.1-2.67 and Tables 2.2-2.10, which follow. For each of the five tests modeled, results include basic information concerning the group, soil,

and test and the following relationships, with measured values shown where appropriate.

a. Load vs. settlement of the reference pile by the hybrid method.

b. Baseline and adjusted load transfer functions for the hybrid method.

c. Load distribution pattern in the reference pile by the hybrid method.

d. Load vs. settlement of the reference pile by the elastic solid method.

e. Load vs. settlement of the reference pile by the finite element method (where appropriate graphical solutions exist).

f. Load distribution pattern in the reference pile by the finite or boundary element method (where appropriate graphical solutions exist).

g. Load vs. settlement of the pile group by the hybrid, elastic solid, and finite element methods.

h. Load distribution patterns in the pile group by the hybrid method.

i. Surface settlements by the elastic solid and finite element methods.

j. Distribution of loads to pile heads by all methods, except where noted.

k. Capacities and efficiencies as estimated from the measured and computed load-settlement curves.

Group load-settlement relationships are shown in some cases for load transfer function or modulus values other than the best ones obtained from modeling the isolated pile for purposes of demonstrating the sensitivity of the models to these inputs.

Some small inaccuracies may exist in the finite element solutions, since parametric graphs do not exist for as wide a variety of length, spacing, and relative pile-soil stiffness parameters as exist for the elastic solid methods, necessitating some interpolation.

AREA Test

All piles in this test were installed by driving. Testing occurred between 19 and 52 days after driving and was of the cyclic, maintained load type. The measured load-settlement curves are envelopes to the cyclic curves. Soil strength data are strongly suggestive that the undisturbed values of undrained cohesion c_u may in fact be remodeled values. The cap was not in contact with the soil surface.

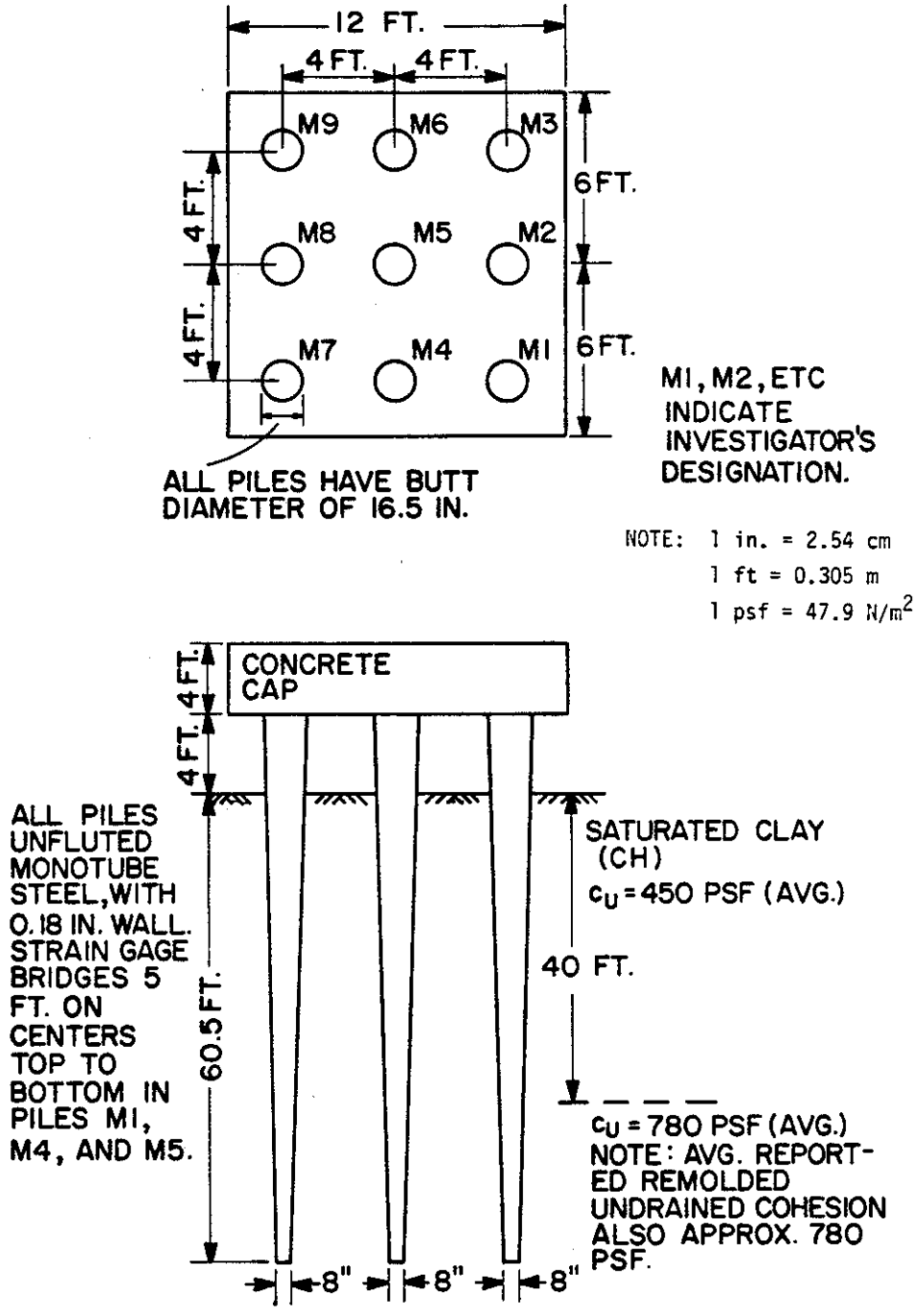

FIGURE 2.1. PILE GEOMETRY AND SOIL CONDITIONS, AREA TEST

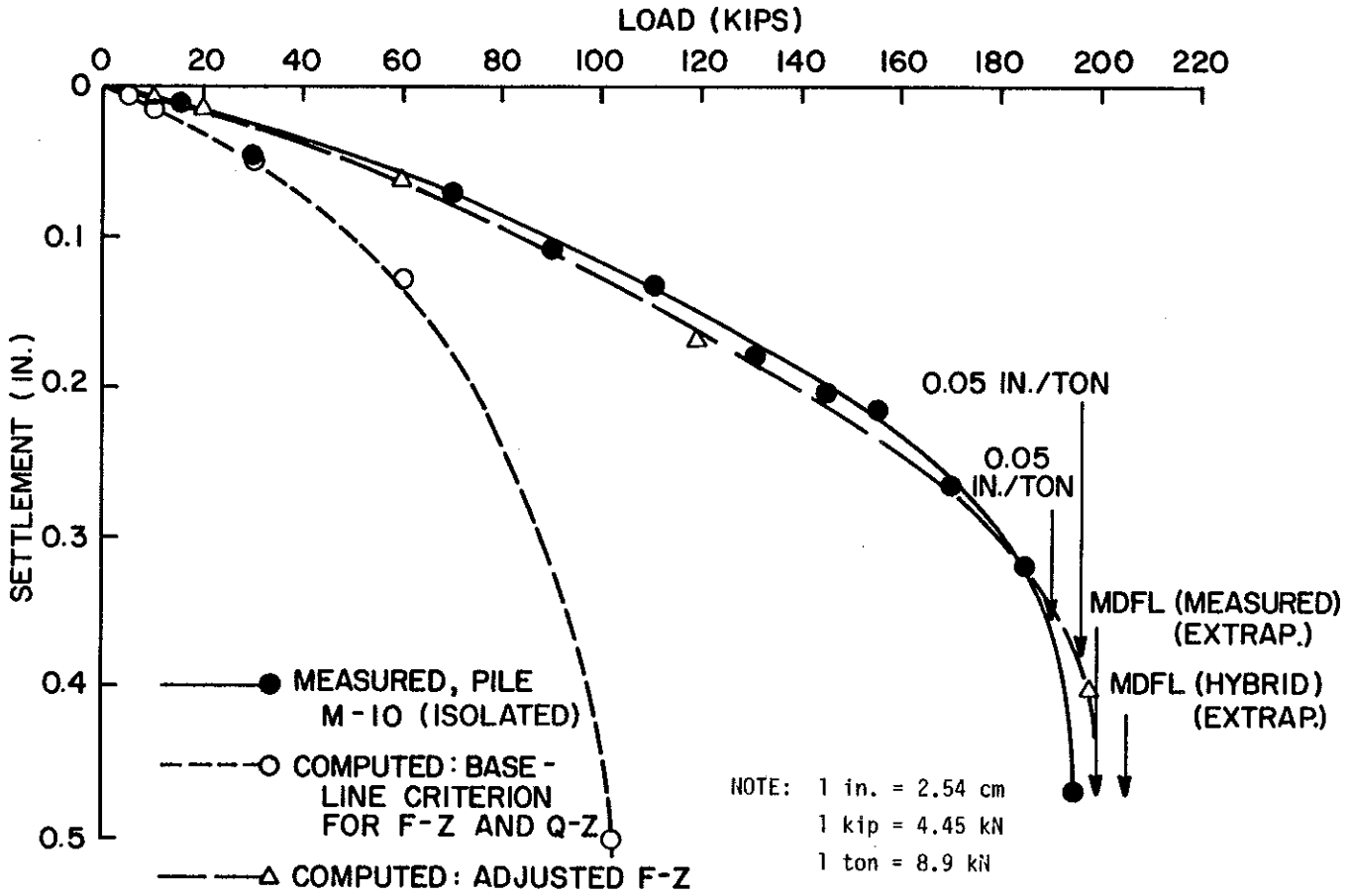

FIGURE 2.2 LOAD VS. SETTLEMENT, REFERENCE PILE, HYBRID MODEL, AREA TEST

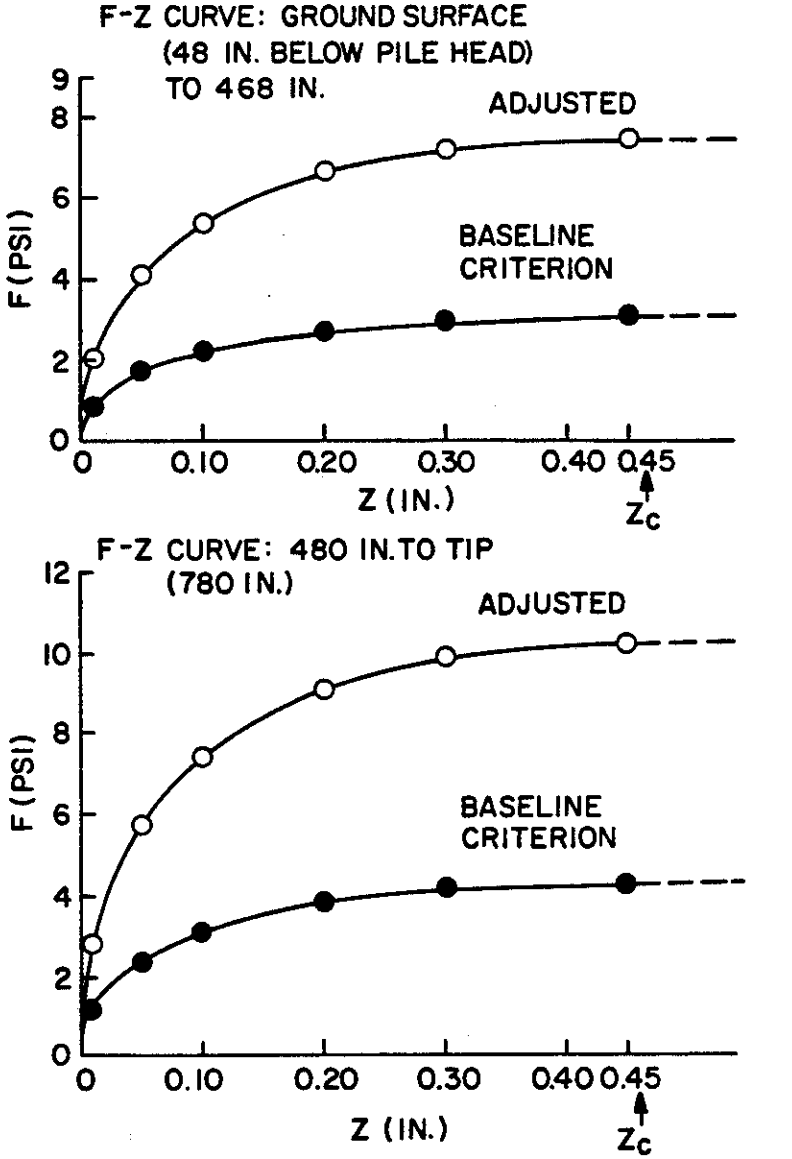

BASELINE CRITERION: $F_{MAX} = \alpha c_u$, WHERE $\alpha = 1.0$ ABOVE 40 FT PENETRATION AND 0.79 BELOW 40 FT.

NOTE: 1 in. = 2.54 cm 1 ft = 0.305 m 1 psi = 6.89 kN/m^2

FIGURE 2.3. F-Z RELATIONSHIPS, AREA TEST

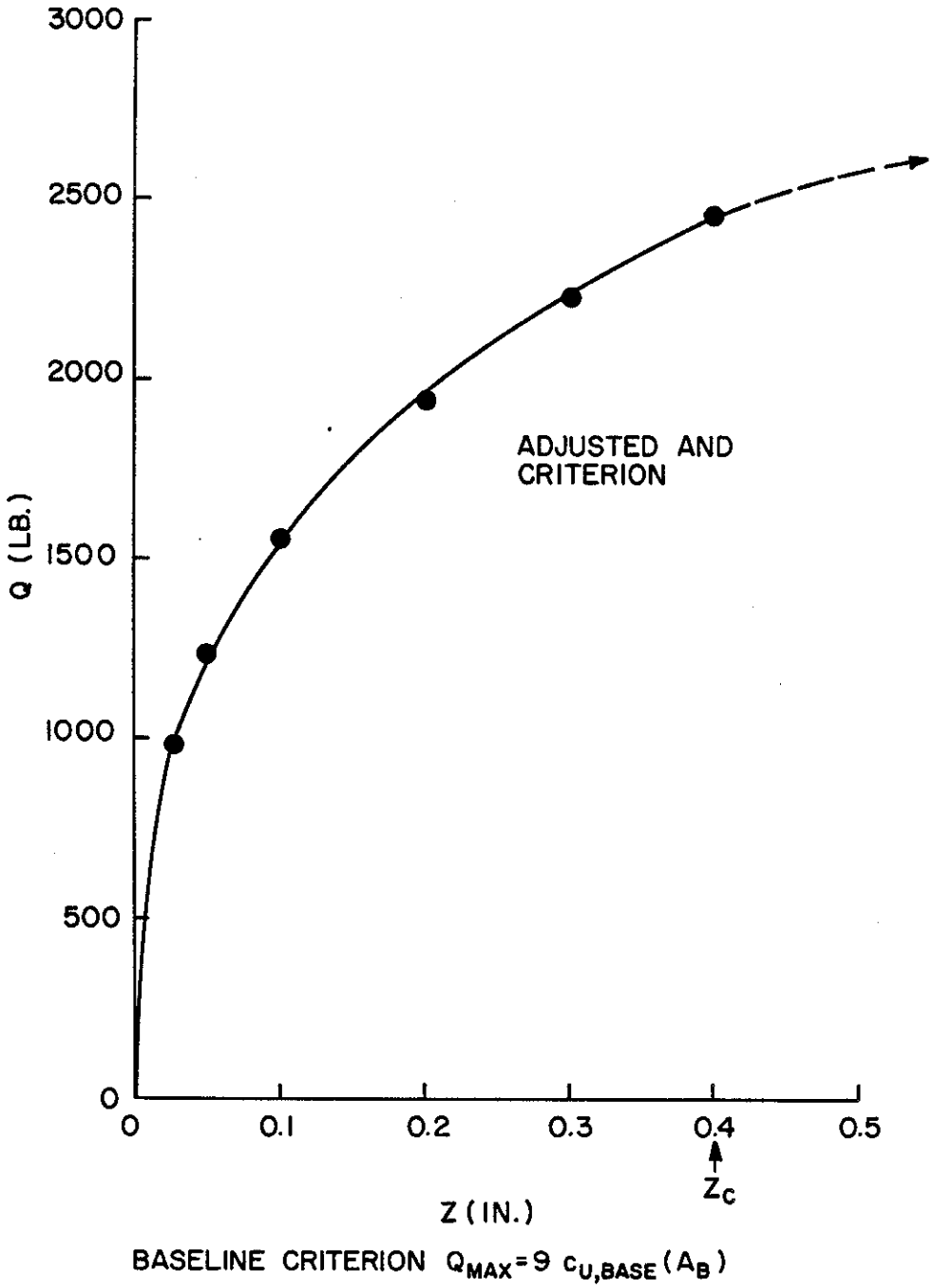

FIGURE 2.4. Q-Z RELATIONSHIP, AREA TEST

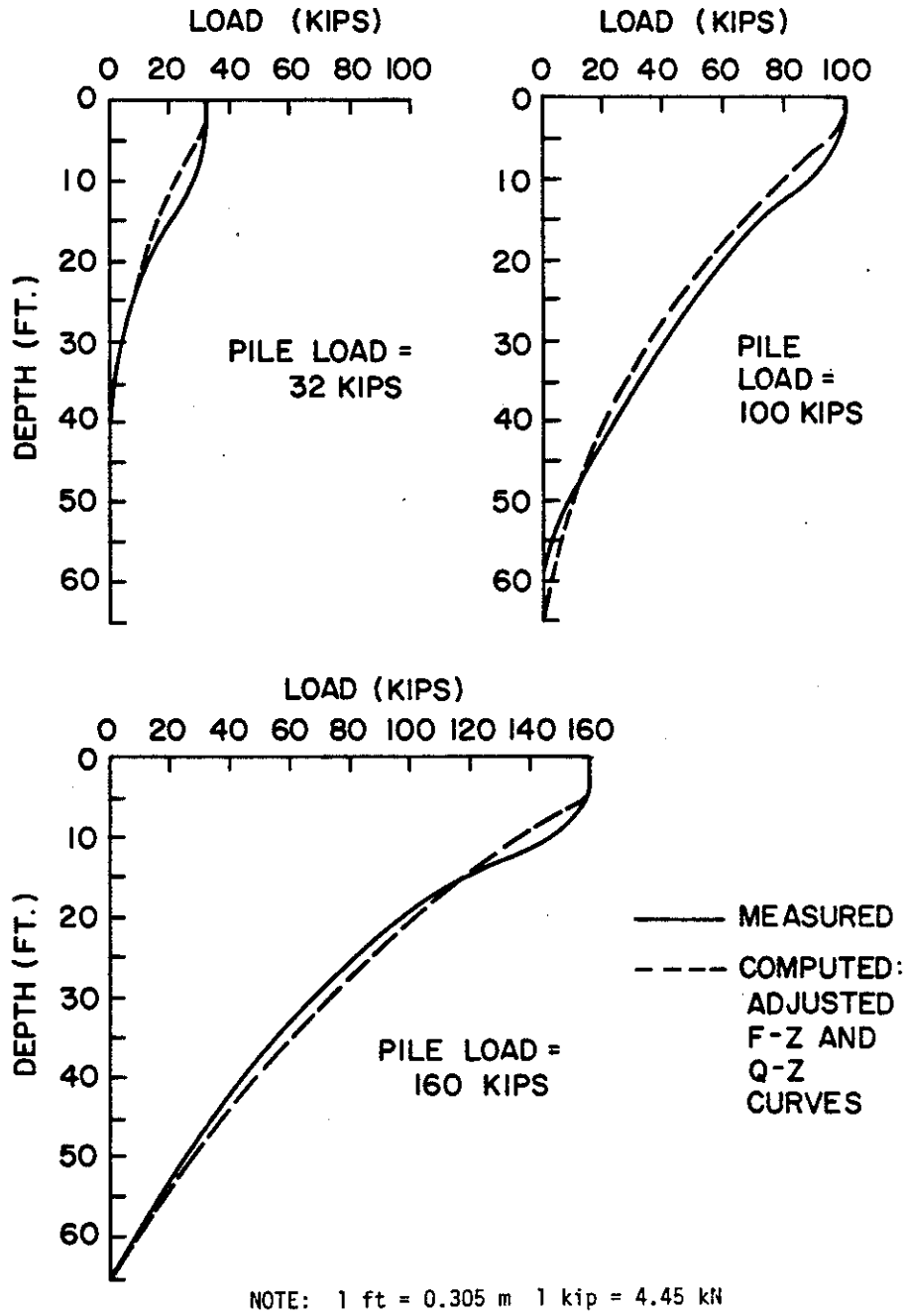

NOTE: 1 ft = 0.305 m 1 kip = 4.45 kN

FIGURE 2.5. LOAD DISTRIBUTION RELATIONSHIPS, REFERENCE PILE, HYBRID MODEL, AREA TEST

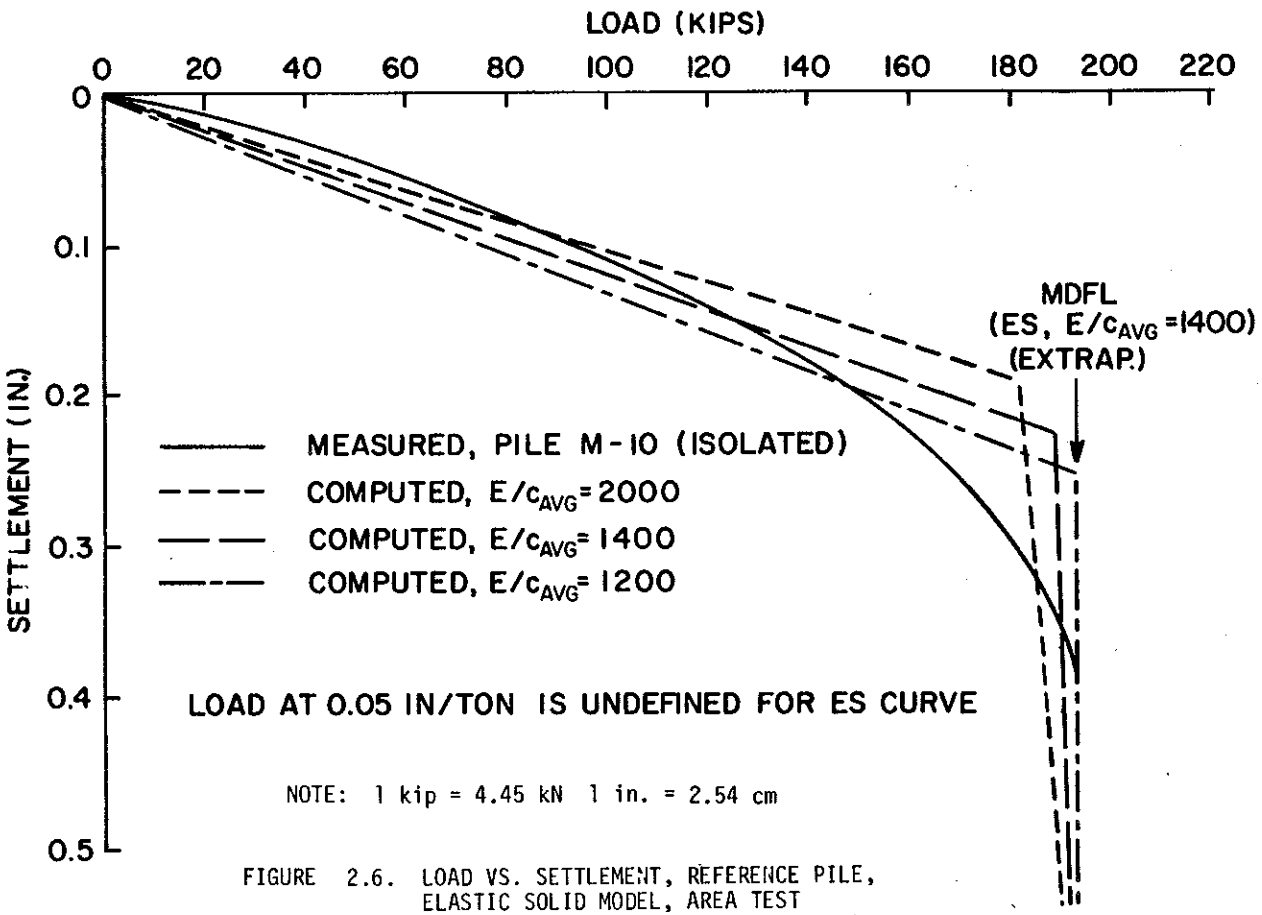

FIGURE 2.6. LOAD VS. SETTLEMENT, REFERENCE PILE, ELASTIC SOLID MODEL, AREA TEST

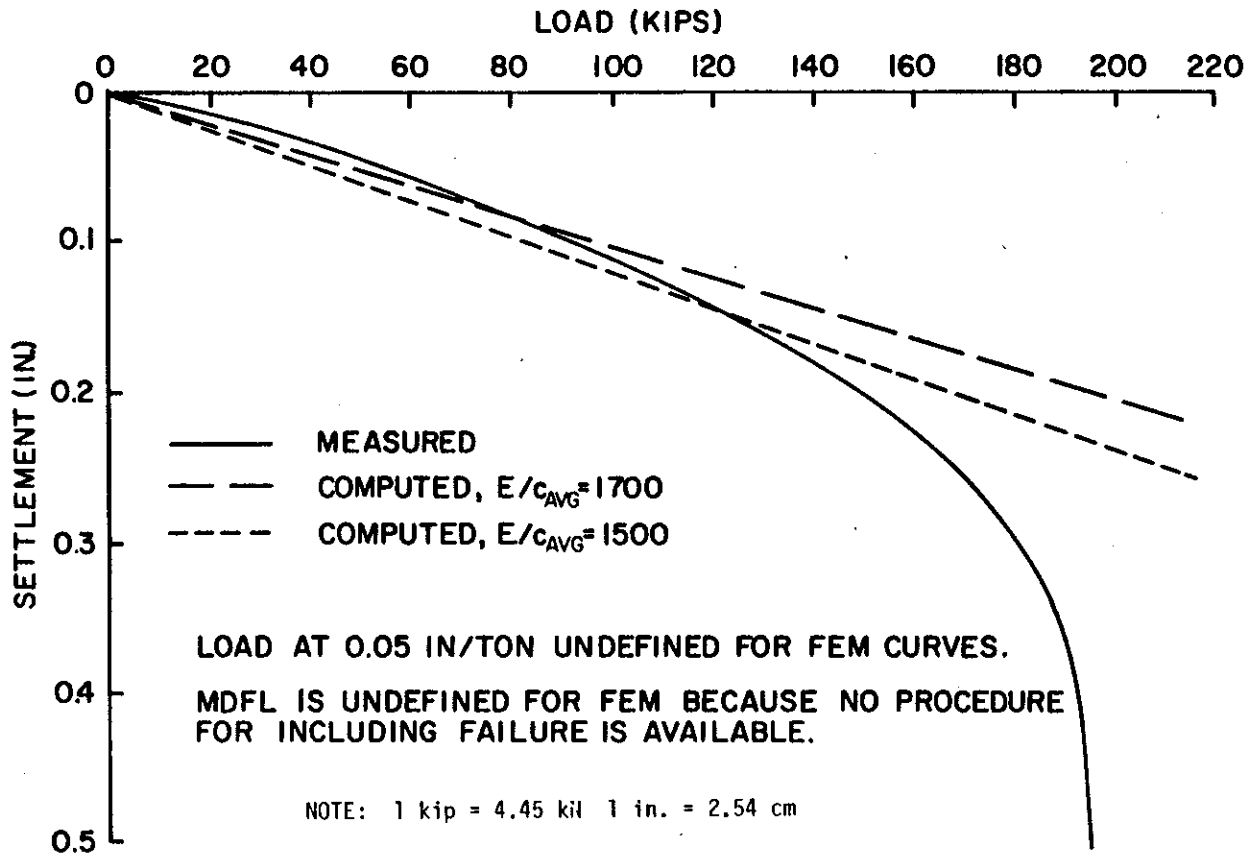

FIGURE 2.7. LOAD VS. SETTLEMENT, REFERENCE PILE, FINITE ELEMENT MODEL, AREA TEST

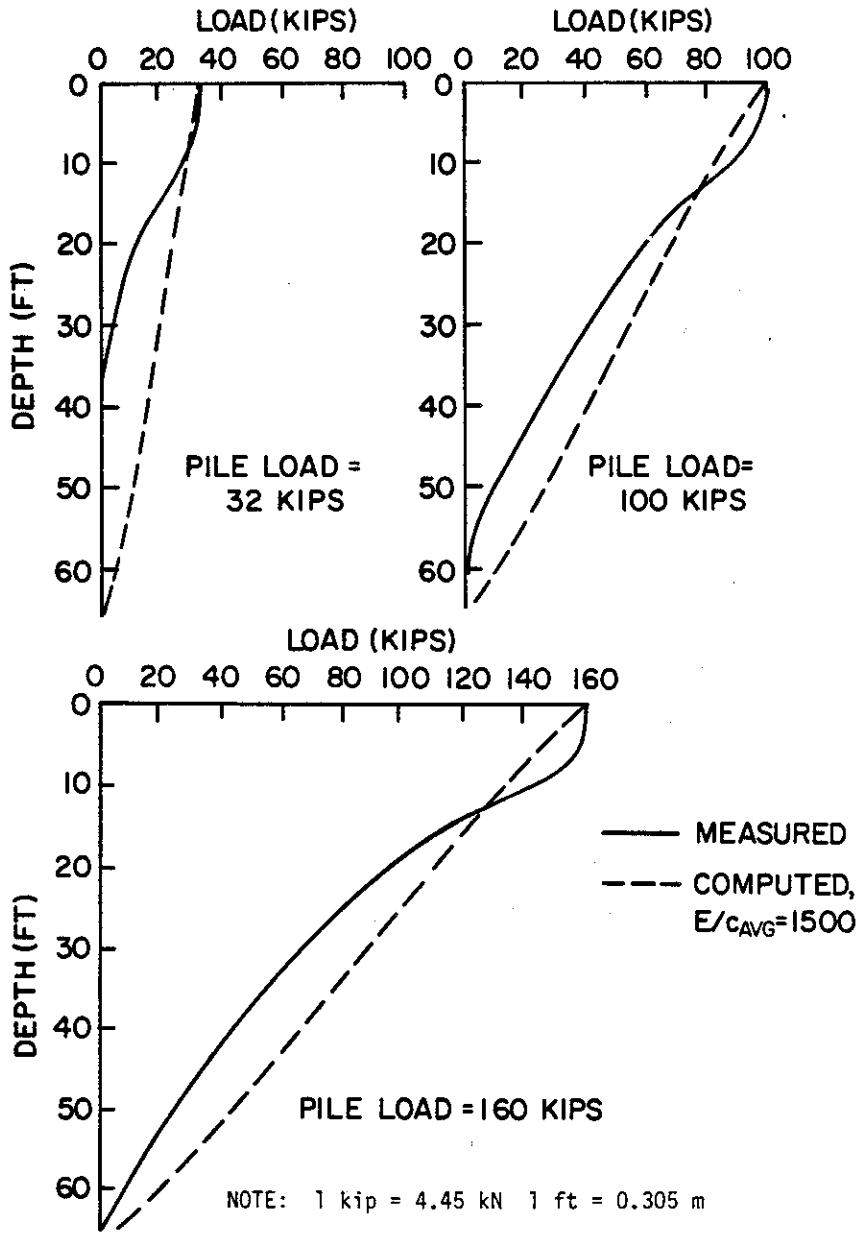

FIGURE 2.8. LOAD DISTRIBUTION RELATIONSHIPS, REFERENCE PILE, FINITE ELEMENT MODEL, AREA TEST

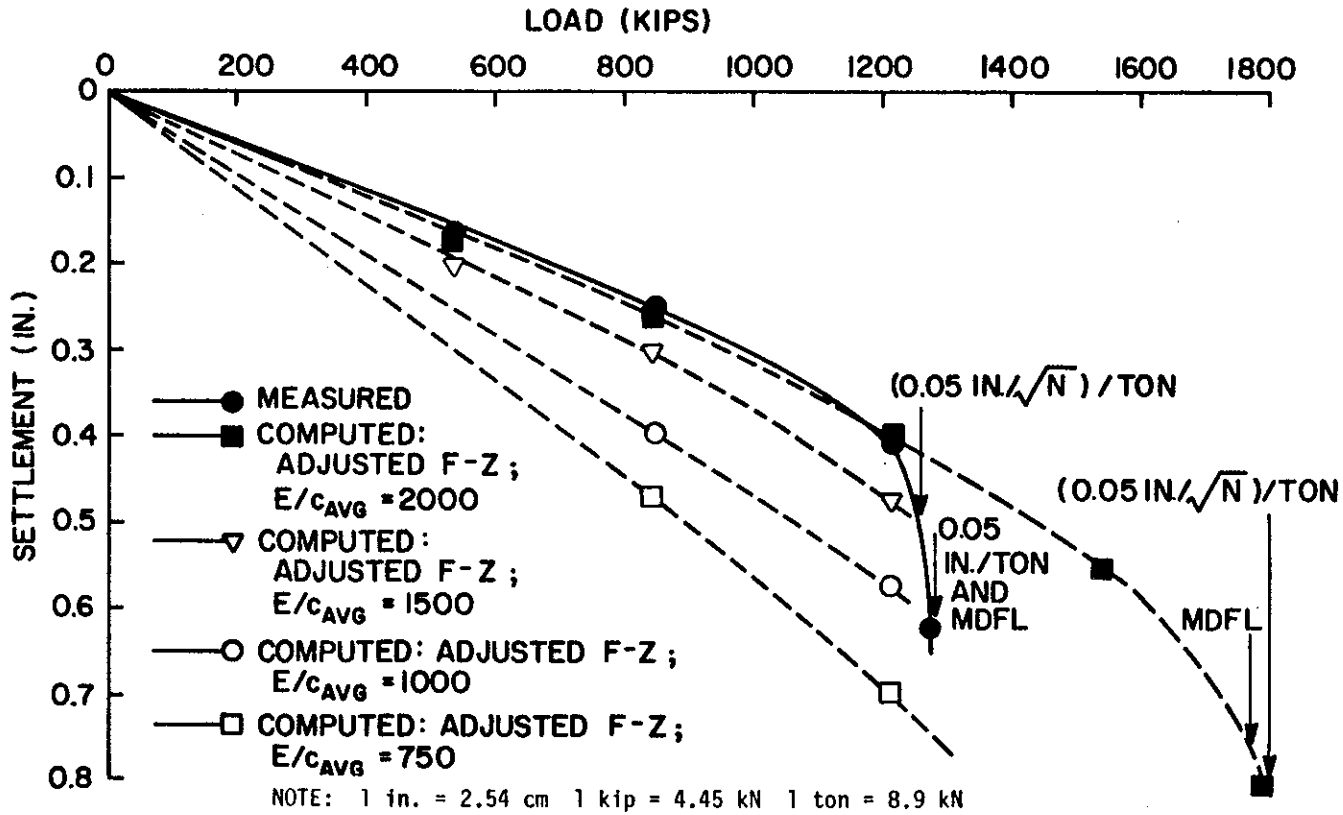

FIGURE 2.9. LOAD VS. SETTLEMENT, GROUP, HYBRID MODEL, AREA TEST

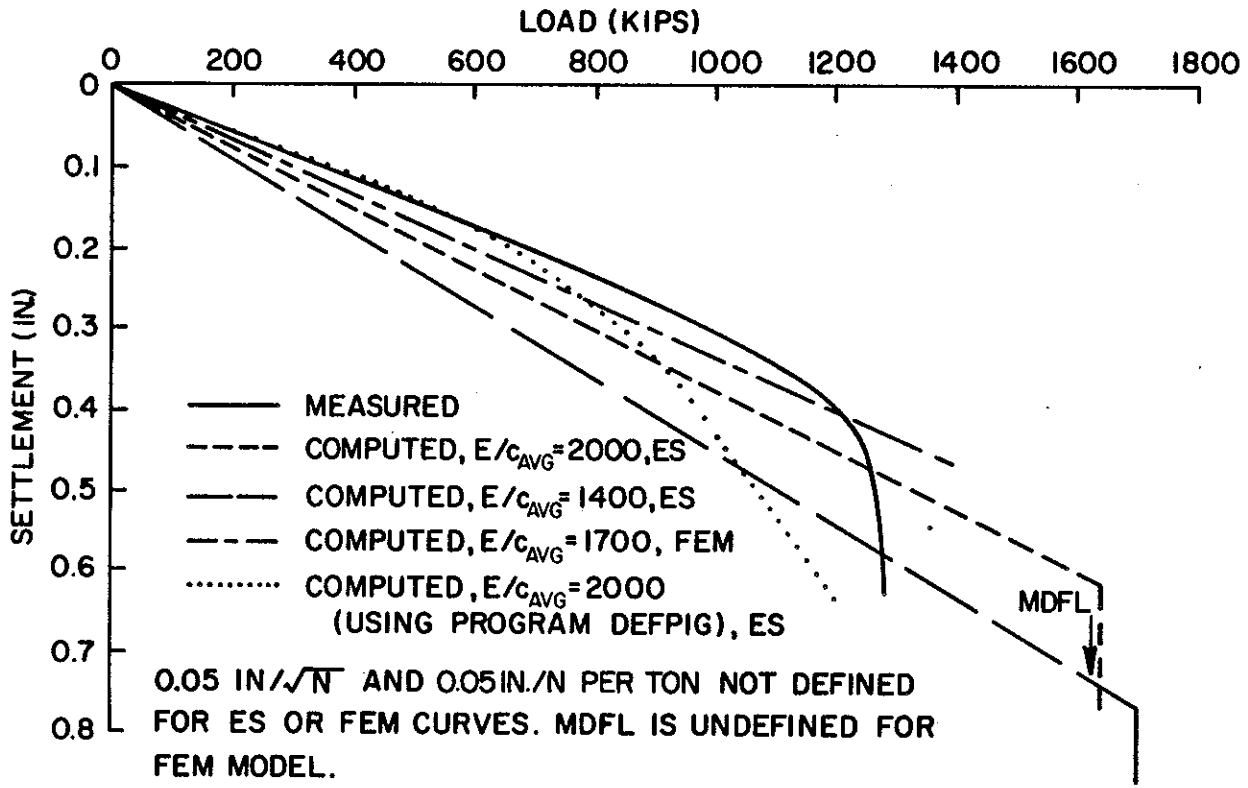

NOTE: 1 in. = 2.54 cm 1 kip = 4.45 kN 1 ton = 8.9 kN

FIGURE 2.10. LOAD VS. SETTLEMENT, GROUP, ELASTIC SOLID MODEL, AREA TEST

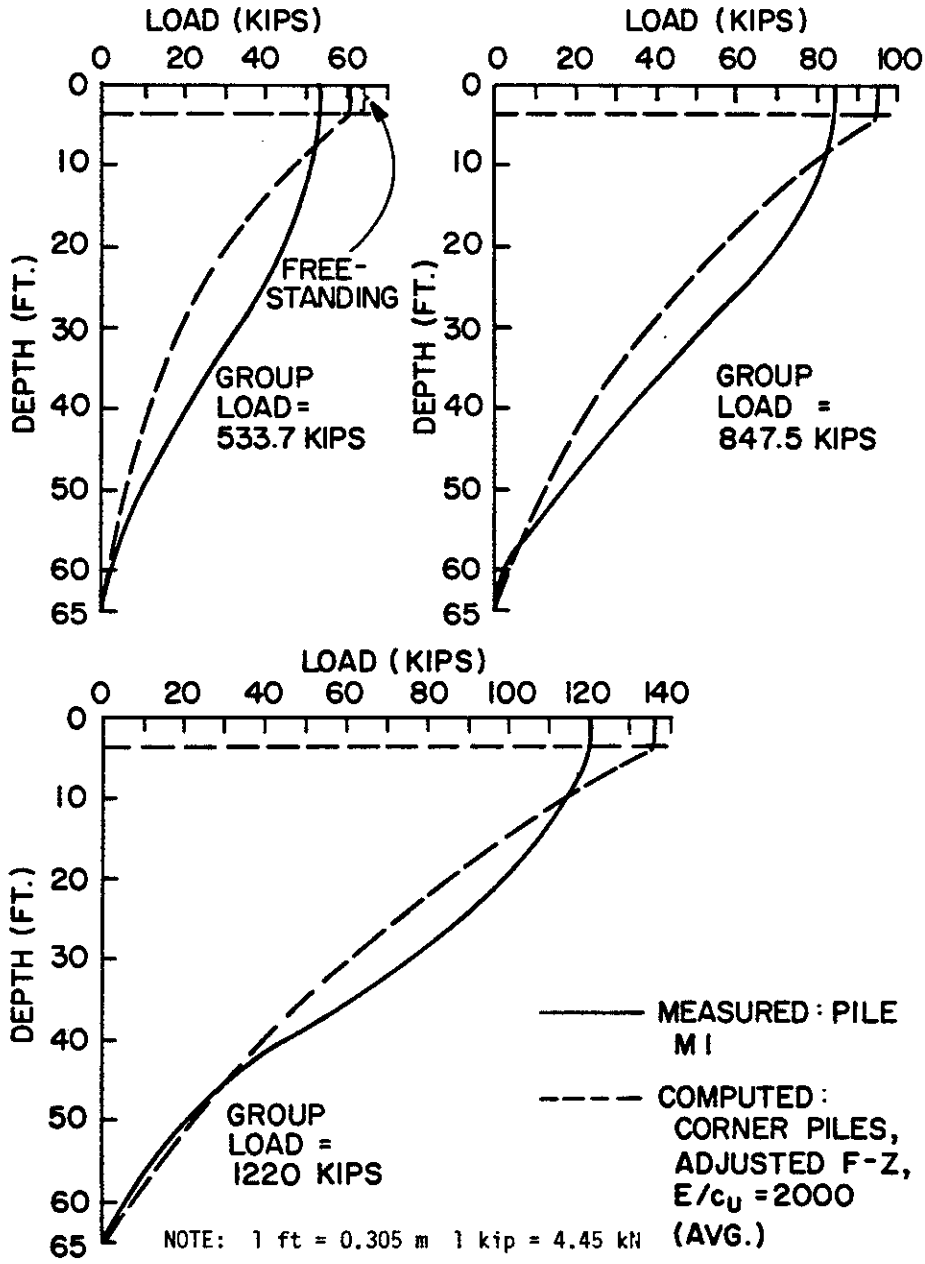

FIGURE 2.11. LOAD DISTRIBUTION RELATIONSHIPS, GROUP, CORNER PILES, HYBRID MODEL, AREA TEST

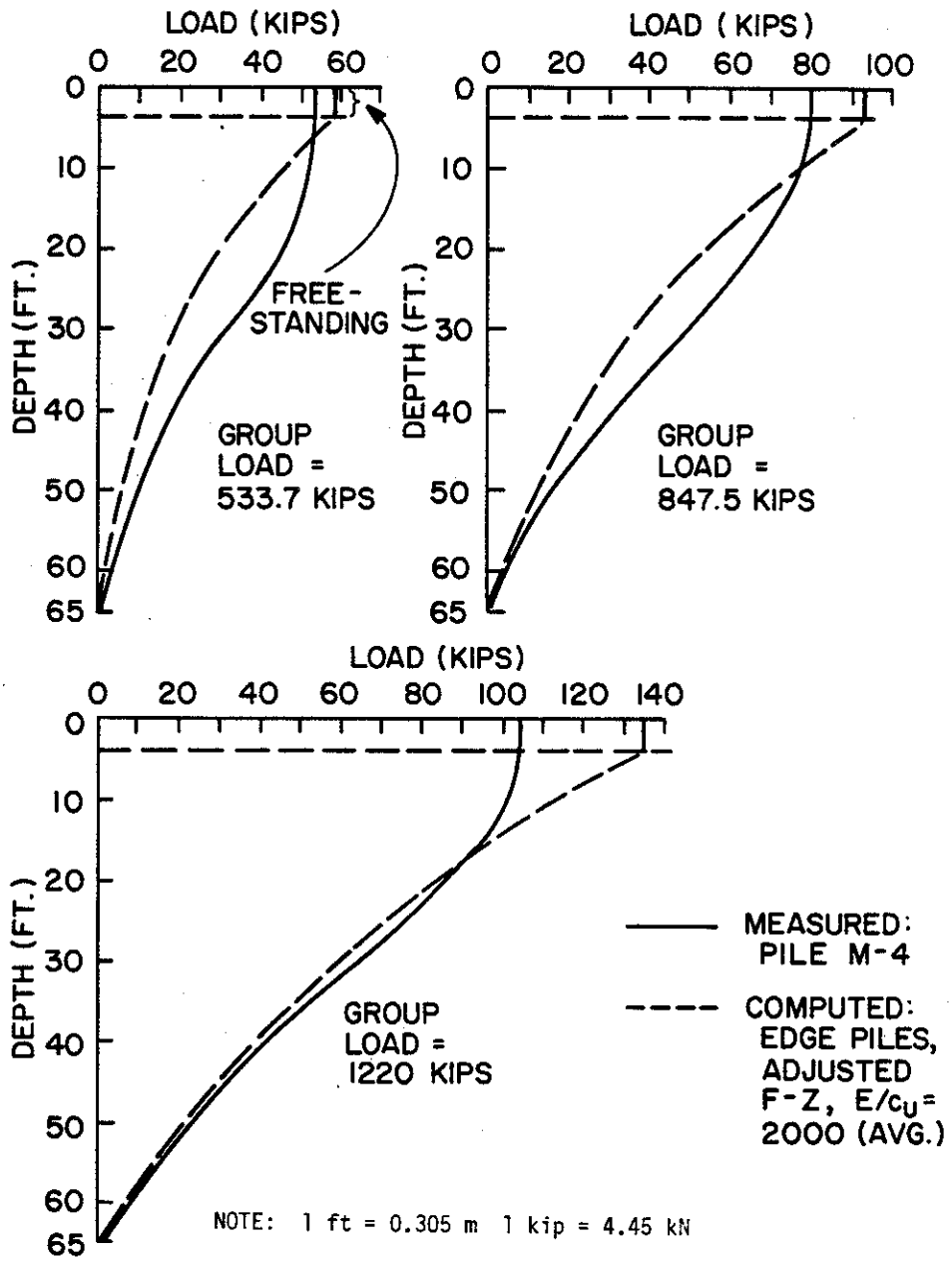

FIGURE 2.12. LOAD DISTRIBUTION RELATIONSHIPS, GROUP, EDGE PILES, HYBRID MODEL, AREA TEST

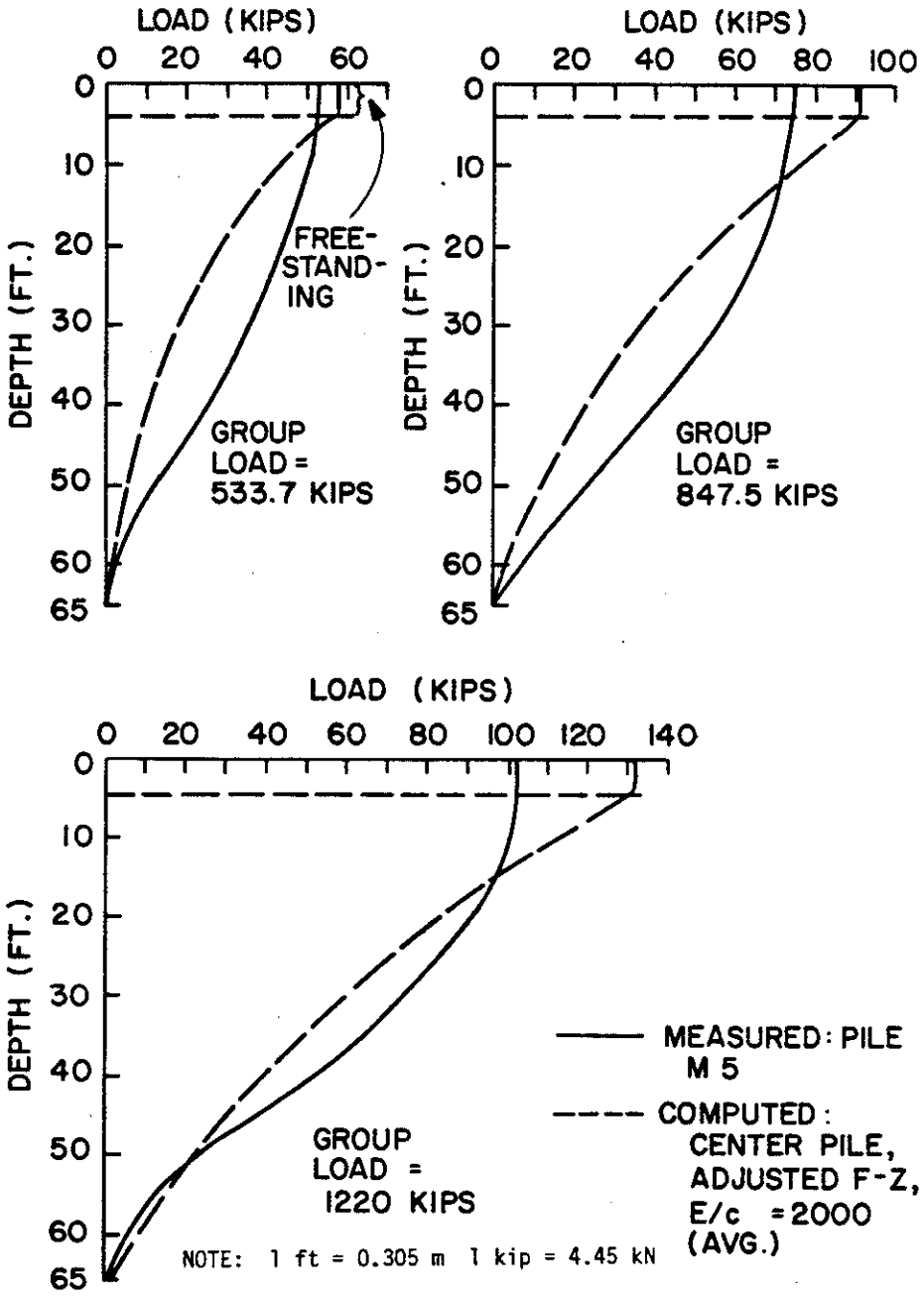

FIGURE 2.13. LOAD DISTRIBUTION RELATIONSHIPS, GROUP, CENTER PILE, HYBRID MODEL, AREA TEST

TABLE 2.2 DISTRIBUTION OF LOADS TO PILE HEADS: AREA 9 PILE GROUP

Applied Group Load (kips)	Method	Load on Corner Piles (kips)	Load on Edge Piles (kips)	Load on Center Pile (kips)
533.7	Hybrid	60.6	58.5	57.5
533.7	Elastic Solid	71.4	54.5	30.0
533.7	FEM	*	*	*
533.7	Measured	53.0**	53.0**	53.0**
847.5	Hybrid	95.3	93.2	93.2
847.5	Elastic Solid	113.5	86.5	47.7
847.5	FEM	*	*	*
847.5	Measured	84.0**	80.0**	75.0**
1220.0	Hybrid	136.1	136.0	132.0
1220.0	Elastic Solid	163.3	124.5	68.6
1220.0	FEM	*	*	*
1220.0	Measured	120.0**	104.0**	102.0**

*Solution for cap suspended off ground not published
**Note: Measured loads are for 1 corner, 1 edge, and the center pile (M1, M4, and M5). Other geometrically similar piles may not have carried these loads.

Hybrid Model: Adjusted f-z curves, $E/c_u = 2000$

Elastic Solid Model: $E/c_u = 1400$

Note: 1 kip = 4.45 kN

TABLE 2.3. COMPUTED AND MEASURED "EFFICIENCIES" FROM AREA TEST

Failure Criterion	Single Pile Failure Load (kips) (M-10)			Group Failure Load (kips)			Group Efficiency				
	H	ES	M	H	ES	M	H	ES	M	B	F
0.05 in./ton	197	-	191	*	-	1290	-	-	0.75		
(0.05 in./)$\sqrt{N}$ton	197	-	191	1780	-	1270	1.00	-	0.74		
MDFL	206**	194**	201**	1780	1640	1290	0.96	0.94	0.71		
										1.07**	0.72

*Beyond limits of curve; therefore, undefined
**Extrapolated
***Based on single pile failure =196 kips (avg. of 0.05in./ton and MDFL)
H - Hybrid method curve
ES - Elastic solid method curve
M - Measured
B - Block (equivalent pier) failure
F - Feld's Rule

Note: 1 in. = 2.54 cm
1 kip = 4.45 kN
1 ton = 8.9 kN

Vesić Test

All piles were installed by jacking. In the case of the group, the entire group was jacked into the soil in one action. Testing was accomplished using a variation of the constant-rate-of-penetration test. The cap was in contact with the soil surface. None of the models employed considered cap-soil contact.

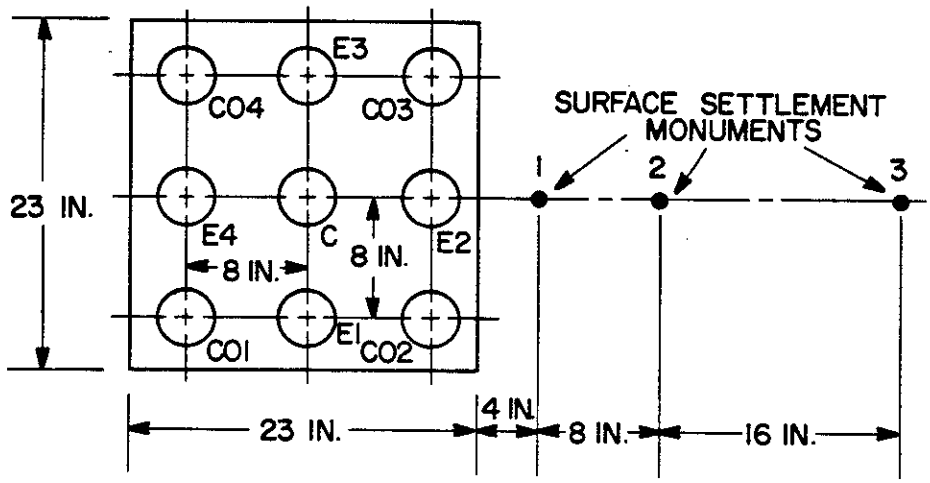

NOTE: 1 in. = 2.54 cm

FIGURE 2.14. PLAN VIEW OF PILE GROUP, VESIĆ TEST (P-93)

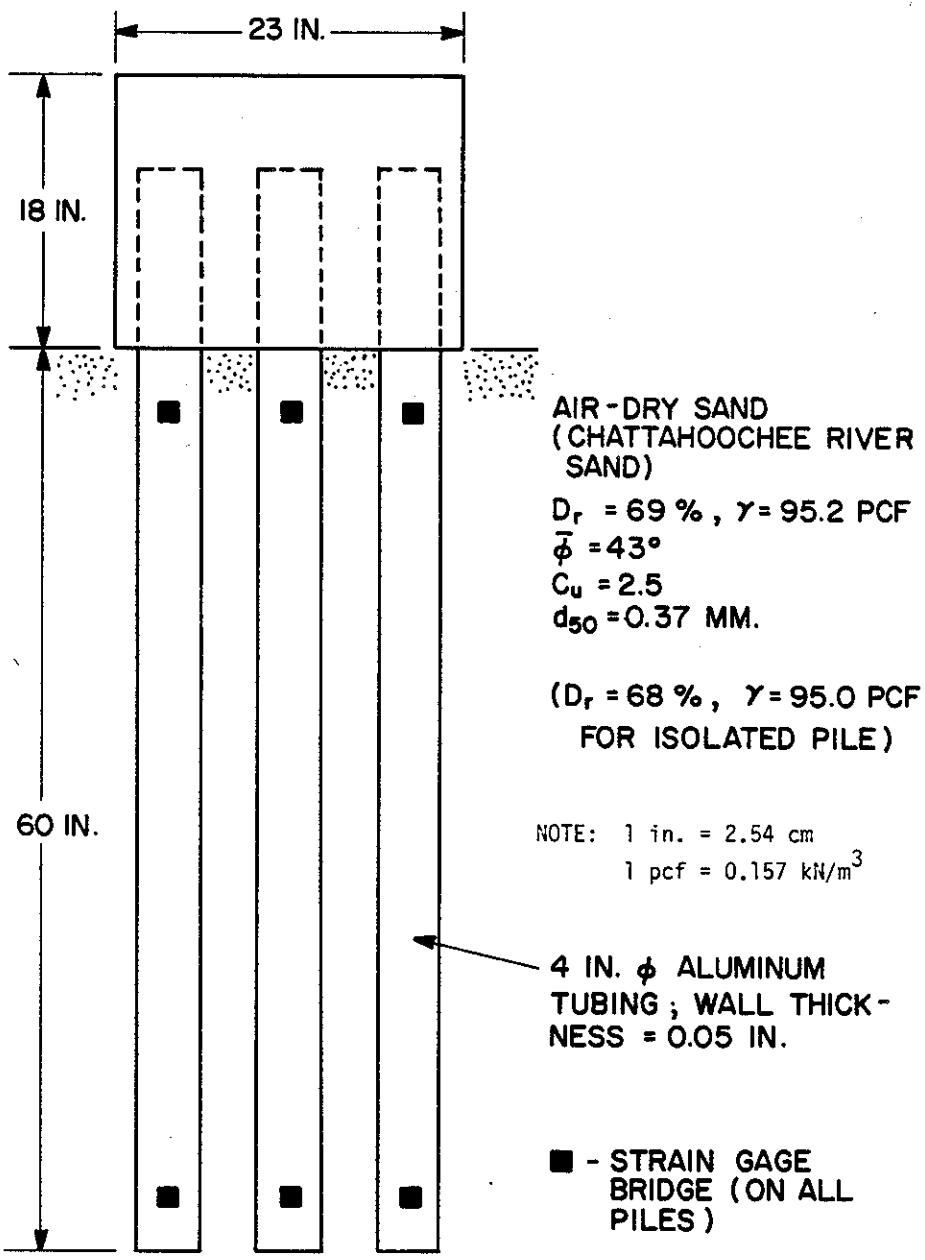

FIGURE 2.15. ELEVATION VIEW OF PILE GROUP AND SOIL DESCRIPTION, VESIĆ TEST (P-93)

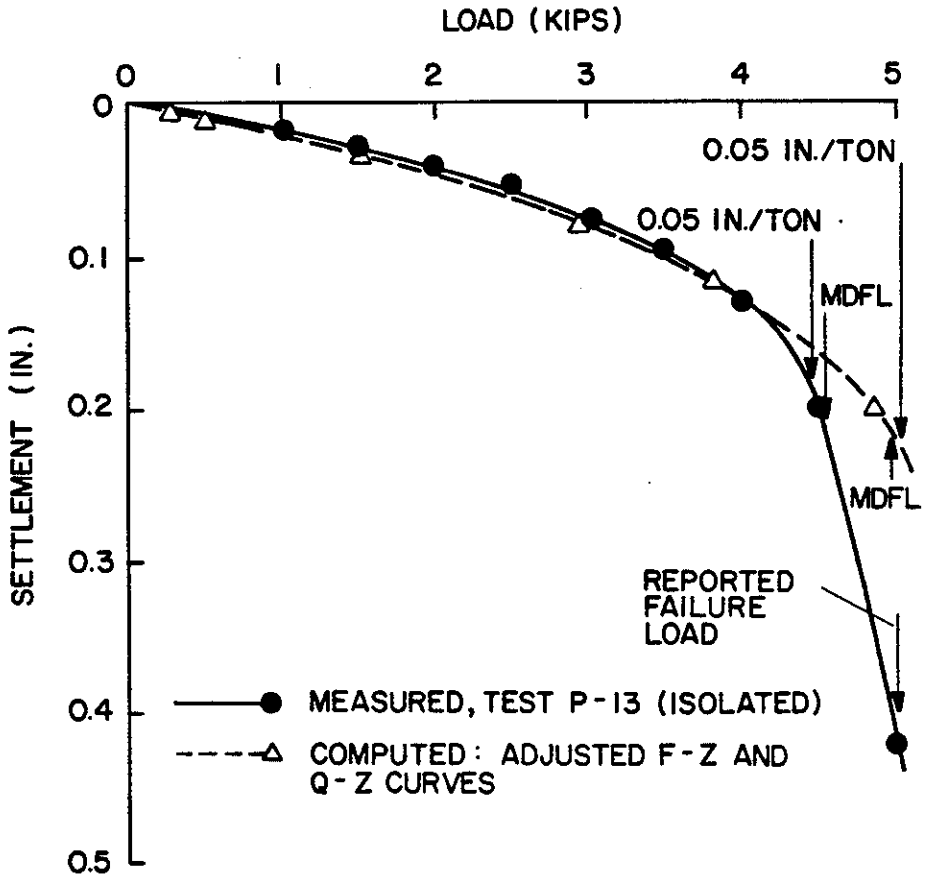

NOTE: 1 in. = 2.54 cm 1 kip = 4.45 kN 1 ton = 8.9 kN

FIGURE 2.16. LOAD VS. SETTLEMENT, REFERENCE PILE, HYBRID MODEL, VESIĆ TEST.

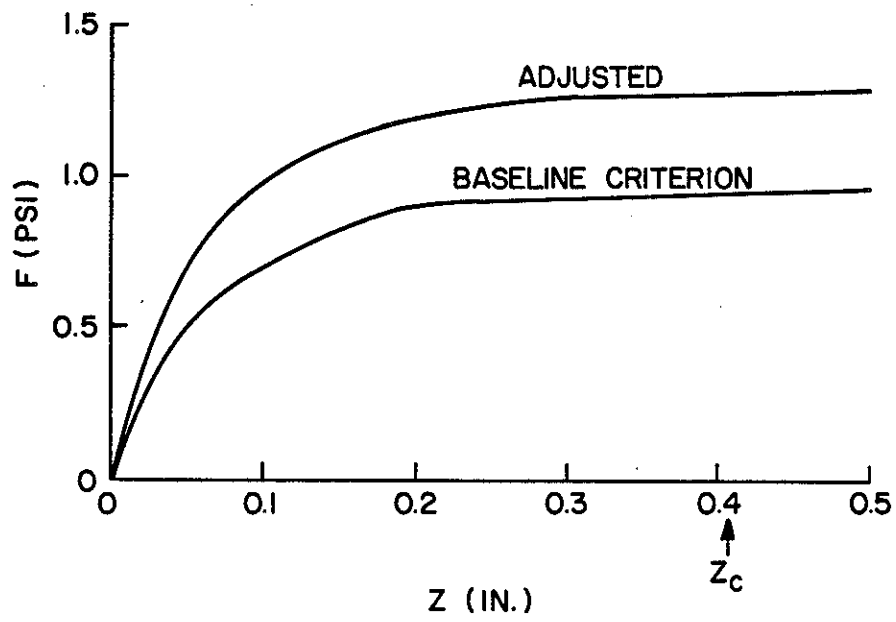

BASELINE CRITERION:

$F_{MAX} = K\bar{\gamma} Z \tan \phi_{PS}$

ASSUME K = 0.7 FOR MODEL PILE

$\phi_{PS} = \phi - 5°$ (SMOOTH METAL) = 38°

AT MIDDEPTH OF PILE:

F_{MAX} = 95.2 (2.5)(0.7) TAN(38°) = 130 PSF = 0.90 PSI

USE MIDDEPTH F_{MAX} ALONG ENTIRE LENGTH OF PILE, SINCE PILE IS SHORT.

NOTE: 1 in. = 2.54 cm 1 psi = 6.89 kN/m^2 1 psf = 47.9 N/m^2

FIGURE 2.17. F-Z RELATIONSHIPS, VESIĆ TEST

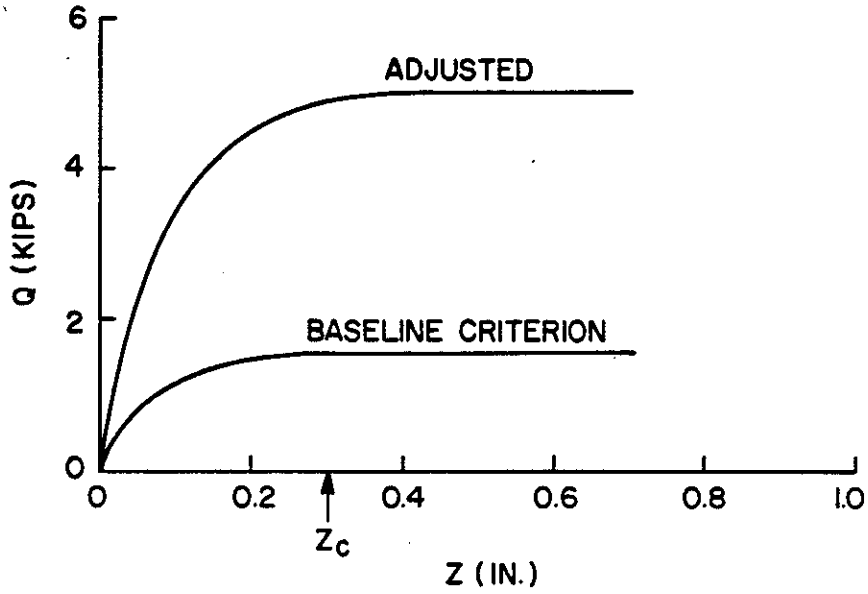

BASELINE CRITERION:

$q_{MAX} = N_q \bar{\gamma} Z$

$= 40(95.0)(5)/144$ ($N_q = 40$ ACCORDING TO BASELINE CRITERION)

$= 132$ PSI

$Q_{MAX} = 132 \times A_B = 1658$ lb.

NOTE: 1 in. = 2.54 cm 1 kip = 4.45 kN 1 lb = 4.4[illegible] N 1 psi = 6.89 kN/m^2

FIGURE 2.18. Q-Z RELATIONSHIPS, VESIĆ TEST

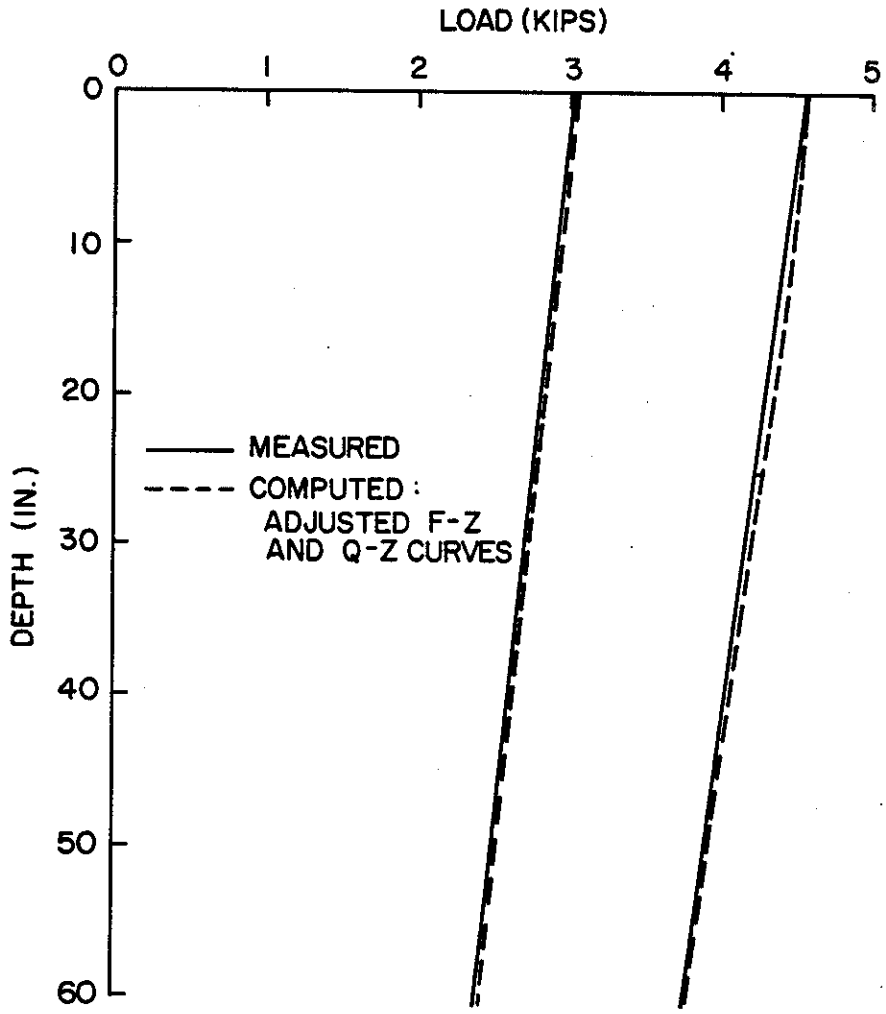

NOTE: 1 in. = 2.54 cm 1 kip = 4.45 kN

FIGURE 2.19. LOAD DISTRIBUTION RELATIONSHIPS, REFERENCE PILE, HYBRID MODEL, VESIĆ TEST

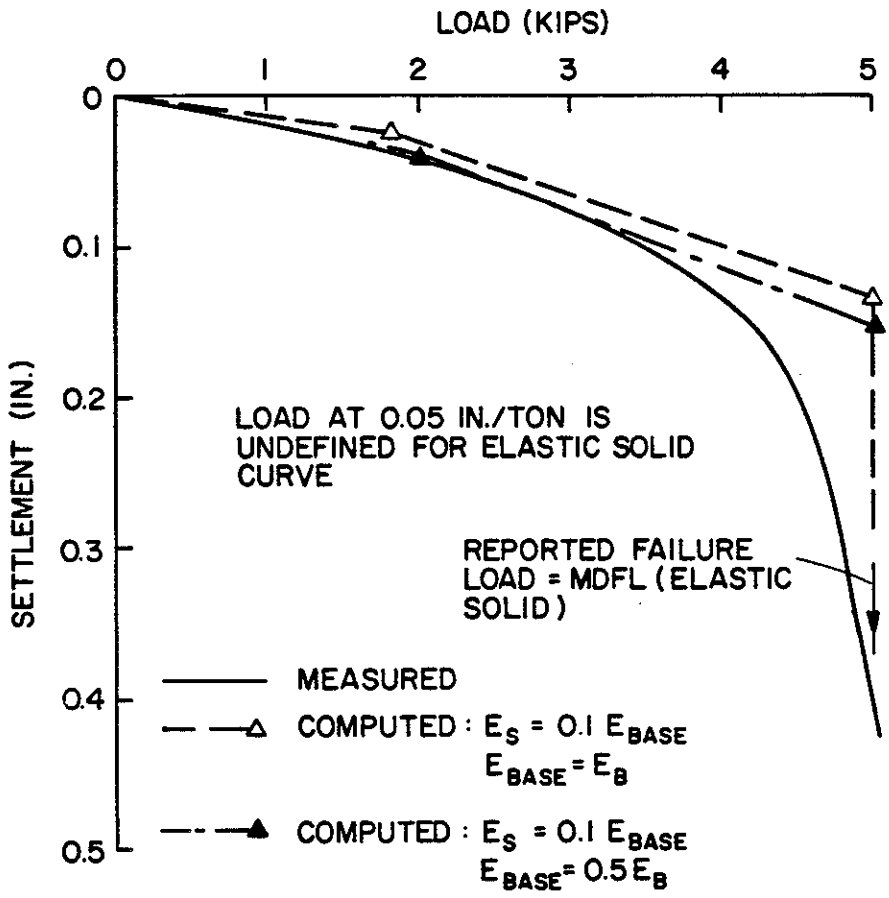

NOTE: 1 in. = 2.54 cm 1 kip = 4.45 kN 1 ton = 8.9 kN

FIGURE 2.20. LOAD VS. SETTLEMENT, REFERENCE PILE, ELASTIC SOLID (POULOS) MODEL, VESIĆ TEST

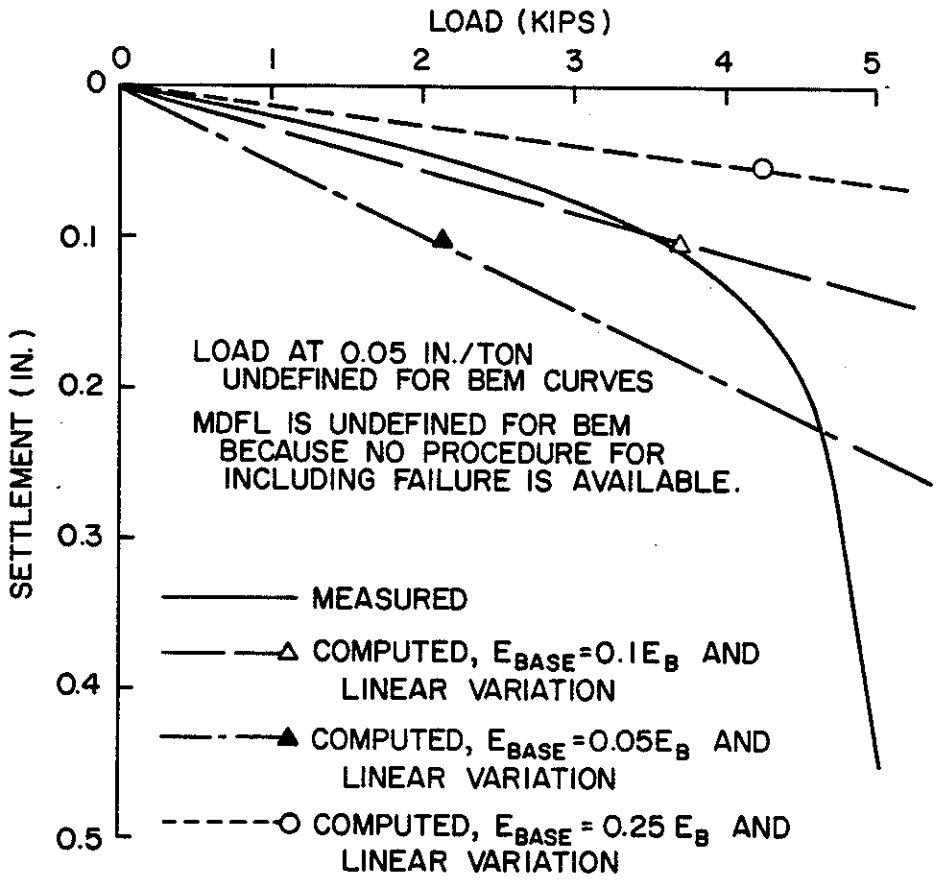

NOTE: 1 in. = 2.54 cm 1 kip = 4.45 kN 1 ton = 8.9 kN

FIGURE 2.21. LOAD VS. SETTLEMENT, REFERENCE PILE, ELASTIC SOLID (BOUNDARY ELEMENT) MODEL, VESIC TEST

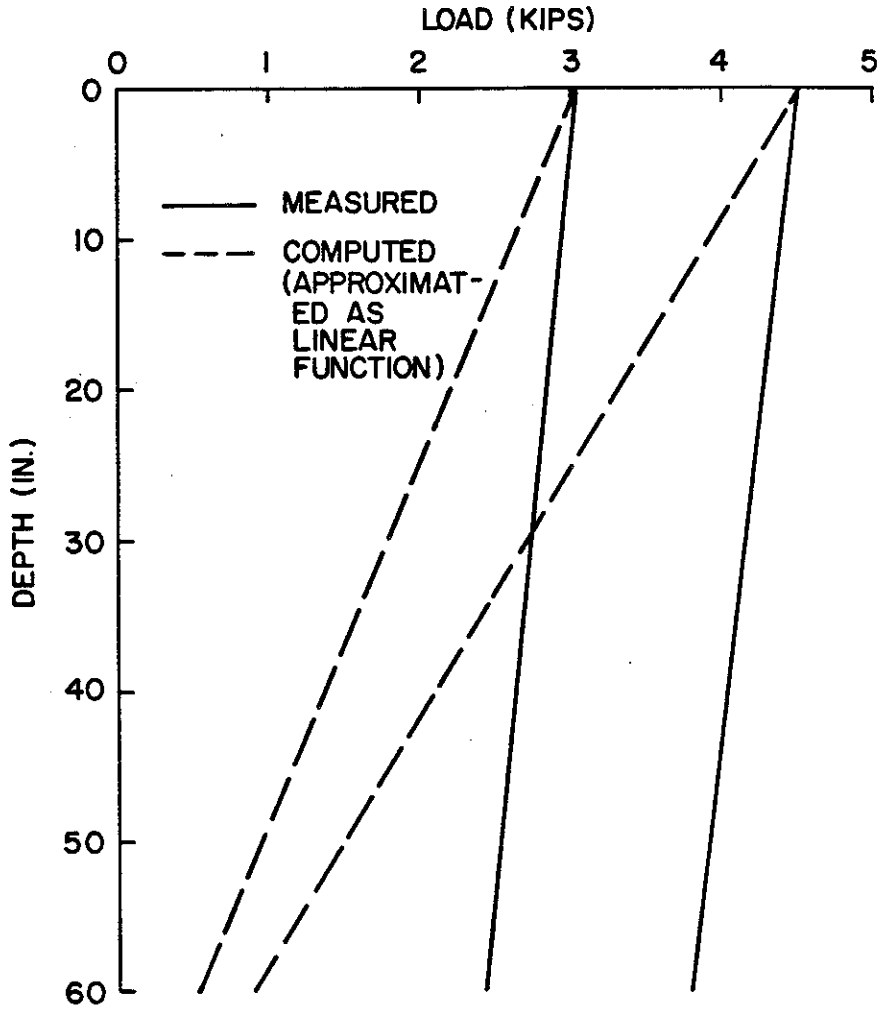

NOTE: 1 in. = 2.54 cm 1 kip = 4.45 kN

FIGURE 2.22. LOAD DISTRIBUTION RELATIONSHIPS, REFERENCE PILE, ELASTIC SOLID (BOUNDARY ELEMENT) MODEL, VESIĆ TEST

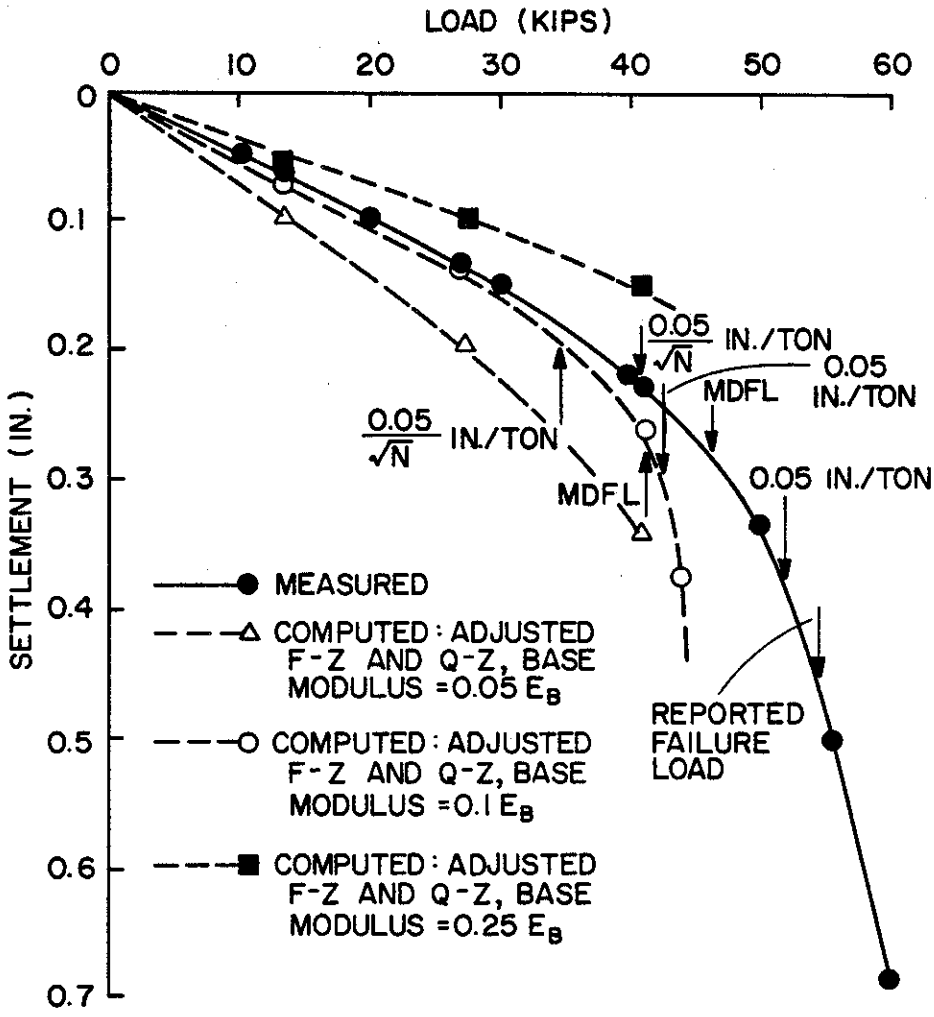

NOTE: 1 in. = 2.54 cm 1 kip = 4.45 kN 1 ton = 8.9 kN

FIGURE 2.23. LOAD VS. SETTLEMENT, GROUP, HYBRID MODEL, VESIC TEST

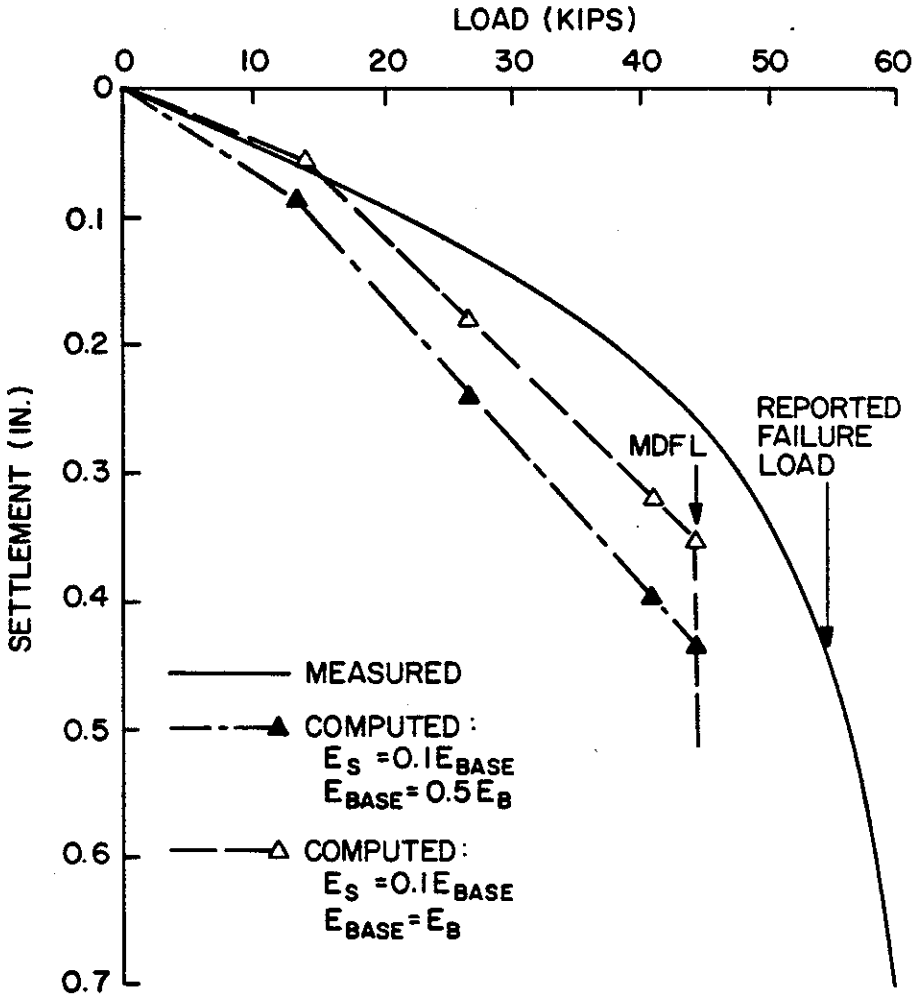

NOTE: 1 in. = 2.54 cm 1 kip = 4.45 kN

FIGURE 2.24. LOAD VS. SETTLEMENT, GROUP, ELASTIC SOLID (POULOS) MODEL, VESIC TEST

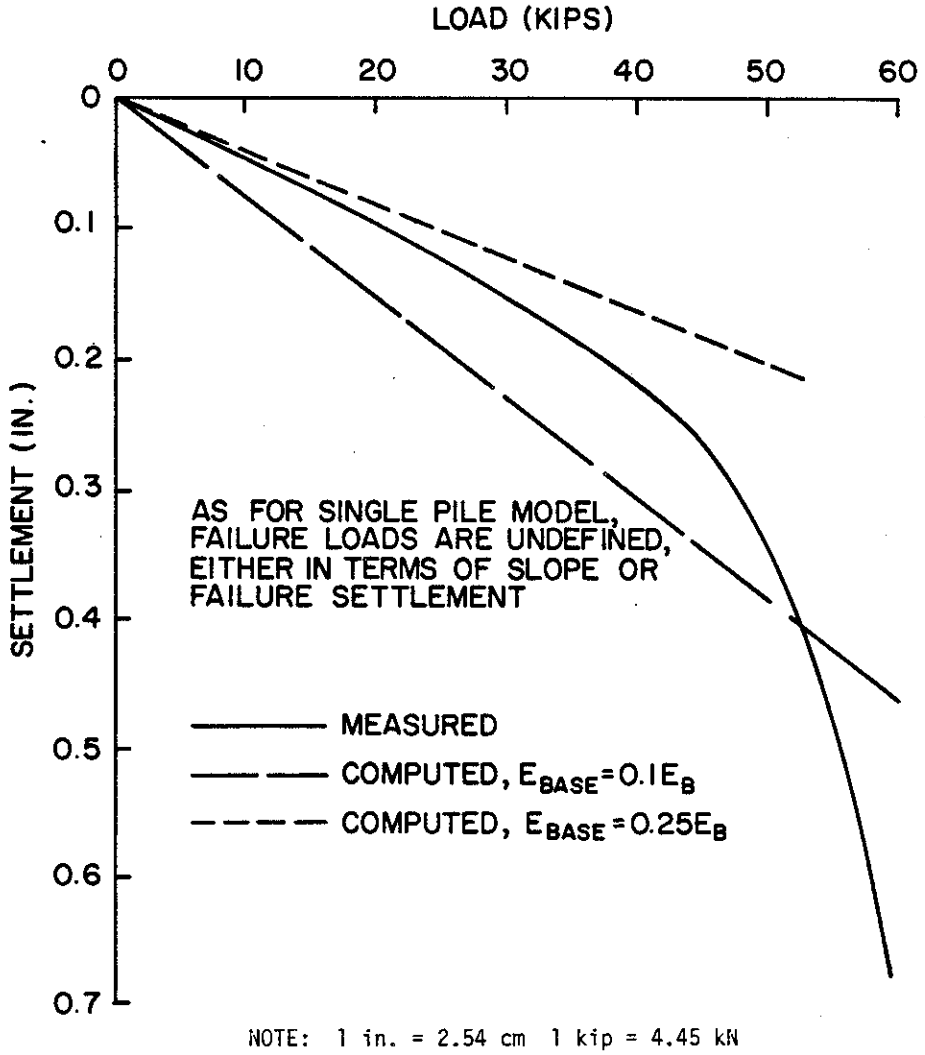

FIGURE 2.25. LOAD VS. SETTLEMENT, GROUP, ELASTIC SOLID (BOUNDARY ELEMENT) MODEL, VESIC TEST

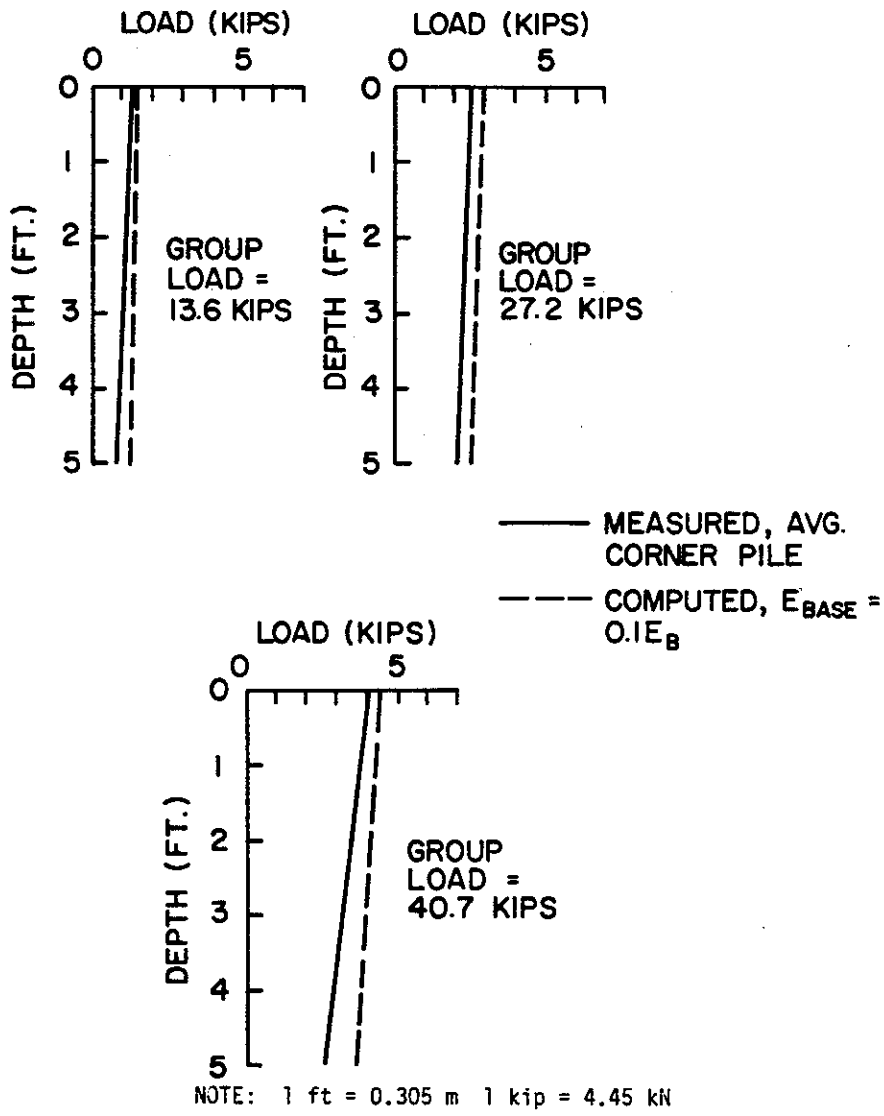

FIGURE 2.26. LOAD DISTRIBUTION RELATIONSHIPS, GROUP, CORNER PILES, HYBRID MODEL, VESIC TEST

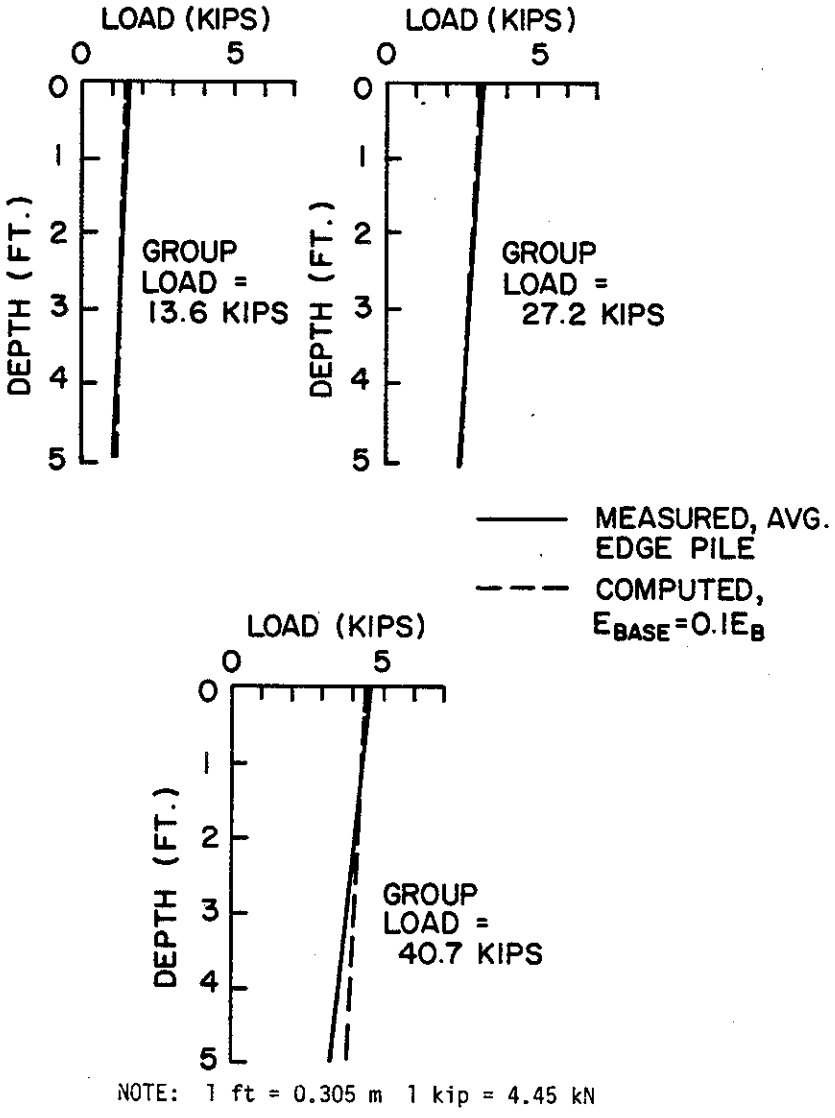

NOTE: 1 ft = 0.305 m 1 kip = 4.45 kN

FIGURE 2.27. LOAD DISTRIBUTION RELATIONSHIPS, GROUP, EDGE PILES, HYBRID MODEL, VESIĆ TEST

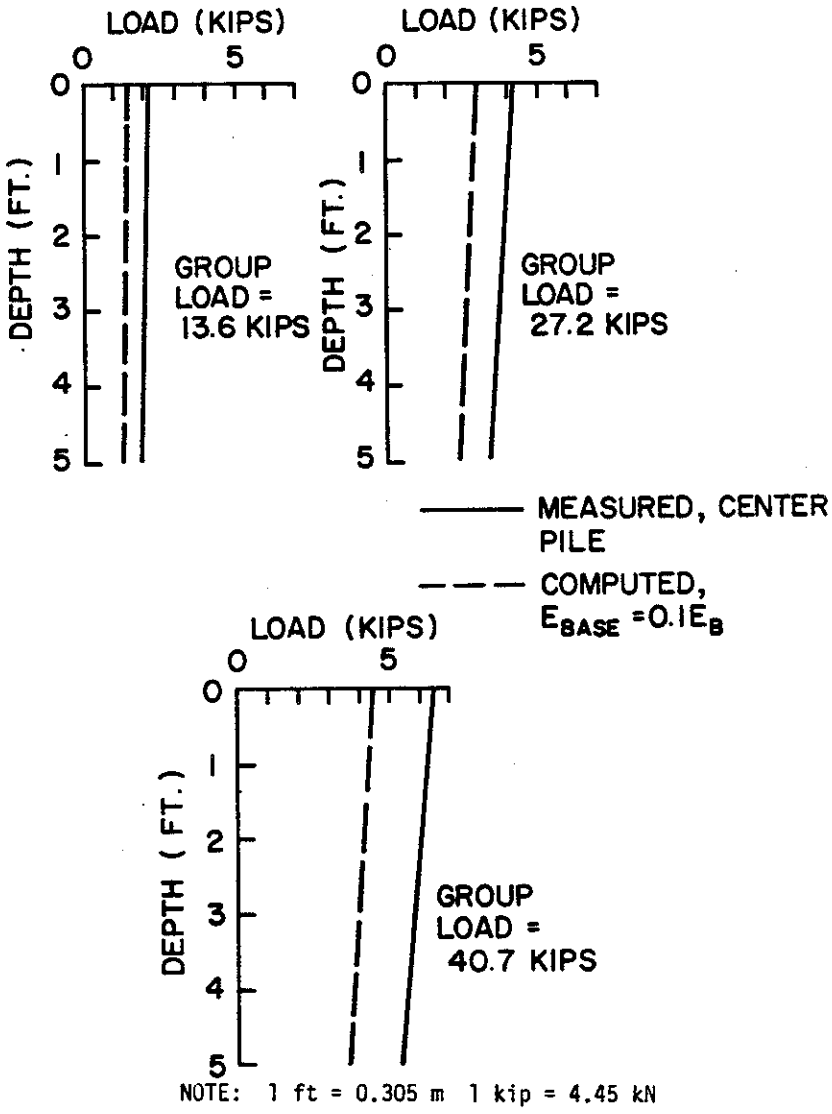

FIGURE 2.28. LOAD DISTRIBUTION RELATIONSHIPS, GROUP, CENTER PILE, HYBRID MODEL, VESIĆ TEST

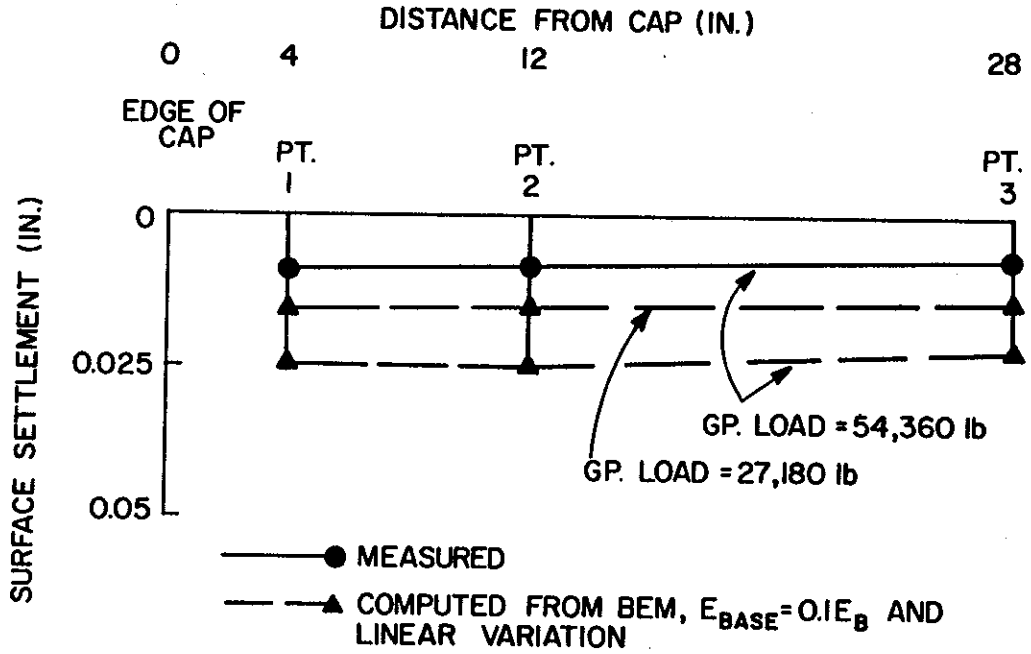

NOTE: 1 in. = 2.54 cm 1 lb = 4.45 N

FIGURE 2.29. SURFACE SETTLEMENTS, GROUP, ELASTIC SOLID AND BOUNDARY ELEMENT MODELS, VESIC TEST

TABLE 2.4. DISTRIBUTION OF LOAD TO PILE HEADS: VESIĆ 9 PILE GROUP; TEST P-93.

Applied Group Load (kips)	Method	Load on Corner Pile (kips)	Load on Edge Piles (kips)	Load on Center Pile (kips)
27.2	Hybrid	3.03	3.01	3.00
27.2	Elastic Solid	3.48	2.80	2.04
27.2	BEM	3.93	2.42	1.06
27.2	Measured	2.55(avg.)	3.20(avg.)	4.20
40.7	Hybrid	4.58	4.48	4.45
40.7	Elastic Solid	5.22	4.20	3.06
40.7	BEM	5.88	3.62	1.58
40.7	Measured	4.10(avg.)	4.45(avg.)	6.50

Note: Measured corner pile loads varied from avg - 13% to avg + 10%. Edge pile loads varied from avg - 12% to avg + 18%.

Hybrid Model: Adjusted f-z and Q-z curves, $E_{BASE} = 0.1\ E_B$

Elastic Solid Poulos Model: $E_{BASE} = E_B$; $E_s = 0.1\ E_{BASE}$

Elastic Solid (BEM): General solution for any "Gibson" soil, or soil with linearly increasing elastic modulus.

Finite Element Model solutions were unavailable for Gibson soil.

Note: 1 kip = 4.45 kN

TABLE 2.5. COMPUTED AND REPORTED "EFFICIENCIES" FROM VESIĆ TEST P-93

Failure Criterion	Single Pile Failure Load (kips) (P-13)			Group Failure Load (kips) (P-93)			Group Efficiency			
	H	ES	M	H	ES	M	H	ES	M	F
0.05 in./ton	5.0	*	4.5	43.3	*	52.7	0.97	*	1.30	
(0.05 in./$\sqrt{N}$)/ton	5.0	*	4.5	35.8	*	41.7	0.80	*	1.03	
MDFL	4.9	5.0	4.6	42.5	45.0	47.0	0.96	1.0	1.11	
Measured (Interp. by Investigator)	-	-	5.0	-	-	54.3	-	-	1.21	0.72

*Undefined due to trilinear nature of curve
H - Hybrid Method curve
ES - Elastic Solid (Poulos) Method curve
M - Measured
F - Feld's Rule

Note: 1 in. = 2.54 cm
1 kip = 4.45 kN
1 ton = 8.9 kN

Schlitt Test

All piles were installed by driving. The load test was of the maintained load type. The loading that was modeled was the second of two loadings, since the first loading had to be aborted due to a malfunction of the loading system. All adjustments to the load transfer functions were made to affect a reasonable match with the reloading relationships for the reference pile, rather than the virgin loading relationships.

Testing of the reference pile (Pile No. 1 in the eventual group) started six days after it was driven, and the reloading test occurred from nine to twelve days after installation. Pile No. 9 had been driven prior to No. 1. After Pile No. 1 had been tested, the remaining piles were driven in the sequence 6, 7, 2, 8, 5, 4, 3. The reload test on the group took place from 17 to 28 days after the last seven piles were driven. The pile cap consisted of a steel frame, suspended off the ground, which was not rigid. Load transfer relationships were measured for seven of the nine piles. Comparisons of measured and computed load transfer curves are shown in the following figures for typical piles.

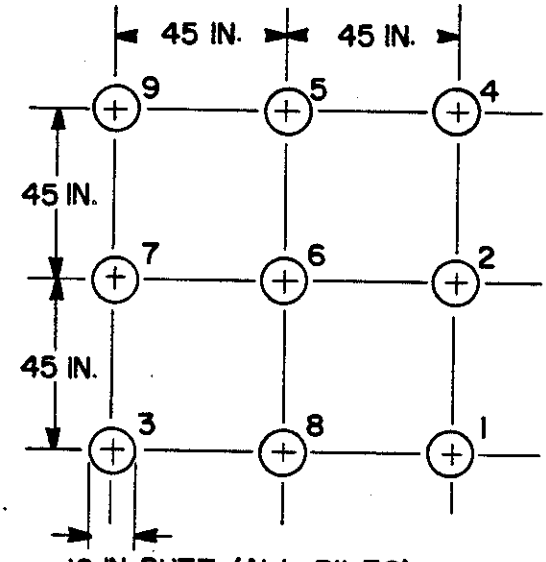

ALL PILES FLUTED MONOTUBE STEEL, WITH 0.25 IN. WALL, EXCEPT 8, WHICH HAD 9 GAGE SHELL. PILES 7 AND 9 WERE CONCRETE FILLED. STRAIN GAGES ON ALL BUT 8 AND 9 AT 5 FT. INTERVALS.

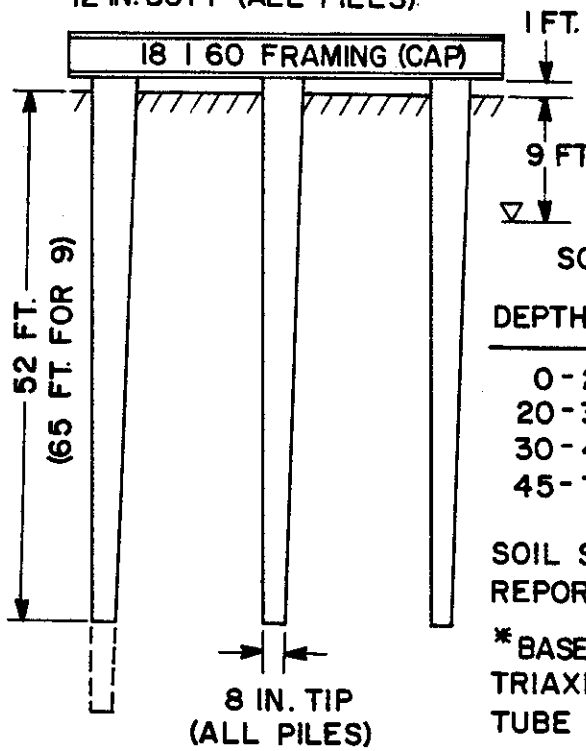

SOIL PROFILE (CL)

DEPTH (FT.)	C_U^* (PSI)	I_P	γ_D (PCF)
0 - 20	5.6	20	87
20 - 30	4.2	18	87
30 - 45	5.6	20	87
45 - 72	9.7	10	92

SOIL SENSITIVITY NOT REPORTED

*BASED ON Q-TYPE TRIAXIAL TESTS FROM TUBE SAMPLES

NOTE: 1 in. = 2.54 cm 1 ft = 0.305 m 1 psi = 6.89 kN/m^2 1 pcf = 0.157 kN/m^3

FIGURE 2.30. PILE GEOMETRY AND SOIL CONDITIONS, SCHLITT TEST

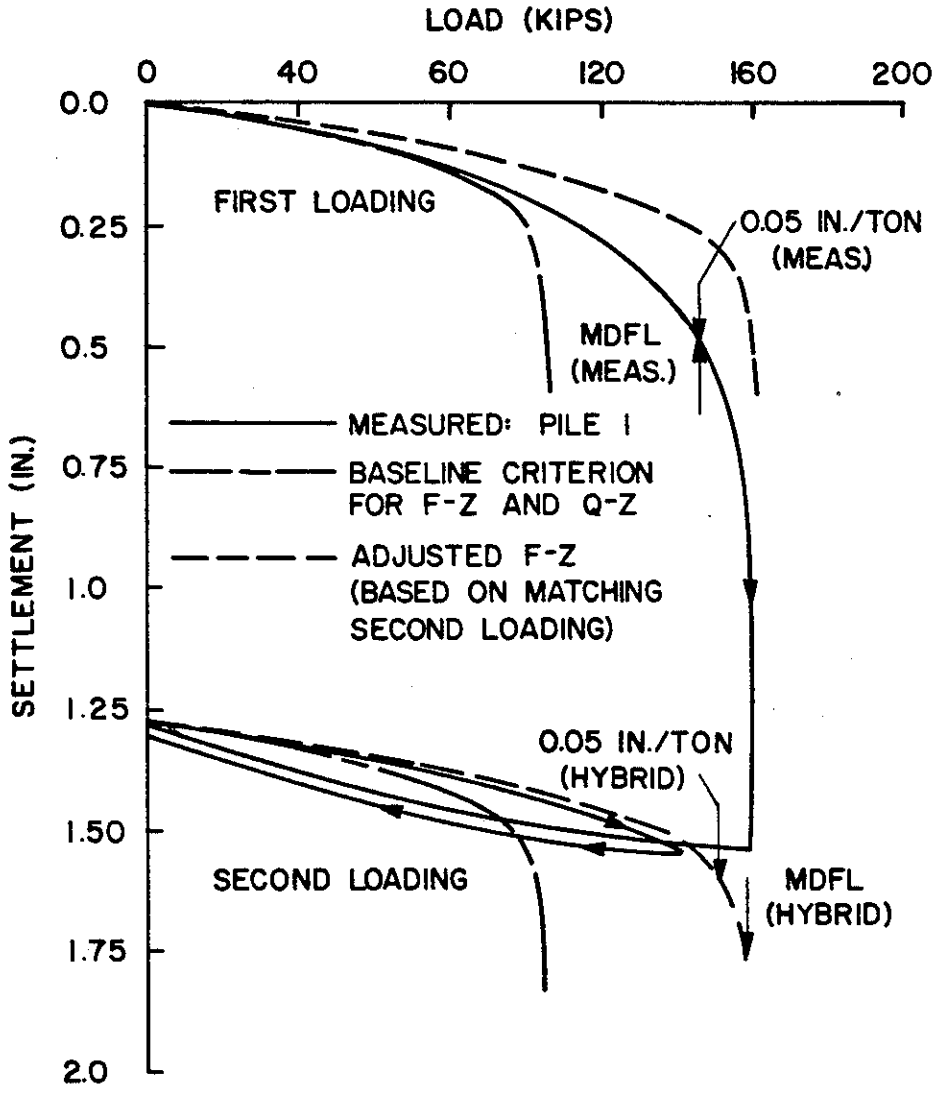

NOTE: 1 in. = 2.54 cm 1 kip = 4.45 kN 1 ton = 8.9 kN

FIGURE 2.31. LOAD VS. SETTLEMENT, REFERENCE PILE, HYBRID MODEL, SCHLITT TEST

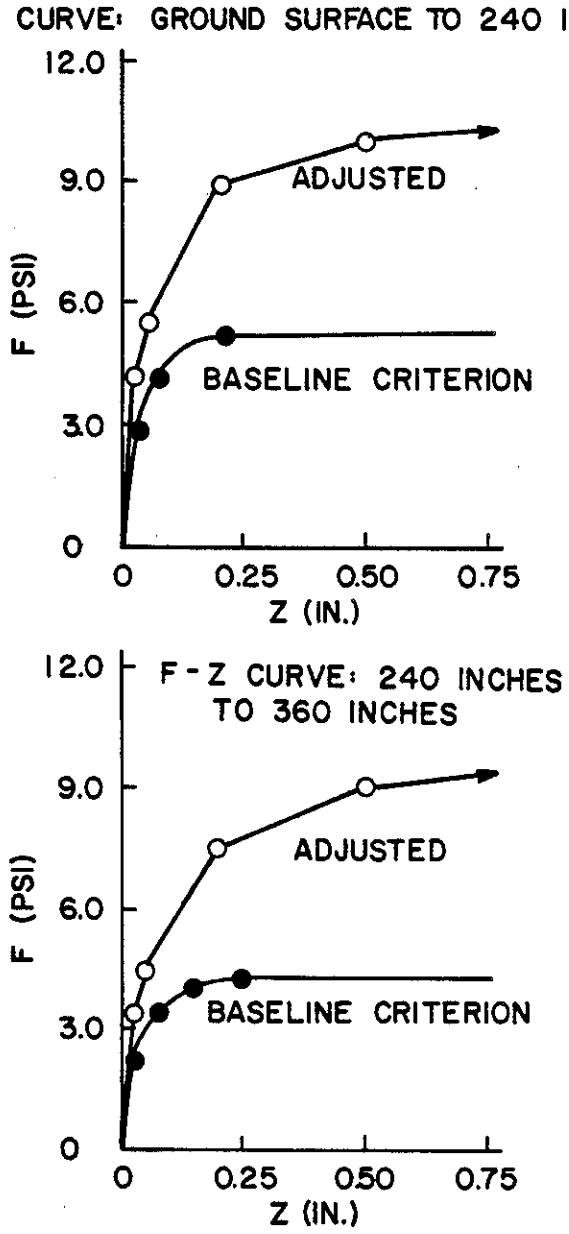

BASELINE CRITERION: $F_{MAX} = \lambda (2 c_{U_{AVG}} + \gamma H)$ WHERE λ IS A FUNCTION OF DEPTH DEFINED IN REF. 80.

NOTE: 1 in. = 2.54 cm 1 psi = 6.89 kN/m^2

FIGURE 2.32. F-Z RELATIONSHIPS, SCHLITT TEST

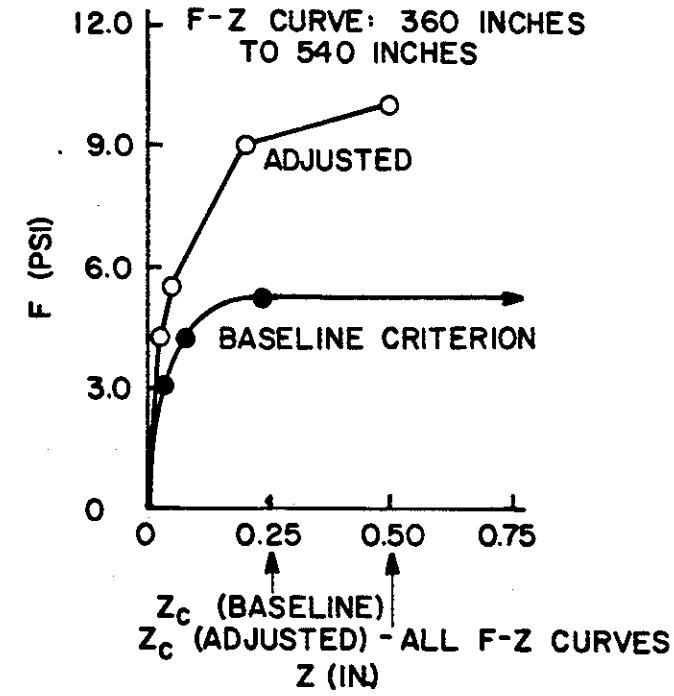

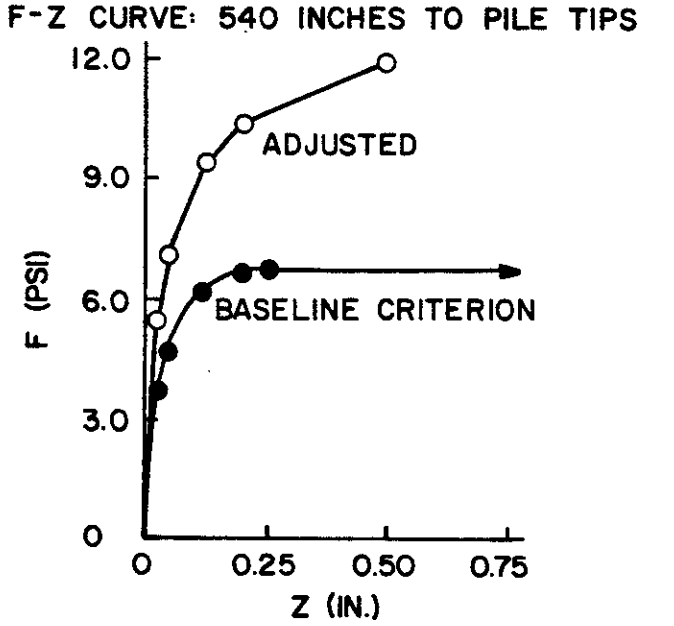

NOTE: 1 in. = 2.54 cm 1 psi = 6.89 kN/m^2

FIGURE 2.32. F-Z RELATIONSHIPS, SCHLITT TEST (CONT'D)

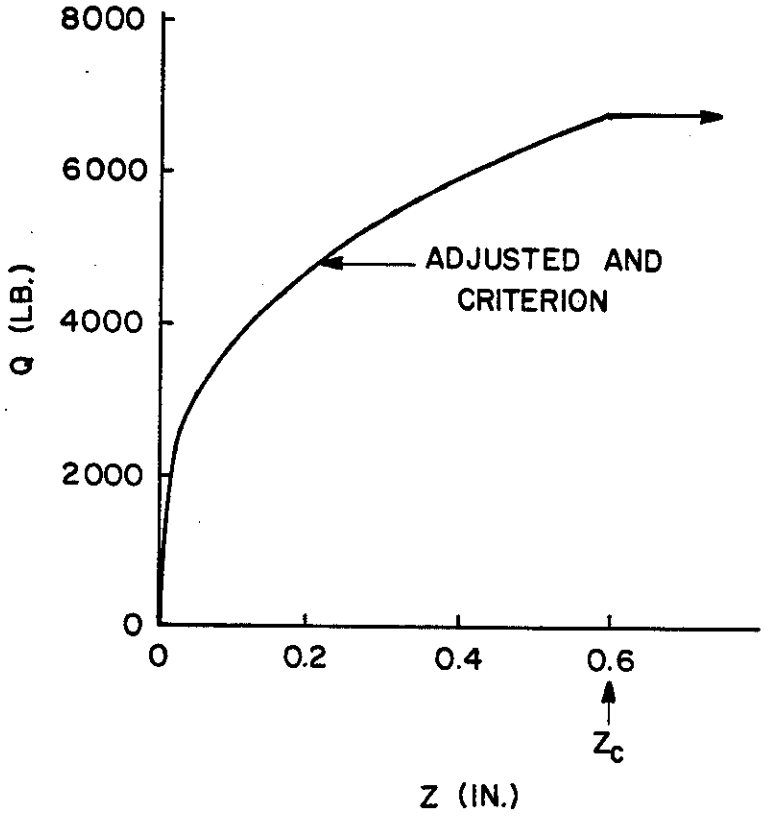

BASELINE CRITERION: $Q_{MAX} = 9\ c_u\ (A_B)$

NOTE: 1 in. = 2.54 cm 1 lb = 4.45 N

FIGURE 2.33. Q-Z RELATIONSHIP, SCHLITT TEST

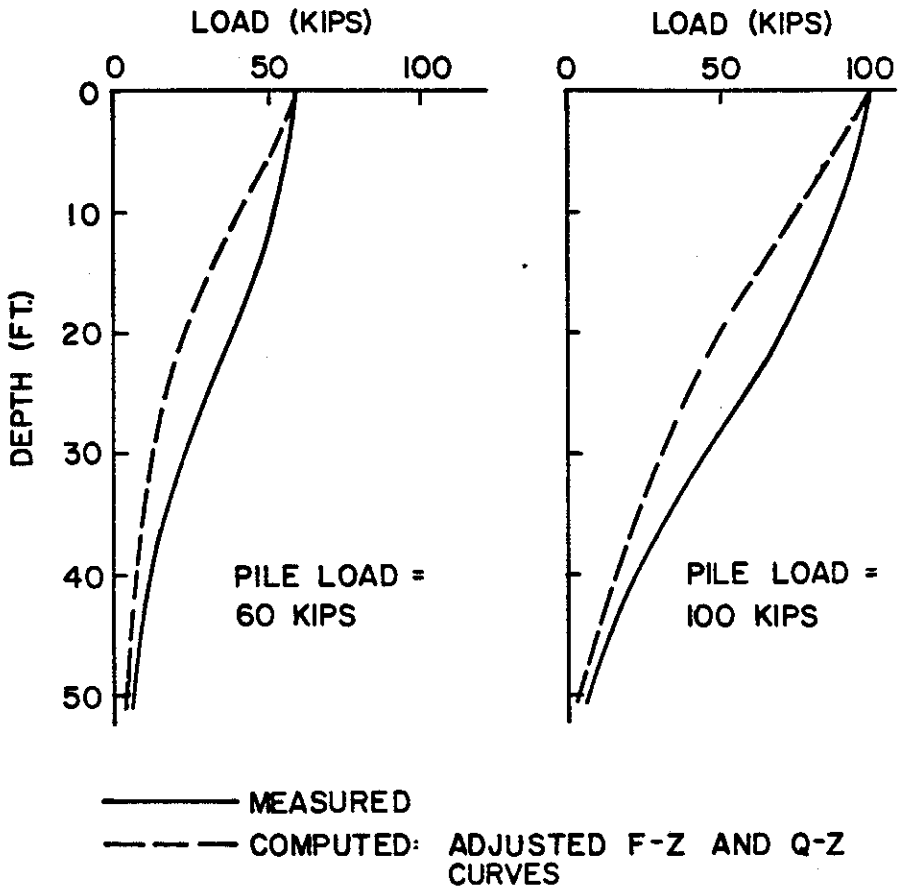

NOTE: 1 ft = 0.305 m 1 kip = 4.45 kN

FIGURE 2.34. LOAD DISTRIBUTION RELATIONSHIPS, REFERENCE PILE, HYBRID MODEL, SCHLITT TEST

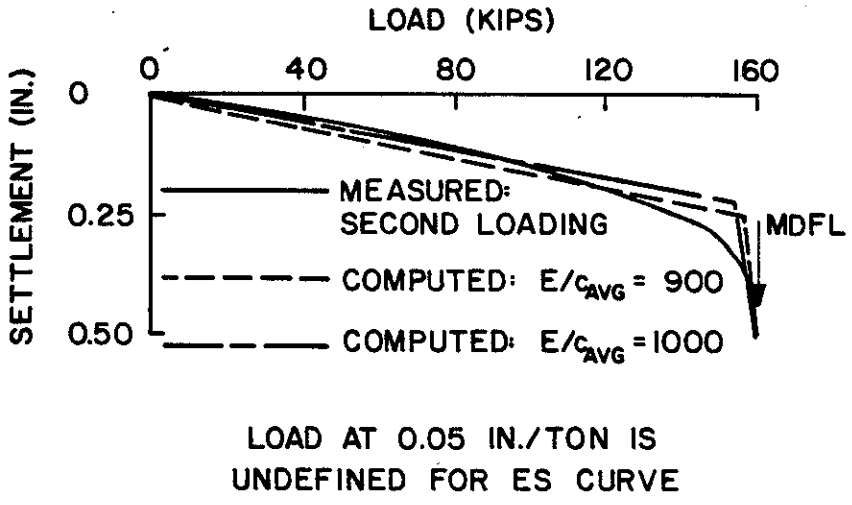

NOTE: 1 in. = 2.54 cm 1 kip = 4.45 kN 1 ton = 8.9 kN

FIGURE 2.35. LOAD VS. SETTLEMENT, REFERENCE PILE, ELASTIC SOLID MODEL, SCHLITT TEST

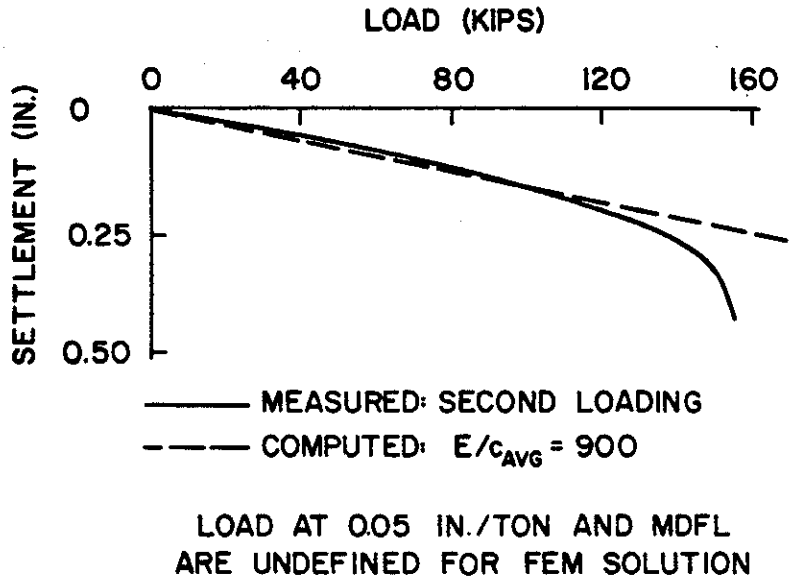

NOTE: 1 in. = 2.54 cm 1 kip = 4.45 kN 1 ton = 8.9 kN

FIGURE 2.36. LOAD VS. SETTLEMENT, REFERENCE PILE, FINITE ELEMENT MODEL, SCHLITT TEST (INCLUDES NON-EXISTENT CAP REACTION)

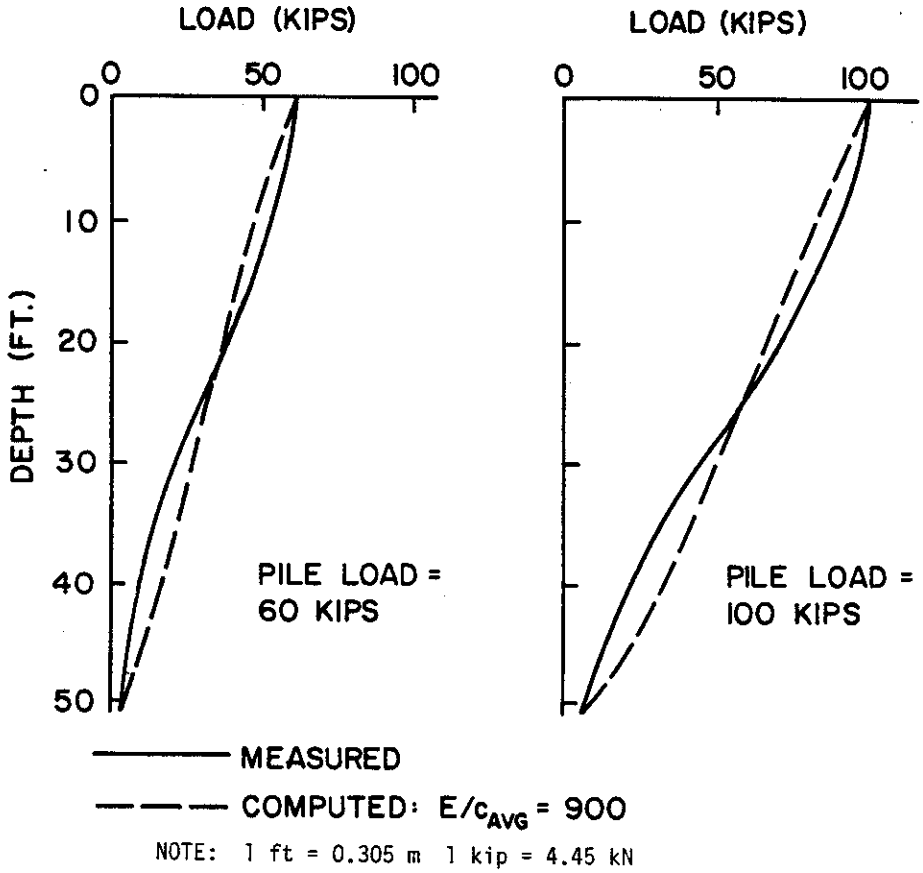

FIGURE 2.37. LOAD DISTRIBUTION RELATIONSHIPS, REFERENCE PILE, FINITE ELEMENT MODEL, SCHLITT TEST

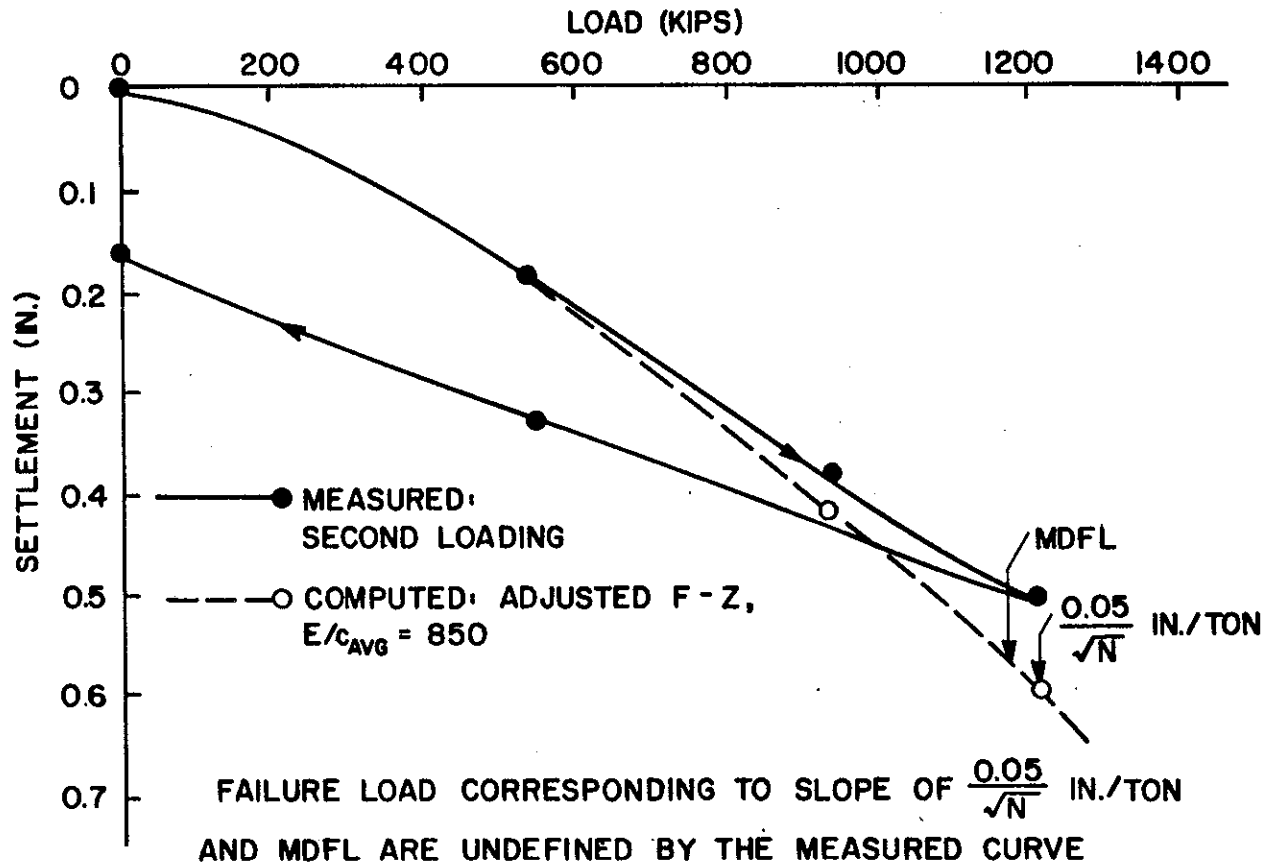

NOTE: 1 in. = 2.54 cm 1 kip = 4.45 kN 1 ton = 8.9 kN

FIGURE 2.38. LOAD VS. SETTLEMENT, GROUP, HYBRID MODEL, SCHLITT TEST

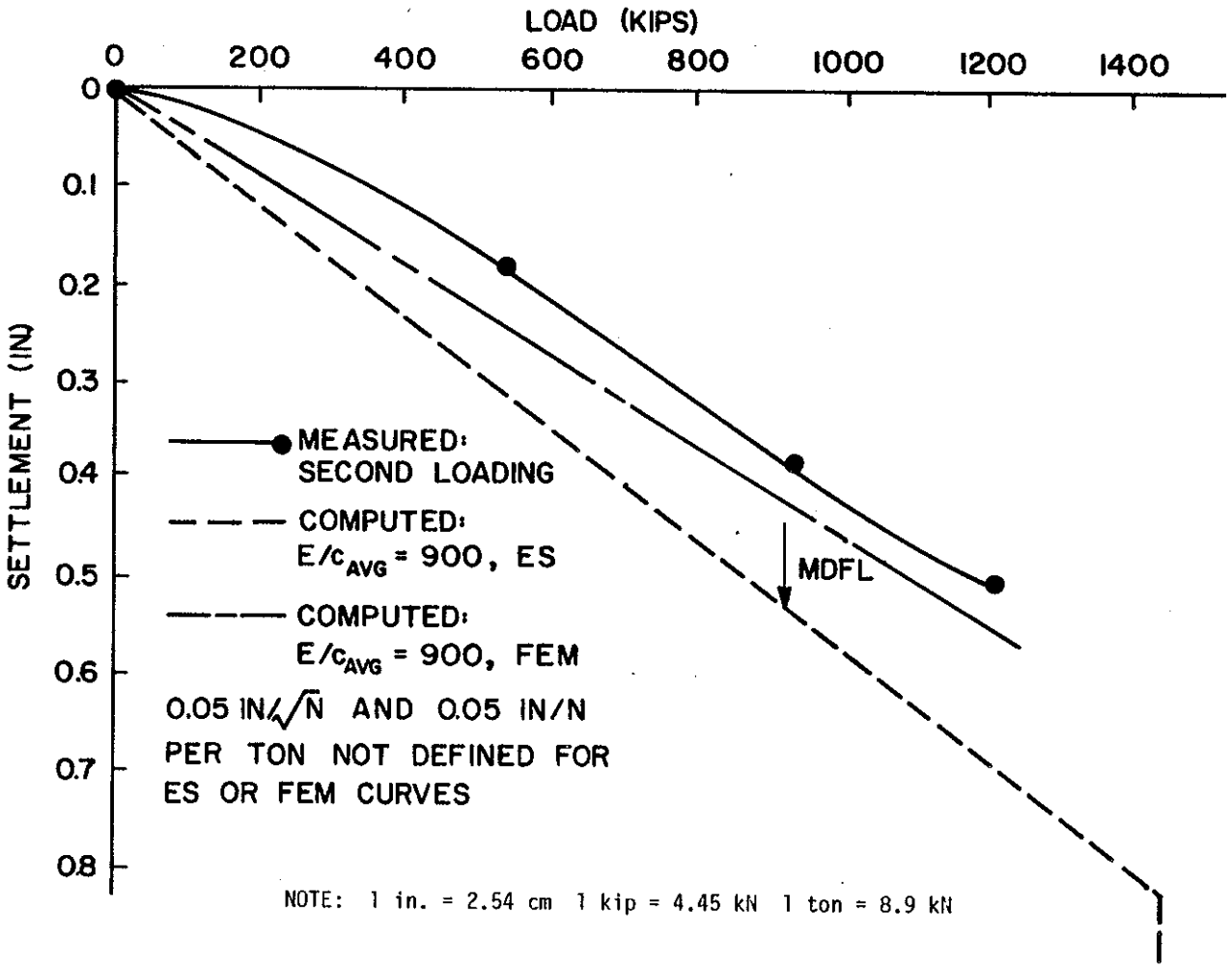

FIGURE 2.39. LOAD VS. SETTLEMENT, GROUP, ELASTIC SOLID AND FINITE ELEMENT MODELS, SCHLITT TEST

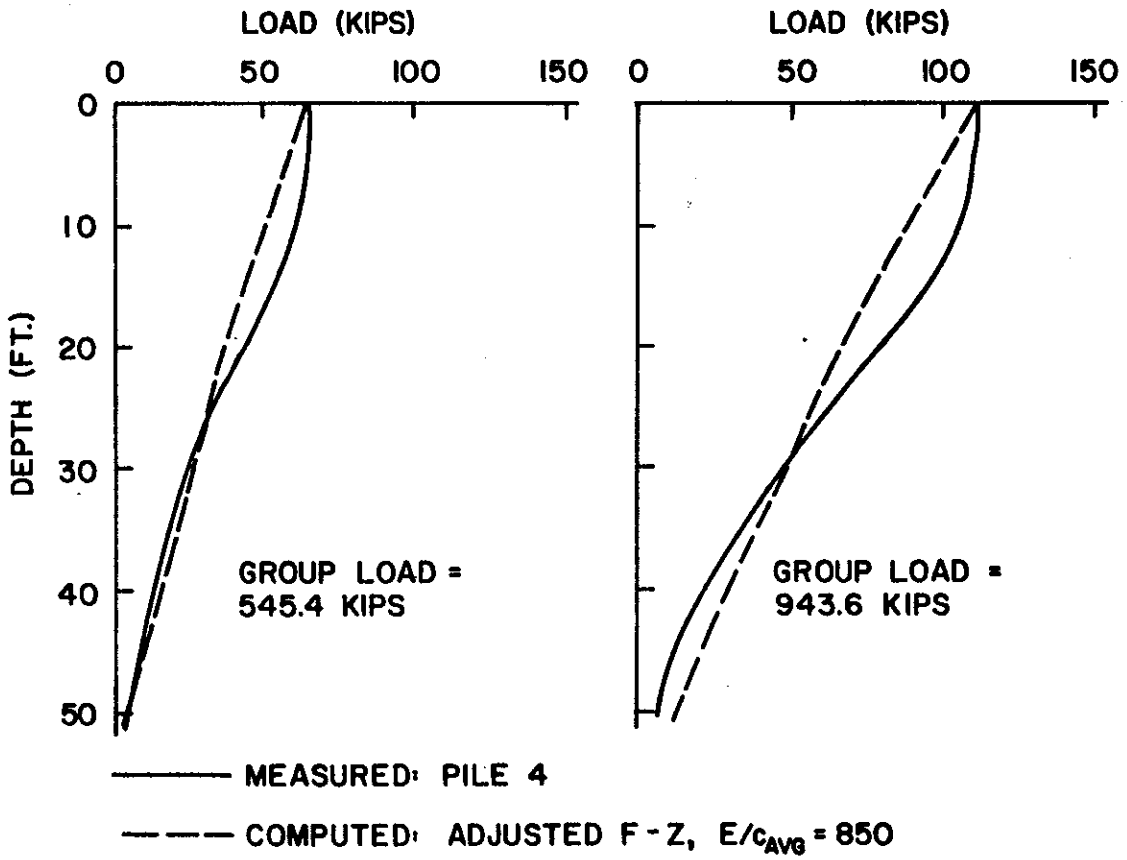

NOTE: 1 ft = 0.305 m 1 kip = 4.45 kN

FIGURE 2.40. LOAD DISTRIBUTION RELATIONSHIPS, GROUP, PILE NO. 4 (CORNER), HYBRID MODEL, SCHLITT TEST

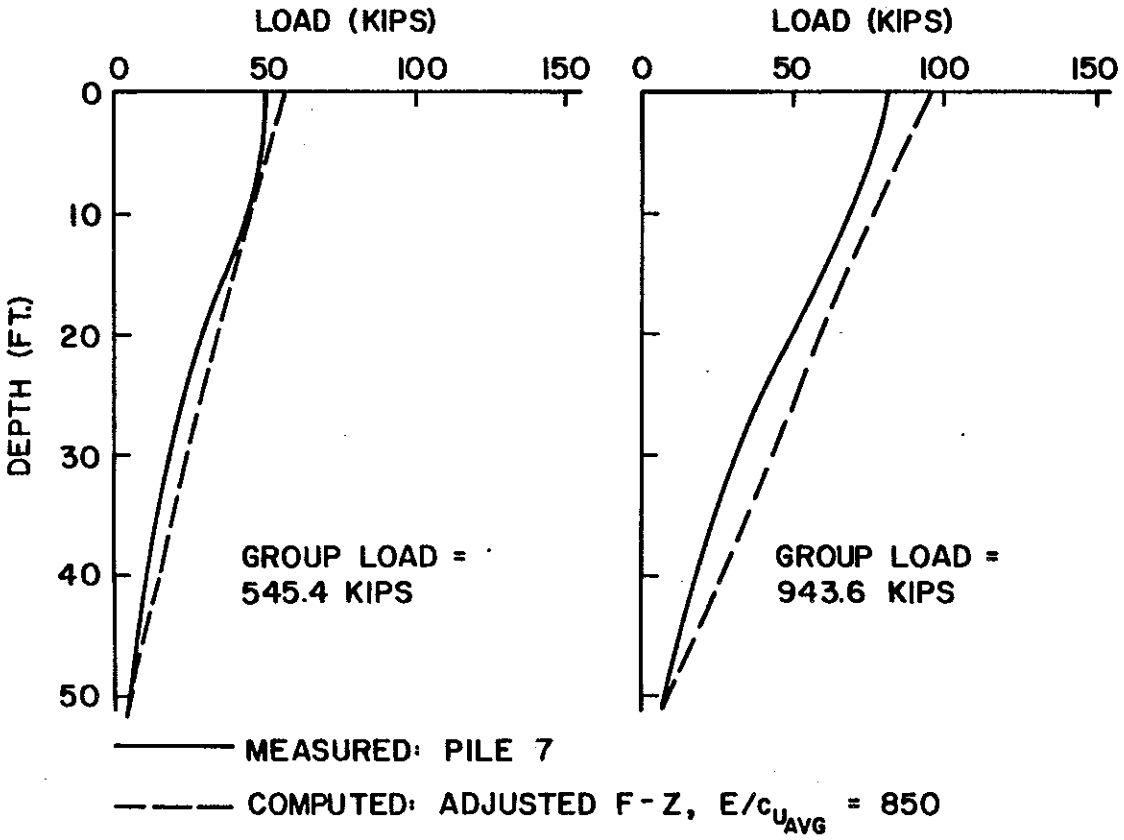

NOTE: 1 ft = 0.305 m 1 kip = 4.45 kN

FIGURE 2.41. LOAD DISTRIBUTION RELATIONSHIPS, GROUP, PILE NO. 7 (EDGE), HYBRID MODEL, SCHLITT TEST

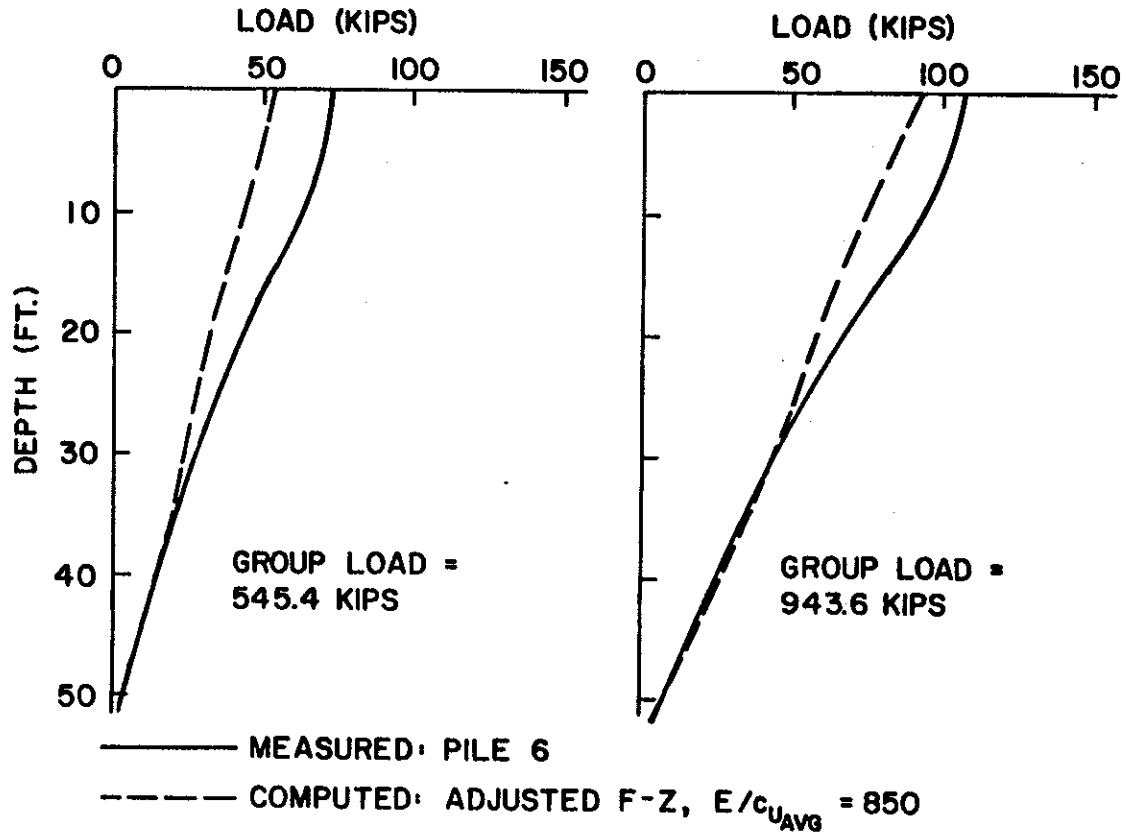

NOTE: 1 ft = 0.305 m 1 kip = 4.45 kN

FIGURE 2.42. LOAD DISTRIBUTION RELATIONSHIPS, GROUP, PILE NO. 6 (CENTER), HYBRID MODEL, SCHLITT TEST

TABLE 2.6. DISTRIBUTION OF LOADS TO PILE HEADS: SCHLITT 9 PILE GROUP

Applied Group Load (kips)	Method	Load on Individual Piles (kips) 1	2	3	4	5	6	7	8	9
545.4	Hybrid	66.2	58.2	63.8	63.8	56.1	54.3	56.1	58.2	68.9
545.4	Elastic Solid	74.6	53.3	74.6	74.6	53.3	33.6	53.3	53.3	74.6
545.4	FEM	*	*	*	*	*	*	*	*	*
545.4	Measured	60.0	77.6	59.0	65.2	42.0	74.4	50.4	43.2	73.6
943.6	Hybrid	115.8	100.3	110.4	110.4	95.5	92.9	95.5	100.3	122.5
943.6	Elastic Solid	129.0	92.3	129.0	129.0	92.3	58.2	92.3	92.3	129.0
943.6	FEM	*	*	*	*	*	*	*	*	*
943.6	Measured	119.0	126.4	91.0	112.8	81.8	110.4	82.2	90.2	129.8
1216.2	Hybrid	166.3	115.2	158.5	158.5	111.7	107.7	111.7	115.2	171.4
1216.2	Elastic Solid	166.3	119.0	166.3	166.3	119.0	75.0	119.0	119.0	166.3
1216.2	FEM	*	*	*	*	*	*	*	*	*
1216.2	Measured	154.8	154.0	116.2	150.2	120.4	130.8	93.8	124.8	171.2

*Solution for cap suspended off ground not published
Hybrid Model: Adjusted f-z curves, E/c_u = 850, Extra length on No. 9 modeled
Elastic Solid Model: E/c_u = 900, Extra length on No. 9 not modeled

Note: 1 kip = 4.45 kN

TABLE 2.7 COMPUTED AND MEASURED "EFFICIENCIES" FROM SCHLITT'S TEST

Failure Criterion	Single Pile Failure Load (kips) (Pile No.1)			Group Failure Load (kips)			Group Efficiency				
	H	ES	M	H	ES	M	H	ES	M	B	F
0.05 in./ton	142	-	146	*	-	>1216*	-	-	-		
(0.05 in./$\sqrt{N}$)/ton	142	-	146	1210	-	>1216*	0.95	-	>0.93		
MDFL	159	160	147	1180	930	>1216*	0.82	0.65	>0.92		
										1.70***	0.72

*Beyond limits of curve; therefore, undefined
**Failure did not occur according to criteria investigated
***Based on single pile failure = 146.5 kips (avg of 0.05 in./ton and MDFL)

H - Hybrid method curve
ES - Elastic solid method curve
M - Measured
B - Block (equivalent pier) failure
F - Feld's Rule

Note: 1 in. = 2.54 cm
1 kip = 4.45 kN
1 ton = 8.9 kN

Koizumi and Ito Test

All piles in this test were installed by jacking in sequence in rows: top row, middle row, bottom row, from right to left. The load tests were conducted about eight months after the piles had been installed, following a series of vibratory tests. Load testing was of the cyclic, quick maintained load type, and the reported measured load-settlement curves were envelopes to the cyclic curves. The cap was in contact with the ground but its reaction was less than ten per cent of the total reaction until after failure of the piles reportedly occurred. Measured load-settlement curves have had the cap reaction deducted from the load value. The finite element solution includes the effect of cap-soil contact, while the hybrid and elastic solid solutions do not.

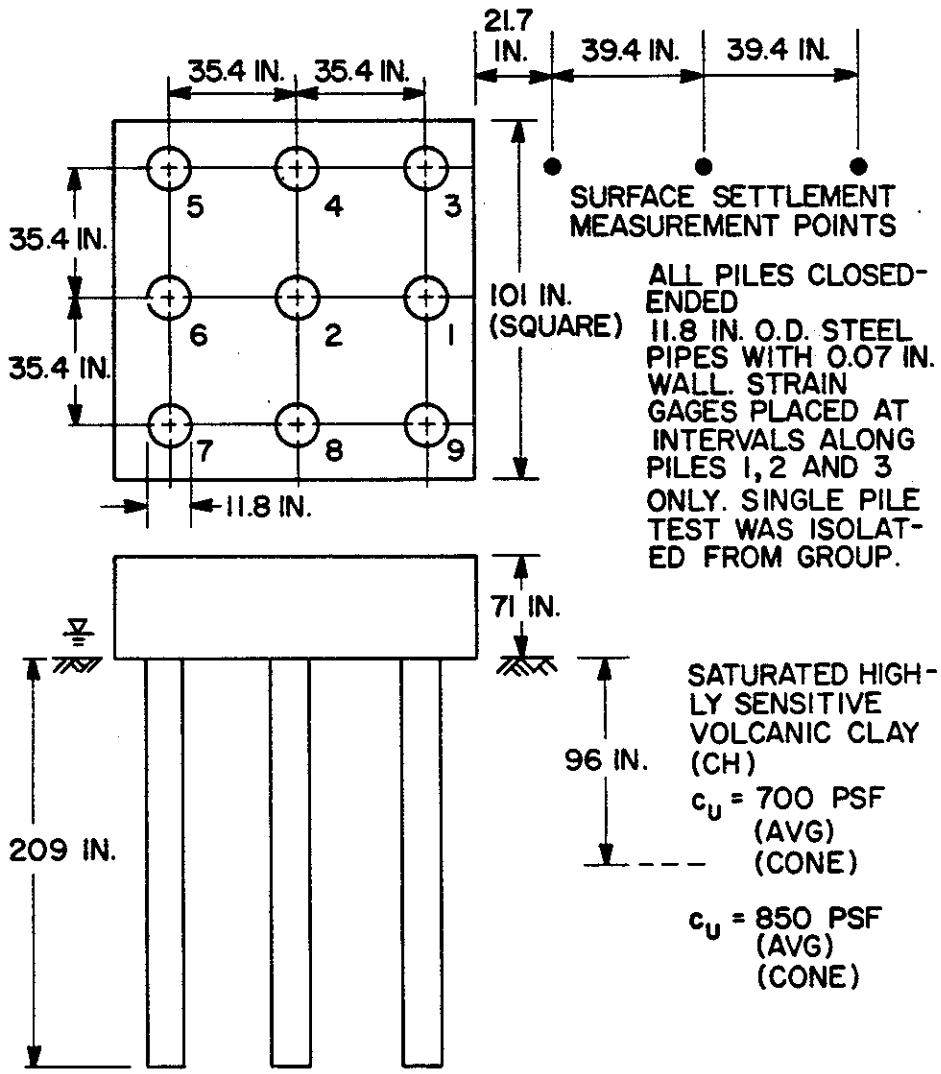

NOTE: 1 in. = 2.54 cm 1 psf = 47.9 N/m^2

FIGURE 2.43. PILE GEOMETRY AND SOIL CONDITIONS, KOIZUMI AND ITO TEST

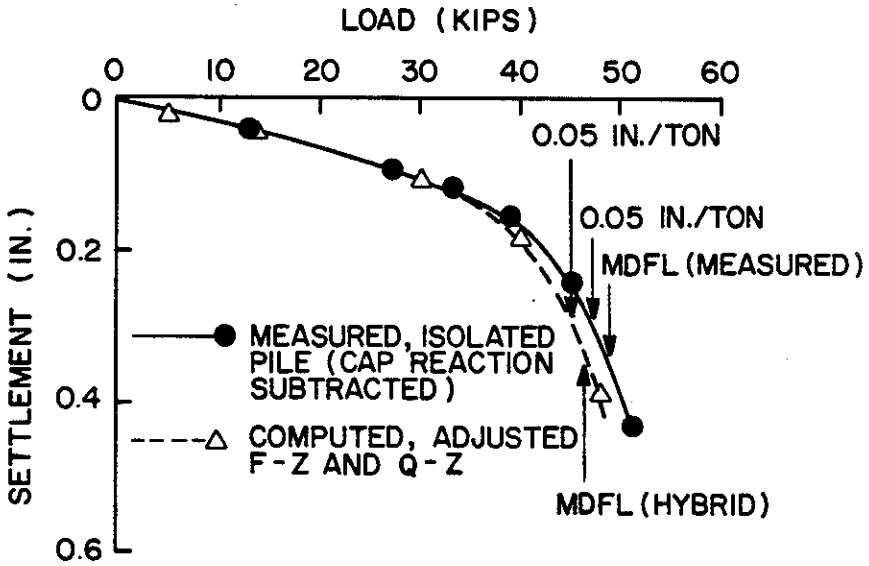

NOTE: 1 in. = 2.54 cm 1 kip = 4.45 kN 1 ton = 8.9 kN

FIGURE 2.44. LOAD VS. SETTLEMENT, REFERENCE PILE, HYBRID MODEL, KOIZUMI AND ITO TEST

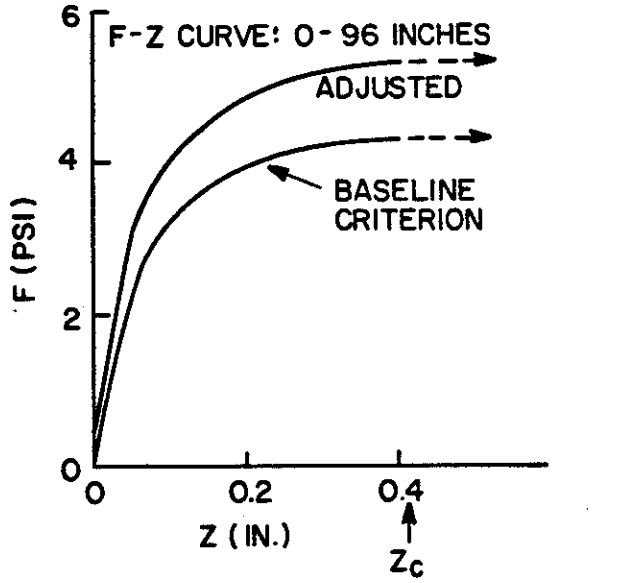

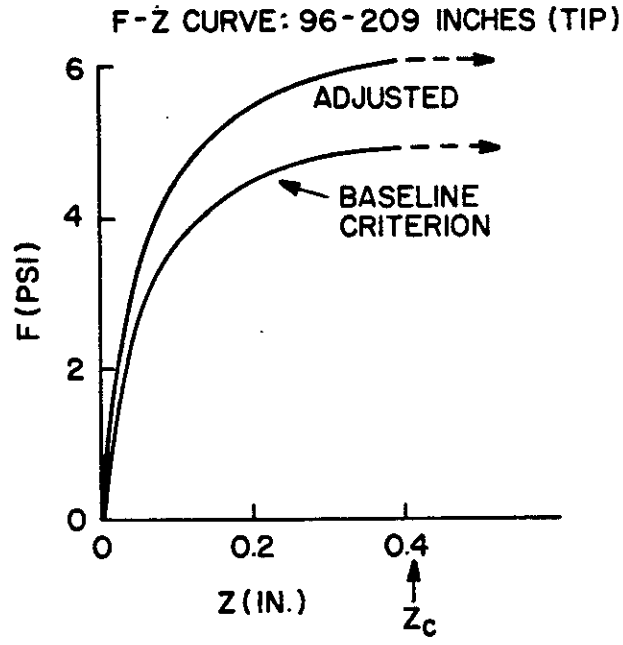

BASELINE CRITERION: $F_{MAX} = \alpha c_U$, WHERE $\alpha = 0.90$ FOR 0-96 IN. AND 0.82 FOR 96-209 IN.

NOTE: 1 in. = 2.54 cm 1 psi = 6.89 kN/m^2

FIGURE 2.45. F-Z RELATIONSHIPS, KOIZUMI AND ITO TEST

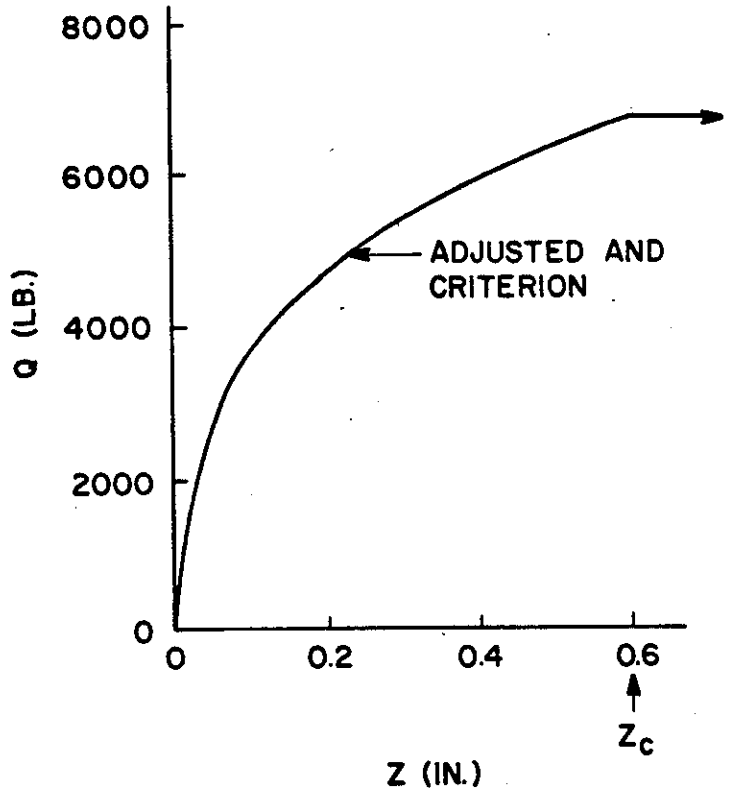

BASELINE CRITERION: $Q_{MAX} = 9\ c_{U_{BASE}}\ (A_B)$

NOTE: 1 in. = 2.54 cm 1 lb = 4.45 N

FIGURE 2.46. Q-Z RELATIONSHIP, KOIZUMI AND ITO TEST

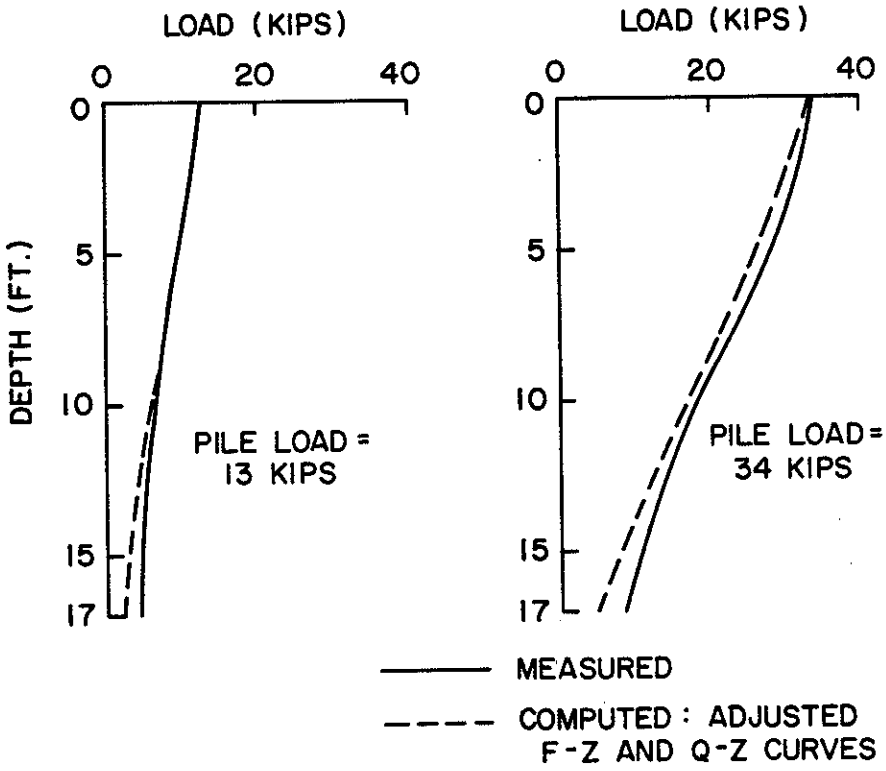

NOTE: 1 ft = 0.305 m 1 kip = 4.45 kN

FIGURE 2.47. LOAD DISTRIBUTION RELATIONSHIPS, REFERENCE PILE, HYBRID MODEL, KOIZUMI AND ITO TEST

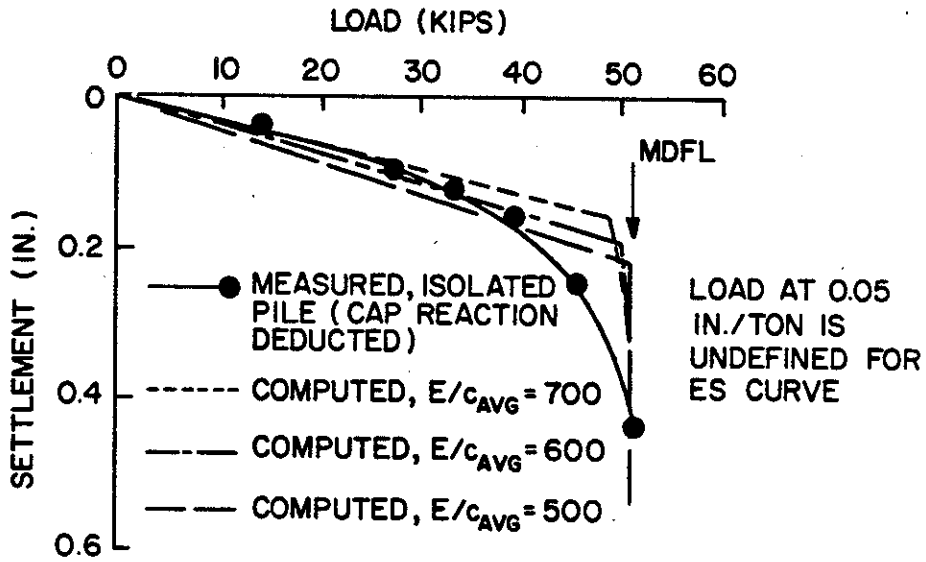

NOTE: 1 in. = 2.54 cm 1 kip = 4.45 kN 1 ton = 8.9 kN

FIGURE 2.48. LOAD VS. SETTLEMENT, REFERENCE PILE, ELASTIC SOLID MODEL, KOIZUMI AND ITO TEST

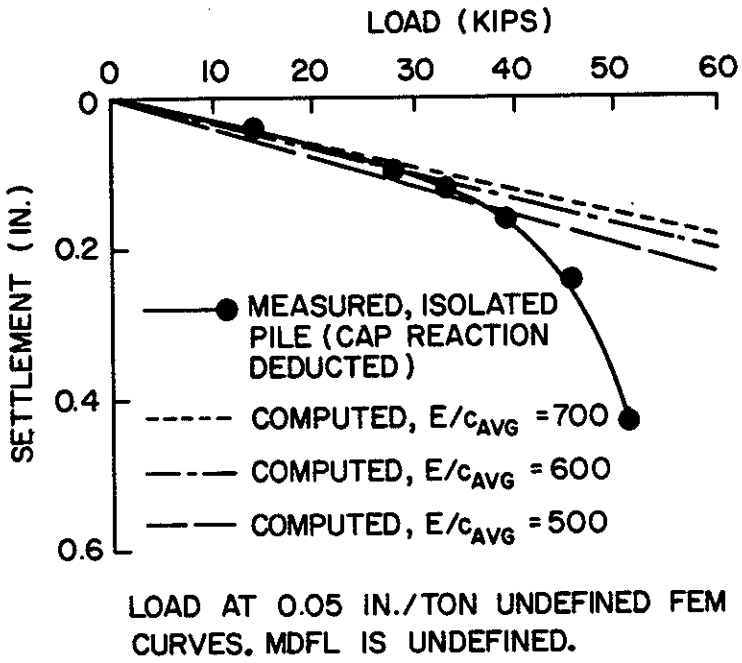

NOTE: 1 in. = 2.54 cm 1 kip = 4.45 kN 1 ton = 8.9 kN

FIGURE 2.49. LOAD VS. SETTLEMENT, REFERENCE PILE, FINITE ELEMENT MODEL, KOIZUMI AND ITO TEST

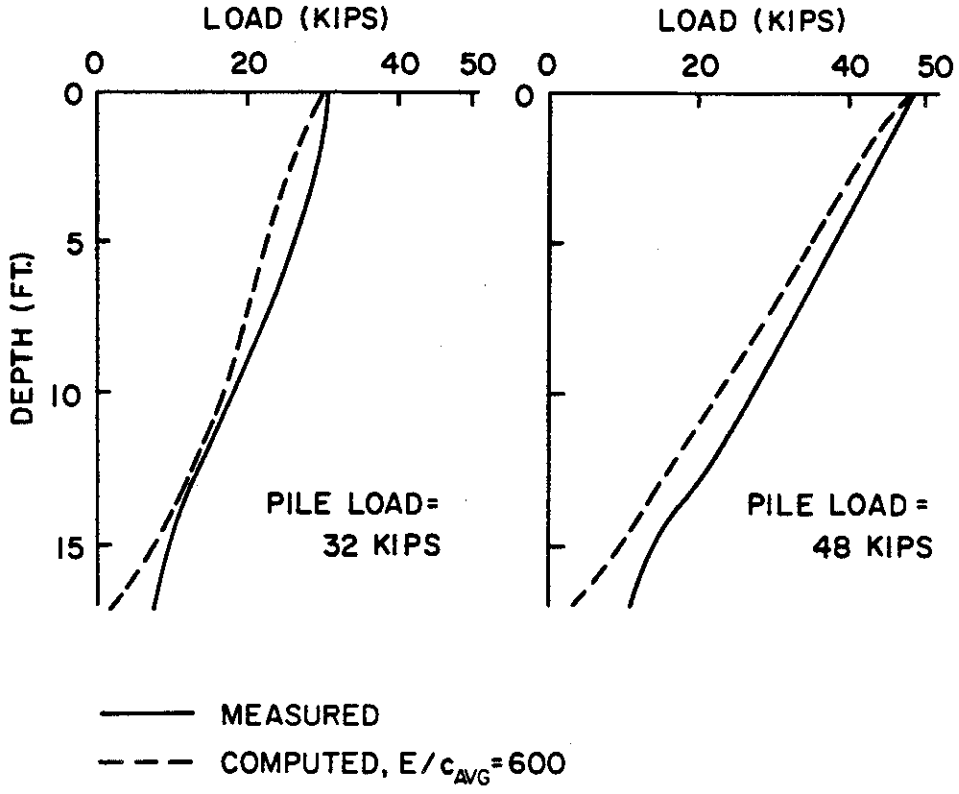

NOTE: 1 ft = 0.305 m 1 kip = 4.45 kN

FIGURE 2.50. LOAD DISTRIBUTION RELATIONSHIPS, REFERENCE PILE, FINITE ELEMENT MODEL, KOIZUMI AND ITO TEST

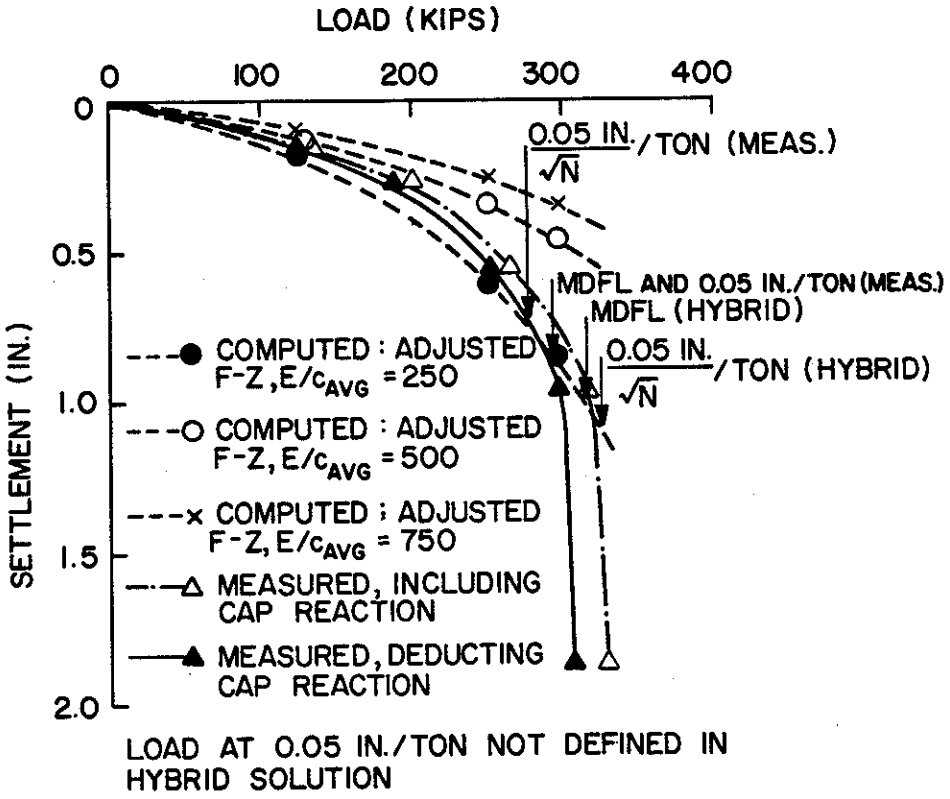

NOTE: 1 in. = 2.54 cm 1 kip = 4.45 kN 1 ton = 8.9 kN

FIGURE 2.51. LOAD VS. SETTLEMENT, GROUP, HYBRID MODEL, KOIZUMI AND ITO TEST

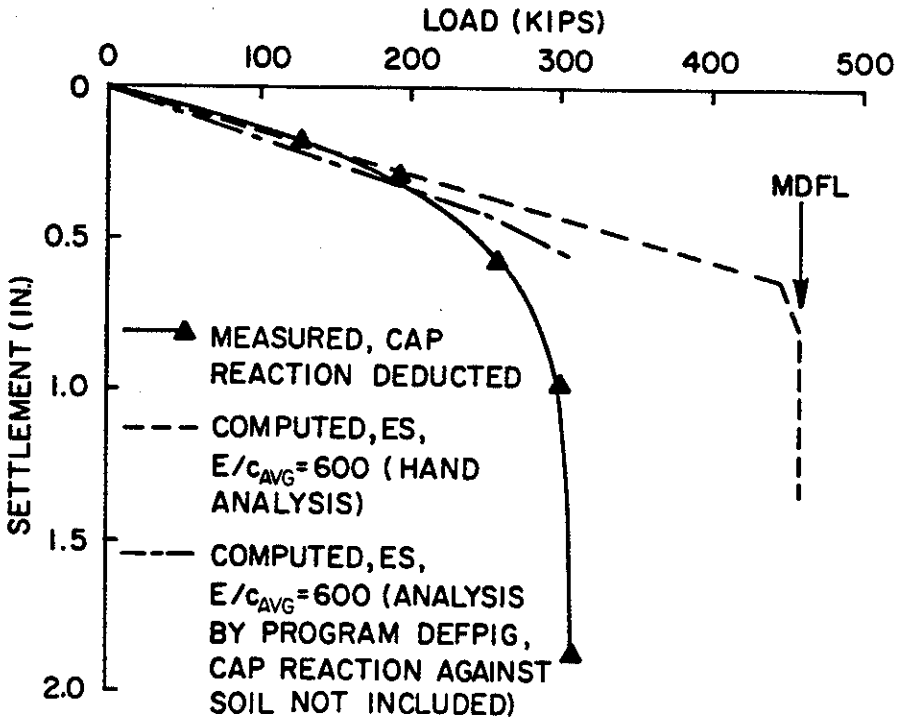

0.05 IN.$\sqrt{N}$ AND 0.05 IN. /N PER TON NOT DEFINED FOR EITHER ES CURVE.
MDFL IS UNDEFINED FOR DEFPIG SOLUTION.

NOTE: 1 in. = 2.54 cm 1 kip = 4.45 kN 1 ton = 8.9 kN

FIGURE 2.52. LOAD VS. SETTLEMENT, GROUP, ELASTIC SOLID MODEL, KOIZUMI AND ITO TEST

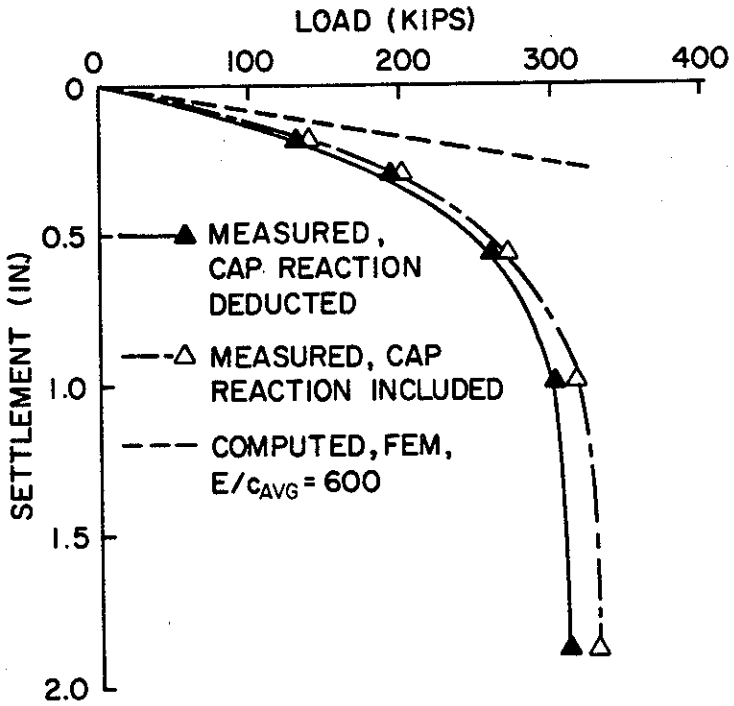

"FAILURE" LOADS ARE UNDEFINED WITH FEM SOLUTION.

NOTE: 1 in. = 2.54 cm 1 kip = 4.45 kN

FIGURE 2.53. LOAD VS. SETTLEMENT, GROUP, FINITE ELEMENT MODEL, KOIZUMI AND ITO TEST

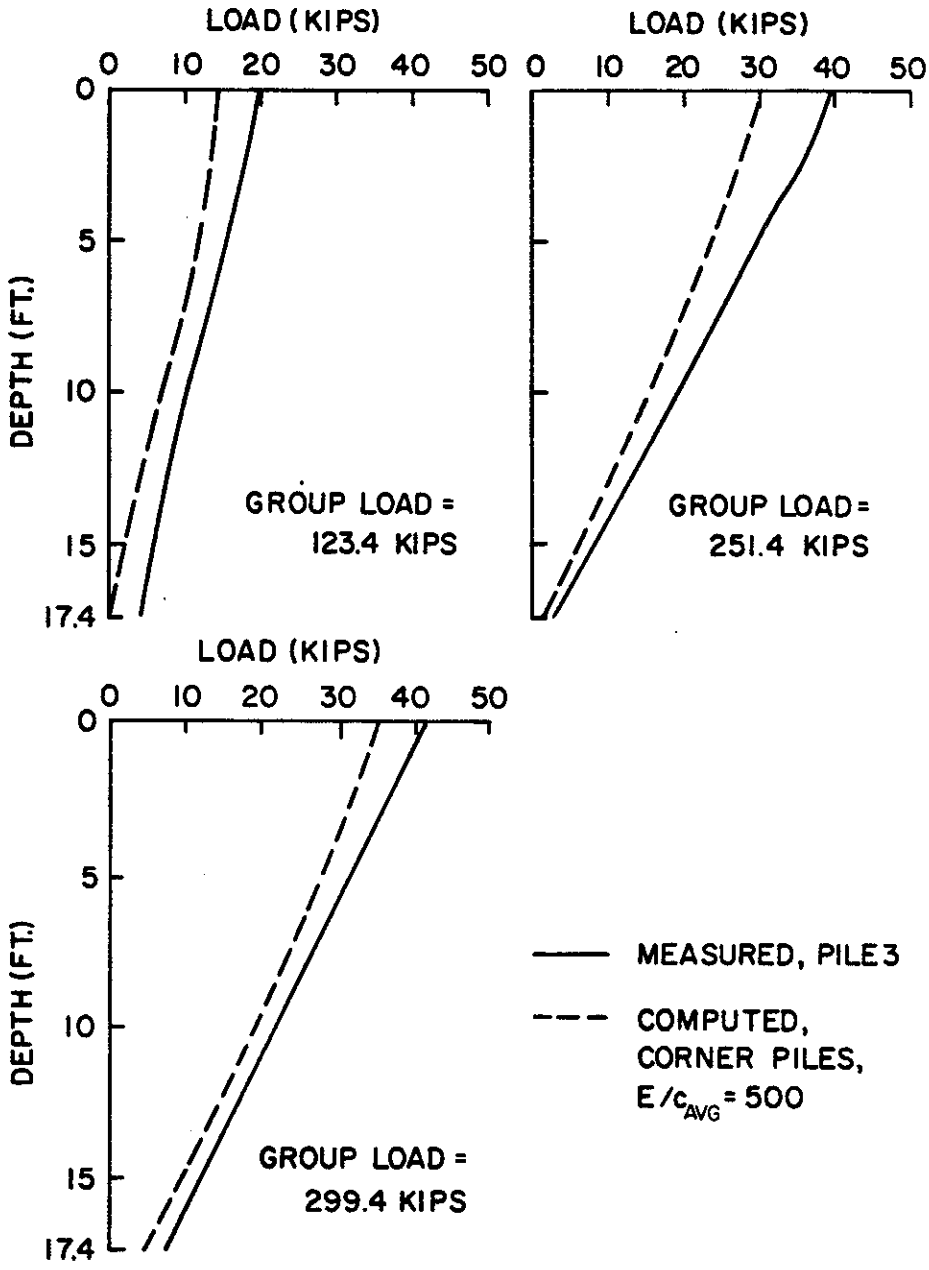

NOTE: 1 ft = 0.305 m 1 kip = 4.45 kN

FIGURE 2.54. LOAD DISTRIBUTION RELATIONSHIPS, GROUP, PILE 3 (CORNER), HYBRID MODEL, KOIZUMI AND ITO TEST

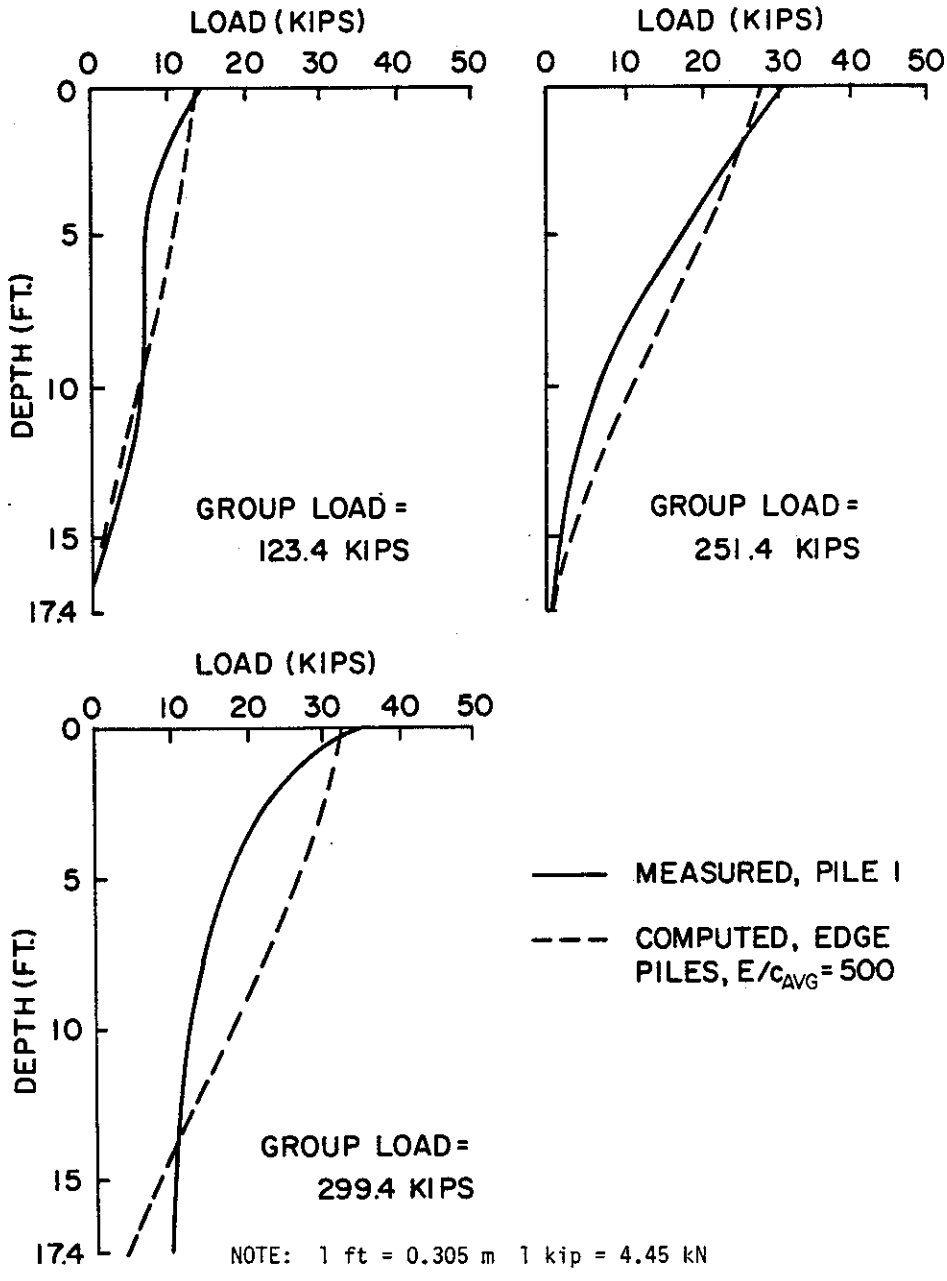

FIGURE 2.55. LOAD DISTRIBUTION RELATIONSHIPS, GROUP, PILE 1 (EDGE), HYBRID MODEL, KOIZUMI AND ITO TEST

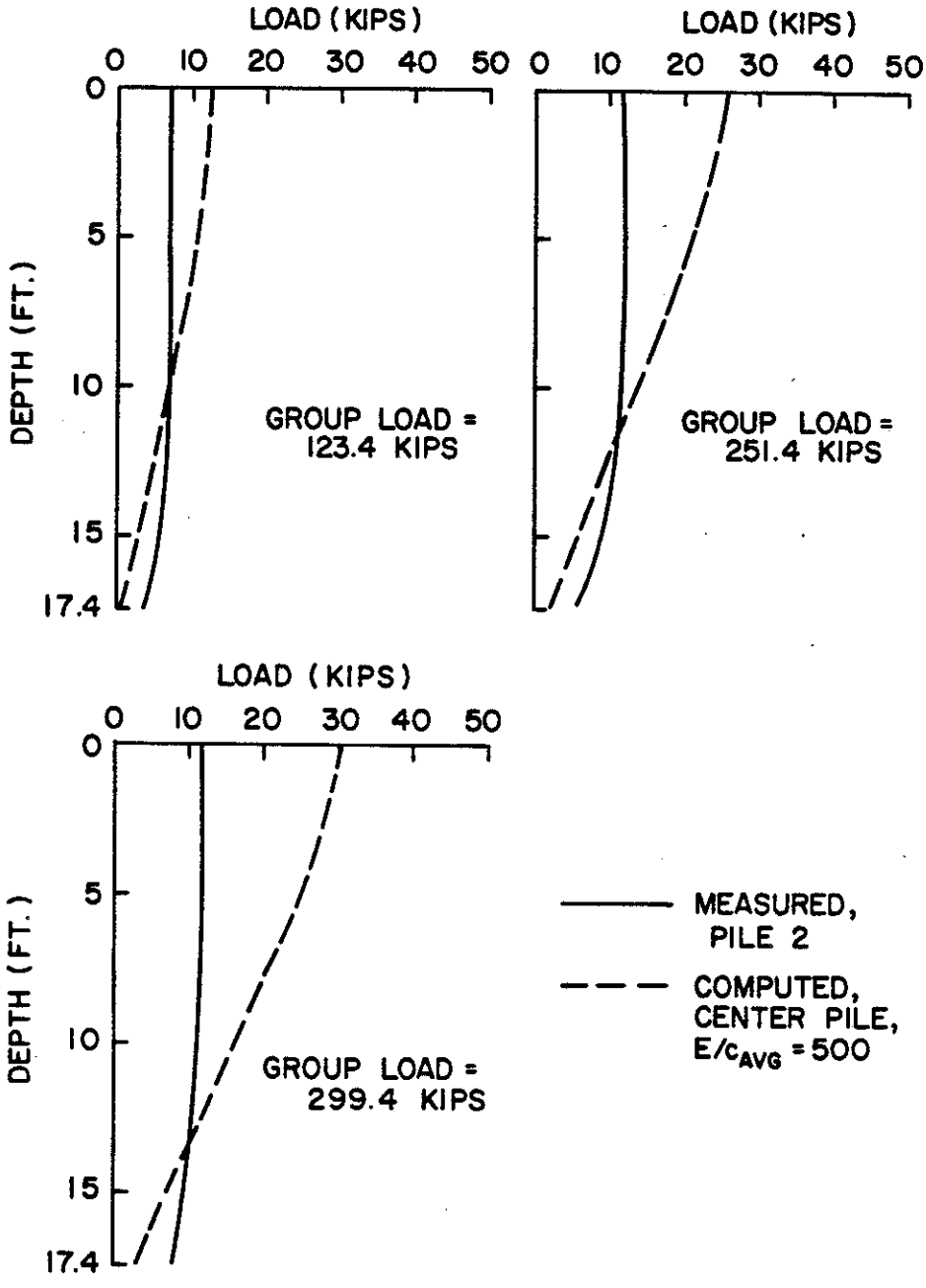

NOTE: 1 ft = 0.305 m 1 kip = 4.45 kN

FIGURE 2.56. LOAD DISTRIBUTION RELATIONSHIPS, GROUP, PILE 2 (CENTER), HYBRID MODEL, KOIZUMI AND ITO TEST

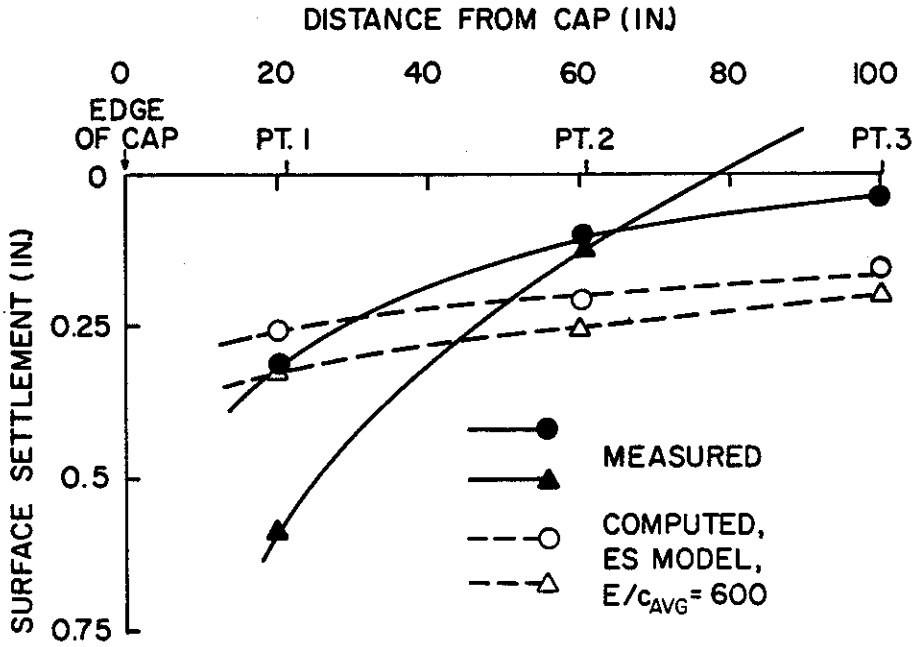

CIRCLES: GROUP LOAD = 251.4 KIPS (SUBFAILURE)

TRIANGLES: GROUP LOAD = 299.4 KIPS (FAILURE, AS REPORTED)

NOTE: 1 in. = 2.54 cm 1 kip = 4.45 kN

FIGURE 2.57. SURFACE SETTLEMENTS, GROUP, ELASTIC SOLID MODEL, KOIZUMI AND ITO TEST

TABLE 2.8. DISTRIBUTION OF LOADS TO PILE HEADS:

KOIZUMI AND ITO 9-PILE GROUP

Applied Group Load (kips)	Method	Load on Corner Piles (kips)	Load on Edge Piles (kips)	Load on Center Pile (kips)
123.4	Hybrid	14.3	13.4	12.5
123.4	Elastic Solid	17.4	12.0	6.0
123.4	FEM	*	*	*
123.4	Measured**	19.0	13.5	6.5
251.4	Hybrid	29.2	27.3	25.3
251.4	Elastic Solid	35.4	24.4	12.3
251.4	FEM	*	*	*
251.4	Measured**	39.5	30.5	11.5
299.4	Hybrid	34.7	32.6	30.2
299.4	Elastic Solid	42.0	29.1	14.6
299.4	FEM	*	*	*
299.4	Measured**	42.1	35.0	11.5

*Solutions unavailable for length/diameter <40.

**Measured values are for 1 corner, 1 edge and 1 center pile only and were obtained by extrapolation of distributed load along piles. Geometrically similar piles may not have carried the indicated loads.

Hybrid Model: Adjusted f-z curves, $E/c_u = 250$
Elastic Solid Model: $E/c_u = 600$

Note: 1 kip = 4.45 kN

TABLE 2.9. COMPUTED AND MEASURED "EFFICIENCIES" FROM KOIZUMI AND ITO TEST

Failure Criterion	Single Pile Failure Load (kips)			Group Failure Load (kips)			Group Efficiency				
	H	ES	M	H	ES	M	H	ES	M	B	F
0.05 in./ton	45	-	47	-	-	293	-	-	0.69		
(0.05 in./$\sqrt{N}$)/ton	45	-	47	325	-	287	0.80	-	0.68		
MDFL	47	51	50	320	460	293	0.76	1.00	0.65	1.69***	0.72

***Based on single pile failure = 48.5 kips (avg. of 0.05in./ton and MDFL)

H - Hybrid method curve
ES - Elastic solid method curve
M - Measured
B - Block (equivalent pier) failure
F - Feld's Rule

Note: 1 in. = 2.54 cm
1 kip = 4.45 kN
1 ton = 8.9 kN

BRE Test

The piles were installed by jacking. Some random variations from the vertical were observed even though great care had been taken to assure perfect alignment. The period of time between installation and testing was one and one-half years. The reference pile was the center pile in the group and was tested after the group test, which is inconsistent with the sequence of tests in the other programs considered in this report.

Several subfailure load tests were conducted over a period of three months on the reference pile, and the initial slope of the load-settlement curve was observed to change over a range of 35%, due apparently to moisture changes in the upper three to four feet of soil. An average curve was used to represent the reference pile for this study.

Tests were a variation of the quick maintained load type and were conducted to only about one-third of ultimate capacity. Thus, no efficiency correlation could be attempted. Finite element solution graphs could not be obtained for the configuration of this group.

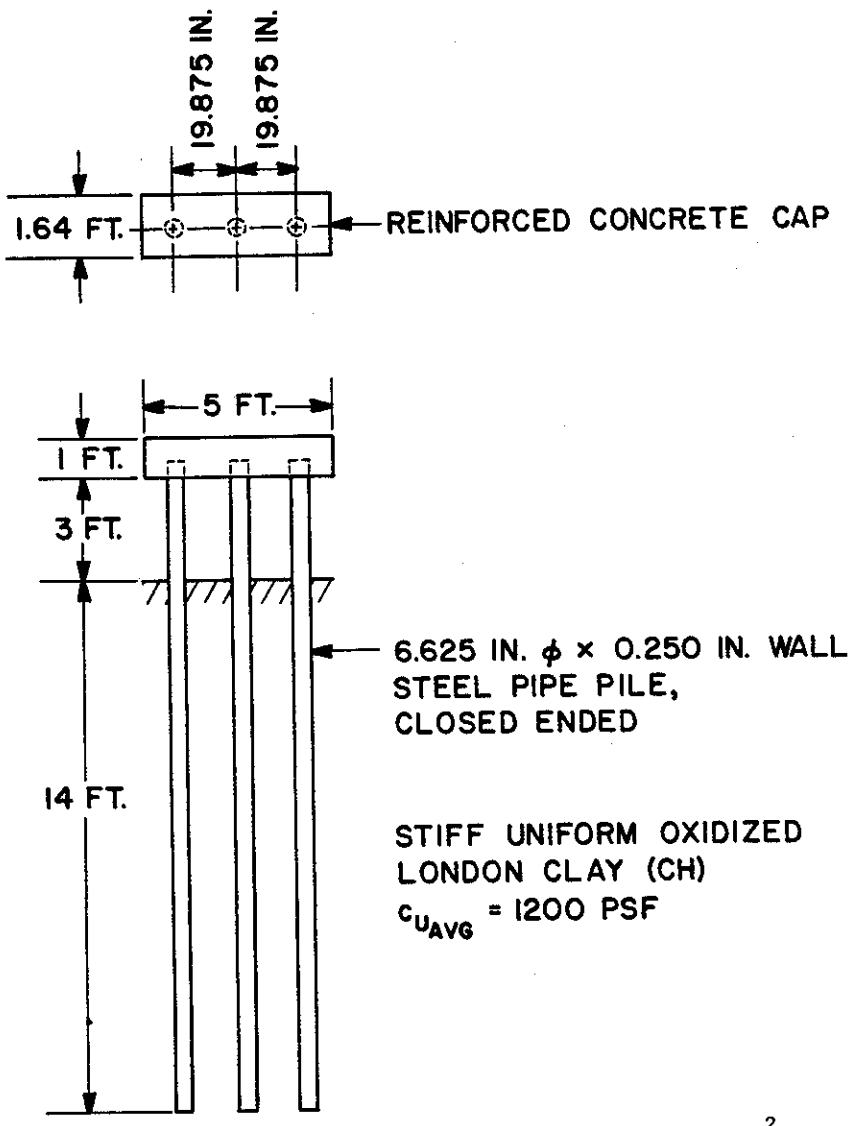

NOTE: 1 in. = 2.54 cm 1 ft = 0.305 m 1 psf = 47.9 N/m^2

FIGURE 2.58. PILE GEOMETRY AND SOIL CONDITIONS, BRE TEST

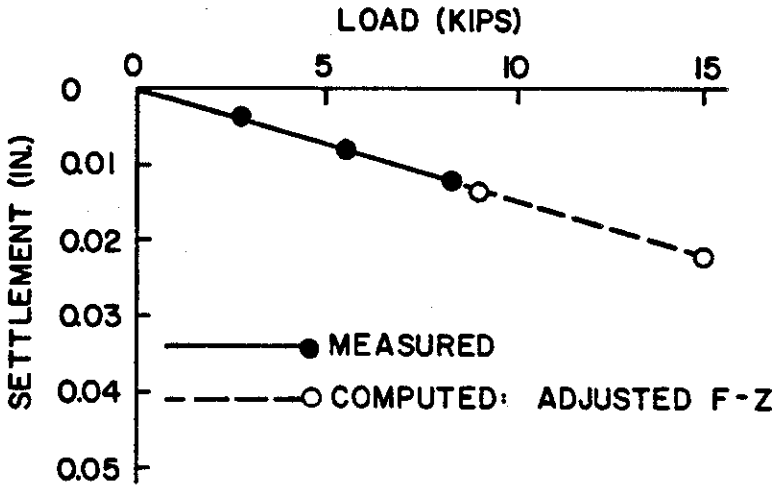

NOTE: 1 in. = 2.54 cm 1 kip = 4.45 kN

FIGURE 2.59. LOAD VS. SETTLEMENT, REFERENCE PILE, HYBRID MODEL, BRE TEST

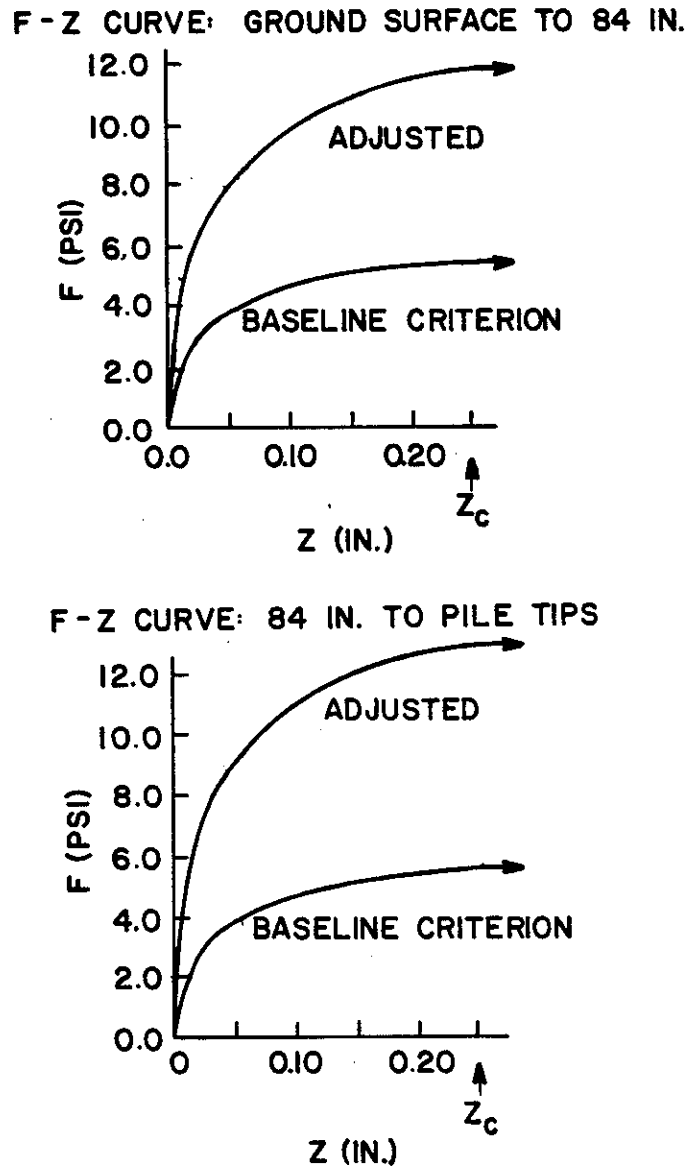

FIGURE 2.60. F-Z RELATIONSHIPS, BRE TEST

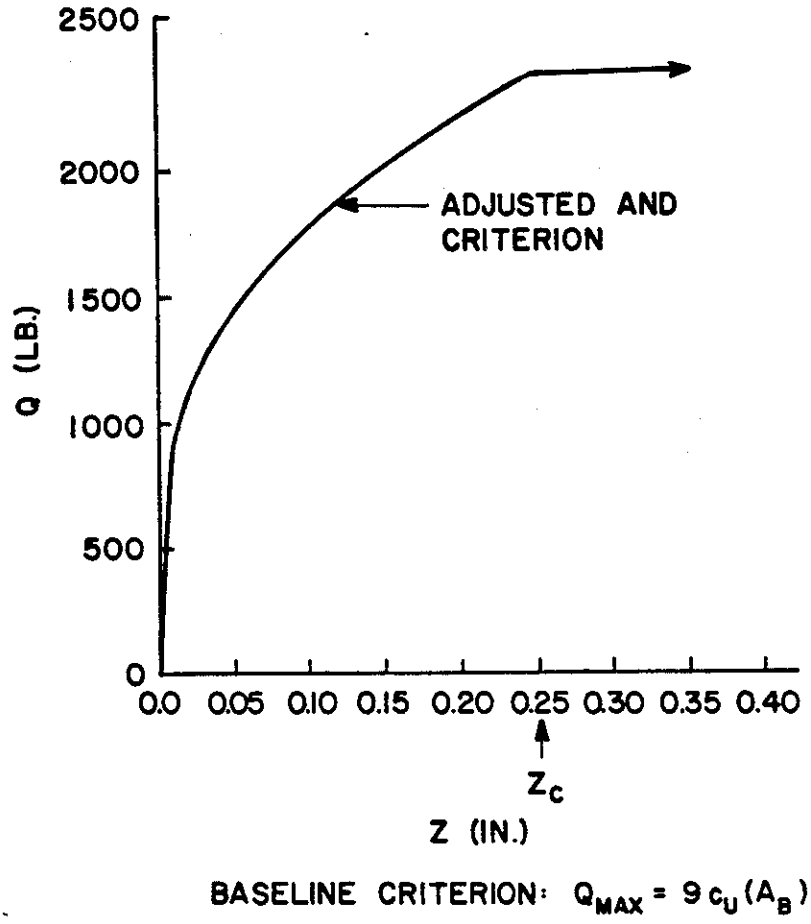

NOTE: 1 in. = 2.54 cm 1 lb = 4.45 N

FIGURE 2.61. Q-Z RELATIONSHIP, BRE TEST

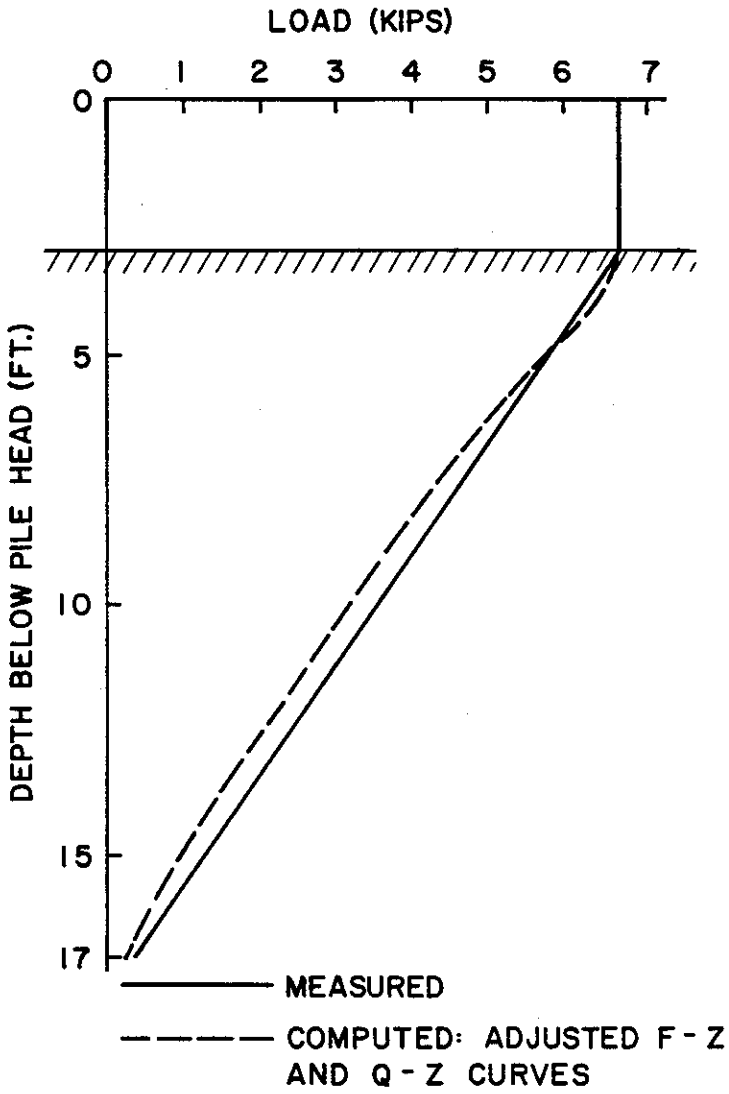

NOTE: 1 ft = 0.305 m 1 kip = 4.45 kN

FIGURE 2.62. LOAD DISTRIBUTION RELATIONSHIP, REFERENCE PILE, HYBRID MODEL, BRE TEST

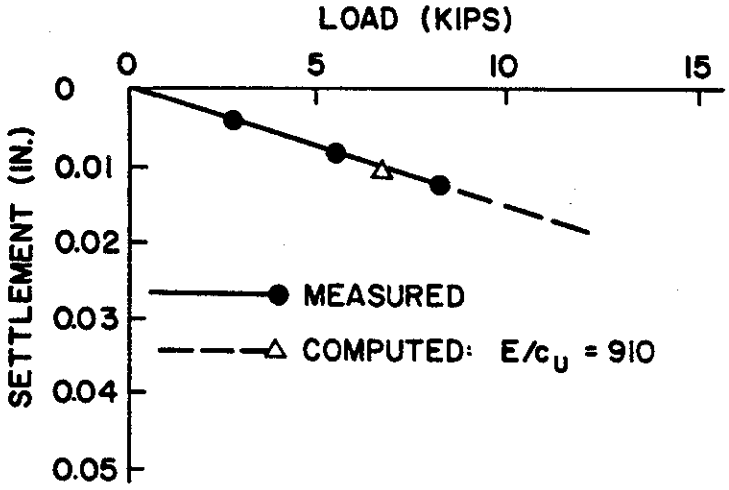

NOTE: 1 in. = 2.54 cm 1 kip = 4.45 kN

FIGURE 2.63. LOAD VS. SETTLEMENT, REFERENCE PILE, ELASTIC SOLID MODEL, BRE TEST

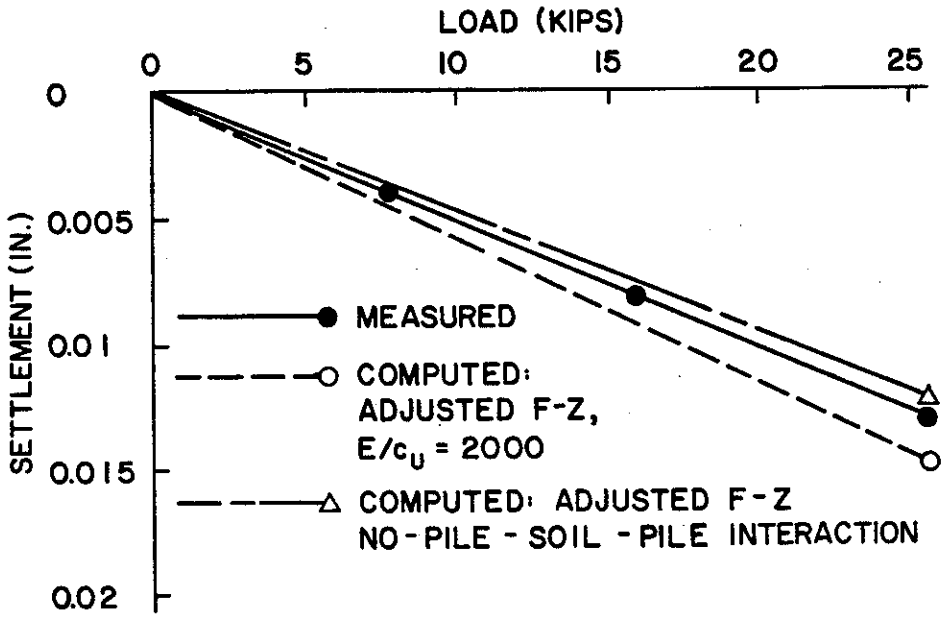

NOTE: 1 in. = 2.54 cm 1 kip = 4.45 kN

FIGURE 2.64. LOAD VS. SETTLEMENT, GROUP, HYBRID MODEL, BRE TEST

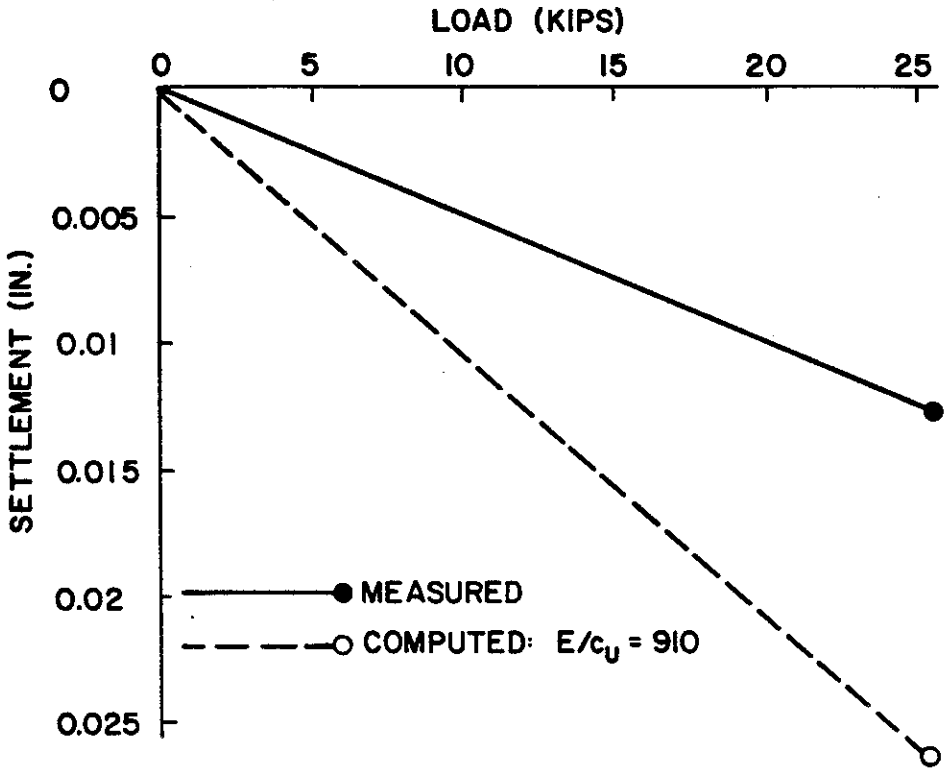

NOTE: 1 in. = 2.54 cm 1 kip = 4.45 kN

FIGURE 2.65. LOAD VS. SETTLEMENT, GROUP, ELASTIC SOLID MODEL, BRE TEST

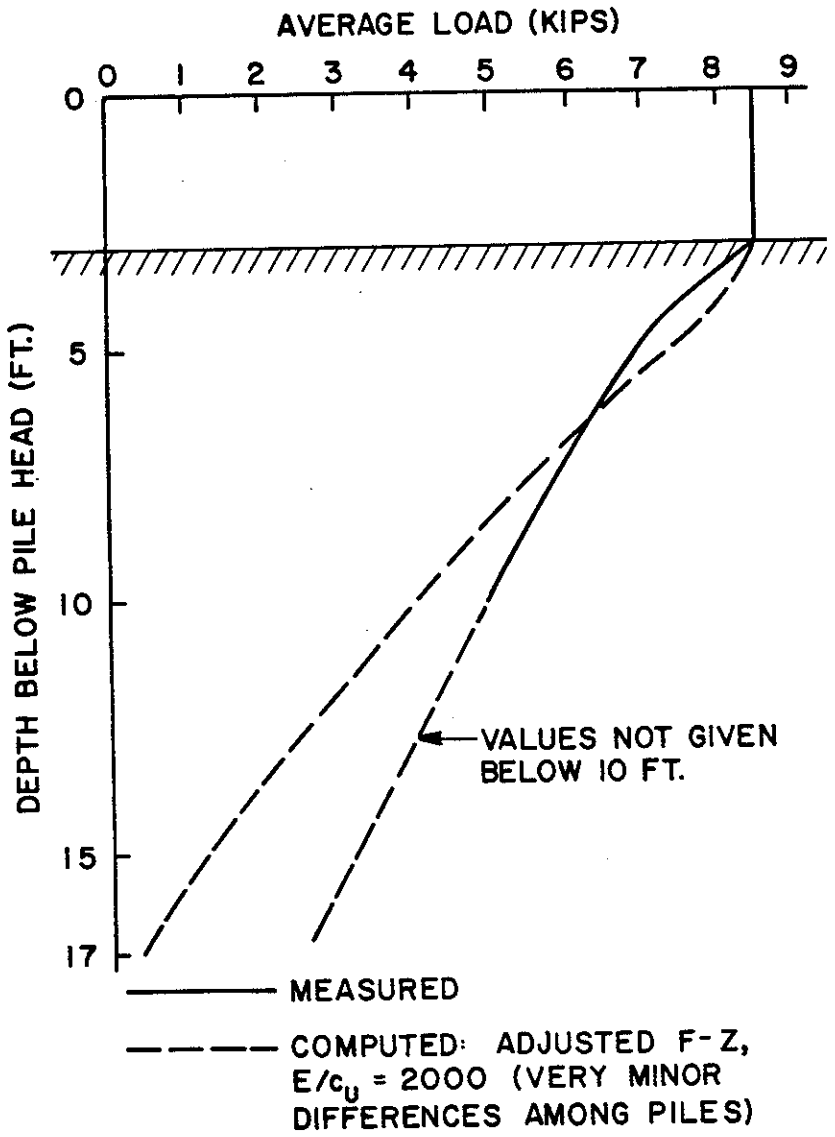

NOTE: 1 ft = 0.305 m 1 kip = 8.9 kN

FIGURE 2.66. AVERAGE LOAD DISTRIBUTION RELATIONSHIP, GROUP, HYBRID MODEL, BRE TEST (ONLY AVERAGE RELATIONSHIP REPORTED)

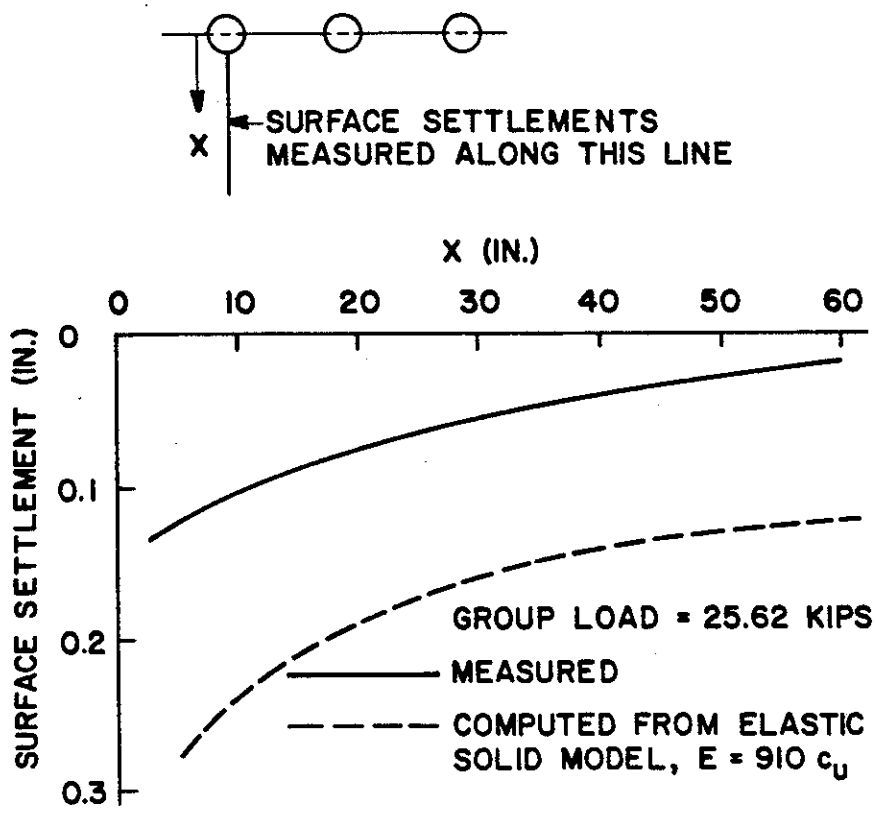

NOTE: 1 in. = 2.54 cm 1 kip = 4.45 kN

FIGURE 2.67. SURFACE SETTLEMENTS, ELASTIC SOLID MODEL, BRE TEST

TABLE 2.10. DISTRIBUTION OF LOADS TO PILE HEADS:
BRE 3-PILE GROUP

Applied Group Load (kips)	Method	Average Load on End Piles (kips)	Load on Center Pile (kips)
25.62	Hybrid	8.56	8.49
25.62	Elastic Solid	9.19	7.23
25.62	Measured*	8.79	8.05

*Inferred from data

Hybrid Model: Adjusted f-z curves, $E/c_u = 2000$
Elastic Solid Model: $E/c_u = 910$

Note: 1 kip = 4.45 kN

Discussion of Results

a. Elastic Modulus Inputs for Groups in Clay. The Young's moduli for the soil that gave the best correlations for the pile-soil-pile interaction effects in the hybrid model were approximately equal to those required to give the best correlations for single pile behavior with the elastic solid and finite element models.

The appropriate E/c_{avg} ratio values were as follows:

Model	Schlitt	Koizumi and Ito	AREA	BRE
Hybrid	850	400 (Interpolated)	2,000	2,000
Elastic Solid	900	600	2,000	910
Finite Element	900	600	1,700	No sol'n

The appropriate ratio for the Schlitt test becomes approximately 500 if the undrained cohesion beneath the pile tips is used as opposed to the average cohesion along the piles. The high AREA values are probably due to the fact that correlations were made to an undrained cohesion value that was apparently near the remolded value and not to the undisturbed cohesion, as was the case for the other three tests.

There is a significant discrepancy in the modulus values in the BRE test. This may be attributed to the fact that the reference pile behavior was somewhat "soft" compared to the other two piles, leading to a need to use a lower value of modulus to model the single pile in the elastic solid model than to model the group in the hybrid model. This problem could be a reflection of normal statistical variation in pile behavior within a group coupled with the existence of only three piles within the group. Stated differently, there was no significant "group effect" in the BRE test. Because of this problem in modeling the BRE test, which was the only test with other than nine piles, it is at present difficult to predict the magnitude of the effect of the number of piles in the group on the choice of the modulus value.

Based on the results reported in the preceding sections, it appears that the range of E/c_{avg} values for all models should be from about 400 in closely spaced groups in sensitive clays to about 850 in widely spaced groups in insensitive clays.

It is apparent that implicit use of the E/c ratio obtained from the reference pile behavior in the synthesis of the load-settlement curve for the group in the elastic solid model tends to produce a group load-settlement curve that is in the order of 25% too soft. This phenomenon may be attributed to the fact that the choice of E at the time a reference pile is modeled does not permit the user to take account of the effect of reinforcement of the soil by the piles in the group, which is automatically accomplished in the finite element model and is accomplished by implication in the choice of E in the hybrid model. In the Koizumi and Ito test, conducted in very sensitive clay, the soil immediately surrounding the perimeter piles may have been stiffer as a result of more rapid reconsolidation near the piles than the soil in the interior soil mass, which leads to a higher modulus to model the single pile than to model the group.

b. Elastic Modulus Inputs for Group in Sand. The best correlations were obtained with the hybrid model, in which a linear variation of Young's modulus from zero at the ground surface through a value of E_{BASE} at the base of the piles and increasing at the same rate below the base of the piles to an infinite depth, when E_{BASE} was taken as $0.1\ E_B$, where E_B is given in Eq. (2.1). This appears to be a reasonable value since the mass of soil beneath the group, which appears to be very influential in the load-settlement properties of the group, is not as highly confined as the soil beneath the tip of a single pile, which was considered in obtaining Eq. (2.1).

In the version of the elastic solid model considered, E can have two discrete values, one at and below the base of the piles (E_{BASE}) and one above the base of the piles E_S. With this method the best correlations for the reference pile were obtained for $E_{BASE} = 0.5E_B$ and $E_S = 0.05E_B$.

The best reference pile correlation with the boundary element model, which permits the same modulus variation as the hybrid model, was the same as that for the hybrid model. This is a rather tenuous

conclusion, as the solution yielded excessive load transfer along the shaft, and relatively little load reached the tip of the reference pile in the model. See Fig. 2.21.

The elastic solid model yielded a group load-settlement curve that, like the models in clay, was too soft. This effect is illustrated in Fig. 2.68 which compares the measured, elastic solid, and hybrid results. This softening may be attributed to the use of a two-layer elastic system to model the group rather than the use of a linear modulus variation. The softening phenomenon was probably magnified for the test that was modeled because the ratio of ultimate shaft resistance to ultimate base resistance in the piles in the group, and by implication E_S/E_{BASE}, was higher in the group than in the reference pile.

c. Load Transfer Functions for the Hybrid Model. The baseline f-z curves proposed by Vijayvergia (80) appear to be of the appropriate form. However, the f_{max} values obtained from the α and λ methods in clay were from 20% to more than 100% low as compared with the values obtained by modeling individual piles. The computed baseline value for f_{max} in the test in sand, based on earth pressure and friction theory, was about 40% low, based on an assumed value of K = 0.7.

If the α method is used for the Schlitt test the computed value for f_{max} is 10% low. The factor α is more than 100% low for the AREA test, presumably due to low reported values of indicated shear strength. It appears to be low for the BRE test, but no conclusion can drawn relative to f_{max} from this test because the test was not carried to failure. The high adjusted value of f_{max} was necessary in order to stiffen the initial portion of the f-z curve. This could also have been done by decreasing z_c and leaving f_{max} as a constant.

Thus, for the tests investigated, it appears that the methods discussed in Chapter 1 for determining baseline values of f_{max} were appropriate, although the λ method was less accurate (more conservative) than the α method in one test in clay, and K should have been increased from 0.7 to about 1.0 in sand. Some caution should be observed in extrapolating the K-value to prototype piles in sand because of depth effects caused by such factors as residual stresses and arching.

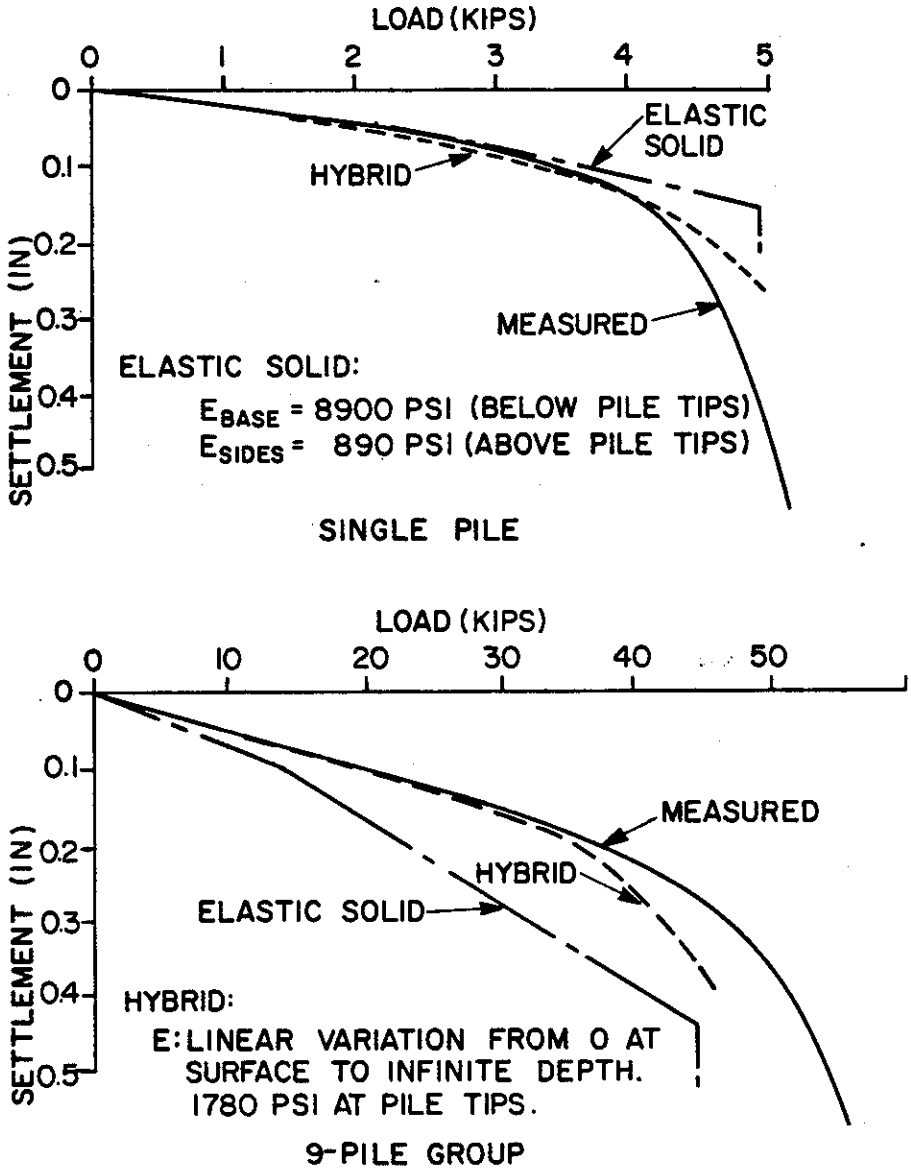

NOTE: 1 in. = 2.54 cm 1 kip = 4.45 kN 1 psi = kN/m^2

FIGURE 2.68. COMPARISON OF HYBRID AND ELASTIC SOLID LOAD-SETTLEMENT CURVES, VESIĆ TEST

The appropriate range of z_c for all tests, except possibly the BRE test, was 0.4 to 0.5 inches (1.0 to 1.3 cm). This is slightly above the range of values suggested by Ref. 80 and may be influenced by the fact that two of the groups modeled contained tapered piles.

The Q-z curve criterion for clay given in Chapter 1 appears valid for $N_c = 9$, although none of the tests in clay were sensitive to the end bearing relationship. An appropriate value for z_c for the Q-z curve is about five percent of the tip diameter. For the test in sand, the criterion also appears to be correct provided the factor N_q^* is taken to be approximately 130, rather than the nominal value of 40 taken to generate the baseline curve, and z_c is taken to be 7.5% of the tip diameter.

d. Load Transfer Characteristics. The hybrid model was "calibrated" for each test to yield load transfer patterns reasonably close to those that were measured in the reference pile. Less control existed over the representation of soil properties in the finite element model. However, fair agreement between calculated and measured load transfer patterns was observed for the reference piles in the clay tests. Poor agreement was observed in the boundary element version of the elastic solid model in the sand test. Representation of the sand around an isolated pile as a medium having uniformly increasing stiffness with depth produced an overestimate of the rate of shaft load transfer. The Poulos version of the elastic solid model did not yield load tranfer patterns, which may account in part for the errors involved in extending the input from the reference pile analysis to the production of the group load-settlement curves (Fig. 2.68). That is, had the single pile load transfer patterns been known there may have been a more optimal way of defining values for E_{BASE} and E_S than is indicated in Fig. 2.20 (such as use of a higher value of E_S and a lower value for E_{BASE}) that would have yielded an equally valid single pile load-settlement curve, while yielding a better load-settlement curve for the group.

Only the hybrid model was used to predict load transfer patterns in the group, as charts or computer codes for obtaining load transfer patterns in pile groups could not be found with the other models. Group load transfer patterns were not replicated as well as those for

single piles, but most of the results are understandable in light of the fact that ideal conditions (plumb pile, average soil conditions, etc.) were used for every pile in the model. The model outputs therefore deviated from the load transfer patterns that were reported for specific instrumented piles in comparable geometric positions in the group, whose load transfer patterns may have been influenced by factors that were not modeled, such as driving sequence and alignment. This quasi-random variation suggests that some probabalastic model, rather than the deterministic models considered in this study, may be more appropriate for computing load transfer differences from pile to pile.

In the pile group in sand some of the deviation is undoubtedly due to the fact that group installation presumably produced higher lateral pressures and possibly densification that caused f_{max} for all of the piles in the group to exceed that for the reference pile. Extreme differences between computed and measured load transfer patterns were observed in the Koizumi and Ito test. Detailed analysis of the distribution of measured loads along the piles casts some suspicion on the measured results; however, the extremely low load transferred by the center pile may be due to the extremely sensitive nature of the soil, the inability of high excess pore pressures in the soil between the piles to dissipate, and the consequent alteration of the f-z relationships not accounted for by the hybrid model.

e. Efficiency. The following observations can be made concerning the attempts to determine "efficiency" through the use of the failure settlement (MDFL) and slope (0.05 in./$\sqrt{\bar{N}}$ per ton) (0.014 cm/$\sqrt{\bar{N}}$ per kN) criteria described earlier. Only the AREA, Koizumi and Ito, and Vesić tests were carried to a high enough load to permit conclusions to be drawn, and only those tests are included in the discussion that follows.

The differences between the efficiencies obtained from the settlement and slope methods from the measured load-settlement curves and the true efficiencies based on plunging or otherwise definable ultimate load were:

MDFL: 3% to 10% low
Slope: 1% high to 15% low

The differences between the efficiencies obtained from those methods from the measured load-settlement curves and the load-settlement curves computed by the hybrid model were:

MDFL: Computed was 14% too low to 35% too high
Slope: Computed was 22% too low to 35% too high

Corresponding errors using the elastic solid model were:

MDFL: Computed was 10% too low to 54% too high
Slope: Not obtainable

Values of "efficiency" could not be obtained with the finite element model.

The block efficiency was 35% too high in the AREA test and 41% too high in the Koizumi and Ito test, based on using observed plunging failure load in the piles and the establishment of an efficiency value equal to unity whenever block efficiency was computed to be greater than unity. If the ultimate load of the Koizumi and Ito group is based on the ultimate capacity of the cap-soil-pile system, which was greater than the capacity of the piles alone due to cap bearing, but which did not occur until a deflection of about one foot (0.3 m) had been achieved, the error in block efficiency is reduced to about 10%. The efficiency values yielded by Feld's rule were within one per cent of those computed from ultimate loads in the AREA and Koizumi and Ito tests, based on defining failure as pile failure and not ultimate capacity of the pile-cap-soil system.

A portion of the errors obtained in the models could be due to the use of reference pile data that may not be entirely representative of the piles in the group, but it is clear that estimating efficiencies from the computed reference pile and group load-settlement curves at load values less than ultimate failure is not an accurate procedure.

f. Distribution of Loads to Pile Heads. As with load transfer patterns in the group, agreement between computed and measured distribution of loads to pile heads is not especially good. None of the models has a clear advantage here. The hybrid model tends to yield

lower differences in pile head loads than the other models. This is in general agreement with the tests studied, except for the Koizumi and Ito test. The reasons for the discrepancies there are thought to be similar to those responsible for the discrepancies in the observed load transfer patterns. In addition, the semi-flexible cap and variable length piling in the Schlitt test may have contributed to the discrepancies in that test, particularly in the elastic solid model, which could not directly consider variable piling lengths.

g. Surface Movements. Surface settlements were overestimated significantly by the boundary element model in the Vesić test. This problem is probably associated with the tensile stresses developed in the soil above the pile tips, at which point the majority of the load was transferred. Better agreement was achieved from subfailure loads in the Koizumi and Ito tests where less soil tension should occur, using the elastic solid model. (No finite element solution was available.) However, heave that was produced about 2.5 meters away from cap at failure was not modeled. Overall, the elastic solid and boundary element models were therefore unreliable as means of computing surface movements. The hybrid algorithm does not compute surface movement.

General Conclusions

A summary of the performance of the three load-deformation models employed in the comparison study is given in Table 2.11.

Since no existing load-deformation model can yield ultimate capacity, it will be necessary to adopt separate models for synthesizing pile group characteristics such as load-settlement, load transfer, and load distribution and for synthesizing ultimate capacity and efficiency. It appears that an efficiency model is only required for friction pile groups in soft clay, and possibly in stiff, overconsolidated clay, and that the group efficiency can be taken as unity elsewhere for design purposes. A simple model such as Feld's rule appears to be the most appropriate efficiency model for friction piles in soft clay.

TABLE 2.11 SUMMARY OF MODEL PERFORMANCE IN COMPARISON STUDY

Model	Performance According To Function					
	Efficiency	Group Settlement	Distribution Of Loads Among Pile Heads	Load Transfer Patterns	Surface Soil Movements	Difficulty of Use
Hybrid	Constrained to give efficiency of 1 based on ultimate load. Computed efficiency based on "failure settlement" varied from 14% low to 35% high compared to similarly defined efficiency from measured load-settlement curves (MDFL)	Accurate in working load range if adjusted load transfer functions were used and soil moduli correlations in Secs. a and b were employed	Comparisons to measured values were not especially good, presumably due to varying stiffness of of individual pile response due to spatially variable soil conditions,variable residual stresses, or variable alignment, effects for which insufficient data existed to permit modeling	Same Comments apply here as apply to distribution of loads among pile heads	Not Obtained	No parametric solutions, so direct solutions had to be made. Several hours required to completely prepare input for each case. Very easy to include variable pile penetration. Execution time on Honeywell 66/60 computer was about 10 seconds per pile.

TABLE 2.11 SUMMARY OF MODEL PERFORMANCE IN COMPARISON STUDY (Cont'd)

Model	Performance According To Function					
	Efficiency	Group Settlement	Distribution Of Loads Among Pile Heads	Load Transfer Patterns	Surface Soil Movements	Difficulty of Use
Elastic Solid	Same as hybrid if pile-soil slip assumption is made, except efficiency based on failure settlement varied from 10% low to 54% high (MDFL)	Slightly less accurate than hybrid due to employment of same soil moduli for single pile and group. Did not track nonlinearity well	Same as hybrid. (Effects listed above could not in general be modeled even if sufficient data existed)	Not obtained	Relatively accurate at subfailure load for one test in clay. Overpredicted significantly for one test in sand	Numerous parametric solutions available. Direct use of computer algorithm of comparable difficulty to hybrid algorithm. Execution time about 20 sec. per pile.
Finite Element	Could not be obtained	Same as elastic solid	Same as hybrid	Not obtained	Not obtained	Some parameteric solutions available. Direct use of model much more difficult and time consuming than hybrid or elastic solid

Chapter 3. Selection of Model to Synthesize Proposed Field Study

General

The present-day approach to the rational design of pile groups consists of several distinctly separate but related tasks:

a. Develop a preliminary layout, pile penetration, and cap size for a given set of loads.

b. Evaluate the cost of the preliminary design.

c. Evaluate the constructability of the preliminary design.

d. Cycle through Tasks a-c with other preliminary designs until the most cost-effective design is apparent.

e. Make a detailed analysis of the candidate design from Task d for

(1) Settlement under a range of working loads, to assure superstructure integrity.

(2) Pile stresses, to assure structural integrity of the piles.

(3) Load transfer to the soil, for purposes of evaluating long-term movements and giving insights into possibility more optimal pile penetrations.

(4) Pile head loads, to permit final design of the pile cap.

f. Evaluate the factor of safety of the group at working load or the ultimate capacity of the group as defined by some failure criterion.

g. Evaluate the candidate design. Accept, discard, or make adjustments where necessary. If discarded, return to Task a with new criteria gained by experience with the candidate design.

Tasks a, b, c, e, and f can be accomplished in a formal sense by the use of separate mathematical techniques or "models." No model exists that will span all five tasks. This study focuses principally on Tasks e and f. All three models studied in detail are appropriate to some degree to Task e. At the current state of the art, Task f must be accomplished separately from Task e, as no mathematical model exists that can adequately simulate the behavior of a group of piles through an entire range of loads up to and including those that produce ultimate failure of the group.

The inability of the models to handle both tasks is a result of different factors from the various models. In order to compute ultimate capacity, a model must be able to simulate failure in the soil wherever it may occur. The location of the failure zones are not in general known in advance, so that the model itself should be capable of generating the location of those zones, of simulating the behavior of failed soil in those zones, and of tracking the expansion of failure zones until complete collapse takes place. Only the finite element model is potentially capable of these tasks.

The requirement exists for the establishment of some kind of failure mechanism in an ultimate failure model, finite element or otherwise, for any point in the system. Some attempts have been made to develop such mechanisms for a single pile-soil system in two dimensions (e.g., Ref. 20) using the finite element model. Such mechanisms include interface elements between pile and soil which yield when the shearing stress exceeds some preset value and provisions for the assignments of zero values for shear modulus in the soil mass if computed stresses exceed the shear strength of the soil. The finite element interface element model requires the analyst to estimate f_{max} before making an analysis, as must be done with the hybrid model or the elastic solid model modified to account for pile-soil slip, so in this respect the finite element model has no advantage over the other models. Furthermore, finite element theory is essentially a small displacement theory. Although it is possible to make allowances for geometric nonlinearities in the finite element mesh as large displacements associated with failure occur, some numerical difficulties still exist, making the calculation of collapse loads presently rather difficult from a practical viewpoint in a two dimensional system.

These failure mechanisms have not been estiablished in general in three dimensions, as would be necessary for the analysis of pile groups. If they could be and a general three-dimensional finite element computer code were written that would perform Tasks e and f, it is likely that a numerical scheme related to that of applying small loads to the groups in increments and accumulating their effects until failure was reached would be necessary. Using the experiences of Ottaviani as a guide (53), a problem possessing a number of elements sufficient for

an accurate solution would require at best several hundred minutes of central processor time on a typical present generation computer.

It is therefore concluded that the finite element model, which is presently usable in three-dimensions as a linear tool, cannot perform both Tasks e and f, nor is it yet reasonable to expand the model to compute ultimate capacity until more efficient numerical processes and faster computing machines can be developed. Of the models studied, however, it has the greatest theoretical potential for expansion into an "ideal" model, incorporating design Tasks e and f, because of its ability to permit failure to occur either along individual piles, in the soil mass, or as a combination of soil mass and soil-pile failure, as would be governed by conditions of pile spacing and soil conditions that could not be predetermined by the analyst.

The hybrid and modified elastic solid models cannot determine ultimate capacity of a pile group, for essentially the same reason in each case. In essence, the collapse load, which is described in terms of f_{max} and Q_{max} for the various piles in the hybrid model and is input directly into the modified elastic solid model, is constrained to be that of the collapse load of an isolated pile times the number of piles in the group. A true collapse mechanism is not defined, and no attempt is made to do so, for the soil surrounding the piles is treated as an elastic medium. Both models exclusively employ a single pile failure concept and cannot rationally replicate failure in cases where "block" failure might predominate.

It has been demonstrated in Chapter 2 that the hybrid model can simulate nonlinear load-movement behavior somewhat better than the modified elastic solid model, such that it can be used to evaluate failure load very approximately if failure is defined by some prescribed settlement or rate of settlement that would be harmful to the super structure rather than by the load causing ultimate collapse of the pile group. Because of its ability to predict load-settlement relationships in the nonlinear range, the hybrid model is judged preferable to the elastic solid model.

The hybrid model could in principle be modified in the future to yield collapse loads other than those that are defined by the sum of the collapse loads of all piles acting as isolated piles, although such a

modification would require a major research and development effort. For example, it would be desirable to develop a routine that would compute the ratios of f_{max} and Q_{max} on group piles to those on isolated piles, resulting from the installation process. It might be possible to accomplish this by assessing the ratios of lateral earth pressures within a group to those around an isolated pile and relating changes in f_{max} and Q_{max} to those pressure ratios. The procedure for predicting the earth pressure differences might be predicated on the theory of expanding cylindrical cavities (77) (which would have to be extended to include interaction effects among cavities) or might incorporate a two-dimensional finite element scheme that has the capability of modeling expanding cavities (pile insertion). In clays it is likely that the changes in the effective earth pressures (and in f_{max} and Q_{max}) would have to be considered by using a numerical procedure to calculate the rate of dissipation of excess pore pressures within the soil surrounding the piles. Another, simpler, way of dealing with f-z and Q-z modifications is to do so when developing input. This is discussed briefly later in this chapter.

With modifications of the type described, the hybrid model would still be constrained to model ultimate failure in a group as individual pile failure and not as the type of failure that would be characterized by soil failure within the soil mass. These modifications are extensive and could not be carried out within the scope and budget of the present study. Undoubtedly, a modified version of the hybrid model would be more costly to execute on a digital computer than is the present version.

In summary, the finite element model appears to have the greatest potential, of the models studied, for long-term development into a model that would encompass both Tasks e and f in the design process. Such development will be difficult and costly and would probably, out of practical considerations, await the development of faster computing machines. The real strength of a future finite element model with a general collapse mechanism would be that it would not be necessary to presuppose whether failure would occur along the piles, within the soil mass, or as a combination of such failure modes.

The hybrid model, on the other hand, is the better candidate for a working model to incorporate in the design process for the near future, provided it is understood that separate efficiency or ultimate capacity models will have to be continued to be used in Task f. The hybrid model could be adapted to compute ultimate failure loads in certain cases with significant modifications. It has the distinct and highly advantageous feature of being able to model the effects of loads other than concentric vertical forces and pile inclinations other than vertical.

Based on the above review and upon the generally positive results achieved with the hybrid model in Chapter 2, the hybrid model is chosen to model the proposed full-scale field tests. This model was seen to yield reasonably accurate predictions of load versus settlement, load transfer patterns, and load distribution to pile heads. It does not output stresses and displacements in the soil mass but does compute displacement at nodes along the piles as described in Chapter 1. Because pile-soil-pile interaction is treated by using elastic halfspace theory, the model can be used directly to calculate long-term settlements in uniform deposits of clay by using values of Young's modulus obtained under drained loading, (for example, from a one -dimensional consolidation test), rather than undrained loading, and a Poisson's ratio value for the soil skeleton (usually, about 0.3), rather than that for the soil-pore water system, as was appropriate for modeling the short-term tests described in Chapter 2.

The principal practical uses of the hybrid model in synthesizing a load test are thus to obtain group settlements under a variety of applied loads, and to obtain thrusts in the piles. The hybrid model is also ideally suited to the investigation of effects produced by eccentric loading such as lateral displacements and bending moments in piles, the effects of nonuniform pile alignment, and other phenomena important to designing certain parts of the experiment, including reaction and deformation measurement systems. Its ability to handle three-dimensional pile geometry and non-vertical loading with little more effort than vertical geometry and concentric, vertical loading makes it appropriate for consideration as a general model for pile groups for a variety of transportation-related design applications.

All of the load-deformation models studied in Chapter 2, including the hybrid model, yield best results when their inputs are "calibrated" to yield reasonable matches with load-settlement and load transfer behavior in a reference test pile at the site at which the prototype group will be installed. This practice is recommended whenever possible if the hybrid model is to be used directly in studying a particular pile group.

Cap-Soil Interaction

The hybrid model has not been developed to include the effects of interaction between the soil and the pile cap. A finite element study by Ottaviani (53) has indicated that, in a square nine-pile group of forty-meter-long by one-meter-square concrete piles spaced three meters on center, the pile cap carries from 9 to 22 percent of the total load in a totally elastic uniform soil. The cap overhang was one-half of the width of a typical pile. The lowest values of cap reaction occurred for piles whose elastic modulus was 2,000 times that of the soil (semi-rigid pile), and the highest value occurred where the pile modulus was 200 times that of the soil (very flexible pile). Using the elastic solid model, Butterfield and Banerjee (13) have observed that square-arrayed five and nine-pile groups of similar relative dimensions to the groups studied by Ottaviani (penetration/diameter = 40, spacing of three diameters, and cap overhang of 0.75 times the pile diameter) carry up to 30 per cent of applied load through the cap when the piles are flexible in relation to the soil.

Experimental evidence, however, does not generally confirm these values. The tests conducted by Koizumi and Ito in clay yielded cap resistance values of about seven per cent of the applied loads until after the piles failed. Cap resistance increased markedly after pile failure, but that resistance was unusable, as it required a displacement of several inches to mobilize. Supplemental tests of the BRE group (61) indicated that cap bearing accounted for about six per cent of the applied load. Similar values for groups in clay can be inferred from the tests reported by Brand, et al. (8). In the group tests in sand reported by Vesić (75,76) the cap bearing was highly variable, being as low as about five per cent of the total load in Test P-93 (the test

modeled in Chapter 2) and as high as about 35 per cent in other tests. Vesić concluded that cap reaction occurred mainly in the overhang portions of the cap, outside the perimeter of the array of piles.

From a practical point of view, cap reaction is likely to be lower in prototype groups than in the groups just described, which were constructed and tested for research purposes, due to the usual practice of not preparing the subgrade that the cap will rest on for bearing. Because of the low and irregular values of cap reaction that have been measured, and that are likely to occur in practice, it is not deemed necessary to conduct the proposed tests with the cap in contact with the ground, nor is it deemed necessary to include the effects of cap-soil interaction in the mathematical model.

Long-Term Settlements

The hybrid model is capable of predicting long-term settlements in uniform soils if drained values are used for E and v. It has not been possible to verify the model in this mode due to the unavailability of appropriate test data. Two other common stratigraphic conditions exist for which long-term settlement computations may be necessary:

a. Piles placed in a non-consolidating layer above a consolidating layer. Long-term settlements can be computed off line using the outputs from a short-term analysis. This is accomplished by summing the shaft resistances output by the model and applying the resulting load uniformly over a ficticious mat located at a depth equal to two-thirds of the pile penetration and computing the settlement in the consolidating layer by using Boussinesq stress distribution. If tip loads are significant, the computed sum of the individual tip loads are applied uniformly over a ficticious mat located at the elevation of the pile tips. The stresses in the consolidating layer are again obtained from Boussinesq theory and superimposed on those obtained from the shaft reactions.

b. Piles driven through soft sensitive or normally consolidated clay into stiff, overconsolidated clay. In this situation, the long-term load transfer characteristics are likely to be significantly different from the short-term characteristics. Load is shed from the shafts and accumulated in the tips. This phenomenon can be synthesized

approximately by the hybrid model in a direct manner by inputting drained values for E and ν in which E varies linearily with depth. The existing algorithm for the hybrid model cannot synthesize this case when the soft layer is loaded by fill and produces negative skin friction in the upper levels of the piles. The model itself, however, is not constrained by the existence of negative skin friction in the pile-soil system.

Computer Code

A computer code based on the hybrid model was developed during Phase I of this study. The code, denoted PILGP1, is a modification of an earlier code, GP3B, which was used in the comparative study reported in Chapter 2. GP3B was also used in analysis of the proposed test group, described subsequently. PILGP1 was written in order to simplify input and to increase computational efficiency. Because of the latter accomplishment, some numerical routines in PILGP1 are somewhat altered from those in GP3B, which leads to slightly different numerical results for the cases studied in Chapter 2.

A User's Guide for PILGP1 is contained in Appendix A of the Final Report, and appropriate program documentation is given in Appendix B of the Final Report. A hard copy of PILGP1 has been made available to the Federal Highway Administration.

Possible Input Modifications

At the present time it is recommended that the load transfer functions be input according to the criteria outlined in Chapter 1 with appropriate modification based on load tests of single piles at specific sites. The premise of the present algorithm (PILGP1) is that the load transfer functions that properly describe single pile behavior may be applied to piles in the group and that group effects are accounted for by automatic adjustment of these functions based on the magnitude and distribution of load transferred to the soil as the group is being loaded. In fact, the installation process alone may alter the load transfer functions in certain situations. For example, Flaate (24) has demonstrated that installing piles in a group in sensitive clay produces a significant time-dependent increase in f_{max} in the interior piles in the

group due to reconsolidation effects. In an eight-pile group it took approximately five years for interior piles to reach the inferred capacity of isolated piles. A similar effect may have occurred in the Koizumi and Ito test described in Chapter 2. Vesić (76) and Kezdi (33) have demonstrated that f_{max} is increased to varying degrees by installing groups of piles in sand.

Residual stresses that exist in the piles after driving piles into hard soils may be input to the hybrid model (PILGP1 version) by offsetting the f-z and Q-z curves as demonstrated in Fig. 1.2. However, little is known about residual stresses in pile groups, which may develop differently than those in single piles, so that criteria for obtaining residual load transfer functions do not exist.

The three problems described above require further research in order for the hybrid model, or any existing model, to be of maximum use. Presently, it may be possible to correct f_{max} values for piles in the interior of a group in sensitive clay by obtaining an appropriate value for undrained cohesion at a given time after installation by interpolating between remolded and undisturbed shear strength. It might be assumed that strength regain is proportional to the degree of consolidation at the location of a particular pile. Degree of consolidation at a given location in the group could be estimated very approximately from superposition of excess pore pressures that can be calculated from single pile radial consolidation theory (28, 68). Critical state theory (21) may also be useful in this respect. It may also be possible to correct f_{max} values in pile groups in loose sand empirically by assuming that installing small pile groups increases the angle of internal friction of the soil by one-half the difference between in situ value and 40 degrees (37). In medium dense to dense sands there is also apparently an increase in K, which can presently be accounted for only by experience based on the few existing group tests that have been conducted in denser sands (7, 33, 76).

Example Parametric Study

As stated earlier, the most appropriate use of the hybrid model in day-to-day practice is to develop parametric charts that can be easily employed by analysts and designers. One straightforward way of

examining group effect is to determine the ratio of the settlement of a pile group of N piles to that of a single pile with an applied load of 1/N times the group load being considered. A number of attempts have been made to predict settlement ratio empirically (e.g., 67); however, the hybrid model allows this effect to be modeled in the computer considering nonlinear soil response. The usefulness of the hybrid model has been illustrated by developing simple parametric charts by which settlement ratio can be determined in uniform soil. Program GP3B was used to develop these charts.

Figure 3.1 shows the hypothetical groups that were modeled in order to obtain the charts; the load transfer functions used are shown in Fig. 3.2; and the parametric solutions for settlement ratio are given in Figs. 3.3-3.6. In these figures, settlement ratios are plotted as functions of pile group load, pile spacing pile penetration, relative initial elastic stiffness of piles and soil, and number of piles in a square array.

The initial elastic modulus of the soil is related to shear strength, as are the load transfer functions. Thus, variation of the initial relative elastic stiffness can involve variation of the pile stiffness (AE) or variation in the soil stiffness (soil modulus and initial slope of load transfer curves). In this study relative stiffness was varied by changing the pile stiffness. Slightly different solutions result if the relative stiffness is varied by changing the stiffness of the soil instead of that of the pile due to the involvement of the load transfer function in the solution.

Figures 3.3 through 3.6 can be used directly and simply to obtain the overall settlement ratio if the stiffness and penetration of the piles is within the range covered by the parameter study, since the settlement ratio contains both tip and shaft compression effects. It is necessary to measure or predict, using PILGP1 or other procedures, the settlement of a single pile under 1/N times the group load in order to obtain numerical values of settlement.

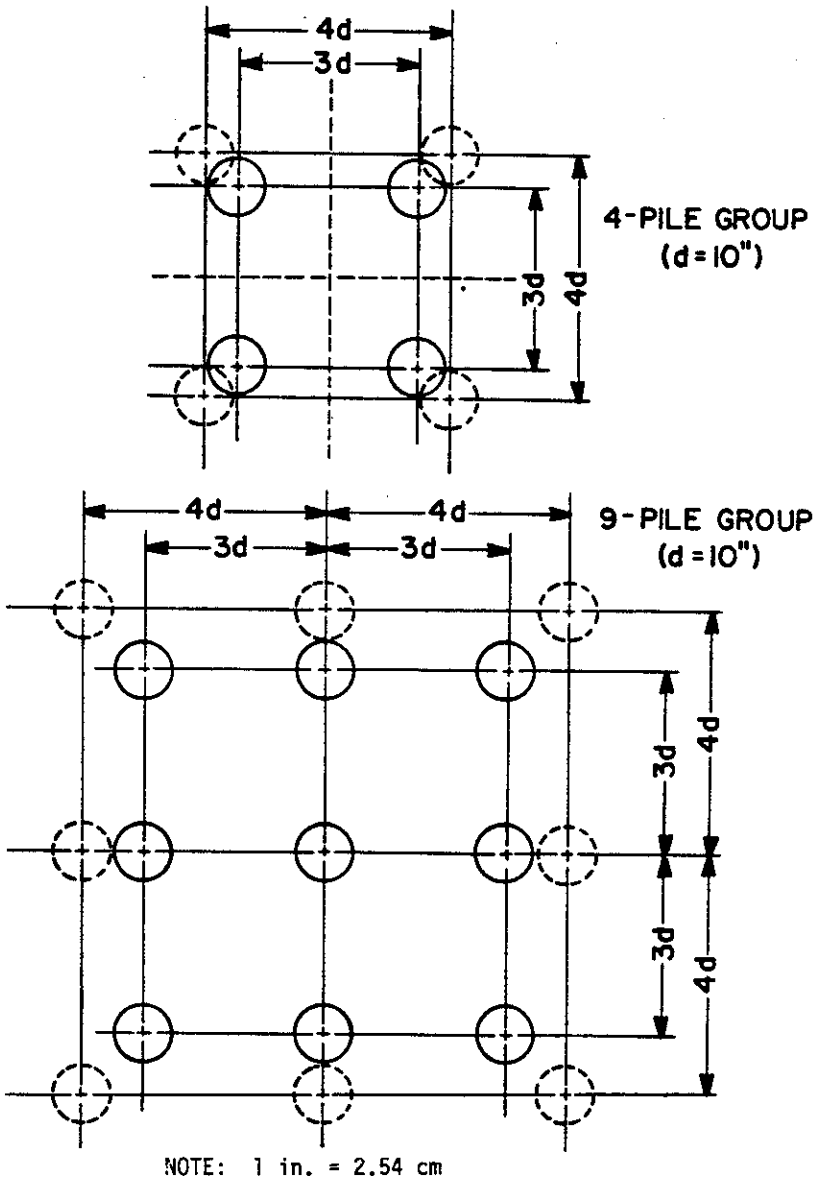

FIGURE 3.1. GEOMETRICS OF HYPOTHETICAL PILE GROUPS IN PARAMETER STUDY

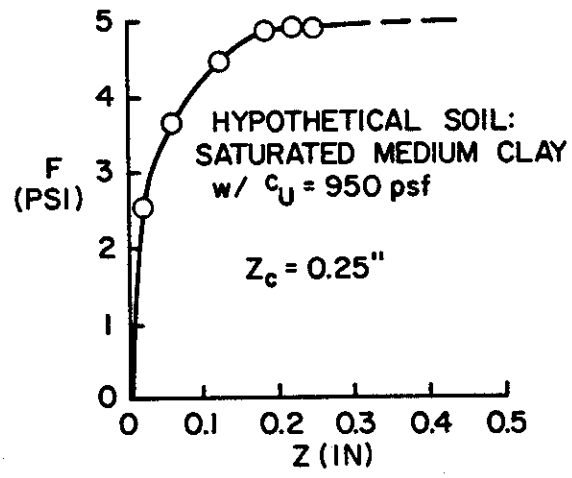

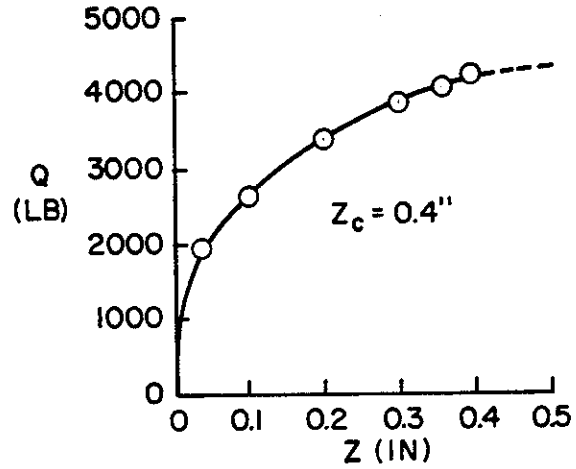

NOTE: 1 in. = 2.54 cm 1 lb = 4.45 N 1 psi = 6.89 kN/m^2 1 psf = 47.9 N/m^2

FIGURE 3.2. HYPOTHETICAL F-Z AND Q-Z CURVES FOR PARAMETER STUDY

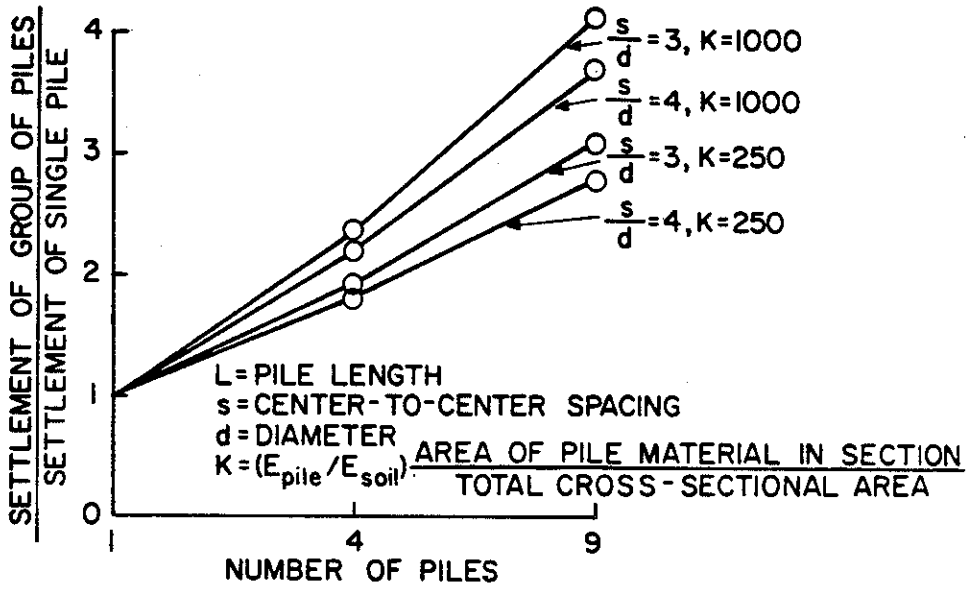

FIGURE 3.3. SETTLEMENT RATIOS; 0.5 x ULTIMATE LOAD; L/D = 25

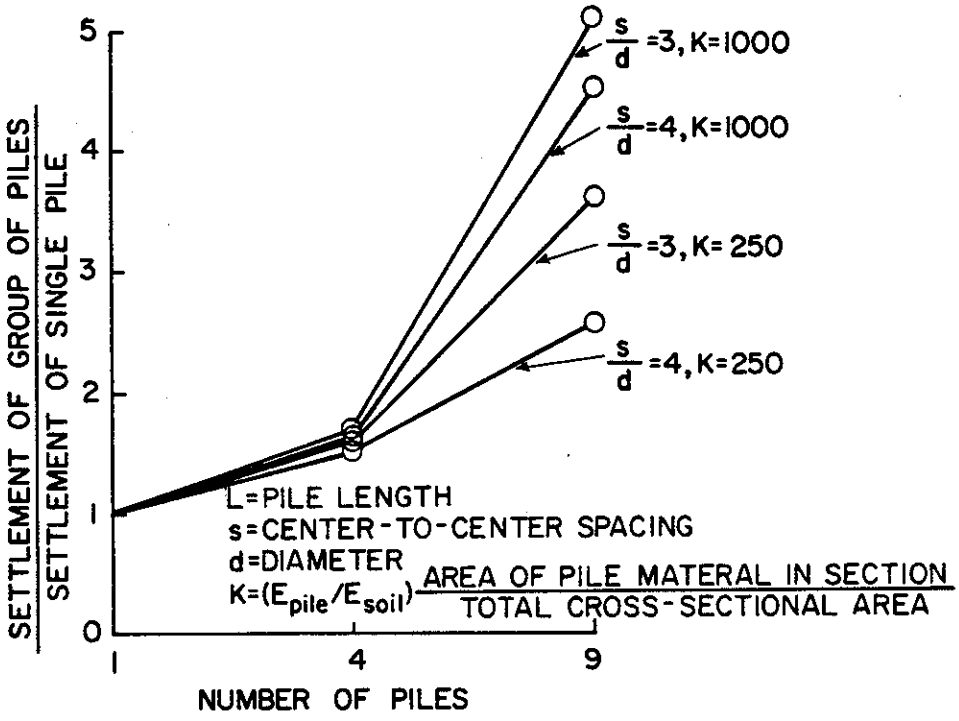

FIGURE 3.4. SETTLEMENT RATIOS; 0.5 x ULTIMATE LOAD; L/D = 50

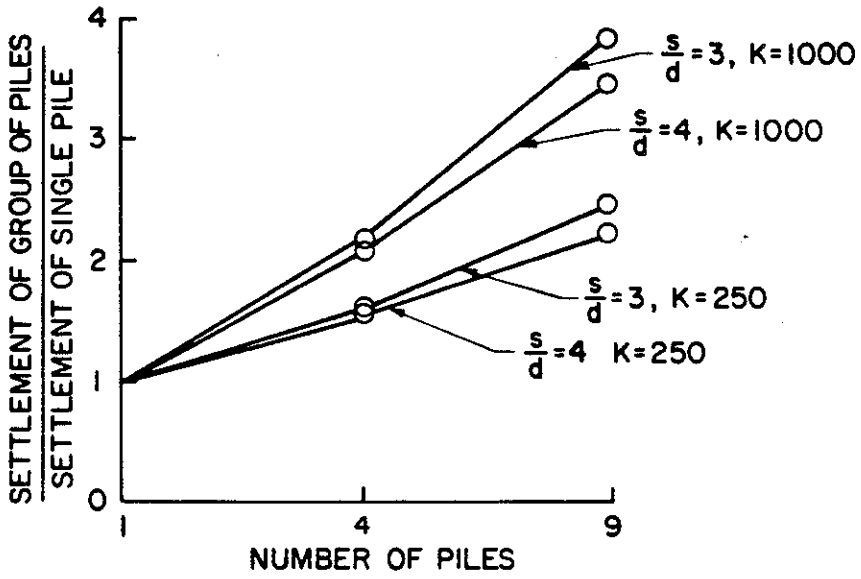

FIGURE 3.5. SETTLEMENT RATIOS; 0.9 x ULTIMATE LOAD; L/D = 25

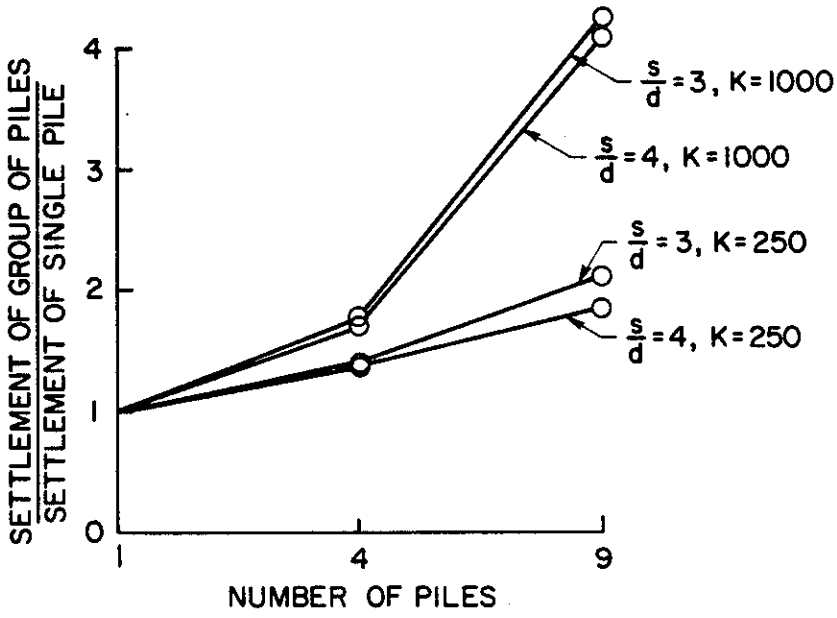

FIGURE 3.6. SETTLEMENT RATIOS; 0.9 x ULTIMATE LOAD; L/D = 50

Figures 3.3 - 3.6 are limited to one special soil type (uniform soil) and are meant only to demonstrate the potential use of the hybrid algorithm in a design office. A considerably more comprehensive parameter study must be undertaken in order to develop general design aids.

Chapter 4. Proposed Group Tests

General

The desirability of load testing full-scale groups of instrumented pile groups is evident for several reasons:

a. A major reason for conducting such tests is to validate and provide improved inputs for an appropriate mathematical model. It is necessary to meet this objective if the test results are to have maximum meaning relative to application of the results to diverse sites. This objective appears to have been absent in most previous studies; however, the hybrid model has been adopted in this study for this purpose. Most previous tests do not have sufficient data to check the hybrid model. As a minimum, the data required for execution of the hybrid model are a profile of undisturbed shear strength; a profile of the elastic modulus and Poisson's ratio; and a documentation of pile alignment, spacing, lengths, etc. (It will be demonstrated subsequently that misalignment of piles can have an important effect on the load-settlement behavior of a pile group.) In order to test the model's output, the group load-settlement relationship should be measured, and load distribution patterns, the loads on the pile heads and load-settlement behavior should be measured for every pile in the system. Similar data should be obtained for at least one reference pile.

The existing tests are deficient in these data. Only three of the group tests studied had reliable soil strength data, but none had adequate information on in-situ moduli, and none had information on true pile alignment. Only one of the tests had load transfer data for every pile in the group. Therefore, additional studies are required to validate the hybrid model.

b. Physical modeling is questionable in this regard because model tests cannot be used to scale such phenomena as in-situ stress magnitudes, rates of pore pressure dissipation, arching in granular soils, and certain microstructural effects in cohesive soils (e.g., tests in compacted or remolded soils may yield different results than those in naturally sedimented soils, particularly those subjected to past stress relief). Installation effects are also very difficult to simulate in model tests. Model tests, while useful in investigating some effects, will not by themselves serve as a model validation.

c. The greatest degree of success in applying load transfer functions to a wide variety of sites would be anticipated to occur when limiting values of load transfer can be expressed in terms of consolidation stresses or effective stresses rather than total stresses, as is now the case. None of the reported tests in clay attempted to correlate load transfer to consolidation stresses or effective stresses.

d. It is uncertain whether an "efficiency" (or block failure) model is required in stiff, overconsolidated clays. A full-scale group test in such soil would be helpful to make this determination.

It is apparent, then, that a field study of the behavior of pile groups is warranted. Philosophically, that study will be designed and conducted in such a way that the parameters that will be measured will serve not only as inputs and as checks on the outputs of the hybrid model but also will be appropriate for investigating other superior models, such as an "ideal" finite element model, that might be developed in the future.

General Conditions for Proposed Tests

The proposed tests will be conducted on the central campus of the University of Houston in an overconsolidated clay. This specific site was selected for several reasons:

a. The behavior of pile groups in overconsolidated clay is not well-understood, and testing in such a soil will be an important contribution. This statement remains true even if gross instrumentation failure were to occur, because valuable information can be gained regarding efficiency in overconsolidated clay.

b. Overconsolidated clay more nearly approximates an elastic halfspace than do sands or normally consolidated clays; hence, it provides a more ideal setting in which to make the first comprehensive test of the hybrid model.

c. The behavior of single piles is fairly well understood in this soil.

d. The geotechnical properties of the principal formation, the Beaumont Clay, have been studied extensively by consultants and researchers.

e. The soil has strength sufficient such that residual stresses in the piles and the effects thereof may be observable. Yet, the soil, whose average overconsolidation ratio in the depth of interest is about five, will develop positive pore pressures when piles are driven, so that time-related effects may also be observable.

f. The soil provides high capacity for uplift anchors, which can be installed relatively inexpensively, while it restricts the maximum compression capacity of the group to a value for which a reaction system can be designed and constructed within the budgetary constraints of the project.

g. The site is convenient, and data acquisition equipment can be operated inexpensively in a controlled environment.

The proposed test site is to the immediate east of the University of Houston Band Annex. A profile of the undrained shear strength at the site, obtained from old borings adjacent to the site is shown in Fig. 4.1. This profile was obtained through a combination of consolidated-undrained triaxial, unconfined compression, and pocket penetrometer tests and should be considered preliminary. (Further detailed studies, conducted after this chapter was written are described in Chapter 5.)

Load tests will be conducted on a group of nine steel pipe piles, depicted in Fig. 4.2, approximately ten, thirty, and sixty days after the group is installed. (Note that the pile numbering system shown here is different from that actually used.) Comparison tests will be conducted at similar times after installation on two reference piles to be located near the group. The two reference piles will be identical to the group piles and will be tested in the same manner, except that the first test on one reference pile will be a "quick test" (modified constant rate of penetration test in which load will be applied in ten-ton (89 kN) increments every 150 seconds until failure occurs. All eleven piles will be sealed at the tip with a boot plate that is flush with the cylindrical surface of the pile. Duplicate testing of two reference piles will give some measure of the potential random variation in single pile behavior at the test site.

After the nine-pile group has been tested the edge piles will be detached from the cap, and the remaining piles will be tested in compression as a subgroup. (Actually, the corner piles were ultimately

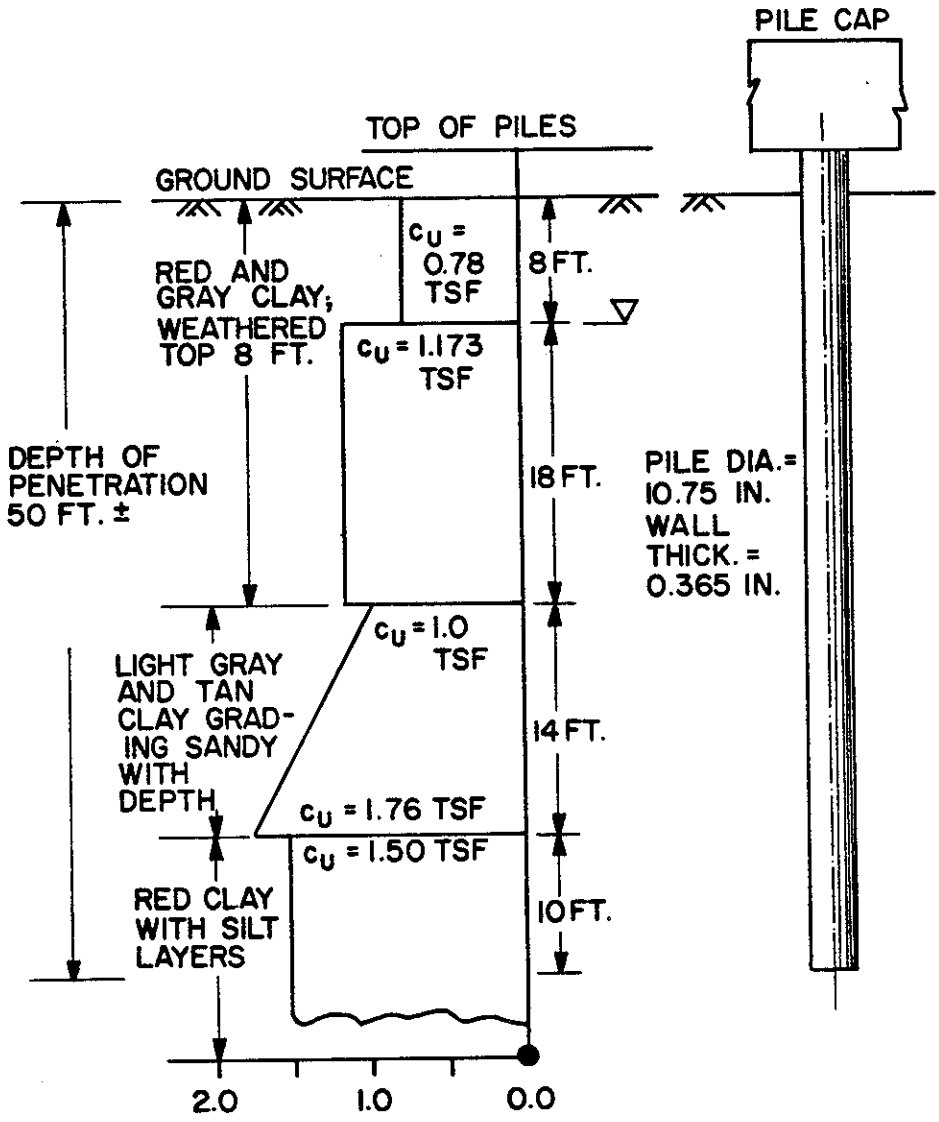

NOTE: 1 in. = 2.54 cm 1 ft = 0.305 m 1 tsf = 95.8 kN/m^2

FIGURE 4.1. PRELIMINARY UNDRAINED SHEAR STRENGTH PROFILE ALONG THE LENGTH OF THE PILES

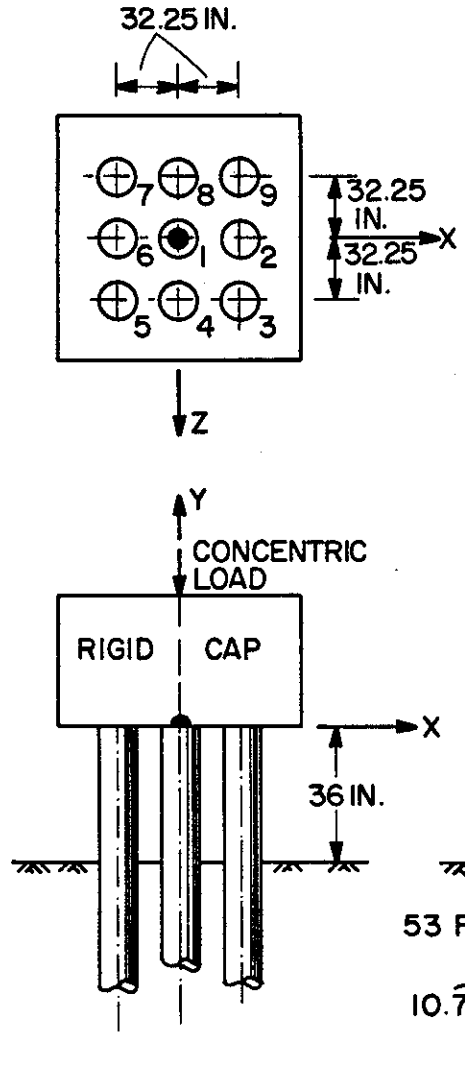

NOTE: 1 in. = 2.54 cm

FIGURE 4.2. NINE-PILE GROUP (CASE A)

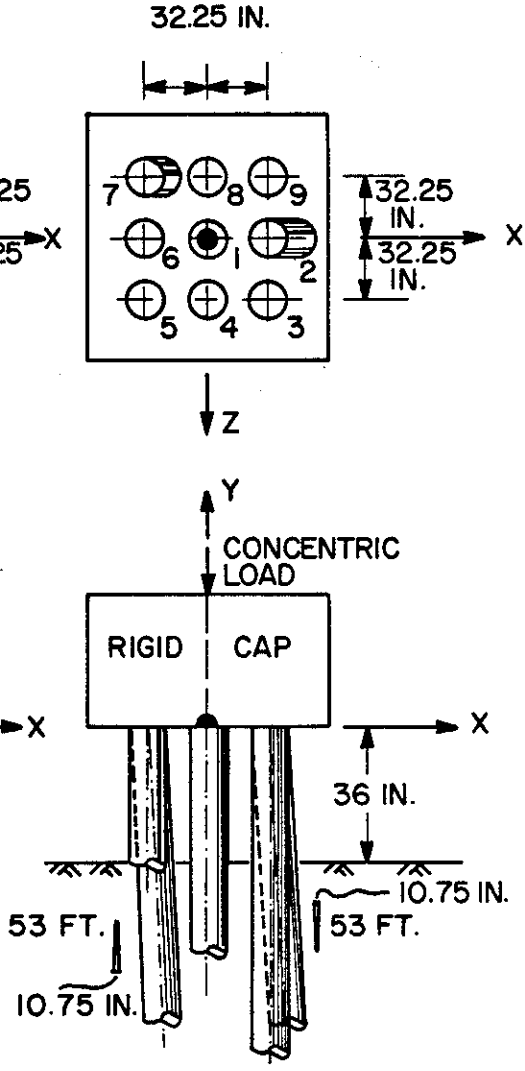

NOTE: 1 in. = 2.54 cm 1 ft = 0.305 m

FIGURE 4.3. NINE-PILE GROUP WITH TWO PILES BATTERED INADVERTENTLY (CASE B)

detached, rather than the edge piles, to provide a tighter grouping for the subgroups.) Following that test, the center pile will be detached from the cap, and the remaining four corner piles will be tested in compression as a subgroup. The tests will be conducted in this sequence to observe time-dependent effects in the nine-pile group and the effects of pile spacing on pile-soil-pile interaction. At the completion of compression testing, four of the group piles and both of the reference piles will be tested in uplift as a gross check of the developed shaft resistance and as a means of studying residual stresses (32).

The test group will consist of 10.75-inch (27.3-cm) o.d. steel closed-ended pipe piles with a nominal 3/8-inch (1-cm) thick wall. The base closure plates will be flush with the sides of the piles. The piles will be spaced three diameters on centers in a square array, representative of a typical bridge foundation. Preliminary site studies (Fig. 4.1) indicated that the piles could penetrate to 50 feet (15.3 m) below grade. The analyses described later in this chapter presume this penetration. (Detailed geotechnical studies described in Chapter 5, made after these analyses were conducted, revealed that dense silt was encountered at a depth of 50 feet (15.3 m) so that the actual design penetration was shortened to 43 feet (13.1 m) below grade. Reanalysis of the group and reference piles with the slightly shallower penetration is made later in the Final Report in conjunction with data analysis.) These dimensions realistically represent a full-scale foundation. Steel pipe piles were chosen as a means of providing maximum protection for instrumentation (most of which will be mounted internally) and for ease of data interpretation.

Since cap-soil interaction is apparently inconsistent and since it is unlikely that cap bearing will be used in the future in the design of pile groups in clay, the cap will not be placed in contact with the ground during this study. It will be suspended approximately three feet (1 m) off the ground to permit insertion of reference beams and dial gages.

It is perhaps desirable to vary parameters such as pile penetration and spacing at time of installation and to test load various piles in the group after the group piles are driven, but before the group is tested as a whole, in order to separate mechanical interaction effects from

effects due only to stress and soil property changes induced by installing nearby piles. However, such considerations have been eliminated from these tests due to budgetary limitations.

Mathematical Modeling of UH Tests

The nine-pile group, four- and five-pile subgroups and reference piles have been modeled on the digital computer using a version of the hybrid model. Baseline load transfer functions have been employed (Eqs. (1.3), (1.4), and (1.6)), and the soil profile and pile penetration shown in Fig. 4.1 has been assumed. Mathematical modeling of the proposed test was done for several reasons:

a. To obtain a "Class A" (before-the-fact) prediction of the behavior of the group as a means of validating the hybrid model for this case.

b. To provide a basis for the final selection of locations, ranges, and sensitivities of instruments to be used in the tests.

c. To provide criteria for shut down of a test due to excessive tilting or lateral translation of the pile cap.

d. To provide load distribution data for the structural design of the pile cap.

Five cases for group analysis were considered, as depicted in Figs. 4.2 - 4.6. Case A (Fig. 4.2) represents the ideal case for the nine-pile group. Case B (Fig. 4.3) represents a model of a possible "as-driven" case, in which a net of two piles are battered slightly as indicated. Case C (Fig. 4.4) represents an extreme case in which the last three piles (7,8, and 9) develop only half the resistance of the remaining piles and are only half as stiff, coupled with an eccentric load applied one foot (0.305 m) from the center of gravity of the group. An extreme freestanding pile length of five feet (1.53 m) has also been assumed for Case C. Case D (Fig. 4.5) represents the ideal case for five-pile subgroup, and Case E (Fig. 4.6) represents the ideal four-pile subgroup. In Cases B and C it was also necessary to input lateral load transfer functions. For the sake of brevity, these relationships are not reproduced here. References on the development of such relationships are contained in Ref. 49. The hybrid model permits a variation of the fixity condition between pile cap and piles (fixed, pinned, or intermediate restraint). Complete fixity was assumed for Cases B and C,

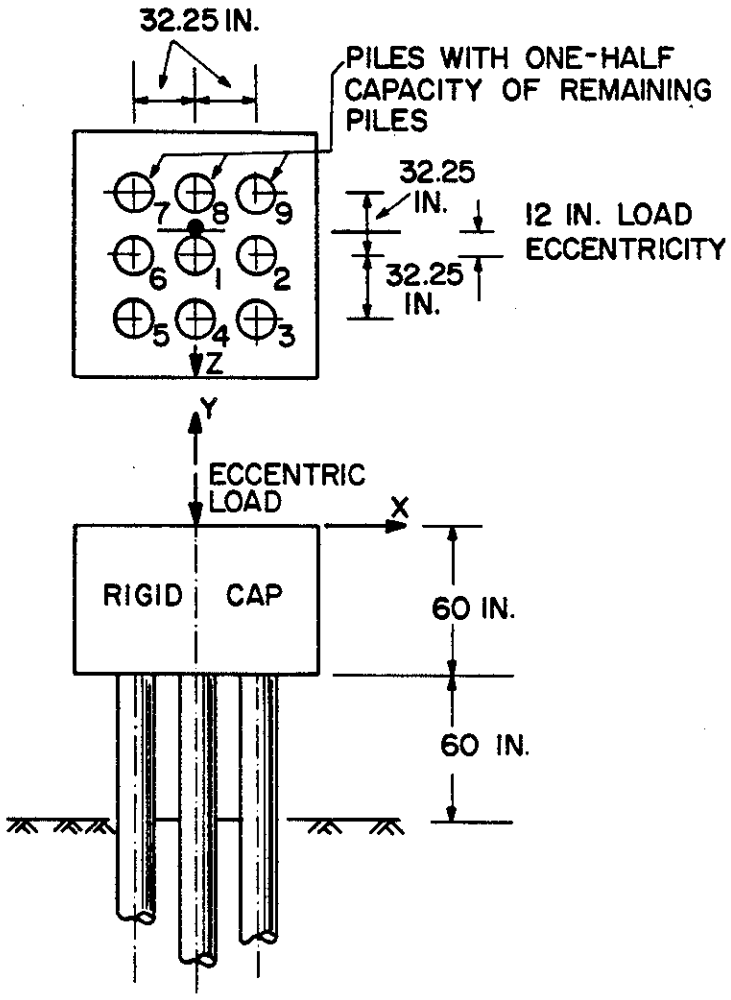

NOTE: 1 in. = 2.54 cm

FIGURE 4.4. NINE-PILE GROUP WITH LOAD 12 IN. (0.305 M) ECCENTRIC TO THE PILE CAP CENTER AND THREE PILES HAVING REDUCED CAPACITY (CASE C)

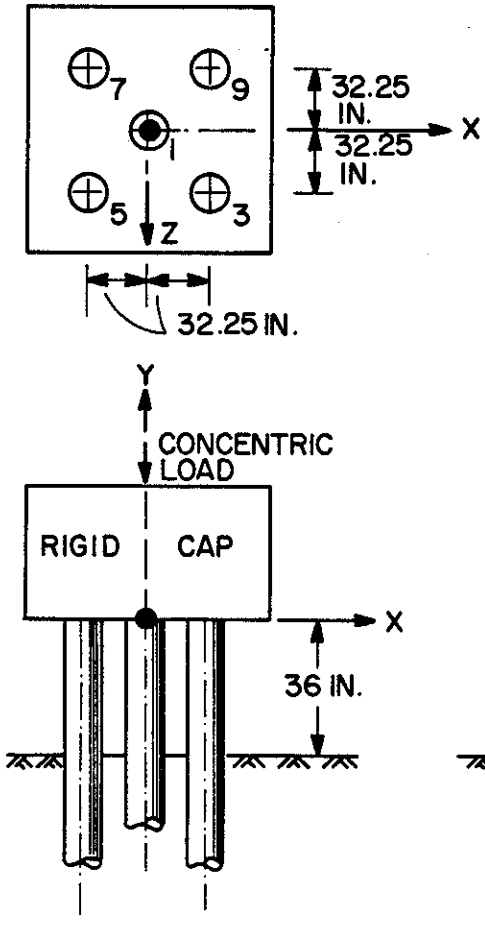

NOTE: 1 in. = 2.54 cm

FIGURE 4.5. FIVE-PILE SUBGROUP (CASE D)

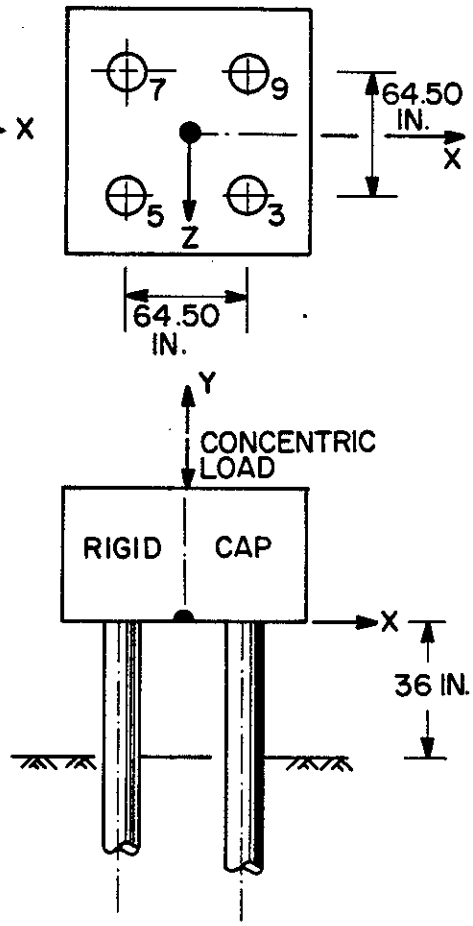

NOTE: 1 in. = 2.54 cm

FIGURE 4.6. FOUR-PILE SUBGROUP (CASE E)

which produce lateral deformations. (The cap detail shown in Chapter 5 will produce essentially complete fixity.)

Tables 4.1 and 4.2 summarize construction of the f-z relationships. In Table 4.1 a relationship has been developed for a standard clay having an undrained shear strength of 1000 psf (47.9 kN/m^2). There are several slight discrete changes in soil strength in Fig. 4.1 from the top of the pile to the bottom, so Table 4.2 was developed to adjust the f-values by the ratio of undrained cohesion at a given depth to 1000 psf (47.9 kN/m^2), the cohesion value for the "standard" soil. The f-z relationships at levels intermediate to those shown in Table 4.2 are obtained internally in the computer program by linear interpolation. Construction of the Q-z relationships for the piles at the site is shown in Table 4.3, and the f-z and Q-z curves are shown graphically in Figs. 4.7 and 4.8. A value of z_c of 0.2 inches (0.5 cm) was chosen based on inferences from the BRE tests and experiences with piling in overconsolidated clay.

Structural properties of the closed-ended pipe piles to be used in the tests are tabulated in Table 4.4. Elastic moduli for the pile-soil-pile interaction calculations were chosen based on the study outlined in Chapter 2. It appears that an appropriate range of values for E is 400-800 c_{uavg}, or 6870 psi (47.3 mN/m^2) to 13,740 psi (94.7 mN/m^2). Calculations were made for both values of E for Case A in order to study the effects of E on the outputs. The remaining cases were studied assuming that E = 13,740 psi (94.7 mN/m^2), which appears to be the single most appropriate value for E based on knowledge of the soil before detailed studies were made. The value of Poisson's ratio was kept at 0.5 because the soil is essentially fully saturated and because the proposed tests will be short-term in nature.

The calculations for predicted capacities of the reference pile and pile groups are shown in Table 4.6. The reference pile capacity is predicted to be 191,000 lbs. (850 kN), and that of the nine-pile group is predicted to be 1,719,000 lbs (860 tons) (7,650 kN) assuming a group efficiency of unity. The cap, loading, and reaction systems will be designed to take safe working loads of 40 percent in excess of these theoretical values (or 1200 tons (10,700 kN)), as it is intended to carry the tests to ultimate failure even if the capacities have been underpredicted.

TABLE 4.1. CONSTRUCTION OF BASIC AXIAL SHAFT LOAD TRANSFER FUNCTION

$$f = f_{max} [2 (z/z_c)^{0.5} - z/z_c]$$

Choose z_c = 0.2 inches (0.5 cm) for Beaumont Clay and assume no residual stresses:

$$f = f_{max} [4.47 (z)^{0.5} - 5(z)]$$

For basic curve let f_{max} = 1000 psf = 6.94 psi (47.9 kN/m^2) arbitrarily.

Z (in.)	f (psi)
0	0
0.067 (z_c/3)	5.79
0.133 (2z_c/3)	6.68
0.20 (z_c)	6.94
10*	7.0*

*Arbitrary input for limiting deflection

For any depth: f = f (above table) x LM (Table 4.2)

Note: 1 in. = 2.54 cm
1 psi. = 6.89 kN/m^2

TABLE 4.2. LOAD MULTIPLIER FOR f-z CURVES

f-z Curve No.	Depth (Below Pile Tops) (ft)	Load Multiplier (LM)*
1	0.0	0.0
2	3.0	0.0
3	4.0	0.780
4	11.0	0.780
5	12.0	1.173
6	29.0	1.173
7	30.0	1.000
8	43.0	1.760
9	44.0	1.500
10	53.0	1.500

*Based on $f_{max} = 0.5\ c_u$ (API criterion, Ref. 1)
LM = one-half of these values for piles 7, 8, and 9, Case C

Note: 1 ft. = 0.305 m

TABLE 4.3. CONSTRUCTION OF TIP LOAD TRANSFER FUNCTION

$Q = (z/z_c)^{1/3} Q_{max}$

$Q_{max} = 9\ c_{u\ tip}$ (tip area)

$= 9\ (3000)\ (0.63) = 17{,}000$ lb (75.7 kN)

Choose $z_c = 0.2$ inches (0.5 cm) and assume no residual stresses

Z (in.)	Q (lb)
0	0
0.05	10,700
0.10	13,500
0.20	17,000
10*	18,000*

*Arbitrary input for limiting deflection. Q-values are one-half these values for piles 7, 8, and 9, Case C.

Note: 1 in. = 2.54 cm

1 lb. = 4.45 N

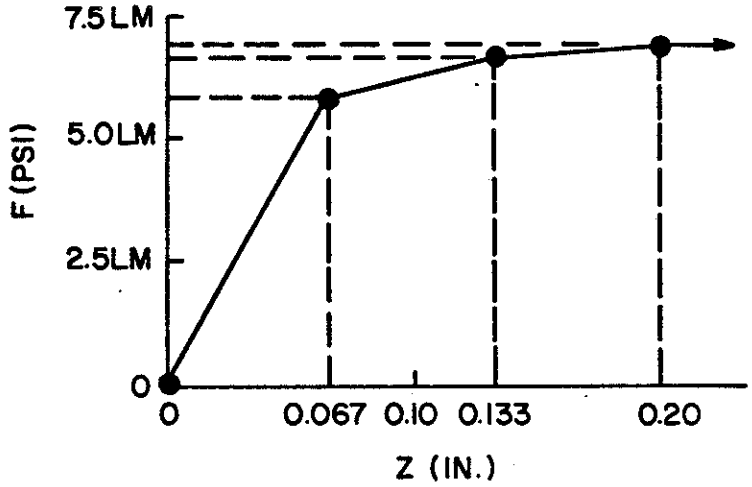

NOTE: 1 in. = 2.54 cm 1 psi = 6.89 kN/m^2

FIGURE 4.7. BASIC AXIAL SHAFT LOAD TRANSFER FUNCTION (F-Z CURVE) (LM=LOAD MULTIPLIER AT DIFFERENT DEPTHS TO CORRESPOND TO CHANGES IN SHEAR STRENGTH)

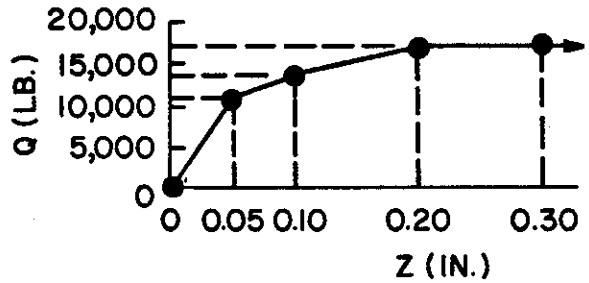

NOTE: 1 in. = 2.54 cm 1 lb = 4.45 N

FIGURE 4.8. TIP LOAD TRANSFER FUNCTION

TABLE 4.4. STRUCTURAL PROPERTIES OF PILES

Cross-sectional area	11.91 in^2
Young's modulus	29,000,000 psi
Tip area	90.8 in^2
Diameter	10.75 in
Perimeter	33.77 in
Wall thickness	0.365 in

Moments of Inertia

About axis parallel to X	160.1 in^4
About axis parallel to Y	160.1 in^4
Polar	320.1 in^4

Note: 1 in. = 2.54 cm
1 $in.^2$ = 6.45 cm^2
1 $in.^4$ = 41.6 cm^4
1 psi = 6.89 kN/m^2

TABLE 4.5. MODULI OF SOIL FOR PILE-SOIL-PILE INTERACTION CALCULATIONS

Poisson's ratio 0.5

Young's Modulus, Constant with Depth

Case 1 . . . . . 400 c_{uavg} = 6870 psi
Case 2 . . . . . 800 c_{uavg} = 13,740 psi

The average value of c_{uavg}, from Fig. 4.1, is 2474 psf = 17.18 psi

Note: 1 psi = 6.89 kN/m^2
1 psf = 47.9 N/m^2

TABLE 4.6. ULTIMATE COMPRESSIVE CAPACITIES OF SINGLE PILE AND PILE GROUPS

Single Pile (Reference)

1.	Average undrained cohesion	2.474 ksf
2.	Factor α (Ref. 1)	0.50
3.	Average f_{max} (1x2)	1.237 ksf
4.	Perimeter distance	2.814 ft
5.	Nominal penetration	50 ft
6.	Perimeter area (4x5)	140.7 ft^2
7.	Shaft capacity (3x6)	174.0 k
8.	Tip capacity (Table 4.3)	17.0 k
9.	Total capacity (7+8)	191.0 k

Pile Groups*

10.	9-pile (9 x total single pile capacity) . . .	1719 k
11.	5-pile subgroup (5 x total single pile capacity)	955 k
12.	4-pile subgroup (4 x total single pile capacity)	764 k

*Based on efficiency of unity for ultimate capacity

Note: 1 ft. = 0.305 m
1 k = 4.45 kN
1 ksf = 47.9 kN/m^2

The salient results of the computer study are given in Figs. 4.9 -4.19 and in Tables 4.7 - 4.9. Figure 4.9 shows the predicted load-settlement curve for a reference pile loaded in compression. No residual stresses were assumed to exist in the pile. If residual stresses are present the initial slope of the curve may be somewhat greater than that shown. The load-uplift curve for the reference piles and for the individual piles in the group are expected to mirror the compression curve shown in Fig. 4.9. The predicted load transfer pattern in the reference piles is shown in Fig. 4.10. Load transfer will apparently be relatively uniform. Thus, placement of load and displacement measurement devices on the piles will be at essentially regular intervals.

Figure 4.11 presents the anticipated range of load-settlement curves for Case A. It is realistically expected that the actual curve will be close to the upper curve. Ultimate failure is expected to occur in each of the three tests at a gross settlement of 1.0 to 1.5 inches (2.5-3.8 cm). Based on these data, the cap height will be established such that adequate clearance will exist between the cap and soil to accommodate the reference system after five load tests have been conducted. That is, assuming zero recovery on rebound and ideal geometry, the cap will be about 6-7 inches (15-18 cm) lower upon completion of the group tests than it was at the time of its installation. (In point of fact, considerable elastic recovery may occur.)

The predicted load transfer patterns in the various piles in Case A are shown in Figs 4.12 - 4.14. Also shown on those figures is a solution in which pile-soil-pile interaction is not considered (i.e., a load transfer function model solution). It is evident that group action will cause shaft load transfer to occur at a slightly lower level in each of the piles and that the tip loads are increased slightly at subfailure loads. The load transfer patterns remain relatively uniform, such that essentially regular spacing of axial load and displacement measuring devices will also be maintained on the group piles. The value of E within the range studied has a relatively small effect on the load transfer pattern.

Distribution of loads among the various pile heads is tabulated for Cases A, B, and C, for several values of load in Tables 4.7, 4.8 and

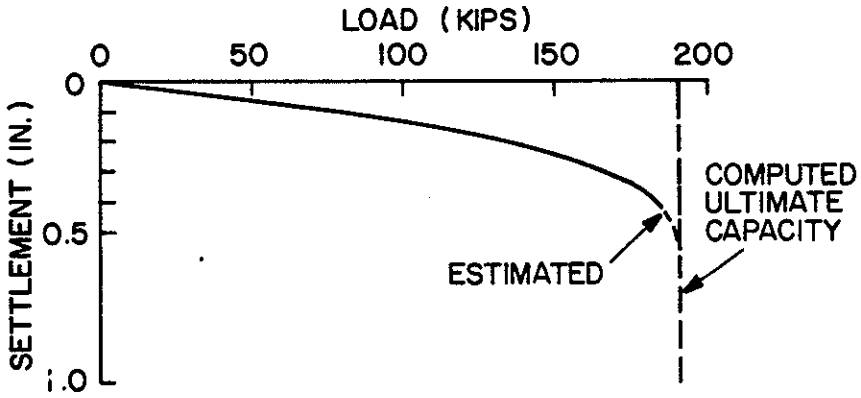

NOTE: 1 in. = 2.54 cm 1 kip = 4.45 kN

FIGURE 4.9. PREDICTED LOAD-SETTLEMENT CURVE FOR REFERENCE PILE

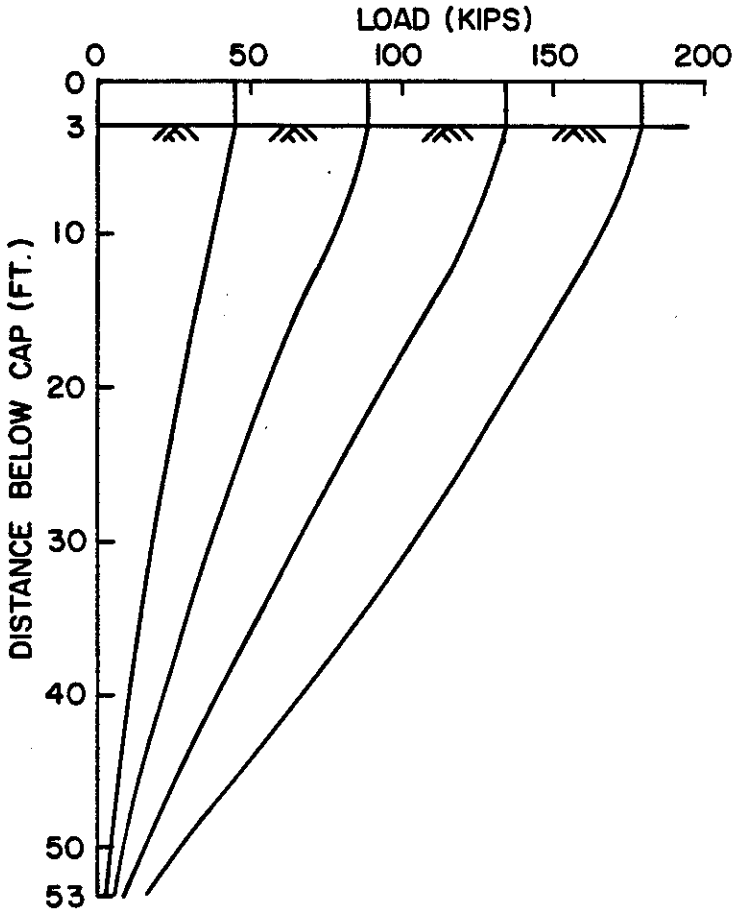

NOTE: 1 ft = 0.305 m 1 kip = 4.45 kN

FIGURE 4.10. PREDICTED LOAD VS. DEPTH PATTERNS FOR REFERENCE PILE

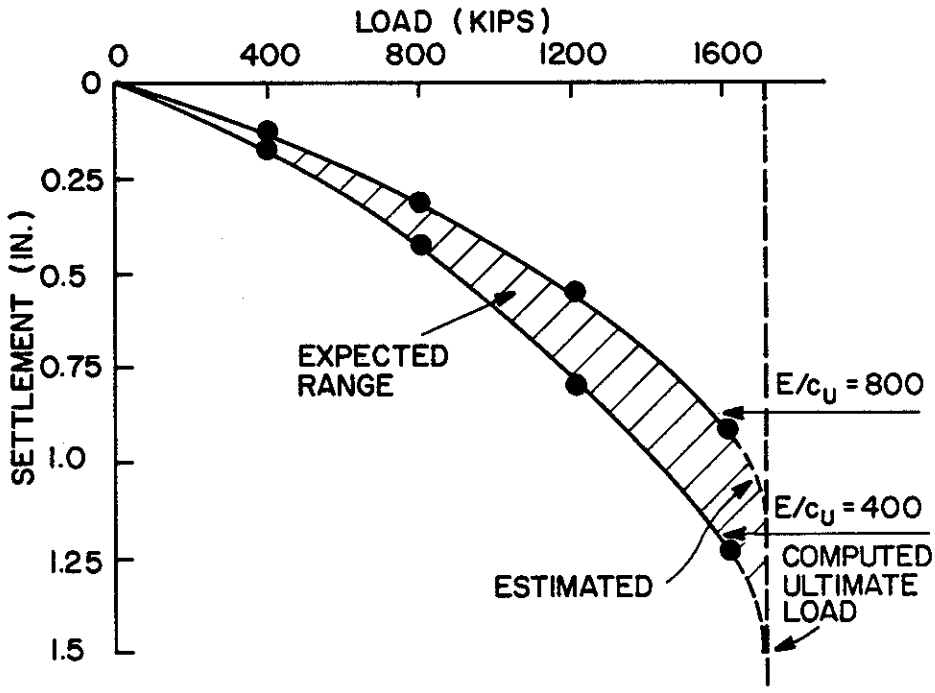

NOTE: 1 in. = 2.54 cm 1 kip = 4.45 kN

FIGURE 4.11. PREDICTED LOAD-SETTLEMENT CURVE FOR NOMINAL NINE-PILE GROUP (CASE A)

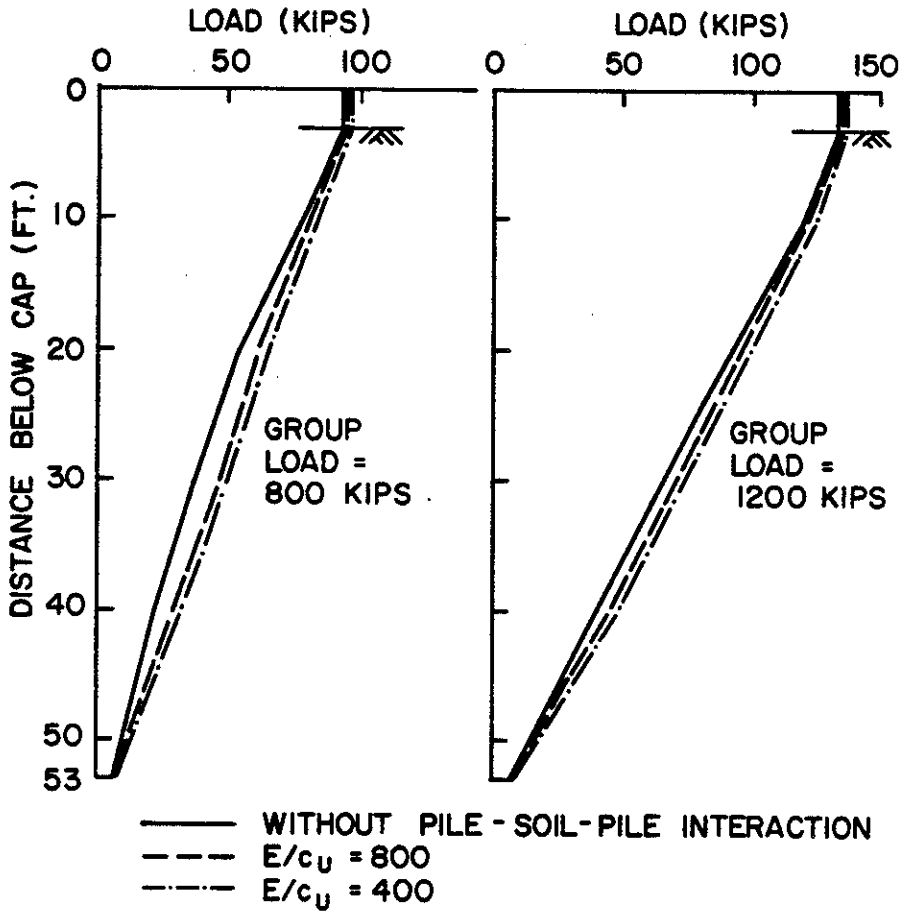

NOTE: 1 ft = 0.305 m 1 kip = 4.45 kN

FIGURE 4.12. PREDICTED AVERAGE LOAD VS. DEPTH PATTERNS FOR CORNER PILES, NINE-PILE GROUP (CASE A)

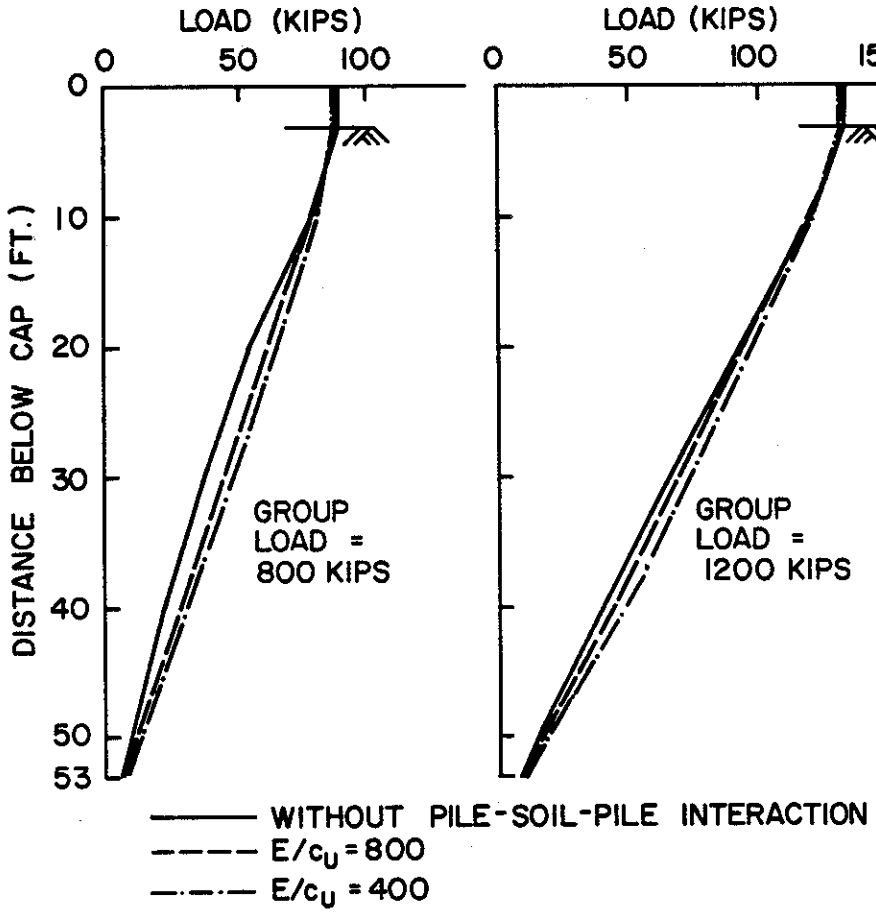

NOTE: 1 ft = 0.305 m 1 kip = 4.45 kN

FIGURE 4.13. PREDICTED AVERAGE LOAD VS. DEPTH PATTERNS FOR EDGE PILES, NINE-PILE GROUP (CASE A)

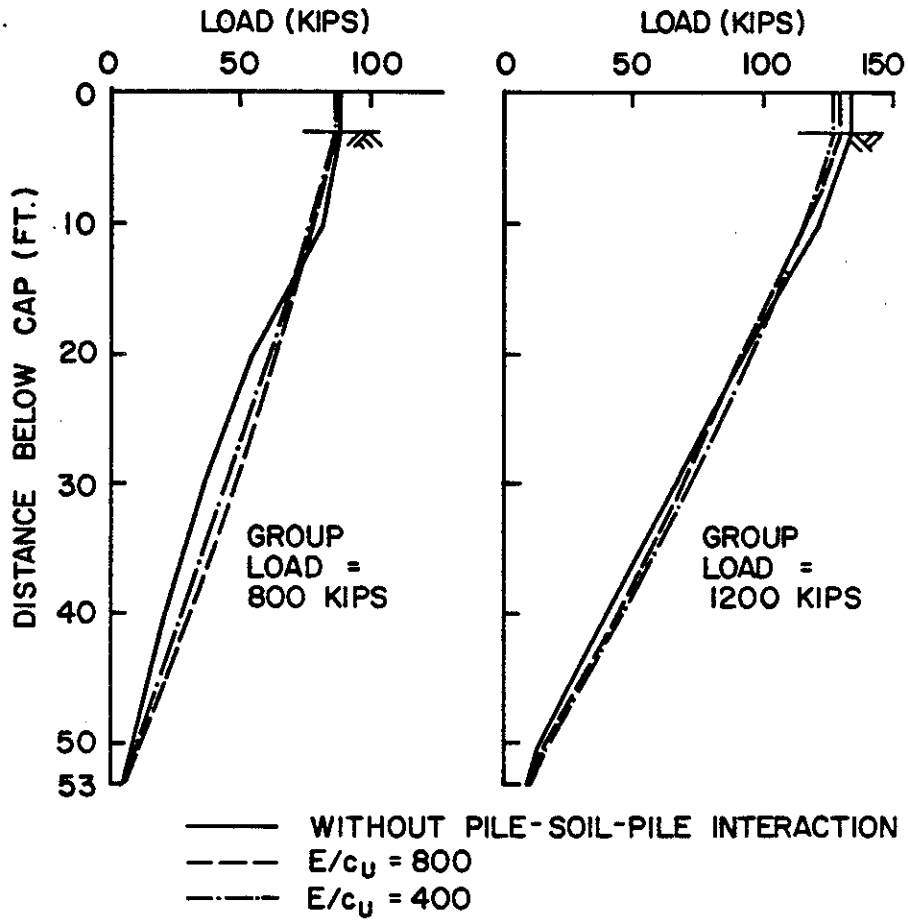

NOTE: 1 ft = 0.305 m 1 kip = 4.45 kN

FIGURE 4.14. PREDICTED LOAD VS. DEPTH PATTERNS FOR CENTER PILE, NINE-PILE GROUP (CASE A)

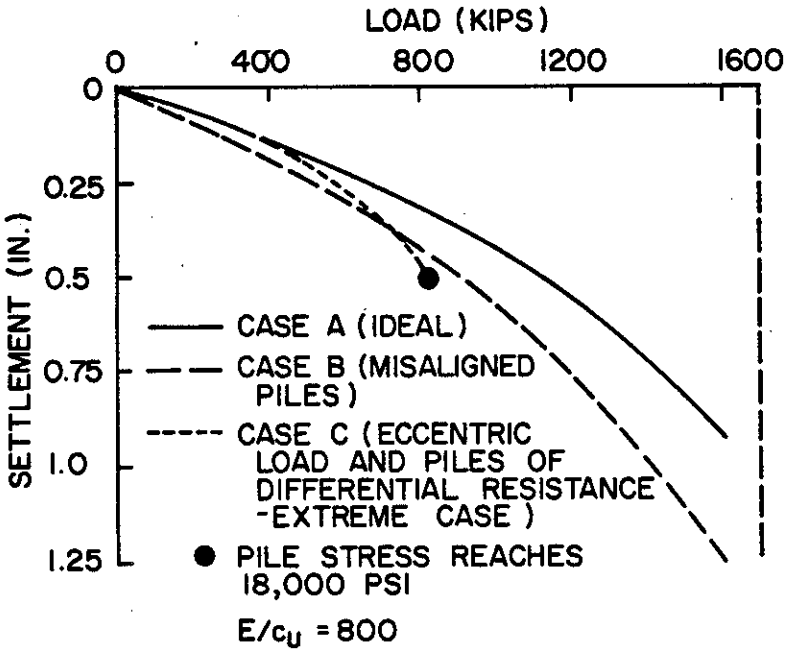

NOTE: 1 in. = 2.54 cm 1 kip = 4.45 kN 1 psi = 6.89 kN/m^2

FIGURE 4.15. EFFECT OF PILE ALIGNMENT, DIFFERENTIAL RESISTANCE, AND ECCENTRIC LOADS, NINE-PILE GROUP

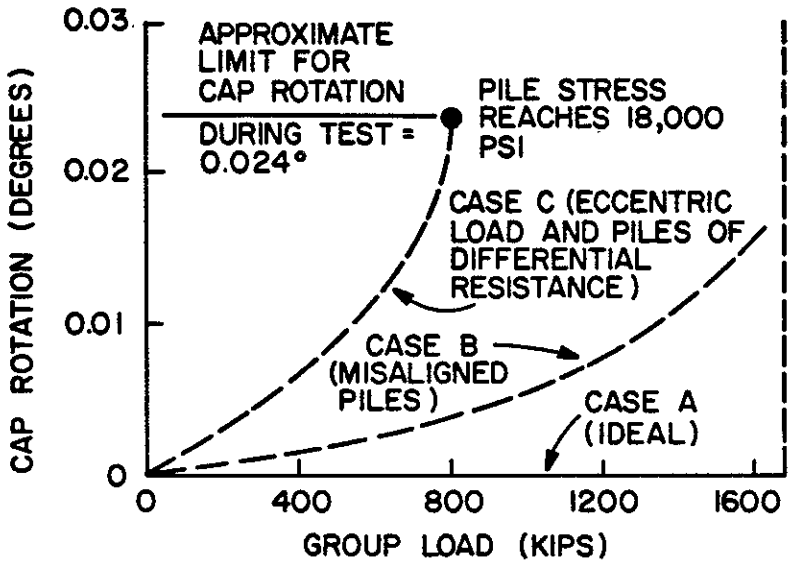

NOTE: 1 kip = 4.45 kN 1 psi = 6.89 kN/m^2

FIGURE 4.16. EFFECT OF PILE ALIGNMENT, DIFFERENTIAL RESISTANCE, AND ECCENTRIC LOADS, NINE-PILE GROUP, E/c_u = 800, ON CAP ROTATION

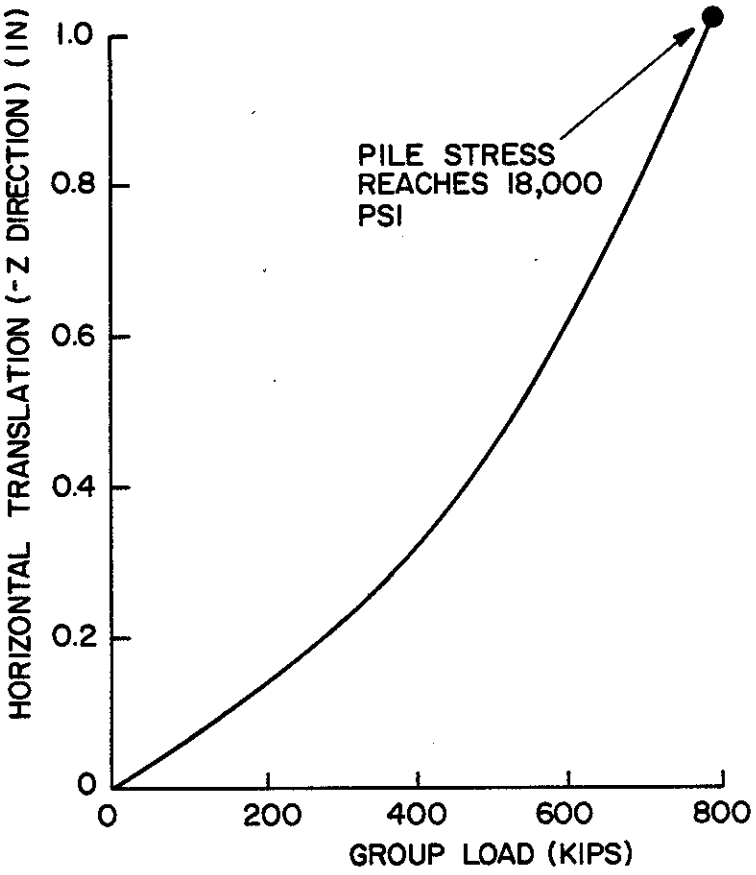

NOTE: 1 in. = 2.54 cm 1 kip = 4.45 kN 1 psi = 6.89 kN/m^2

FIGURE 4.17. PREDICTED HORIZONTAL TRANSLATION OF TOP OF PILE CAP FOR CASE C, E/c_u = 800

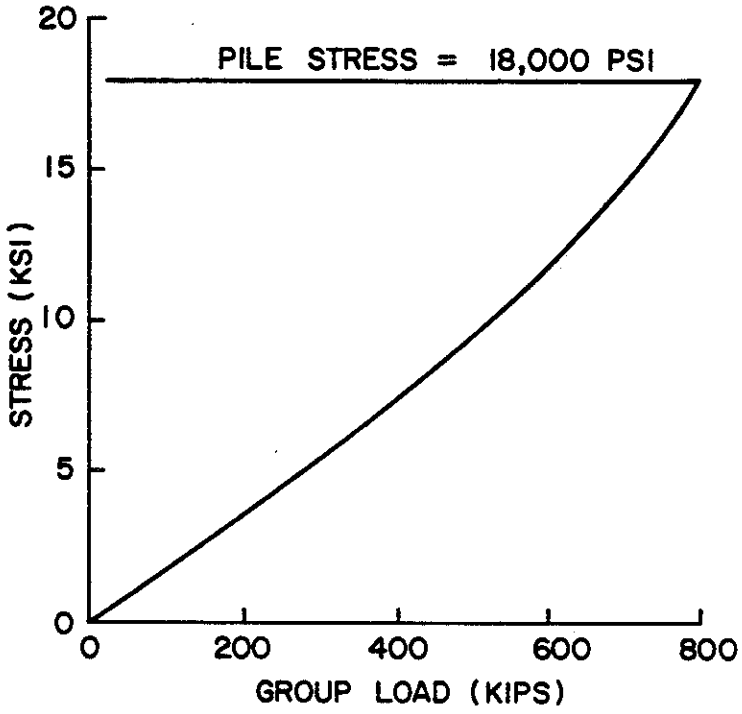

NOTE: 1 kip = 4.45 kN 1 psi = 6.89 kN/m^2 1 ksi = 6.89 mN/m^2

FIGURE 4.18. PREDICTED MAXIMUM COMBINED AXIAL AND FLEXURAL STRESS, CASE C, E/c_u = 800 (OCCURS AT HEADS OF PILES 7 and 9)

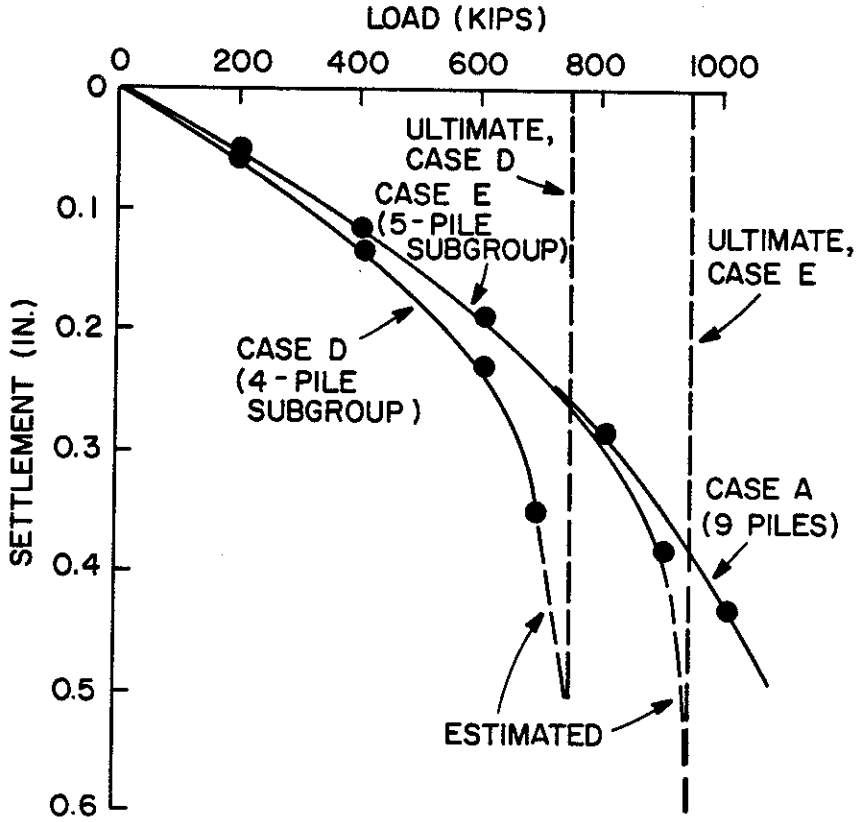

NOTE: 1 in. = 2.54 cm 1 kip = 4.45 kN

FIGURE 4.19. PREDICTED LOAD-SETTLEMENT CURVES FOR FOUR- AND FIVE-PILE SUBGROUPS (CASES D AND E) COMPARED WITH PREDICTED CURVE FOR NINE-PILE GROUP

TABLE 4.7. COMPUTED DISTRIBUTION OF LOADS TO PILE HEADS, CASE A

Group Load (kips)	Pile	Load on Pile Head (kips)	
		$E/c_u = 400$	$E/c_u = 800$
400	Corner (3, 5, 7, 9)	45.0	44.8
	Edge (2, 4, 6, 8)	44.2	44.3
	Center (1)	43.2	43.6
800	Corner (3, 5, 7, 9)	90.4	90.0
	Edge (2, 4, 6, 8)	88.2	88.4
	Center (1)	85.7	86.6
1200	Corner (3, 5, 7, 9)	136.2	135.3
	Edge (2, 4, 6, 8)	132.0	132.4
	Center (1)	127.4	129.3
1600	Corner (3, 5, 7, 9)	181.2	
	Edge (2, 4, 6, 8)	176.4	*
	Center (1)	169.8	

*Not obtained

Note: 1 kip = 4.45 kN

TABLE 4.8. COMPUTED DISTRIBUTION OF LOADS TO PILE HEADS, CASE B

Group Load (kips)	Pile	Axial Load on Pile Head $E/c_u = 400$
400	1	43.3
	2	43.8
	3	44.4
	4	44.2
	5	45.5
	6	44.7
	7	45.3
	8	44.2
	9	44.6
1200	1	127.6
	2	131.7
	3	134.1
	4	131.8
	5	137.8
	6	134.0
	7	136.6
	8	131.9
	9	134.7

Note: 1 kip = 4.45 kN

TABLE 4.9. COMPUTED DISTRIBUTION OF LOADS TO PILE HEADS, CASE C

Group Load (kips)	Pile	Axial Load on Pile Head $E/c_u = 800$
400	1	55.7
	2,6	56.8
	3,5	16.5
	4	16.2
	8	59.5
	9,7	61.0
600	1	86.4
	2,6	88.7
	3,5	24.2
	4	23.7
	8	86.5
	9,7	88.8

Note: 1 kip = 4.45 kN

4.9. For cap design purposes the data indicate that for Case A (ideal) the corner piles will carry two to three percent more load than the average pile load. The center pile will carry four to five percent less than the average, and the edge piles will carry about one percent less than the average up to a load of 1600 kips (7,120 kN). It is assumed that these ratios are also valid at the ultimate capacity of 1720 kips (7,650 kN). Based on analysis of the tests described in Chapter 2 and upon analysis of Cases B and C, which indicate wide variations in loads due to irregular geometry, eccentric loading, and variable pile behavior, it appears reasonable to design the cap for the full nine-pile group assuming that the corner piles will carry seven percent more than the average failure load of 191 kips (850 kN), the center pile will carry twelve percent less than the average load, and the edge piles will carry four percent less than the average load. In the case of extreme eccentricity of the loads or extreme irregularity of pile capacity (Case C), neither of which is expected to occur, the maximum load that can be placed on the pile group will be governed by flexual considerations in the piles and rotation of the pile cap. Pile loads will not, in such a case, approach the computed ultimate failure loads before the test must be stopped, such that Case C is not critical for design of the pile cap. The same general percentages are applied to the four- and five-pile subgroups as a reflection of possible variable alignment and minor load eccentricites in those tests.

Figure 4.15 compares the predicted load-settlement curves for Cases A, B, and C with $E/c_u = 800$. It is evident that pile misalignment of the type depicted in Case B can produce settlements that are up to one-third higher than those produced in the ideal case. It may thus be possible that the total deflection of the cap for the series of group load tests may exceed seven inches (18 cm) by up to one third. However, considering elastic rebound, it should be adequate to consider a total displacement of eight inches (20 cm) for design purposes. Figure 4.15 also shows that the load-settlement curve for Case C will be very nonlinear, owing to premature failure of the row of weak piles. At a load of 800 kips (3,650 kN), cap rotation and lateral translation will be so large that combined flexural and axial stresses in Piles 7 and 9 will reach 18,000 psi (124 mN/m^2). The nominal yield

point of the steel in the piling (35,000 psi) (241 mN/m^2) would be reached well below the predicted nominal ultimate capacity of 1,720 kips (7650 kN). Thus, with the situation shown in Case C it will be imprudent to attempt to fail the group in the vertical mode.

Predicted cap rotations for Cases B and C are shown in Fig. 4.16. It can be seen that a combination of cap rotation of 0.024 degrees (about the -X axis), which produces a differential settlement of 0.05 inches (0.13 cm) over the 108-inch (2.74-m) span of the cap (described in Chapter 5), and lateral translation (in the Z-direction) of 1.03 in. (2.6 cm) (Fig. 4.17) produce pile stresses of 18 ksi (124 mN/m^2) at the base of the cap for a group load of 800 kips (3.56 mN). This indicates that the pile group cannot be carried to failure in the vertical mode without risking plastic yield of the steel for a pile group in this condition. These predictions suggest that horizontal translations and differential settlement of the pile cap are important and should be measured along and about two orthogonal horizontal axes and that the test should be terminated if they are exessive.

The reaction beams for the test group will be "mobile" during compression testing in that they will be supported by slender tension bars (Dywidag type) that will be anchored over 70 feet (21 m) below the point of connection with the beams. Thus, any lateral deformations that occur will be permitted and will not be resisted by moments or shears in the jacking system, which is described in Chapter 5.

Figure 4.18 shows the rate of build-up of combined stresses in the outer fibers of Piles 7 and 9 in Case C. The predicted load-settlement relationships for the subgroups, Cases D and E, are shown in Figure 4.19. It is apparent that group settlement is not highly sensitive to the number of piles in the group for small values of load.

Criteria for Termination of a Test

The following criteria will be employed to determine when a compression test is to be terminated.

a. Primary Criteria. The normal mode of failure will be failure by some form of excessive movement in the vertical direction. The following criteria will be followed, in the order listed, to ascertain when vertical failure of a reference pile or of a pile group has occurred.

When failure has occurred according to the highest-ranked criterion, the load will be removed in two or three decrements.

(1) Plunging. All compression tests will be conducted to plunging failure (increasing settlement with no increase in applied vertical load) if possible.

(2) Change in Rate of Tip Load Versus Settlement. If plunging failure is not achieved, failure will be defined as follows: Tip load, as obtained by strain gages, will be plotted against tip settlement, as obtained by mechanical extensometers, in the final 30 minutes of a load increment. The point at which a discernable change occurs in the slope of this plot on all piles will be defined as failure.

(3) Rate of Butt Settlement. Granular soils are known to be present several feet below the planned elevation of the pile tips. It is conceivable that their presence may prevent plunging or discernable tip failure. In such a case it is anticipated that the butt load-settlement curve will become linear after a distinct nonlinear zone if the test is conducted by applying uniform load increments at relatively short intervals of time (for example, one hour). The load at which this "terminal linearity" occurs will be defined as failure.

(4) Capacity of the System. If failure as defined by 1, 2, or 3 above has not occured by the time the capacity of the reaction system (1200 tons (10.68 mN)) has been reached, the test will be terminated.

b. Secondary criteria. In order to prevent overstressing of the piles in flexure, a compression test will be terminated if either of the following events occurs.

(1) Relative vertical deformation exceeds 0.35 inches (0.9 cm) over the width of the cap (9 ft (2.75 m)) in either of two horizontal directions.

(2) Lateral translation of the pile cap exceeds 0.30 inches (0.8 cm) in either of two horizontal directions.

The above criteria are based on an independent linear analysis of a group of plumb piles.

Uplift tests will be conducted on six individual piles. Failure for these tests will be defined as the load at which uplift occurs without further increase in load.

In the event of accidental unloading, as may occur with a hydraulic leak, the load will be returned to the load at which the accidental unloading occurred and increased in increments from that point. The criteria for failure in such a case will remain as indicated above.

The 0.05 in./$\sqrt{\text{N}}$ per ton (0.014 cm/$\sqrt{\text{N}}$ per kN) failure criterion examined in Chapter 2 is an arbitrary criterion which does not consider fully the effect that failure is apparently governed by displacement or displacement rate of the pile tips and will therefore not be used in the evaluation of failure in the tests. The MDFL criterion is more rational, but it is unproven in group load tests. Therefore, it also will not be used in the tests.

Specific Measurements

The measurements for the field tests will be designed to provide complete data for developing inputs to and checking outputs from the hybrid model. Additionally, data will be taken that will not be directly applicable to the hybrid model but which are intended to serve as inputs and output checks for "ideal" models that may be developed in the future. Specifically, stress-strain properties of the undisturbed soil, displacements in the soil mass and at the soil surface during installation and load testing, wave propagation within selected piles as they are being driven, and residual stresses in the piling will be measured for this purpose. The following subsections describe the measurements to be made and the requirements for instrumentation, where appropriate. Details of the site investigation, instrumentation, and data acquisition schedules are discussed in Chapter 5.

Soil. The following soil measurements will be made:

a. Classification tests. Moisture content, dry density, Atterberg limits, and grain-size distribution analyses, sufficient in number to classify the soil to a depth of at least three group widths beneath the tips of the piles and to provide data as necessary for installing anchor systems to a greater depth, will be conducted. Tests will be assigned in the laboratory based on visual classification of the samples. It is anticipated that Atterberg limits tests will be conducted on about 30 samples. Moisture content and dry density tests will be conducted on every undisturbed sample to be subjected to a laboratory strength or

consolidation test and on such other samples as may seem desirable. About 60 moisture content and density tests will be performed. Several grain size distribution tests will be conducted to assess sand content as a function of depth.

b. Tests for routine load transfer correlations. It may be desirable to obtain f_{max} and Q_{max} in practice in terms of routinely obtained soil strength data. Therefore, the soil shear strength profile will be represented in terms of the following tests:

(1) Pocket penetrometer and torvane
(2) Standard penetration
(3) Unconfined compression
(4) Unconsolidated-undrained triaxal compression
(5) Static cone penetration (bearing and sleeve friction)

Pocket penetrometer and torvane tests will be made on undisturbed shelby tube samples of cohesive soil. About 60 such samples are anticipated to be recovered.

Standard pentetration tests will be made in one boring at approximately five-foot intervals. (A closer interval will be used in the depth range of 35-45 feet (11-14m) to aid in the selection of a precise tip elevation for the piles.) A final tip elevation will be selected that will reasonably preclude situation of pile tips in a thin silt or sand layer, which will lead to excessive capacity and possibly to more nonuniform capacities. Unconfined compression tests will be conducted at approximately equal depth intervals.

Unconsolidated-undrained single stage triaxial compression tests will be conducted, with a similar distribution to that for the unconfined compression tests. Confining pressures will be isotropic and will be set equal to the total overburden pressure less the geostatic pore pressure indicated in observation wells (borings that have been pumped free of drilling fluids to below the water table and have been allowed to stand open to obtain static free water levels).

Three static cone soundings using the Fugro cone will be made to an approximate depth of 65 feet (20 m) prior to installing the pile group. Continuous records of tip bearing and sleeve resistance will be made. These tests will also be used to assess the proper depth of the pile tips, and they will serve as baselines for static cone measurements

to be made after the conclusion of the compression tests for purposes of assessing disturbance patterns in the soil due to pile installation.

c. Tests to investigate soil disturbance due to installation of piles. In order assess the degree of soil nonuniformity within and around the pile group and reference piles due to pile installation, five continuous static cone penetration tests will be made after completion of the tests. Penetration tests made after the tests will be located at varying distances from single piles and from the group. All tests will be carried to a depth of approximately two group widths beneath the pile tips. These tests are needed to determine rationally any gain or loss of strength from the pre-driving in-situ condition.

d. Tests to determine in-situ stress-strain properties of the soil. Because of stress relief, patterns of secondary structure will become magnified in the samples that are recovered from the overconsolidated clay. Unconsolidated-undrained triaxial compression and unconfined tests are therefore inappropriate to ascertain important aspects of soil stress-strain behavior, especially the initial tangent Young's modulus. In order to circumvent this problem, the following tests will be conducted to obtain stress-strain relationships.

(1) Pressuremeter. A self-boring pressuremeter will be used in two boreholes to obtain undrained cohesive shear strength and stress-strain behavior. However, the success of this instrument to advance itself into very stiff clays at depths greater than about 30 feet (9 m) without damage to its components is uncertain and, therefore, the depth of pressuremeter testing may be limited. Subject to this limitation, six to seven pressuremeter tests are planned in each of two boreholes.

(2) Seismic tests. A seismic crosshole procedure will be used to obtain upper bound values for shear modulus of the soil at one location on the site as a general check on the validity of the pressuremeter test results. One source hole (the standard penetration test borehole) and two receiver holes will be employed. Crosshole tests will be conducted to a depth of about 60 feet (18 m).

(3) Consolidated-undrained triaxial tests. Undisturbed samples will be consolidated in a triaxial cell to approximately twice the

average preconsolidation pressure indicated from one-dimensional consolidation tests, and the cell pressure will be reduced isotropically to the point at which the samples in the cells are at variable overconsolidation ratios, in the range of those that exist in-situ. The samples will then be loaded in undrained shear. Isotropic stress reduction will be used because the soil is not highly anisotropic in-situ.

The above tests presume that loading from the pile group will be of a short duration and that undrained stress-strain behavior is appropriate. Approximately four samples will be subjected to K_o consolidation and eight to isotropic consolidation tests. Two sets of tests are expected to be in the red and gray clay and two sets below that soil. All samples will be rebounded to one of three values of overconsolidation ratio. Pore pressure will be measured. The K_o tests will be employed to assess the in-situ at rest earth pressure coefficients.

e. Consolidation. One-dimensional consolidation tests on shelby tube samples will be performed to determine overconsolidation ratios and compressibility factors to aid in establishing final cell pressures for the above tests and to infer at-rest earth pressure coefficients in the overconsolidated clay. One-dimensional consolidation tests will be performed at random depths from near the surface to below the pile tips.

f. Tests to determine effective stress parameters. Rational correlations may exist between f_{max} and the effective stress parameters c' and ϕ'. An attempt will be made to measure the total and pore water pressure against the shafts of five of the test piles. Therefore, it would be possible to relate f_{max} to c' and ϕ'. If such a relationship is found, the effective stress at failure against the piles can then be related to in-situ geostatic vertical effective stresses to obtain appropriate earth pressure coefficients that could be used to compute f_{max} for similar conditions using effective stresses. Isotropically consolidated, undrained (CIU) triaxial compression tests on undisturbed samples (back-pressure saturated) with pore pressure measurement will be used to obtain the effective stress parameters. Six sets of three samples each, with confining pressure in the range of in-situ pressures and above in-situ pressures, within each set are planned. Several consolidated-drained direct shear tests will also be conducted to obtain

the residual strength parameters, as failure may be progressive along the shafts of the piles.

g. Tests to determine remolded strength. A potentially simple and rational means of obtaining f_{max} in overconsolidated clays, which may be superior to the procedure described in Chapter 1 (1), is to relate f_{max} to the consolidated-undrained strength of the remolded soil, since soil adjacent to the face of the shaft is remolded before being reconsolidated. CAU tests (using computed values of K_o) on remolded samples will be conducted at varying cell pressures on one set of three samples from the red and gray clay and one set from the light gray and tan clay to obtain the consolidated undrained strength parameters c_{rr} and ϕ_{rr} (remolded reconsolidated). Two other sets of tests, one in the red and gray clay and one in the light gray and tan clay, will be conducted using isotropic consolidation.

h. Soil pressures. In connection with Item f, above, pore water pressure will be measured at various points in the soil mass, within the pile group, below the group, and at locations peripheral to the group. Similar measurements will be made on and in the vicinity of one of the reference piles. Specific pore water and total pressures acting at four different levels on the faces of five piles (four within the group) will also be measured. The ranges of these instruments have been calculated from the theory of expanding cylindrical cavities in an incompressible cohesive soil mass (77), and all pore water pressure sensors are assumed to require that range. The choice of sensitivity is based on equipment availability at moderate cost and upon the sensitivity with which f_{max} is to be calculated:

Range: 0-300 psi (0-2070 kN/m^2) (total pressure)
0-150 psi (0-1030 kN/m^2) (pore water pressure)

Sensitivity: 1 psi (6.89 kN/m^2)

A plan of instrument locations is given in Chapter 5.

i. Soil deformations. Surface deformations that occur during installation and during load testing will be read from several monuments situated at the soil surface and from soil telltales at three levels beneath the ground in two locations relative to the group. These data will aid in investigating zone of surface influence of pile driving for

this group. The range and sensitivity of these instruments can not be calculated accurately from theory, so experience, based partially on the Koizumi and Ito and BRE tests described in Chapter 2, has been used:

Range: -1.0 to 1.0 in. (-2.5 to 2.5 cm)

Sensitivity: 0.01 in. (0.025 cm)

A plan of instrument locations and further details on the system are given in Chapter 5.

Reference Piles and Pile Group. The following measurements will be made on the piles.

a. Overall load. During each test, the overall load applied to the group or to a reference pile will be measured by means of calibrated load cells positioned above the loading rams. These load cells will be sensitive to the nearest ton (9 kN). For the reference piles a single ram and load cell will be used. For the group, four jacks and four load cells will be used, so that each load cell will have a range of 0-300 tons (0-2670 kN). Both jack pressure and load cells will be independently monitored as independent checks on the sum the load measurements to be made at the heads of the individual piles.

b. Cap and pile head translation. During each single pile test, pile head settlement or uplift will be measured by means of two dial gages mounted diametrically opposite each other on the circumference of the piles at the ground level and suspended from reference beams.

Similar measurements will be made on each of the piles in the group during the group tests. In addition the vertical displacement and horizontal displacement of the cap in two orthogonal directions will be measured by positioning dial gages in sets of three at the lower corners of the pile cap. The requirements for the dial gages are

Settlement gages:

Range: 0-2 inches (0-5.1 cm)

Sensitivity: 0.001 inch (0.0025 cm)

Horizontal translation gages:

Range: 0-0.5 inch (0-1.27 cm)

Sensitivity: 0.001 inch (0.0025 cm)

Vertical control will be maintained on the supports for the reference beams during the tests by means of a microhead level and scale to the nearest 0.01 inch (0.025 cm). The level will also be used to

make sightings on the pile cap with the same sensitivity as a back-up to the dial gage measurements. The level will be checked periodically during the operations by reference to a temporary bench mark that will be established on a structure about 100 feet (30 m) from the test site.

Reference beams and dial gages will be protected from direct sunlight and wind during each compression test by means of a canvas shroud.

c. Load distribution in individual piles. Load at the top of each pile will be measured by means of two separate full-bridge electrical foil resistance strain gage circuits situated at and slightly above the ground surface in each pile and wired to cancel flexure, magnify axial stress, and compensate for temperature. Load will also be measured using a similar arrangement at approximately five-foot (1.5-m) intervals along every pile in order to obtain the load transfer patterns. The range of the individual strain gage elements, which will be temperature compensated for mild steel, is dictated by the following:

Ultimate static load on pile = 150 tons (1335 kN) (based on 67% overload)
Corresponding average axial stress = 25.2 psi (174 kN/m^2)
Peak force during driving = 150 tons (1335 kN)
Corresponding peak stress = 25.2 ksi (174 kN/m^2)
Maximum strain, static or dynamic = 869 microinches per inch

The dynamic forces and stresses were obtained from a one-dimensional wave equation analysis, described in Figs. 4.20 and 4.21, using a Raymond 1S hammer (single acting, 19,500 ft-lb (26.5 m-kN) per blow) to drive the pile, an aluminum-micarta hammer cushion, and no pile cushion.

Gage sensitivity was established by requiring resolution of 25 psf (1.2 kN/m^2) side shear stress between two adjacent strain gage stations located five feet (1.5 m) apart vertically. This requirement forces strain gage circuits to resolve a load in the pile of approximately 350 pounds (1.56 kN), which produces a strain of one microinch per inch.

The propagation of the stress waves during driving will be monitored with analog data acquisition equipment in four of the piles in

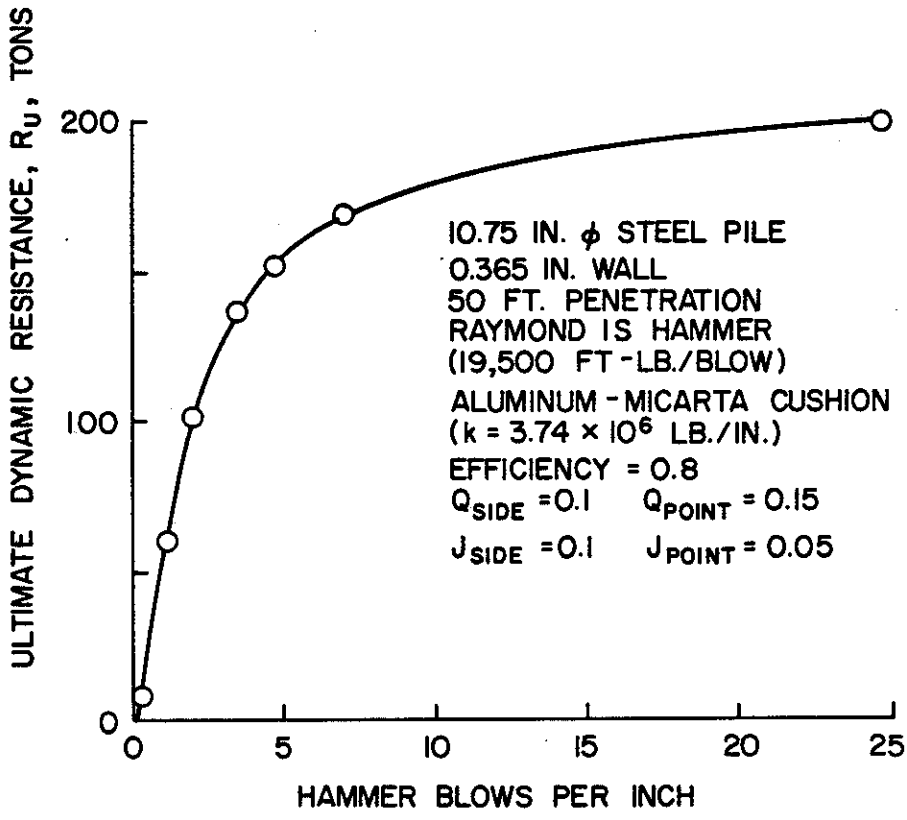

NOTE: 1 in. = 2.54 cm 1 ft-lb = 1.36 m-N 1 lb = 4.45 N 1 ton = 8.9 kN

FIGURE 4.20. DYNAMIC RESISTANCE VS. HAMMER BLOWS PER INCH (2.54 CM) FOR PROPOSED TEST PILES BY ONE-DIMENSIONAL WAVE EQUATION

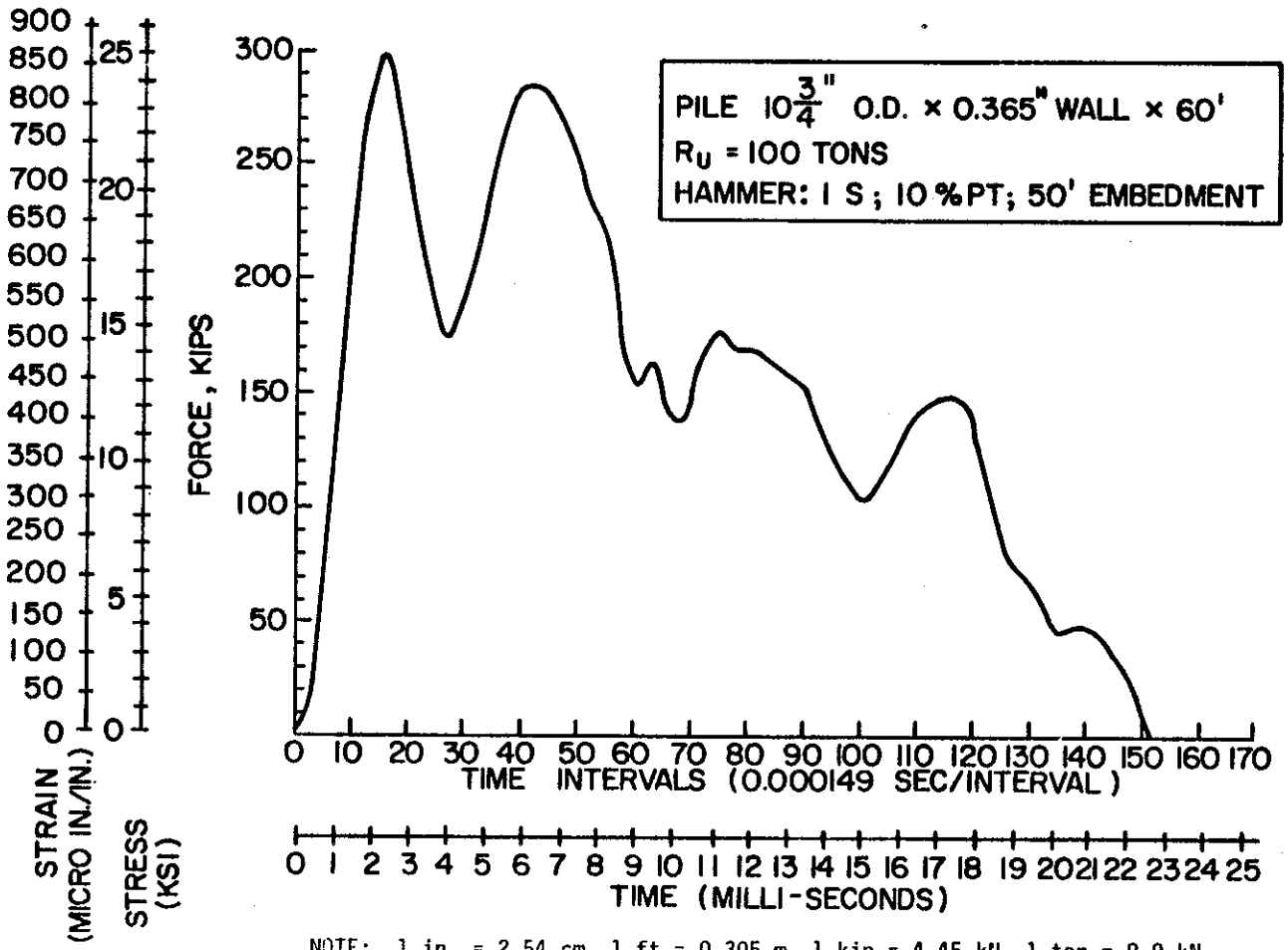

NOTE: 1 in. = 2.54 cm 1 ft = 0.305 m 1 kip = 4.45 kN 1 ton = 8.9 kN
1 ksi = 6.89 mN/m^2

FIGURE 4.21. MAXIMUM FORCE, STRESS, AND STRAIN AT PILE HEAD DURING DRIVING

order to obtain an approximate assessment of any variation of dynamic response to driving that may occur among piles in a group in stiff clay. This measurement will be accomplished by obtaining traces of the strain gage bridge output at several levels on each of the four piles for several blows of the hammer near maximum penetration. These gages will be separate from the strain gate system described above for measuring static loads. They will be single gages, with full-bridge completions on the surface by means of dummy gages. In order to obtain an accurate trace of strain versus time (Fig. 4.21), two requirements must be met:

(1) The frequency response of the gages should be about 100 times the frequency of the propagating wave. Figure 4.21 reveals that this frequency of the wave will be about 250 Hz. Gages will be used that will have a frequency response of 25,000 Hz.

(2) The gage length of the sensing elements should be no longer than one-one hundreth of the wave length of the wave. The wave length of the propagating wave in Fig. 4.21 is about 60 ft (18 m). Hence, any strain gage of reasonable length will be appropriate. One-quarter-inch (0.64-cm) gages will be used in this study.

The requirements for the strain gage circuits therefore are:

Range: ±1000 microinches per inch
Sensitivity: 1 microinch per inch
Frequency Response: 25,000 Hz
Gage Length: less than 0.6 ft. (18 cm)
Temperature Compensation: mild steel

In addition, gage resistances of 350 ohms will be employed to permit relatively high power levels to be used.

As a learning experience, the University of Houston will place accelerometers (vertically oriented) adjacent to each of the "dynamic" strain gages and will measure their output. For completeness, these instruments are described in Chapter 5. However, they are not explicitly a part of this project.

An electrical resistance strain gage system is sensitive to moisture intrusion onto the gage elements or lead wires. The gages and lead

wire will be protected by

(a) Mounting the gages internally.

(b) Using encapsulated gages.

(c) Using coatings of two separate waterproofing compounds (for example, Vishay M-Coat A and M-Coat G) over the gage locations.

(d) Pressurizing the piles with a dry nitrogen system that will be flushed periodically to remove water vapor.

The active gages in the strain circuits will be bonded to the interior surface of the steel piles with an RTC epoxy. Mild heat and pressure curing will be used to insure that a no-creep bond is achieved.

A set of zero readings will be obtained on all circuits prior to driving the piles in an attempt to measure residual loads in the piles.

d. Pile foreshortening and alternate load measurement. As a means of providing redundancy to the strain gage system and as a means of directly measuring the tip displacement for use in failure criteria considerations, mechanical extensometers will be installed in every pile. Total foreshortening of each pile is anticipated to be on the order of 0.15 inches (0.38 cm). A reasonable resolution for purposes of measuring tip defection is 0.005 inches (0.013 cm) ; therefore, a system with such a resolution will be used.

Reference points (anchors) will be placed at the pile tips, the ground surface, and at four equally spaced points between in order to measure strain at several levels in the pile in the event of a failure of the electrical strain gage system. The device that will used to measure relative displacements mechanically will be a commercially available multiple position borehole extensometer (Terrametrics, Model 6CS-LT(R)) with a range of two inches (5 cm) and a theoretical resolution of 0.001 inch (0.0025 cm). The extensometers will be installed after the piles are driven. Readout will be by means of dial gages with sensitivities of 0.001 inch (0.0025 cm).

e. Lateral pressures. As previously stated, total and pore water pressures will be measured against the shafts of four piles in the group (center, corner, and two edge piles) and in one reference pile. The system will be totally pneumatic in order to provide long-term stability. Four different measuring points at approximately equal

intervals along the piles will be used. All pore water pressure cells will be flushed just prior to driving and periodically thereafter to prevent air entry. Readings will be made immediately after a pile is driven, periodically thereafter during and after installation of other piles, and after application of each load increment during the load tests. Ranges and sensitivities are as described in the earlier section on "Soil pressures."

f. Pile geometry. The relative location of the heads of each of the piles in the group will be measured after all piles are driven. Horizontal location will be determined using a transit, relative to a horizontal reference point at the northeast corner of the Band Annex. Vertical position will be determined with a level using a procedure similar to that described for vertical control on the reference beam anchors. Vertical position will also be checked on every pile after each pile is driven to assess heaving.

Although the soil at the test site is relatively uniform and contains no rocks, and the piles are relatively rigid flexurally, some deviation from perfect plumb geometry is possible. Undersized pilot holes to a depth of about 20 feet (6 m) and a diameter of eight inches (20 cm) will be drilled to permit better alignment of the piles and to reduce heave. The true alignment will be determined by means of an electrical inclinometer. The sensitivity of the inclinometer is chosen so that it can resolve a horizontal displacement of the tip relative to the butt of one inch (2.54 cm). This sensitivity can be achieved with a SINCO Model 50325 Microtilt sensor. Deviation of each of the piles will be measured after all of the piles have been driven by running the sensor down a square tube which will be affixed to the inside of the pile, in two perpendicular orientations and taking tilt readings at ten-foot (3-m) intervals.

Inclinometer measurements are necessitated for three reasons:

(1) To obtain an accurate picture of the location of pressure cells on the pile surface relative to those that are in the soil.

(2) To provide an accurate value for batter for purposes of after-the-fact mathematical modeling with the hybrid model.

(3) To make certain that no "dog-legging" of the piles has occurred.

Chapter 5. Test Details

General Soil Characterization

This chapter contains a general description of the soil properties at the test site and detailed drawings of the ground instrumentation and piling instrumentation for the test program proposed in Chapter 4. It also describes the test procedures. The testing program consisted of six single pile compression tests, three nine-pile-group compression tests, a subgroup compression test on five piles (corner piles omitted from original group), a subgroup compression test on four piles (center pile omitted from five-pile subgroup), and six single pile uplift tests, as described in Chapter 4.

Figure 5.1 shows a general profile of the soil at the test site and SPT records obtained from the detailed geotechnical study performed as a part of this research and reported in Appendix C of the Final Report. It is evident that two primary strata exist in the upper approximately 47 feet (14.3 m): a stiff to very stiff highly plastic, highly overconsolidated, slickensided clay (CH) above a depth of about 26 feet (7.9 m) and a stiff to very stiff overconsolidated sandy clay (CL) with some fine sand pockets below 26 feet (7.9 m). Interbedded layers of dense silt and hard clay were encountered below a depth of 47 feet (14.3 m). The 26-foot (7.9 m) depth apparently marks the contact between the Beaumont formation (upper layer) and the Montgomery formation (lower layer), which are two late Pleistocene formations of the Houston Group that were deposited in a deltaic environment. The approximately four feet (1.3 m) of soil immediately below the contact was somewhat softer in consistency than the soil above or below. Alphabetic layer and sublayer designation have been established for later load transfer correlations and are shown on Fig. 5.1. Further geological and geographical details may be found in Appendix C of the Final Report.

The soil in both formations was preconsolidated through a process of desiccation in the geological past when the sea level of the nearby Gulf of Mexico was several hundred feet lower than it is at present. This process has lead to rather high strengths, as summarized partially in Fig. 5.2. Figure 5.2 shows smoothed undrained shear strength profiles obtained from limit pressures in the pressuremeter tests, UU

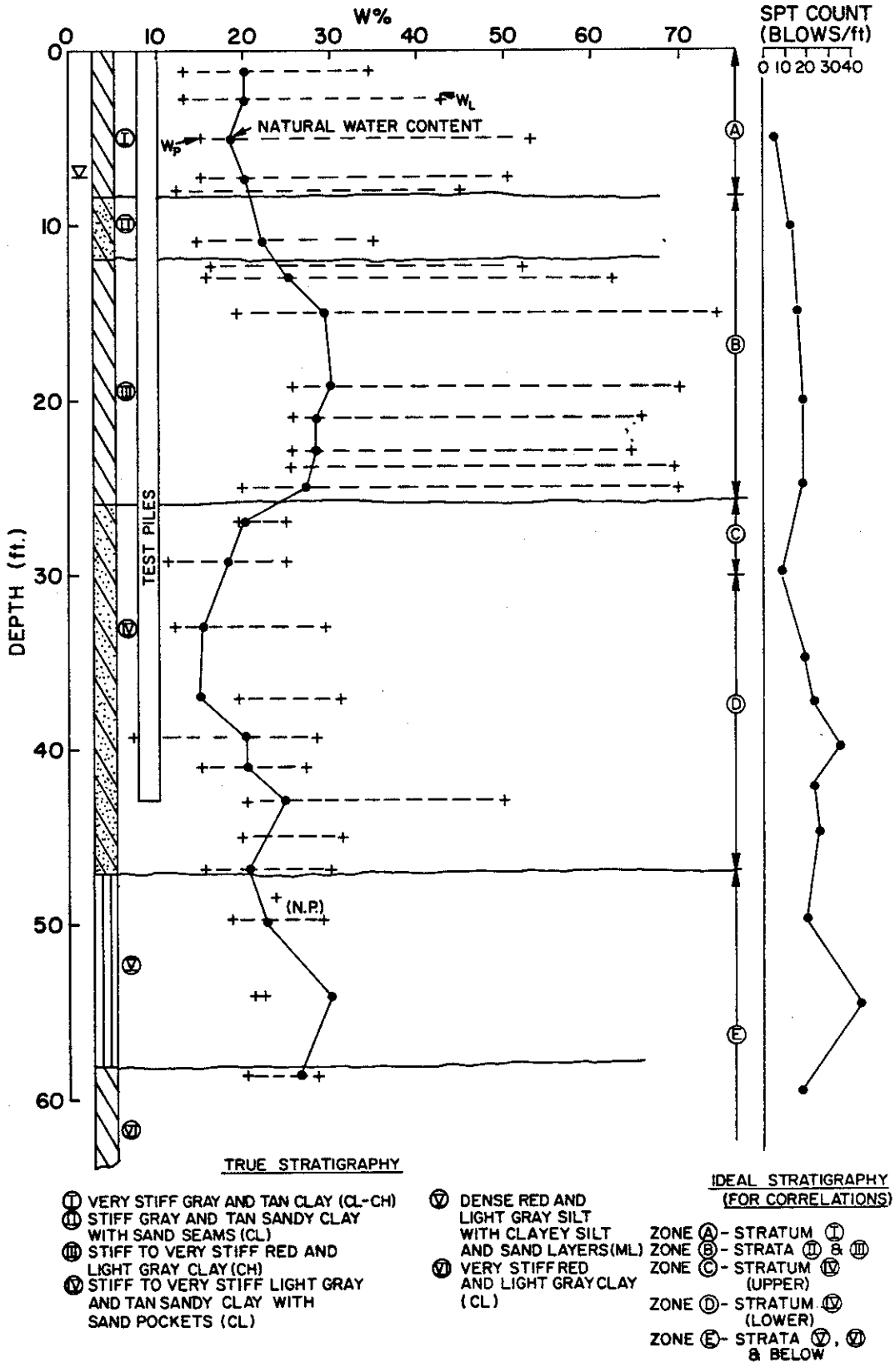

FIGURE 5.1. GENERAL SITE STRATIGRAPHY (1 ft = 0.305 m)

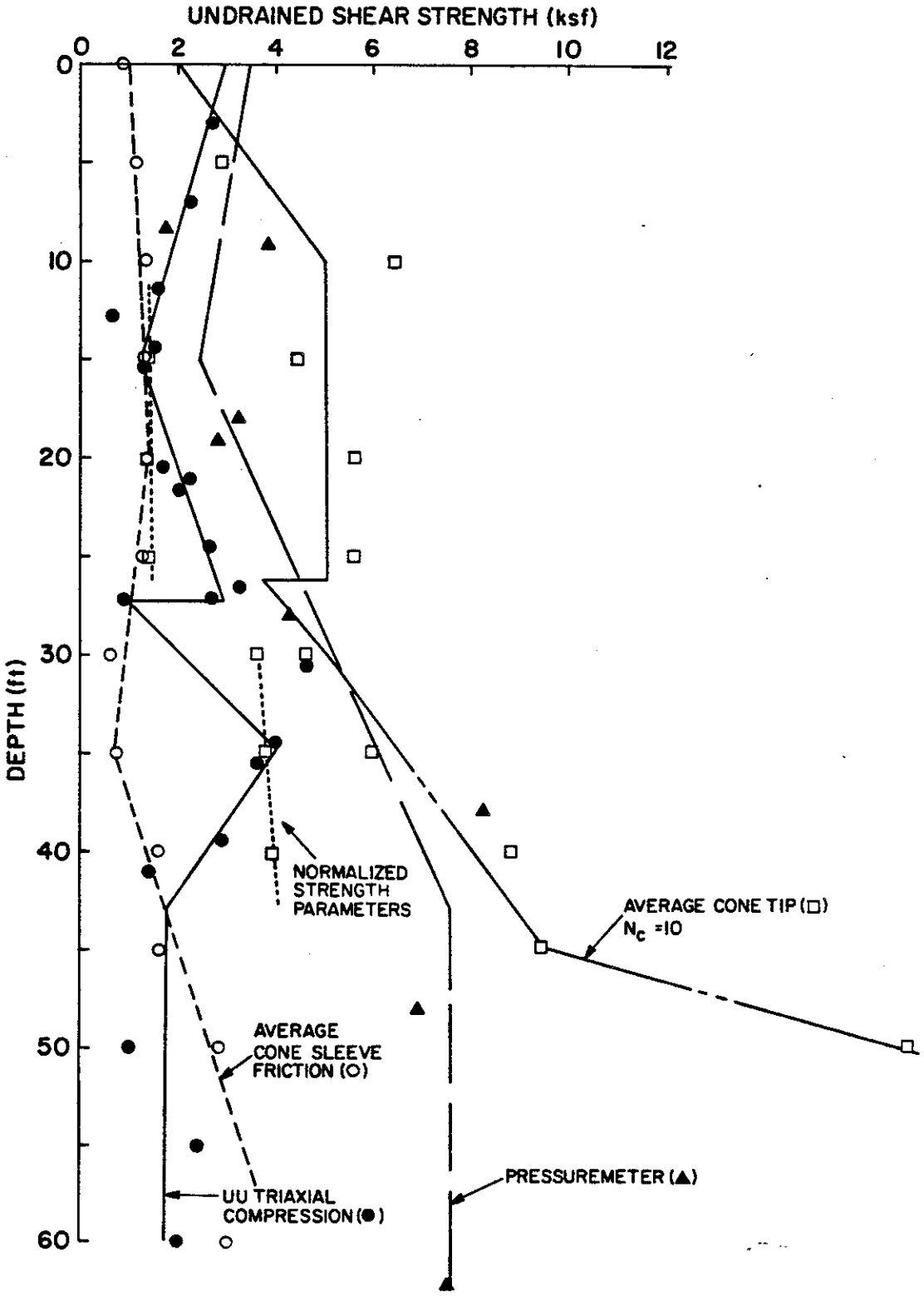

FIGURE 5.2. SUMMARY OF SHEAR STRENGTH DATA (1 ft = 0.305 m; 1 ksf = 47.9 kN/m^2)

triaxial compression tests, from the average cone sleeve friction and tip bearing records and a profile of the undrained shear strength as calculated from the triaxial compression tests described in Chapter 4 in which samples were consolidated to a state of apparent normal consolidation and then rebounded isotropically to a given OCR. The calculations for shear strength for these tests were made by first obtaining from Fig. 5.3 a value of OCR for the depth of interest. (OCR was developed in Fig. 5.3 by taking the ratios of best-fit indicated preconsolidation pressure from the one-dimensional consolidation tests and isotropic consolidation stages of the triaxial tests to the existing in-situ vertical total stress minus free pore water pressure defined from a piezometric surface at a depth of seven feet (2.1 m) (defined herewith as the vertical quasi-effective stress)). Curves relating OCR to undrained shear strength from these tests for various materials encountered, contained in Appendix C, Final Report, were then entered with OCR to obtain the undrained strength values that are plotted in Fig. 5.2. The profiles of measured earth pressure coefficients and overconsolidation ratios are summarized in Fig. 5.3, and the profiles of quasi-effective vertical stress and octahedral normal quasi-effective stress, computed from the earth pressure coeffcients in Fig. 5.3, are shown in Fig. 5.4. Figure 5.5 depicts a profile of the Skempton A parameter at failure (A_f) from the CU triaxial tests (each point representing an average value for all tests run at a particular depth).

Other depictions of shear strength shown in Fig. 5.5 are those computed from the strength parameters for the total stress triaxial compression tests that were conducted on both undisturbed and remolded samples, described in Appendix C, Final Report, and the in-situ octahedral quasi-effective stress existing at a given depth. Here, the shear strength at a given depth was ascertained as that value obtained from the Mohr-Coulomb strength parameters of a soil specimen representative of that depth, in which the appropriate confining pressure is isotropic and is equal to the in-situ octahedral normal quasi-effective stress at that depth.

Other methods of defining the shear strength profile, including pocket penetrometer and torvane tests, unconfined compression tests,

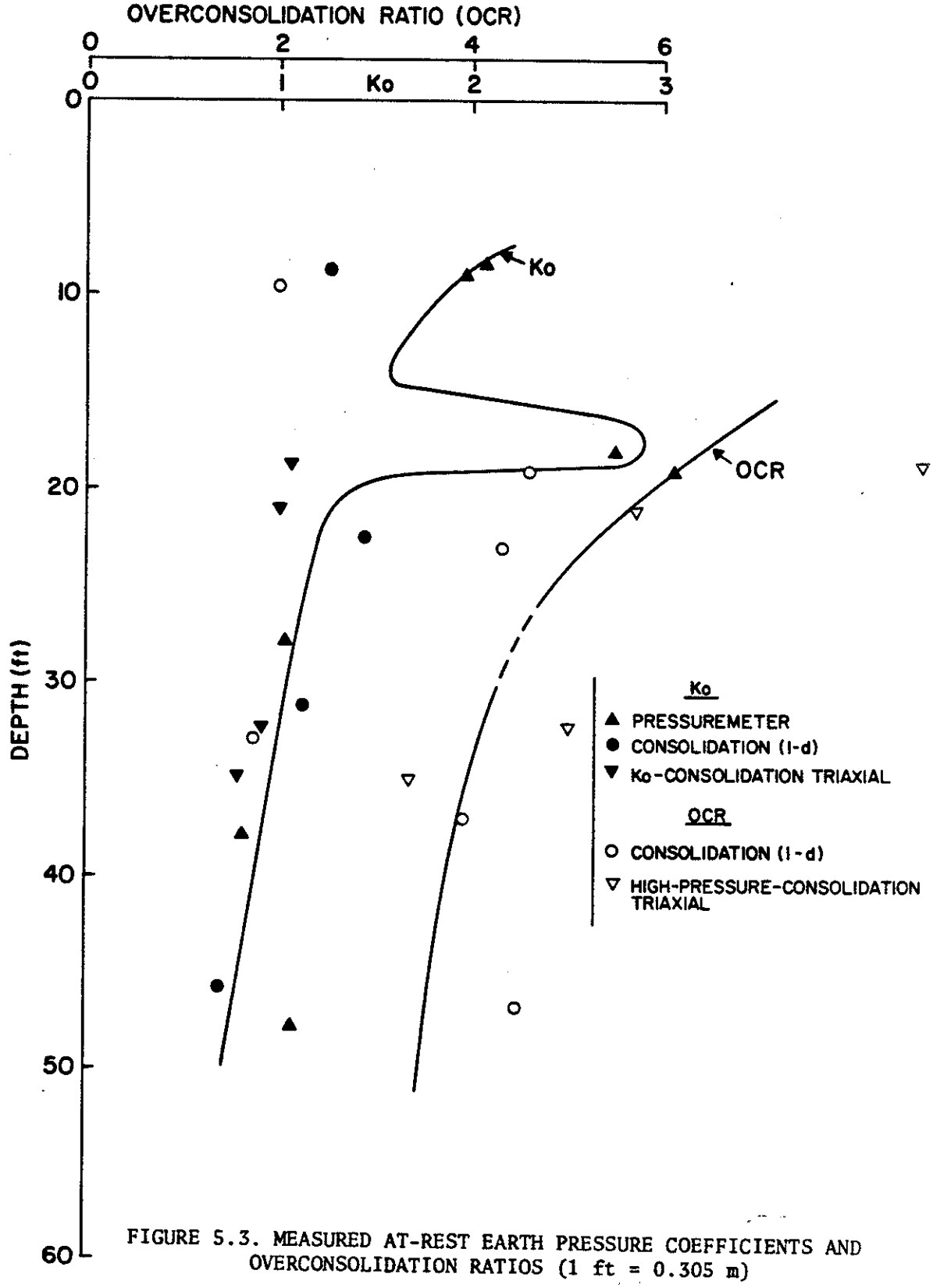

FIGURE 5.3. MEASURED AT-REST EARTH PRESSURE COEFFICIENTS AND OVERCONSOLIDATION RATIOS (1 ft = 0.305 m)

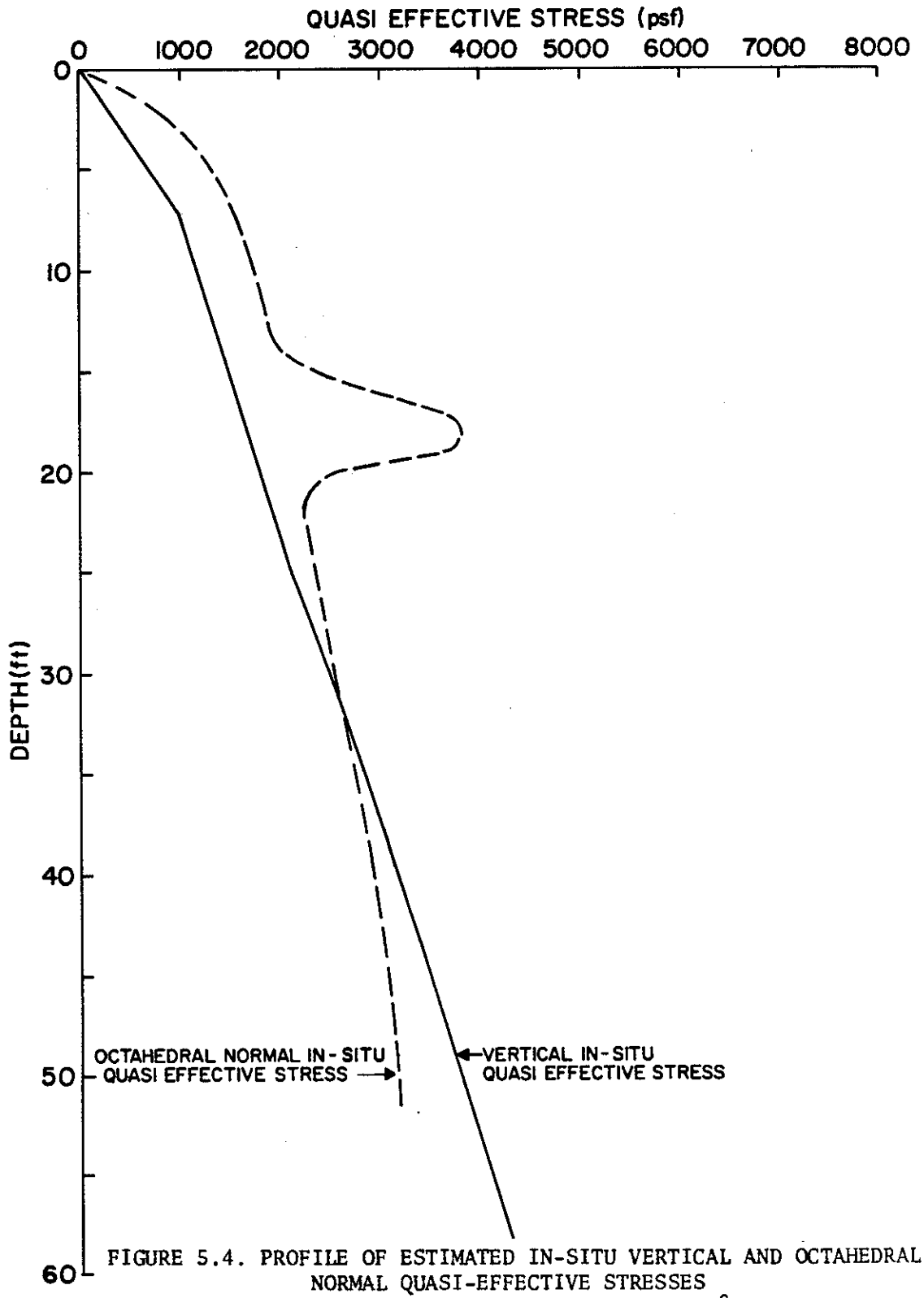

FIGURE 5.4. PROFILE OF ESTIMATED IN-SITU VERTICAL AND OCTAHEDRAL NORMAL QUASI-EFFECTIVE STRESSES
(1 ft = 0.305 m; 1 psf = 47.9 N/m^2)

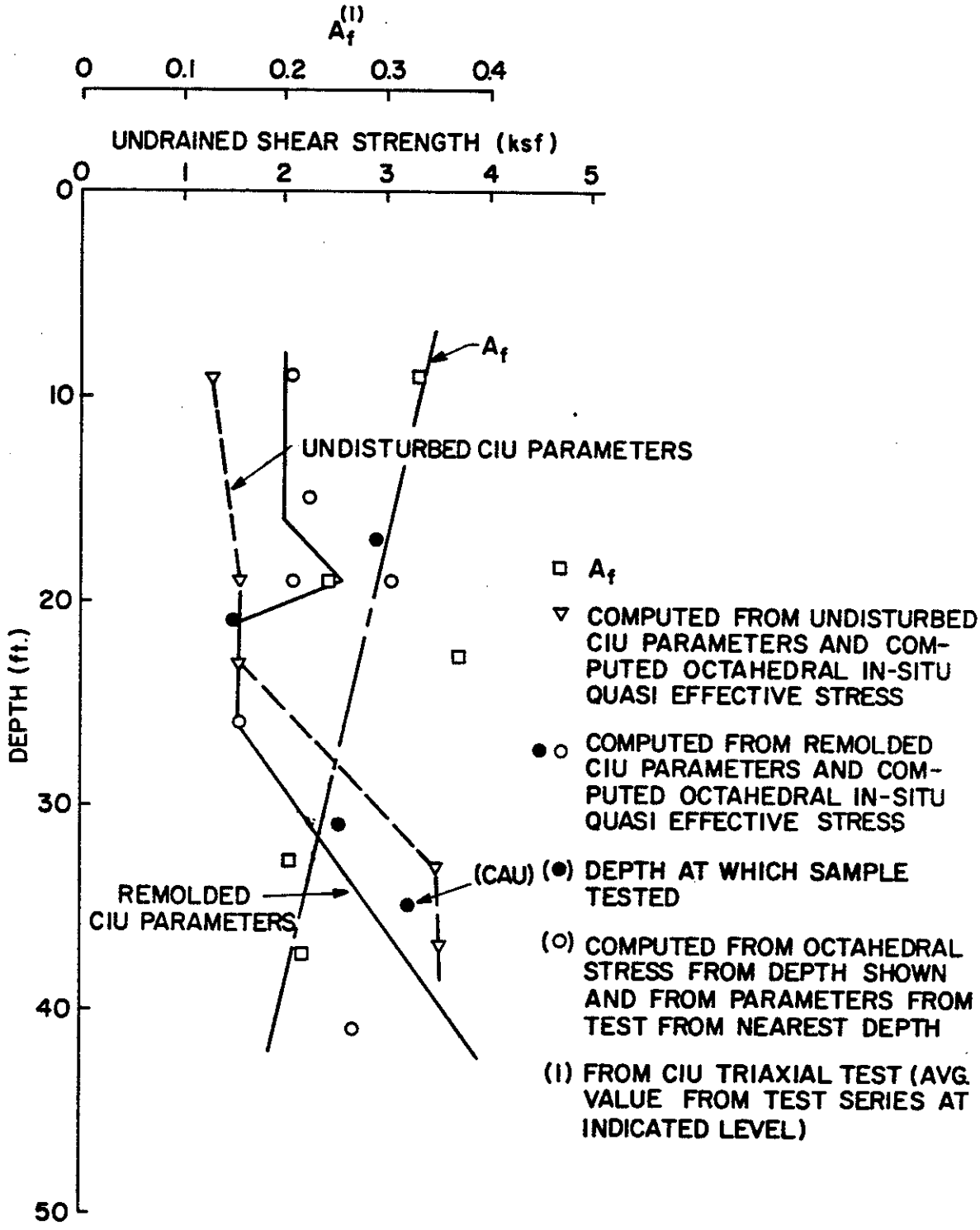

FIGURE 5.5. PROFILE OF A_f AND SHEAR STRENGTHS COMPUTED FROM STRENGTH PARAMETERS AND ESTIMATED OCTAHEDRAL NORMAL QUASI-EFFECTIVE STRESSES (1 ft = 0.305 m; 1 ksf = 47.9 kN/m^2)

and drained direct shear residual strength tests, are described in Appendix C, Final Report, which also describes the tests summarized on Figs. 5.2 and other soil tests in detail.

It is evident from Figs. 5.2 and 5.5 that each of the several methods summarized produces different shear strength profiles as well as different degrees of data scatter. These differences can generally be explained by variations in test procedures and in the effects of secondary structure described subsequently. More scatter is observed in the strength data gathered from the undrained laboratory tests on undisturbed samples, such as the unconfined compression test and the UU triaxial compression test. This is primarily due to the fact that the process of desiccation lead to a random network of secondary structure (slickensides and fissures), particularly in the Beaumont formation, which strongly influenced the laboratory test results because of stress relief and subsequent opening of slickensides and fissures during the sampling process.

The strength profiles from the in-situ tests (SPT, CPT, and pressuremeter) are somewhat smoother and better defined than those from the undrained laboratory tests. These tests probably represent a more realistic picture of strength variability (although not necessarily of absolute strength values) within the soil mass.

The profiles of computed shear strength from the consolidated-rebounded laboratory tests and from the remolded CU triaxial tests are generally smooth, partially because a smoothed variation in K_o was used in the calculations. The proximity of the strengths and moduli to those obtained by UU test suggests that this procedure may have destroyed some natural cohesion.

Based on the data summarized in Figs. 5.1 and 5.2, it was decided to elevate the tips of the test piles from 50 feet (15.3 m) to 43 (13.1 m) below grade due to the presence of erratic, dense, interbedded silt and hard clay deposits beneath a depth of 47 feet (14.3 m) below grade which were not evident in the preliminary information employed in the analyses in Chapter 4. The choice was made in order to minimize random, differential pile capacities due to differential tip capacities and to maintain as uniform a soil profile as possible above the pile tips. All drawings and details shown in this chapter presume this penetration. Piles were installed in 8-inch (20-cm) diameter dry-drilled pilot holes

that were made to a depth of 10 feet (3.1 m). The driving system described in Fig. 4.20 was used.

Figure 5.6 characterizes the stress history and compressibility data for the test site. In addition to the preconsolidation pressure, compression index data and consolidation coefficient data (at stress levels slightly in excess of the indicated preconsolidation pressure) are also summarized. The latter data were produced from one dimensional consolidation tests.

Figure 5.7 shows a summary of the quasi-elastic properties of the soil, namely the indicated Young's modulus as obtained from the stress-strain curves of the in-situ pressuremeter tests, the indicated Young's modulus obtained from crosshole tests, the indicated Young's modulus obtained from the laboratory UU triaxial compression tests on undisturbed samples defined at a stress difference level equal to twenty percent of the peak principal stress difference, and from the consolidated-rebounded undrained triaxial compression tests at a twenty precent stress level, using a rationale similar to that used to compute shear strength from this test. Supporting data again may be found in Appendix C of the Final Report.

The locations of the various sample borings and in-situ tests relative to the test piles are shown in Appendix C, Final Report.

Pile Fabrication

The group piles protruded through the pile cap, which was precast reinforced concrete, 4 feet, 3 inches (1.3 m) thick, and which was suspended 3 feet, 0 inches (0.92 m) off the ground. In this way instrument lead wires were brought out of the piles above the cap, and all internal extensometer readings were made at the top of the cap. This procedure precluded interference of extensometer readings with pile settlement readings, which were made beneath the cap. Reference piles extended 40 inches (1.02 m) above grade and were loaded through a slip-on loading head. The precast cap on the group piles was attached to the piles by epoxy grout having 10 ksi (68.9 mN/m^2) shear strength.

During assembly the test piles were cut into segments to permit access to internal strain gage locations. The segments, which were

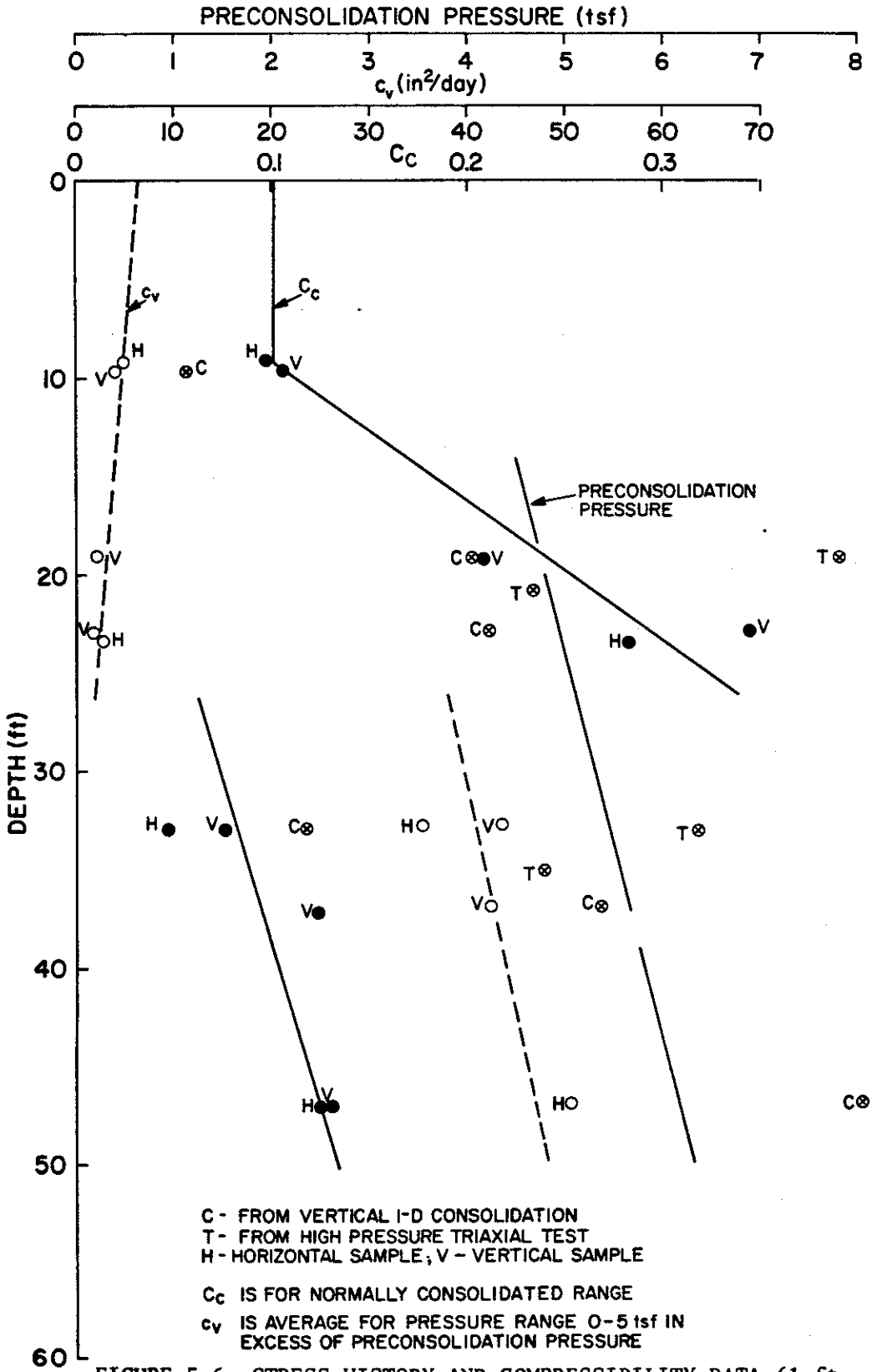

FIGURE 5.6. STRESS HISTORY AND COMPRESSIBILITY DATA (1 ft = 0.305 m; 1 tsf = 95.8 kN/m^2; 1 in^2/day = 0.00765 mm^2/sec.)

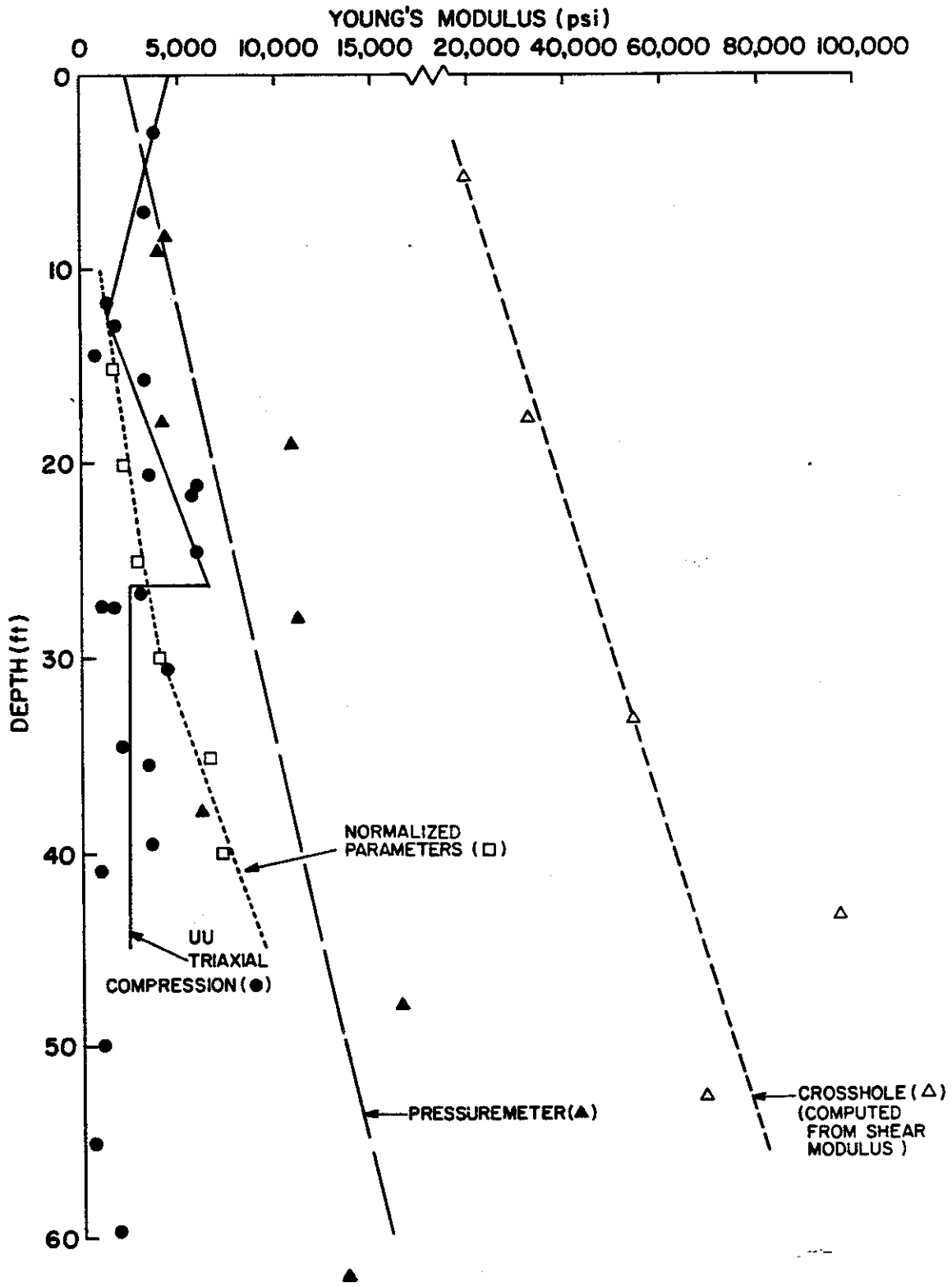

FIGURE 5.7. YOUNG'S MODULUS DATA FOR SOIL (1 ft = 0.305 m; 1 psi = 6.89 kN/m^2)

typically five feet (1.5 m) long, were welded back together using special precautions to prevent overheating of lead wires and fluids within lateral pressure cells. Wire-fed welders (short arc MIG welders) were used to minimize heat, and sensitive areas such as the lateral pressure cells were cooled with chilled water baths while welding occurred. Axial alignment during reassembly of the piles was maintained by using a special alignment jig consisting of a heavy machined H-section and chain clamps. The mechanical extensometers were not placed in the piles until after the piles were driven in order to prevent damage to the anchors and extensometer rods. Prior to finalizing production procedures for instrumenting the piles, a three-segment test section was constructed and test driven against a rigid block by a Raymond 1S hammer to insure that assembly techniques produced adequate welds and alignment and to insure satisfactory performance of strain gages and instrument leads.

The strain gage circuits on all piles were calibrated in compression to a load of 150 tons (1335 kN) on the floor of the shop building in which the piles were assembled after "exercising" the piles to a load of 150 tons (1335 kN) for three cycles. Calibration readings were made by the data acquisition system that was used during the field tests as a means of "debugging" the data acquisition system.

Lateral pressure cells were constructed and calibrated by a separate supplier. All details are presented later; however, certain aspects of the cells, which affected the construction process, are described here. The supplier's calibration revealed that the total pressure sensors were very sensitive to changes in temperature, so that it was necessary to install an electronic thermal sensor on the steel backing plate of each cell. All of the total pressure cells were then calibrated in air under zero gage pressure in a temperature-controlled room in order to obtain corrections for cell pressure as a function of temperature as indicated by the electronic temperature sensors. Laboratory calibration curves were successfully developed. During this process it was discovered that slight buckling of the total pressure cell sensor plate occurred when the temperature of the plate exceeded approximately 40°C, causing a shift in the pressure correction curve and also affecting the usable pressure range of the cell. This made it

necessary to maintain the temperature of this plate at less than 40°C throughout the construction and installation process.

Checks of the validity of making direct pore water and total pressure readings with the lateral pressure cell system were made by submerging the cells in a water tank to a depth of 18 feet (5.5 m). Indicated pressures (with due consideration for temperature changes) were found to be correct in the water tank to within about 1 psi (6.89 kN/m^2).

Finally, the lateral total pressure cells were read after they were affixed to the piles during compression calibration of the piles in order to obtain a second correction to the readings relating the indicated pressure produced due to the presence of a compressive load in the cell parallel to the sensor face. This "cross-sensitivity" effect was found to be minor compared to the temperature effect decribed earlier.

Further details of the pile instrumentation and calibration procedures are contained in Appendix E of the Final Report.

Instrumentation Details

Figures 5.8 and 5.9 depict the ground instrumentation locations. The general site layout for testing is shown in Fig. 5.10. Note that anchorage for the main reaction frame was provided by two 600-ton (5.34 mN) underreamed drilled piers, which are described in detail later. Details of the ground piezometers are shown in Fig. 5.11, and details of the vertical movement points are shown in Fig. 5.12.

Figure 5.13 depicts the elevation of a typical test pile, showing the segments of the pile into which it was cut for the purpose of placing instruments as well as the pressure tight cap system. Note that the detail of the extension segments (those portions of the piles above site grade) differs between the group piles and the reference piles. An elevation of a typical five-foot (1.5 m) segment of a test pile is indicated in Fig. 5.14, and a section of a typical segment is shown in Fig. 5.15. Explanatory notes for the elevations and sections are given in Table 5.1.

The elevation of the bottom segment of a test pile is shown in Fig. 5.16, and an elevation and section of the extension segment for the group piles (Nos. 2-10) are given in Figs. 5.17 and 5.18. Figure 5.19 shows the extension segment for the reference piles (Nos. 1 and 11).

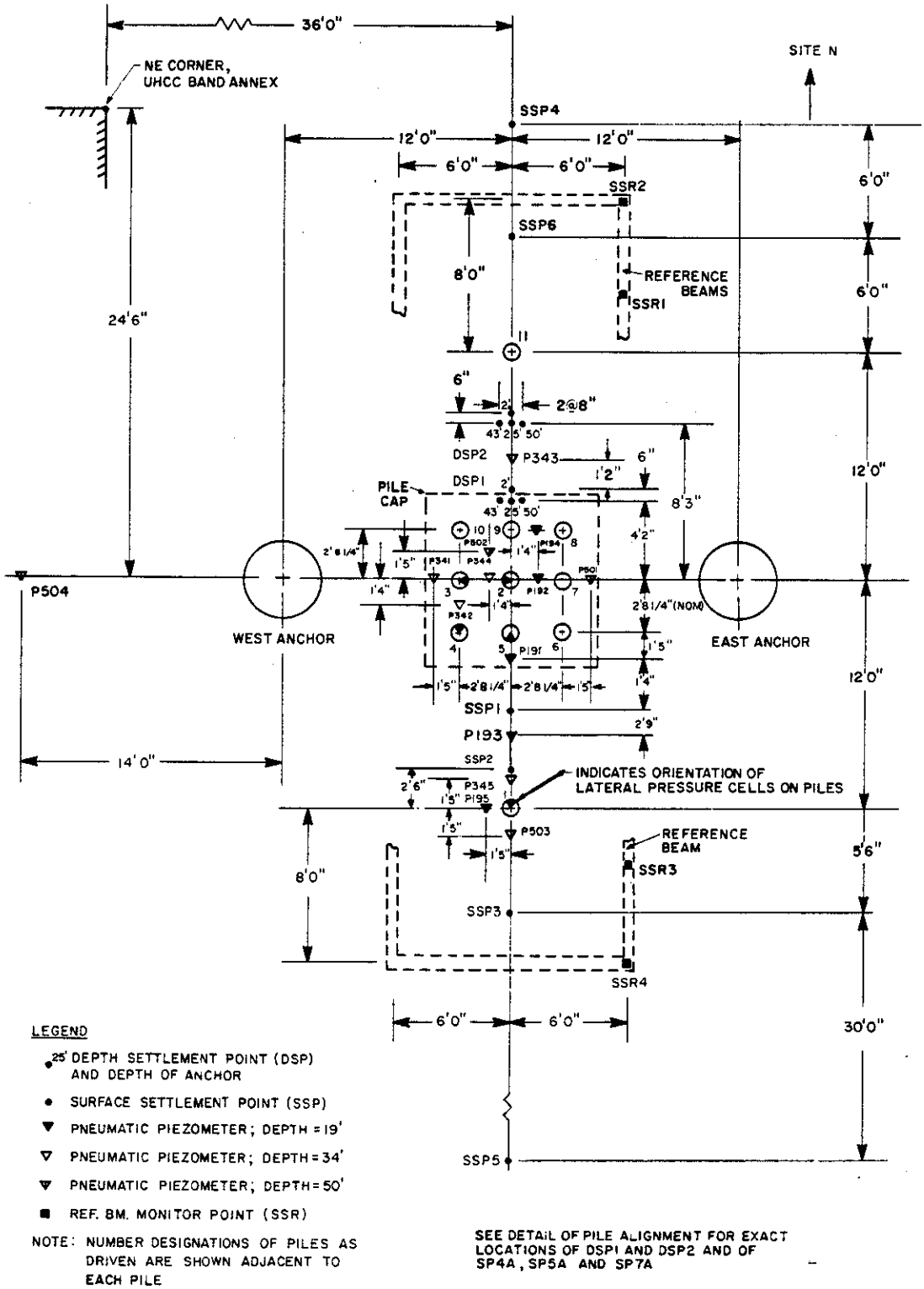

FIGURE 5.8. GROUND INSTRUMENTATION PLAN (1 ft = 0.305 m; 1 in = 25.4 mm)

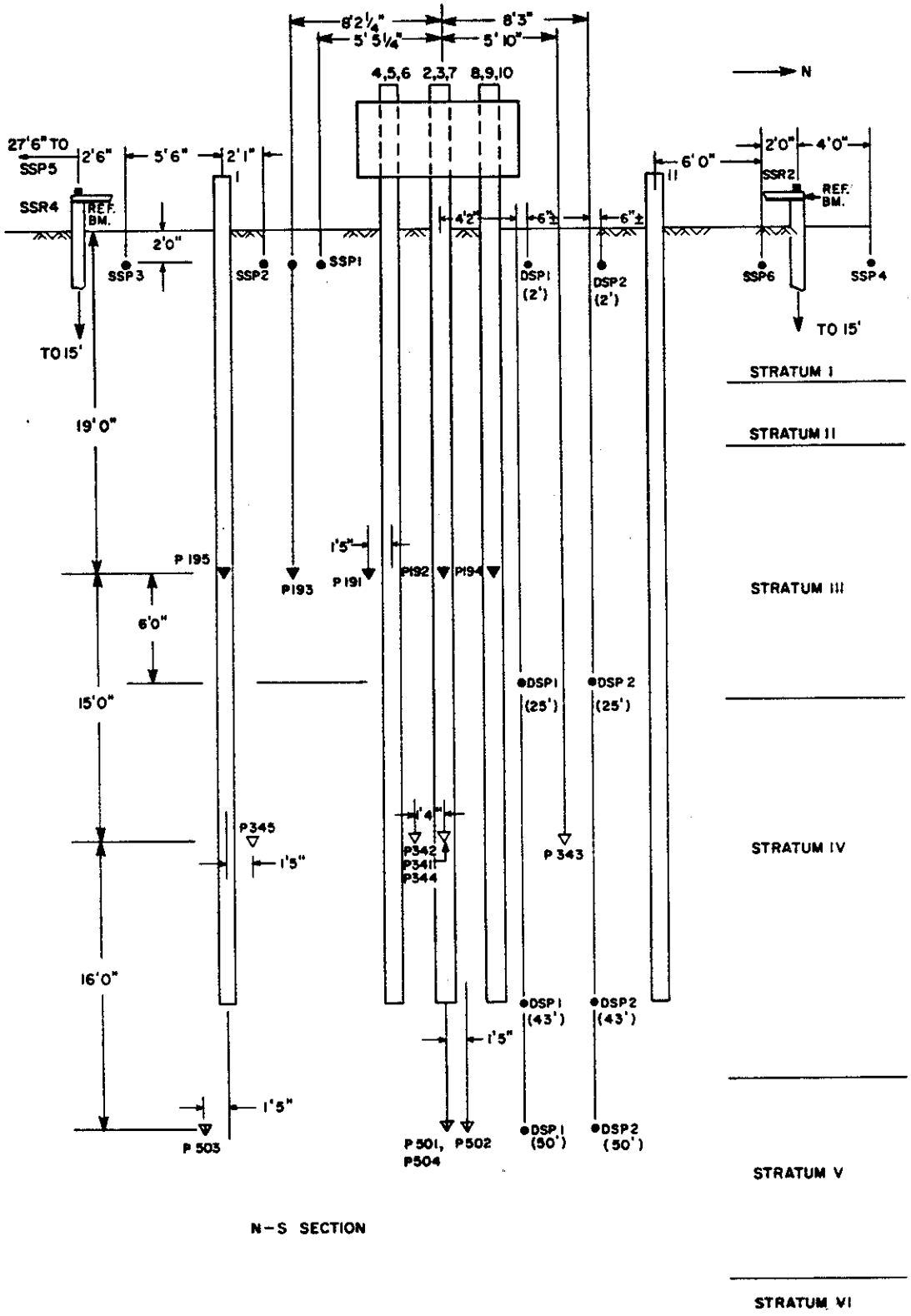

FIGURE 5.9. ELEVATION VIEW OF GROUND INSTRUMENTS (1 ft = 0.305 m; 1 in = 25.4 mm)

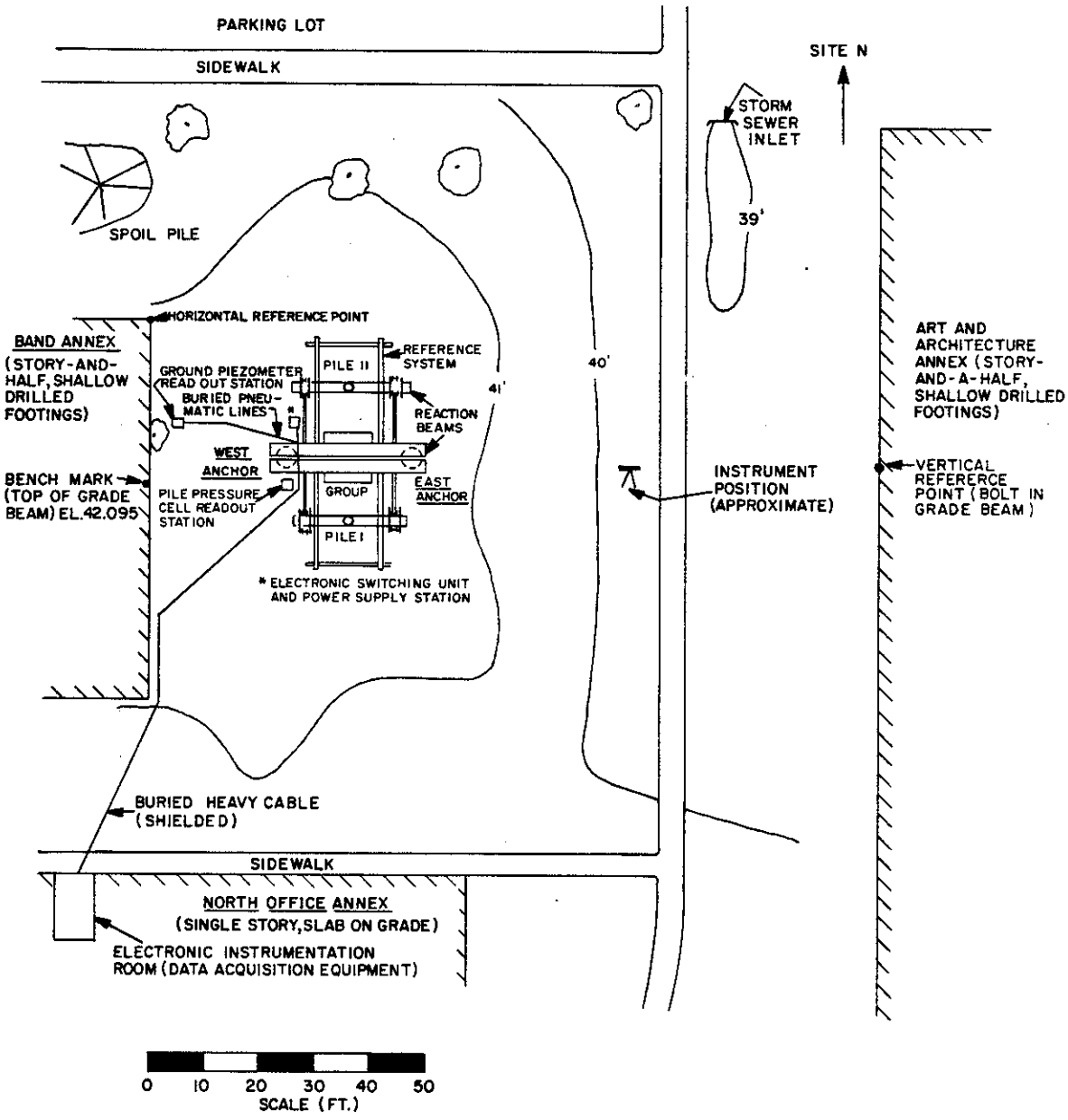

FIGURE 5.10. GENERAL SITE LAYOUT (1 ft = 0.305 m)

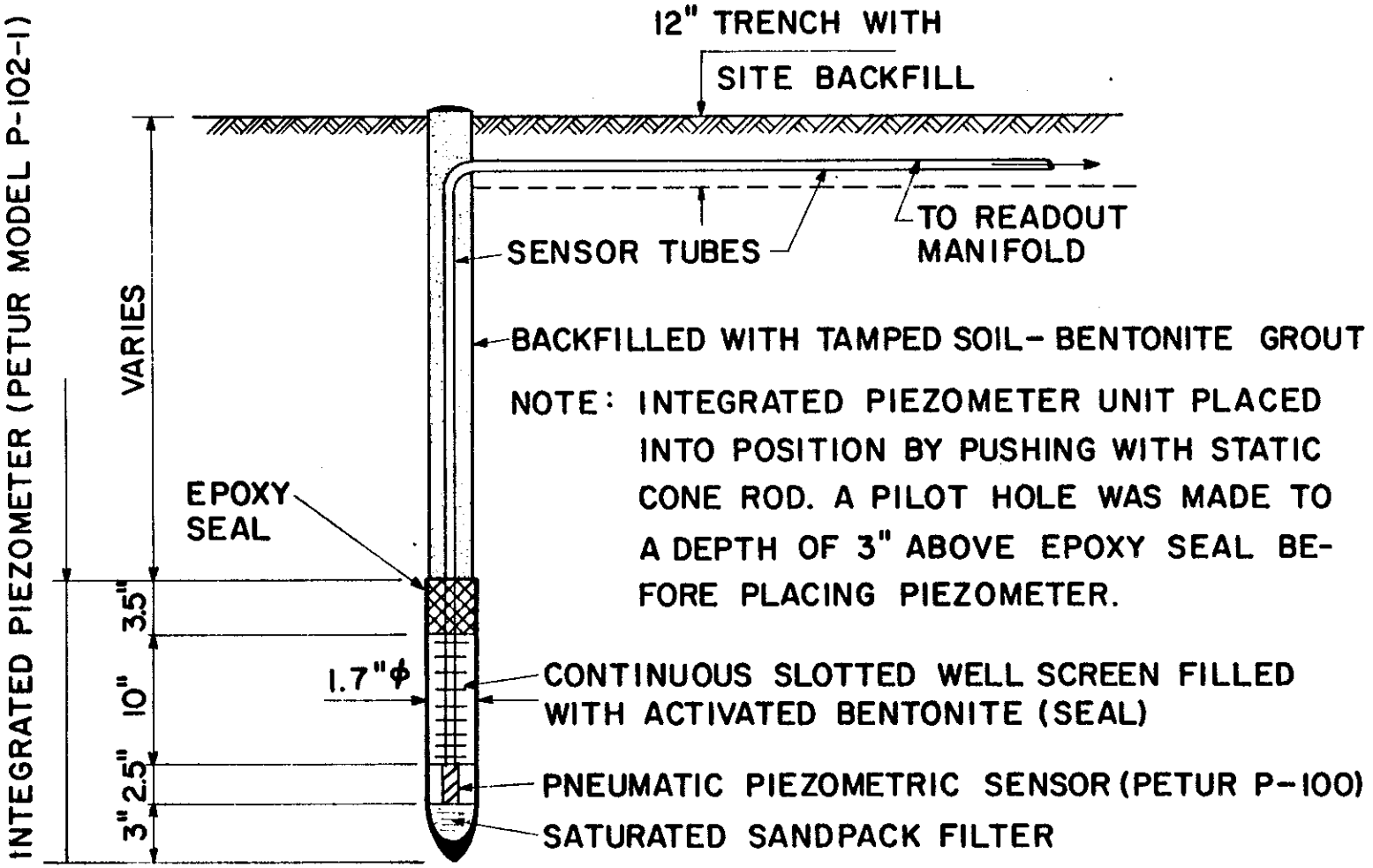

FIGURE 5.11. GROUND PIEZOMETER DETAIL (1 ft = 0.305 m; 1 in = 25.4 mm)

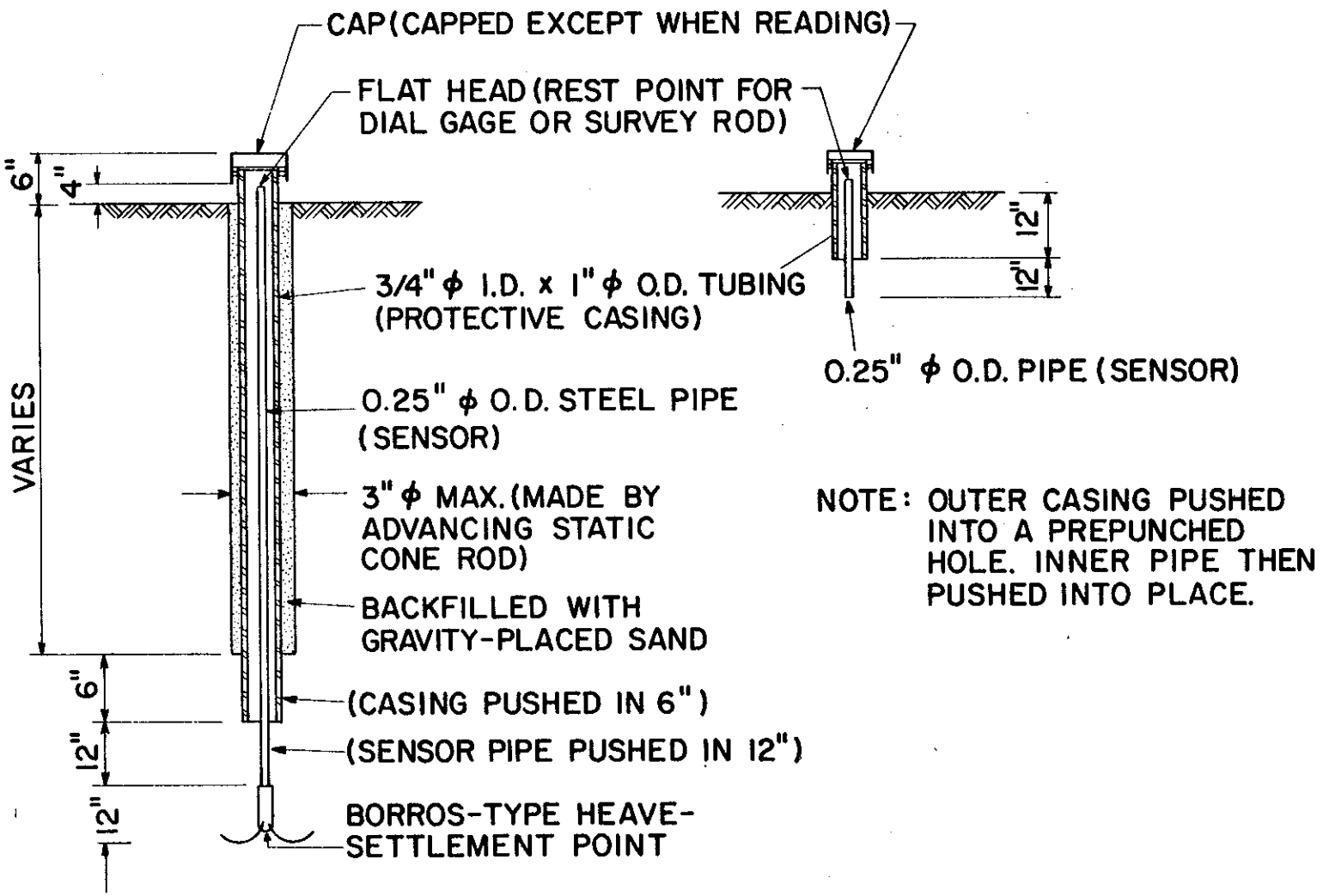

FIGURE 5.12. VERTICAL GROUND MOVEMENT POINT DETAILS (1 ft = 0.305 m; 1 in = 25.4mm)

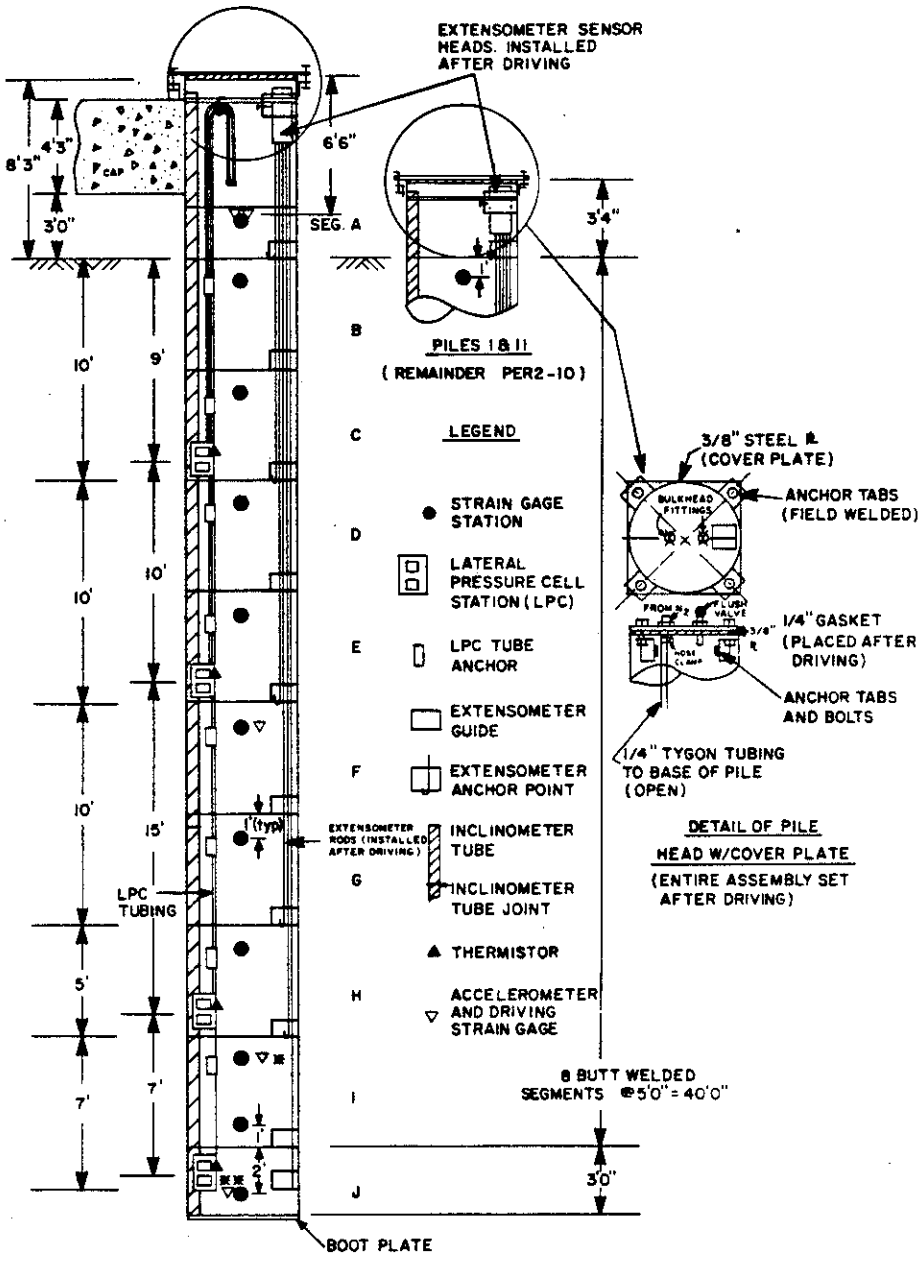

ITEMS NOT SHOWN: RIBBON CABLE, ACCELEROMETER CABLE, THERMISTOR WIRE.
SEE INDIVIDUAL DRAWINGS FOR DETAILED DIMENSIONS. ABOVE DIMENSIONS ARE NOMINAL.

LPC'S, LPC ANCHORS, LPC TUBING, THERMISTORS OMITTED ON PILES 6-11
ACCELEROMETER AND DRIVING STRAIN GAGES OMITTED ON ALL PILES EXCEPT 1,2,4,5.

* POSITION ON PILES 4 & 5 ** POSITION ON PILES 1 & 2

FIGURE 5.13. ELEVATION VIEW OF A TYPICAL TEST PILE (1 ft = 0.305 m; 1 in = 25.4 mm)

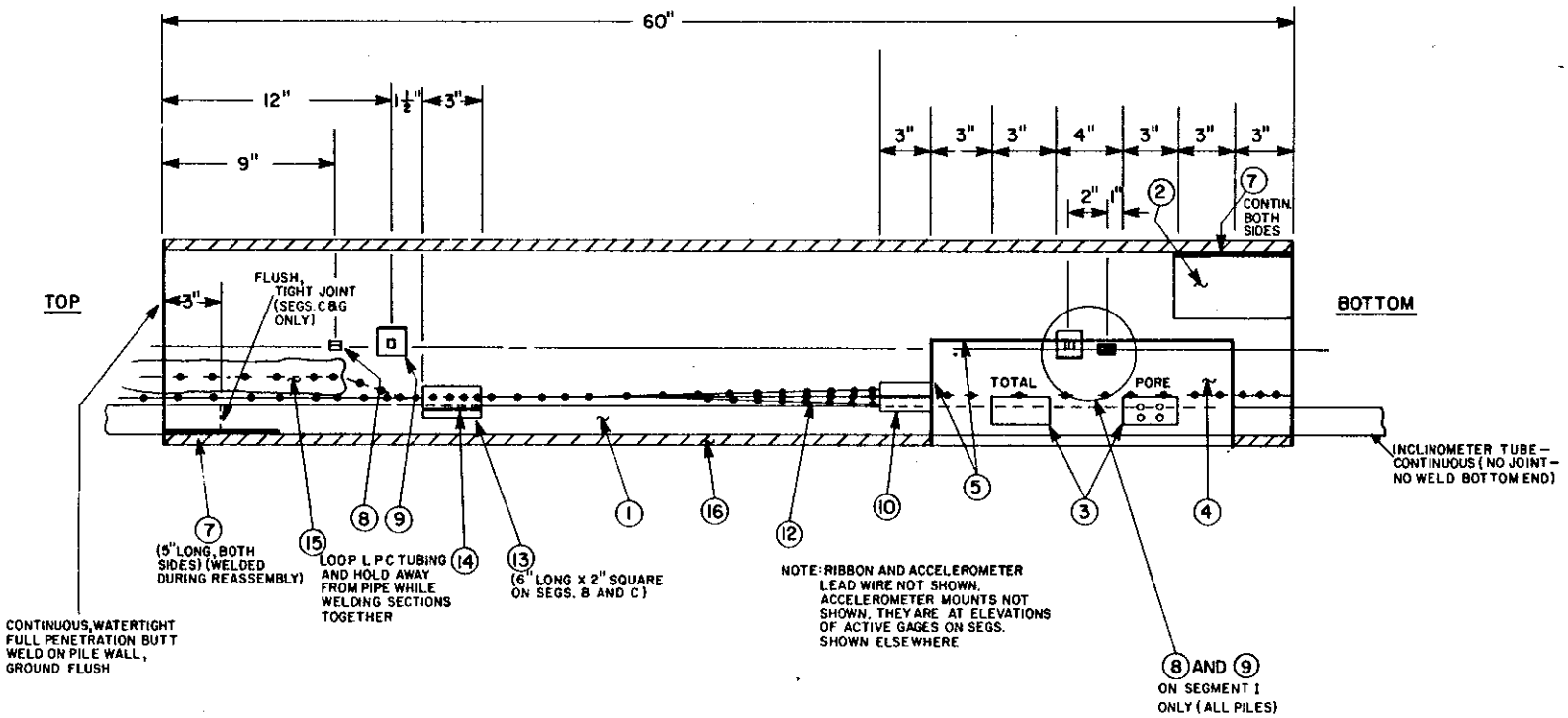

FIGURE 5.14. ELEVATION CUTAWAY OF TYPICAL FIVE-FOOT (1.5-M) PILE SEGMENT (1 in = 25.4 mm)

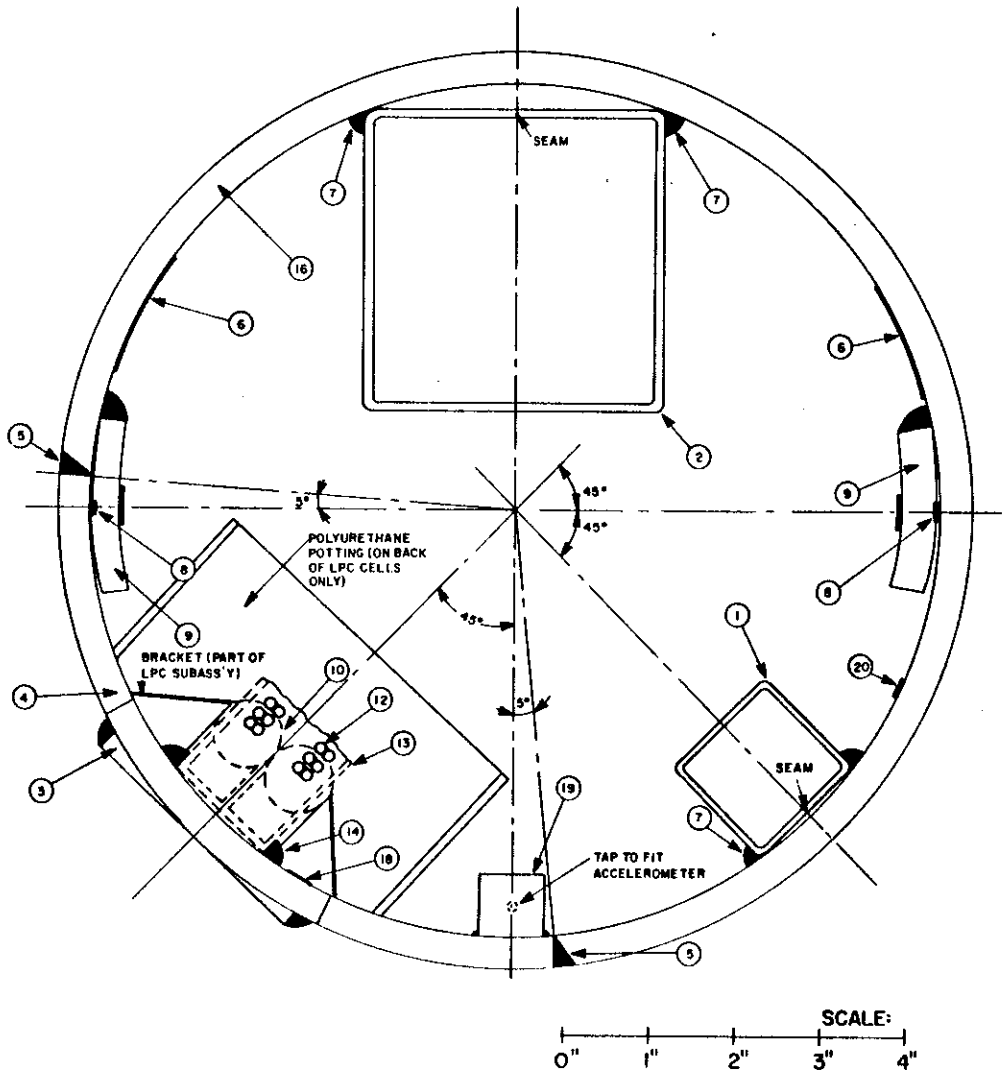

FIGURE 5.15. CROSS-SECTIONAL VIEW OF TYPICAL FIVE-FOOT (1.5-M) PILE SEGMENT (1 in = 25.4 mm)

TABLE 5.1. DETAIL TABLE; SHOWING INFORMATION FOR INDICATED NUMBERED ITEMS FOR INSTRUMENTED PILE SEGMENTS

Notes: Items 3, 4, 10, and 12 were provided as a unit by contractor

1. INCLINOMETER GUIDE TUBE. 1.5" square A-36 steel tubing (outside) by 0.12" wall. Flush fit and aligned axially at tube connection point. Note, this tube is in the relative position of Item 13 on Piles 6-11 (as-built).

2. EXTENSOMETER ANCHOR POINT AND GUIDE TUBE. 3.5" square A-36 steel tubing (outside) by 0.12" wall. Aligned axially.

3. LATERAL PRESSURE CELL SENSOR FACES. 3" by 3" flat fluid-filled cells (total pressure) w/thermal sensor. 3" by 3" rounded porous stainless steel cells (pore water pressure) with air flushing lines. Activated by differential gas pressure. Manufactured by Petur Instrument Co., Seattle, Wa. ELIMINATE ON PILES 6-11 AND ON SEGS. B, D, F, G, I, PILES 1-5.

4. LATERAL PRESSURE CELL MOUNTING PLATE. ASTM A-53, Grade 2 steel pipe with 10.75" o.d. and 0.365" wall. ELIMINATE ON PILES 6-11 AND ON SEGS. B, D, F, G, I, PILES 1-5.

5. SHOP WELD: LPC MOUNTING PLATE TO PILE WALL. 45° butt weld to full penetration; ground flat on outside. Weld all 4 sides with concurrent cooling of sensor faces to 100°F. ELIMINATE ON PILES 6-11 AND ON SEGS. B, D, F, G, I ON PILES 1-5.

6. LEAD WIRE RIBBON. 34-strand ribbon attached to pile full length with hot melt bonding compound with 6" slack section (unbonded) at end of each segment. Heavily epoxied at top of Seg. B. Mechanically clamped at bottom of Seg. A.

7. INTERNAL TUBING WELDS. ¼" round fillet welds. 6" both sides on Items 1 and 2, except were noted. Where joints occur in Item 1 make weld length 3" on either side of the joint.

8. ACTIVE STRAIN GAGE. Vertically mounted foil resistance gage, encapsulated type, bonded to pipe with heat-pressure cured epoxy. Water-proofed. Gage type: EA-06-250BF-350-W.

9. DUMMY GAGE AND TAB. Horizontally mounted gage, per 8, above, on 2" by 2" steel tab attached as indicated by 1/4" round fillet weld on one side only. Tab raised 1/16" on side opposite weld. See Detail.

10. LATERAL PRESSURE CELL SENSING ELEMENTS. Petur P-100 elements. See Detail. ELIMINATE ON PILES 6-11.

11. EXTENSOMETER ROD AND HOOK ANCHOR. Terrametrics 3/16" prestraightened aluminum rod with hook (tension) anchor.

12. LATERAL PRESSURE CELL PRESSURE, RETURN, AND FLUSHING TUBING. 3/16" ϕ polyethelyne tubing, jacketed in pairs. Slightly slack from sensing elements, Item 10, to holding anchors, Item 13. Potted into every holding tube with flexible epoxy; taped to Item 10 at passover points of higher cells. ELIMINATE ON PILES 6-11. Includes thermal sensor wire.

13. LATERAL PRESSURE CELL TUBING HOLDING ANCHORS. 1.5" potted square steel tube (outside) by 0.12" wall. One side cut away. 3" length except 6" on Segment B. Installed on all segments, except J, as shown. ELIMINATE ON PILES 6-11. Place pair side-by-side on segments B-E, Piles 1-5.

14. SHOP WELD: 1/4" round full length fillet each side of anchor.

15. ASBESTOS CLOTH WRAP. Temporary protection for LPC tubing. Removed after making butt weld.

16. PILE WALL. 10.75" o.d. by 0.365" wall, API 5L, GRADE B pipe. U.S. manufacture (Jones and Laughlin).

17. BOOT PLATE. 10.75" o.d. by 1.0" thick mild steel plate butt welded w/ 45° full penetration continuous weld on all piles. Weld ground flush.

18. THERMAL SENSOR. 0.1°F-sensitive thermal sensor, compatible with Budd P-350 readout. Epoxied onto backing plate at total pressure cell location. Sensor wire bundled with LPC tubing.

19. ACCELEROMETER MOUNT. Placed internally on Segments I (J on Piles 1 and 2) and F, and externally on A only on Piles 1, 2, 4, and 5. ±250-g, current-type (piezoelectric) accelerometers to be attached to bottom of mounts and lead wire bundled with LPC tubing. ±1000-g devices at Seg. A and at Seg. J on Piles 1 and 2. Mounts are mild steel, 1.0" cubes, tapped to accommodate accelerometer.

20. STRAIN GAGE, DRIVING MONITOR. Single element strain gage mounted internally at same level as each accelerometer mount on Piles 1, 2, 4, and 5. Lead wire separate from ribbon (Item 6) and brought out 1/2" ϕ hole during driving. Two diametrically opposite gages mounted on extension segment.

NOTE: 1 in. = 25.4 mm.

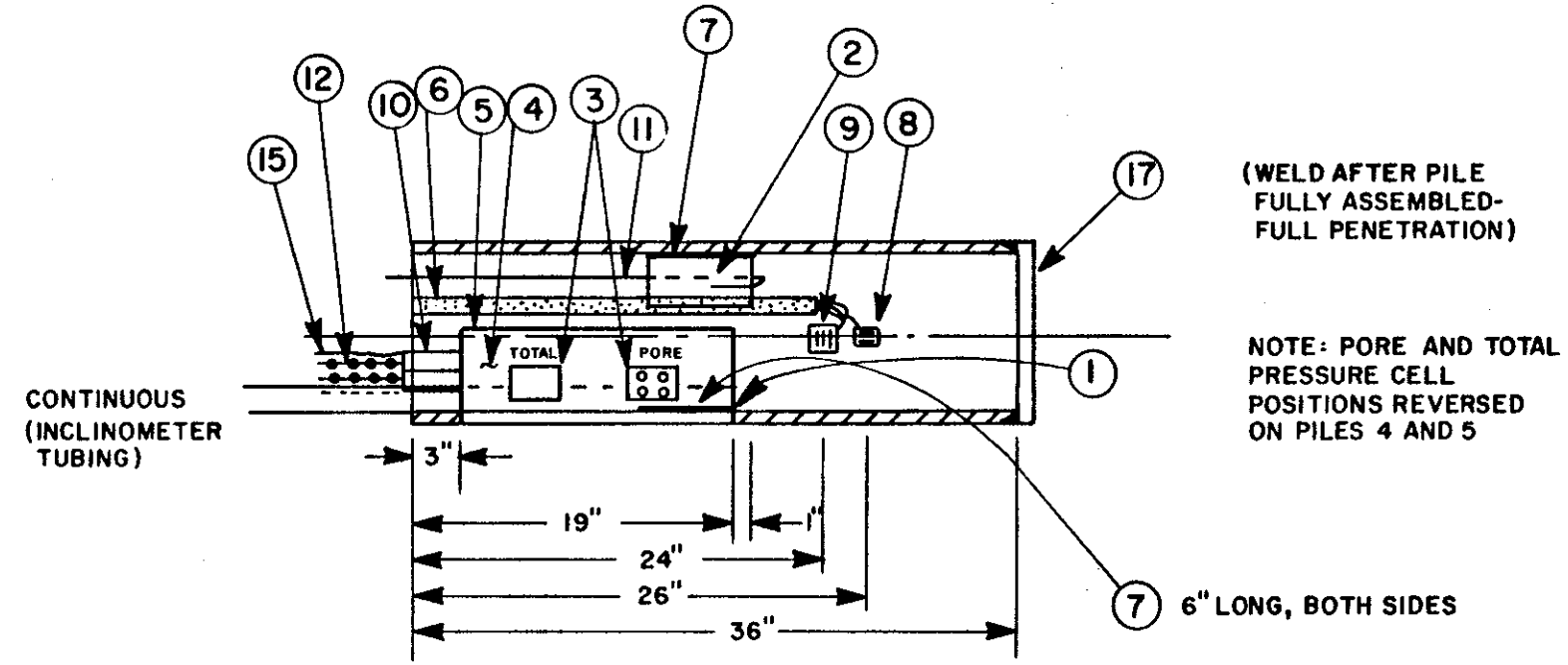

FIGURE 5.16. ELEVATION CUTAWAY OF END SEGMENT (1 in = 25.4 mm)

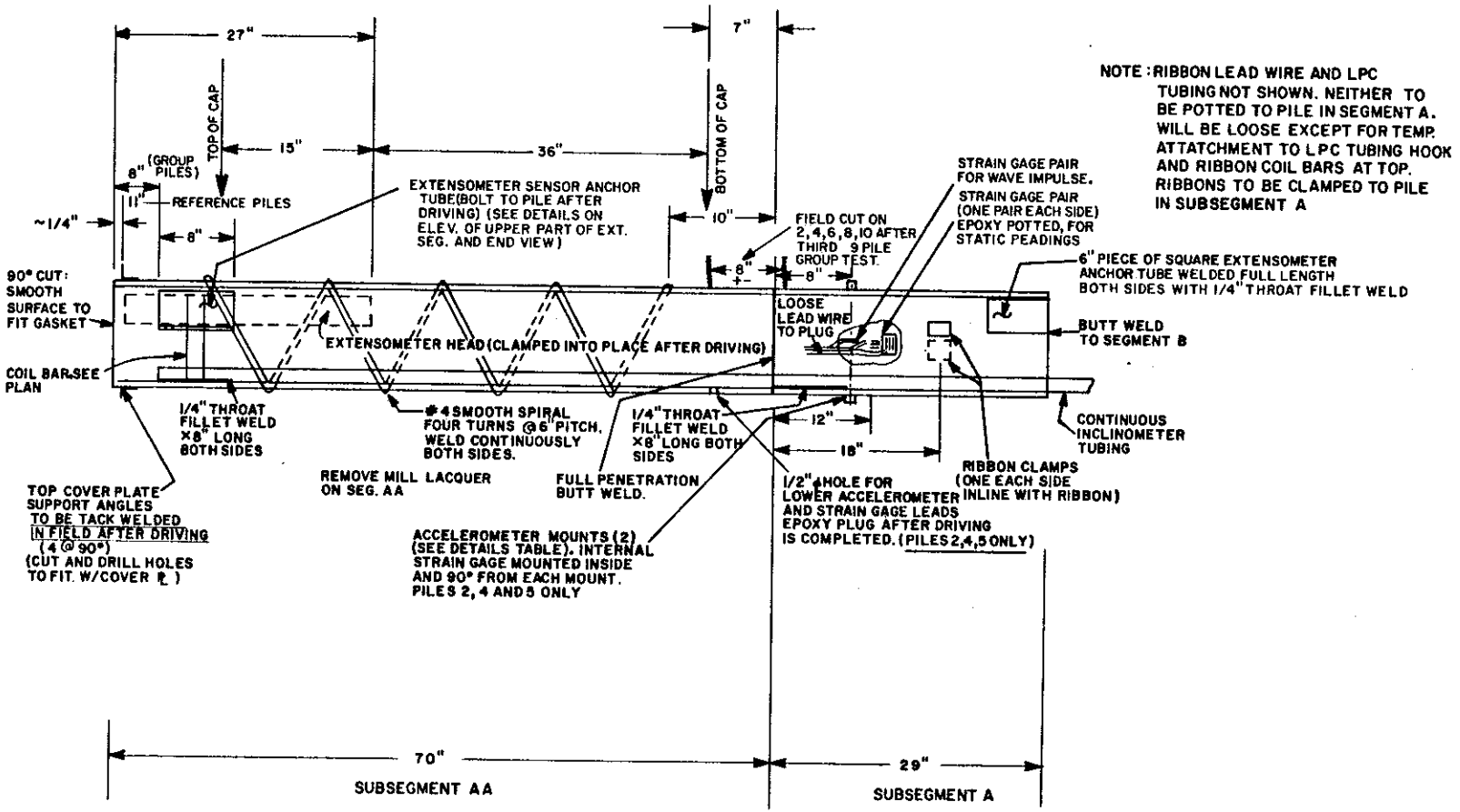

FIGURE 5.17. ELEVATION CUTAWAY OF EXTENSION SEGMENT FOR GROUP PILES
(1 in = 25.4 mm)

Details of the extensometer head mounting, extensometer anchors, and extensometer heads are indicated in Figs. 5.20, 5.21, 5.22 and 5.23. Details of the strain gage installations and lateral pressure cells are given in Figs. 5.24 and 5.25, respectively. The loading head for the reference piles is shown in Fig. 5.26.

Schematic drawings of the electrical and pneumatic data acquisition systems, described in more detail later, are shown in Figs. 5.27 - 5.29.

The instrumentation systems were all designed to give maximum redundancy. Backup systems were provided for measuring load at the tops of piles, load variation along the piles, and settlement, which were the most critical variables to be measured. No provisions were made to install replacement elements of a given instrument system in the event of a failure of an element (e.g., piezometer tube struck by driven pile). Extreme care was taken to ensure that all elements were in proper working order before placement into the ground. The philosophy followed in choosing or designing the various instrumentation and readout systems was that all systems should be as simple, rugged, and stable as possible, commensurate with range and sensitivity requirements, in order to reduce the chances for malfunction.

Specifications for Instrumentation

a. Ground Instruments

(1) Piezometers. All ground piezometers were Petur Instrument Model P-102-1 wellpack pneumatic piezometers, with Model P-100 pressure sensor. Integral leads were provided from the piezometer to the readout device (gas pressure gage) on the surface. The length of the integral leads was equal to the depth of the piezometer plus the distance of the piezometer from the center of the cap plus thirty feet (9 m). See Fig. 5.11 for further details.

(2) Piezometer readout. All ground piezometers were read with a SINCO standard pneumatic readout device with 300 psi (2.07 mN/m^2) range, accurate to 1 psi (6.89 kN/m^2) for the full range. An integral nitrogen pressure tank was built into the readout device. Readings on individual instruments were made by plugging and unplugging directly from the readout device using quick-connect couplings. The readout device was situated just outside of the east

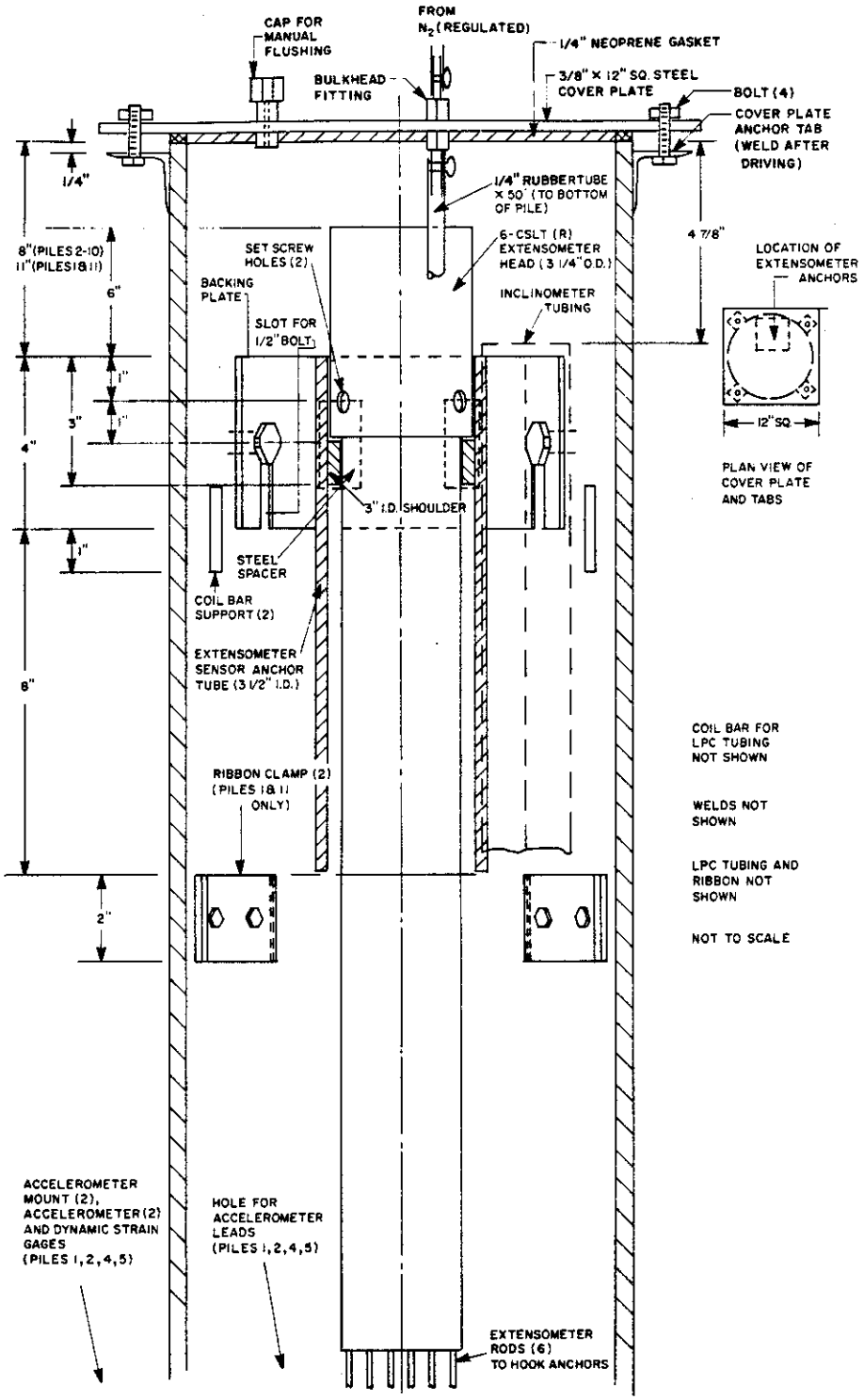

FIGURE 5.20. DETAIL OF EXTENSOMETER HEAD MOUNTING (1 in = 25.4 mm)

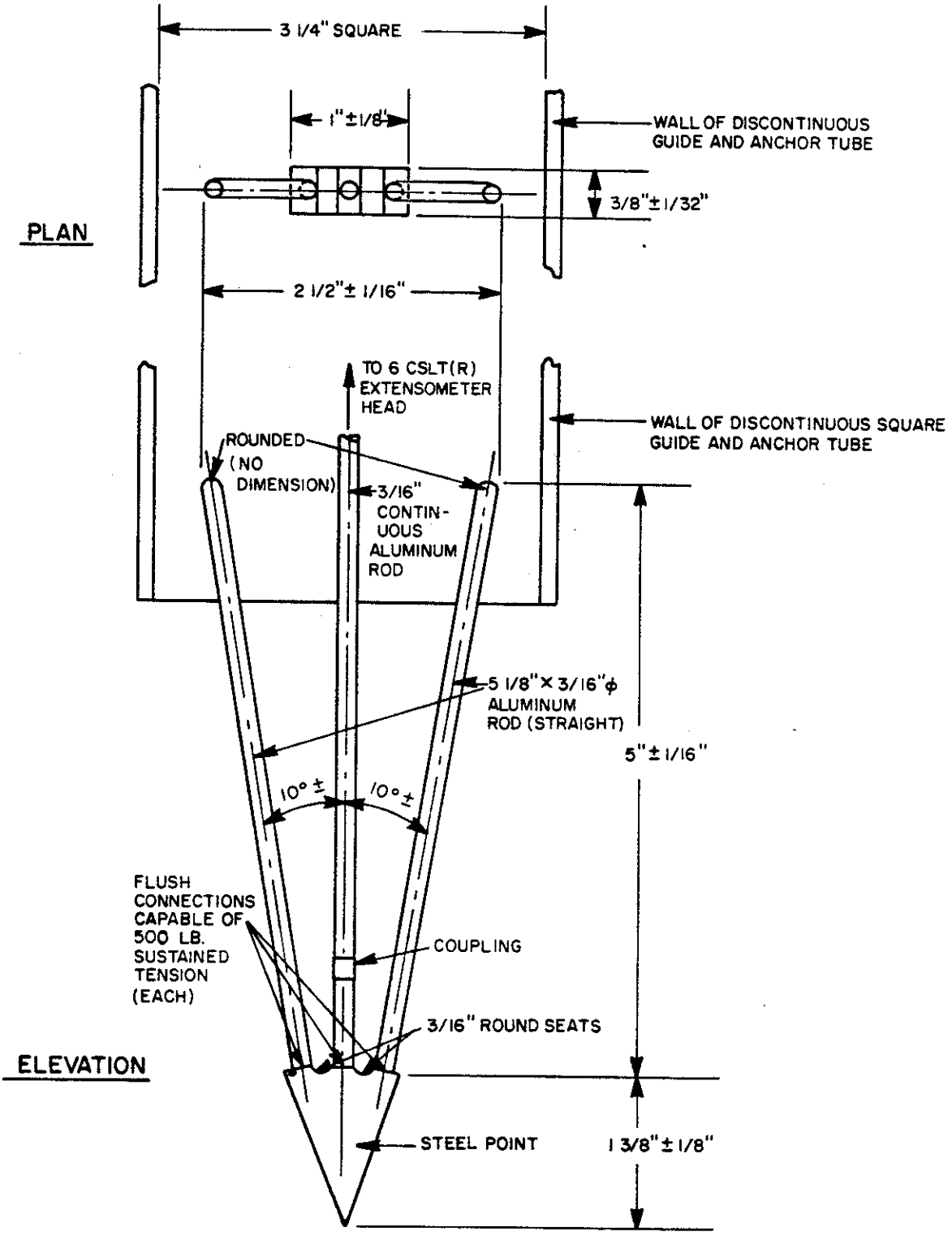

FIGURE 5.21. DETAIL OF EXTENSOMETER ANCHOR (A) (1 in = 25.4 mm; 1 lb = 4.45 N)

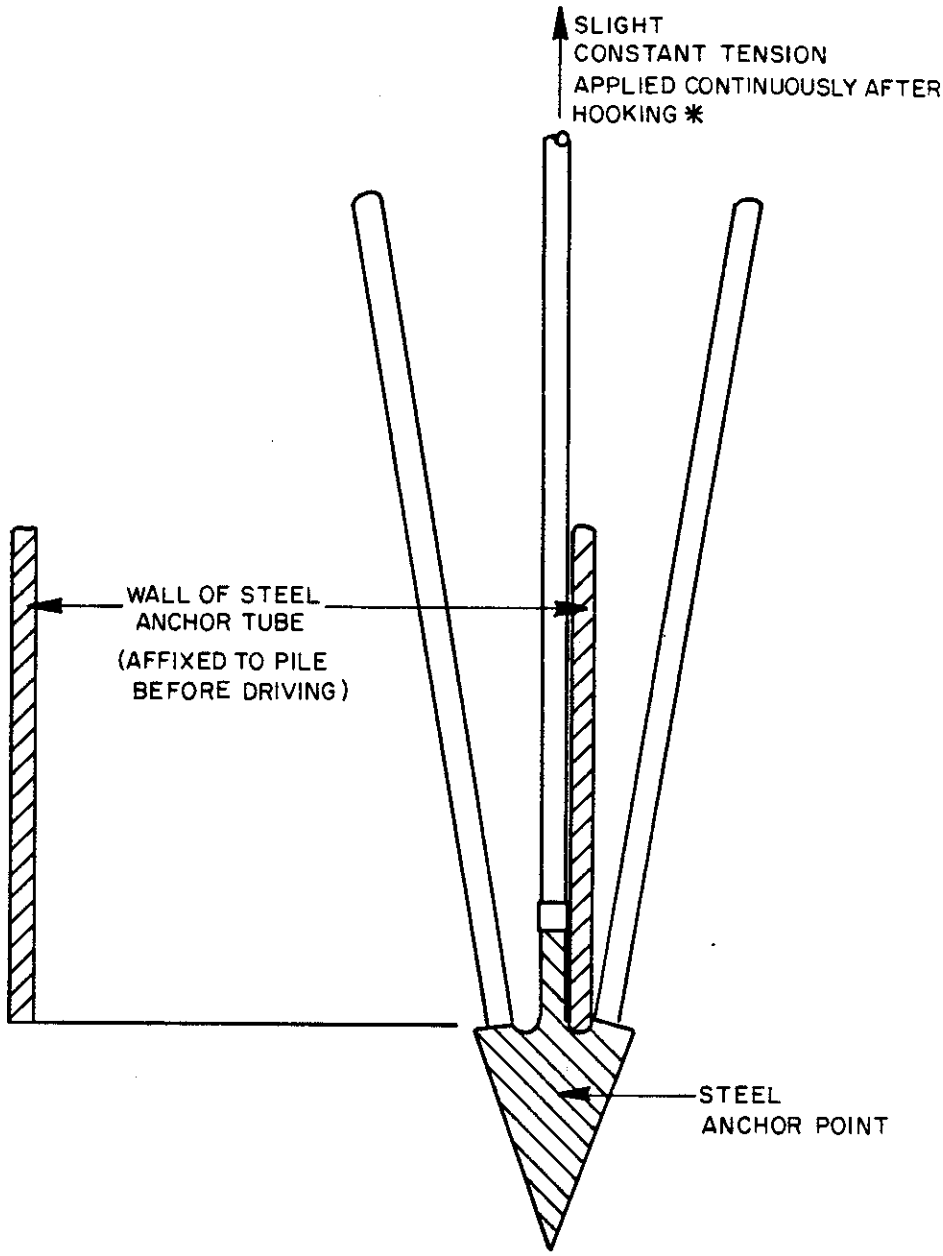

*REQUIRES 3 FT. EXTRA ROD SO THAT ROD CAN BE CLAMPED TO TOP OF PILE, THE 6 CSLT(R) EXTENSOMETER HEAD SLIPPED OVER THE EXTENDED 3 FT. OF ROD, THE ROD UNCLAMPED AND HELD SIMULTANEOUSLY IN TENSION ABOVE EXTENSOMETER HEAD, THE EXTENSOMETER HEAD SLIPPED INTO POSITION INSIDE THE PILE AND CLAMPED INTO PLACE, THE RODS CLAMPED INTO THE EXTENSOMETER HEAD, AND THE EXCESS ROD CUT OFF.

FIGURE 5.22. DETAIL OF EXTENSOMETER ANCHOR (B) (1 ft = 0.305 m)

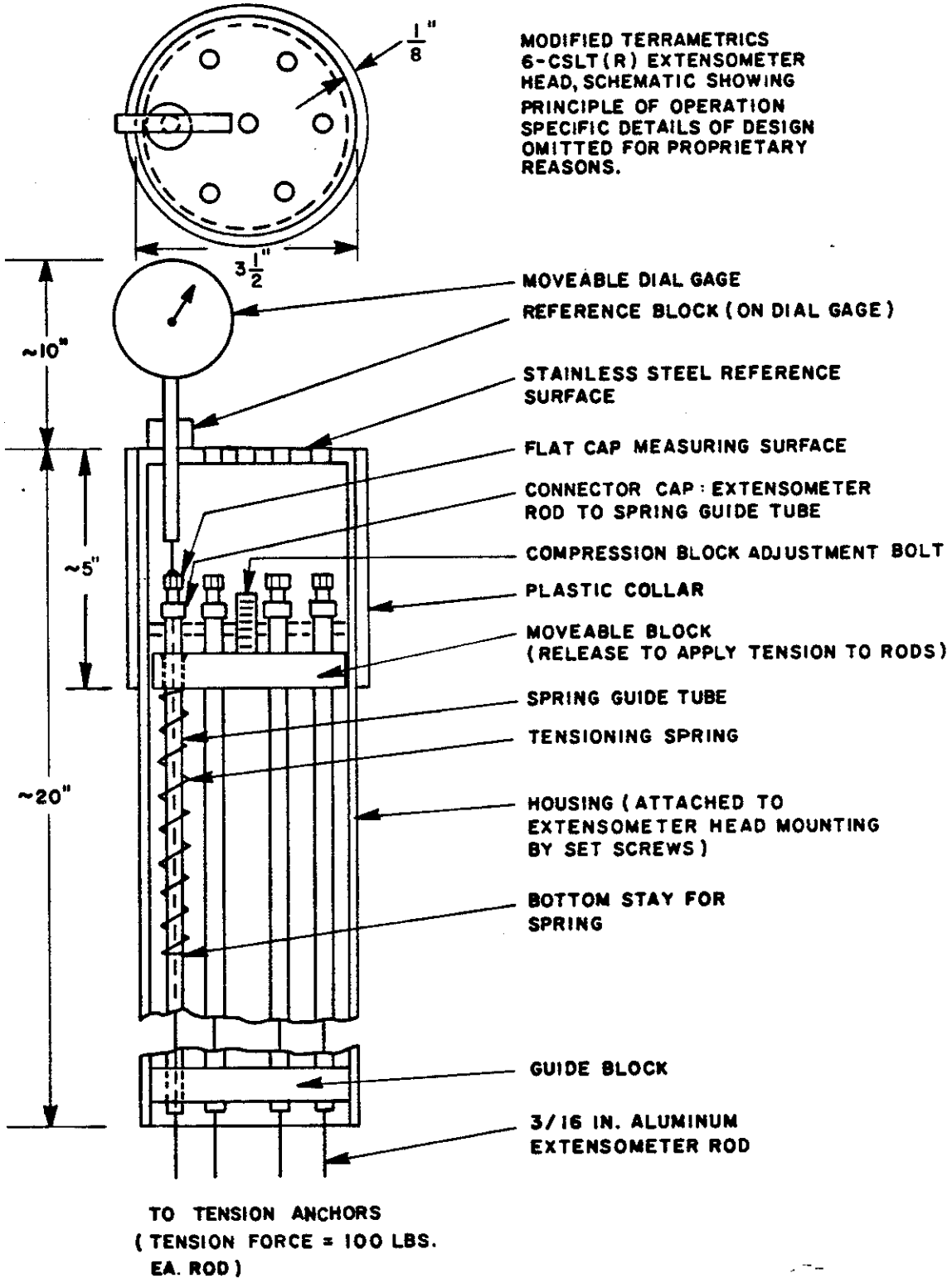

FIGURE 5.23. DETAIL OF EXTENSOMETER HEAD (1 in = 25.4 mm)

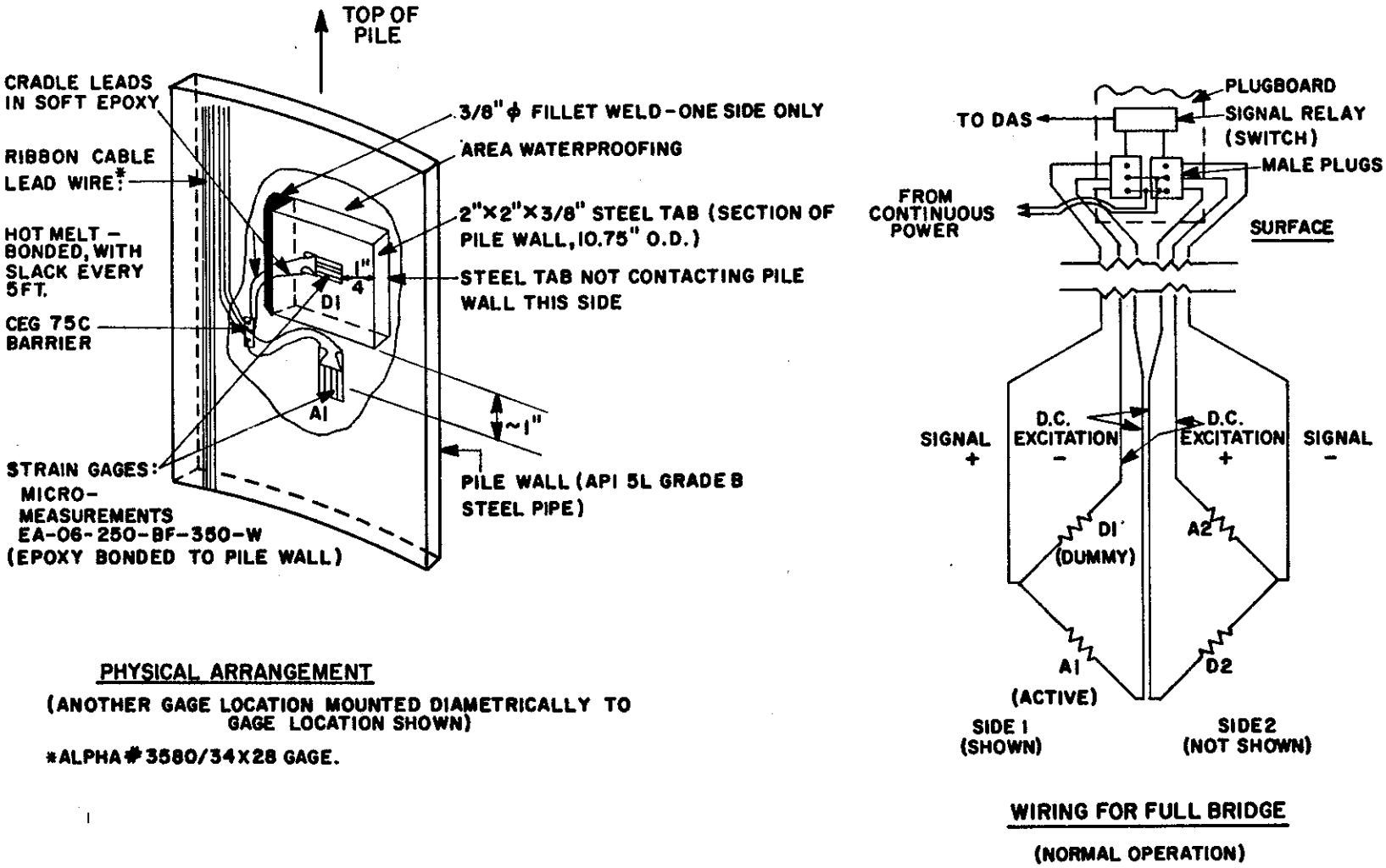

FIGURE 5.24. DETAIL OF STRAIN GAGE LOCATION (1 in = 25.4 mm)

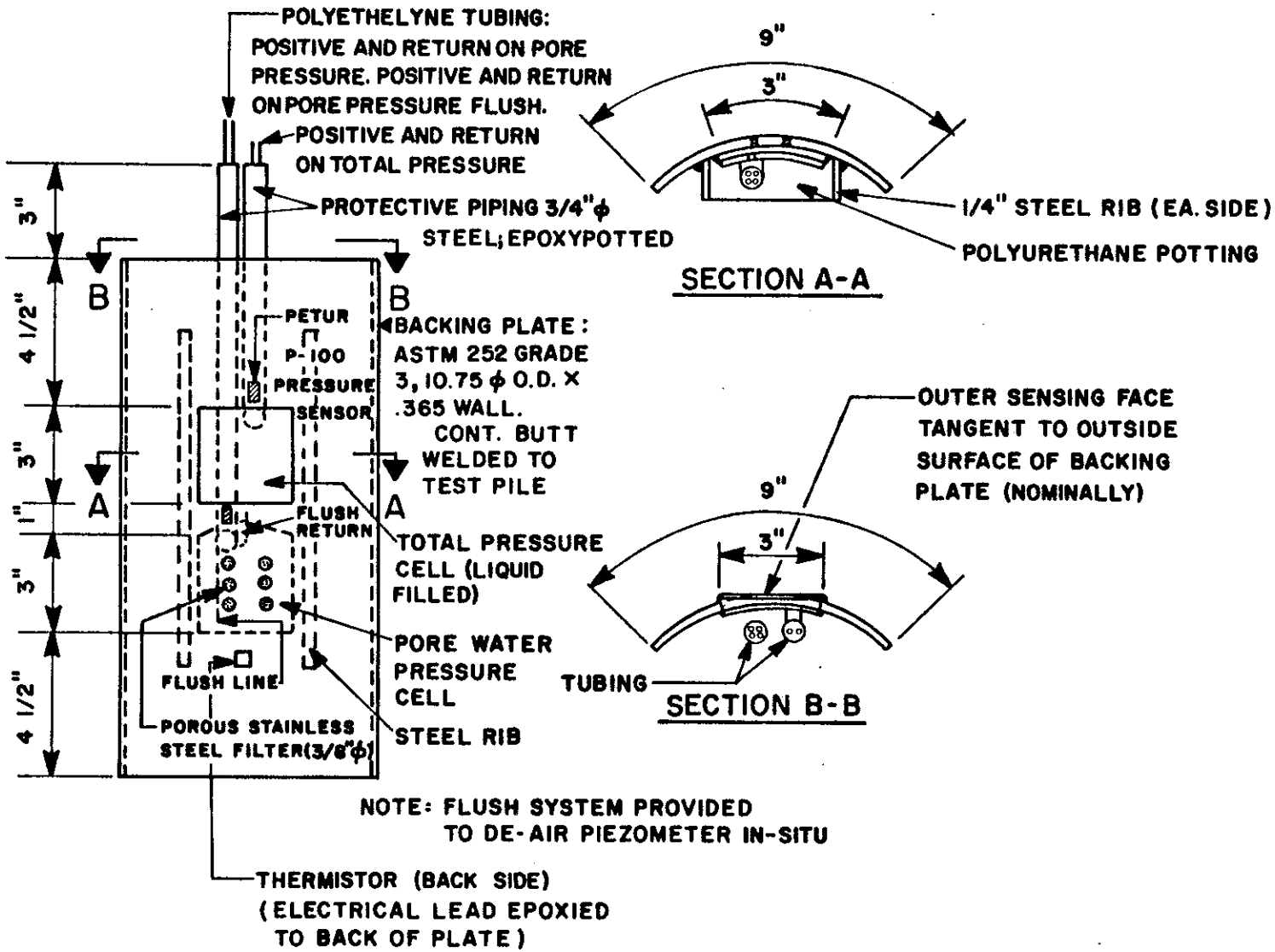

FIGURE 5.25. DETAIL OF LATERAL PRESSURE CELL (LPC) (1 in = 25.4 mm)

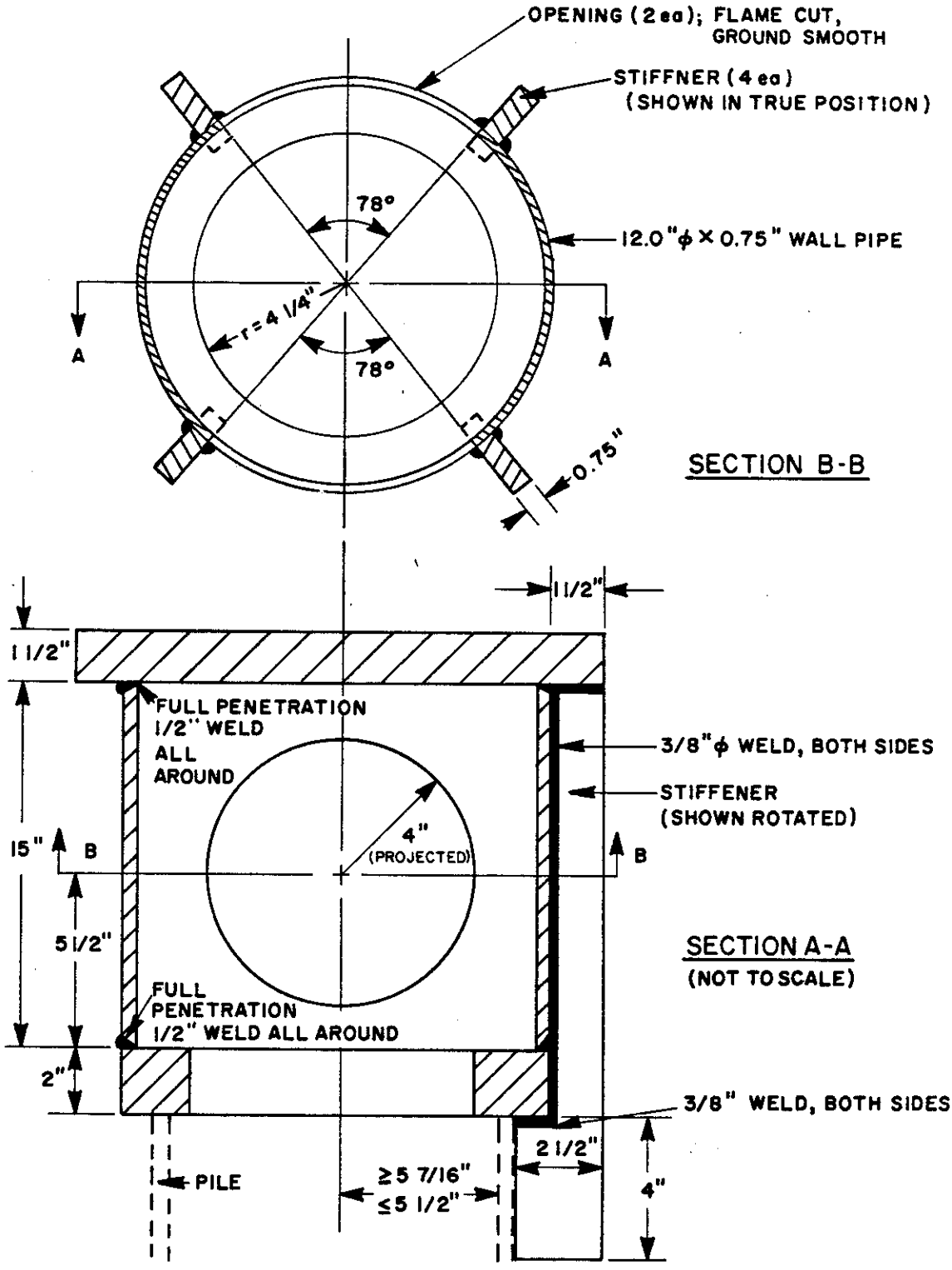

FIGURE 5.26. LOADING HEAD FOR REFERENCE PILES (1 in = 25.4 mm)

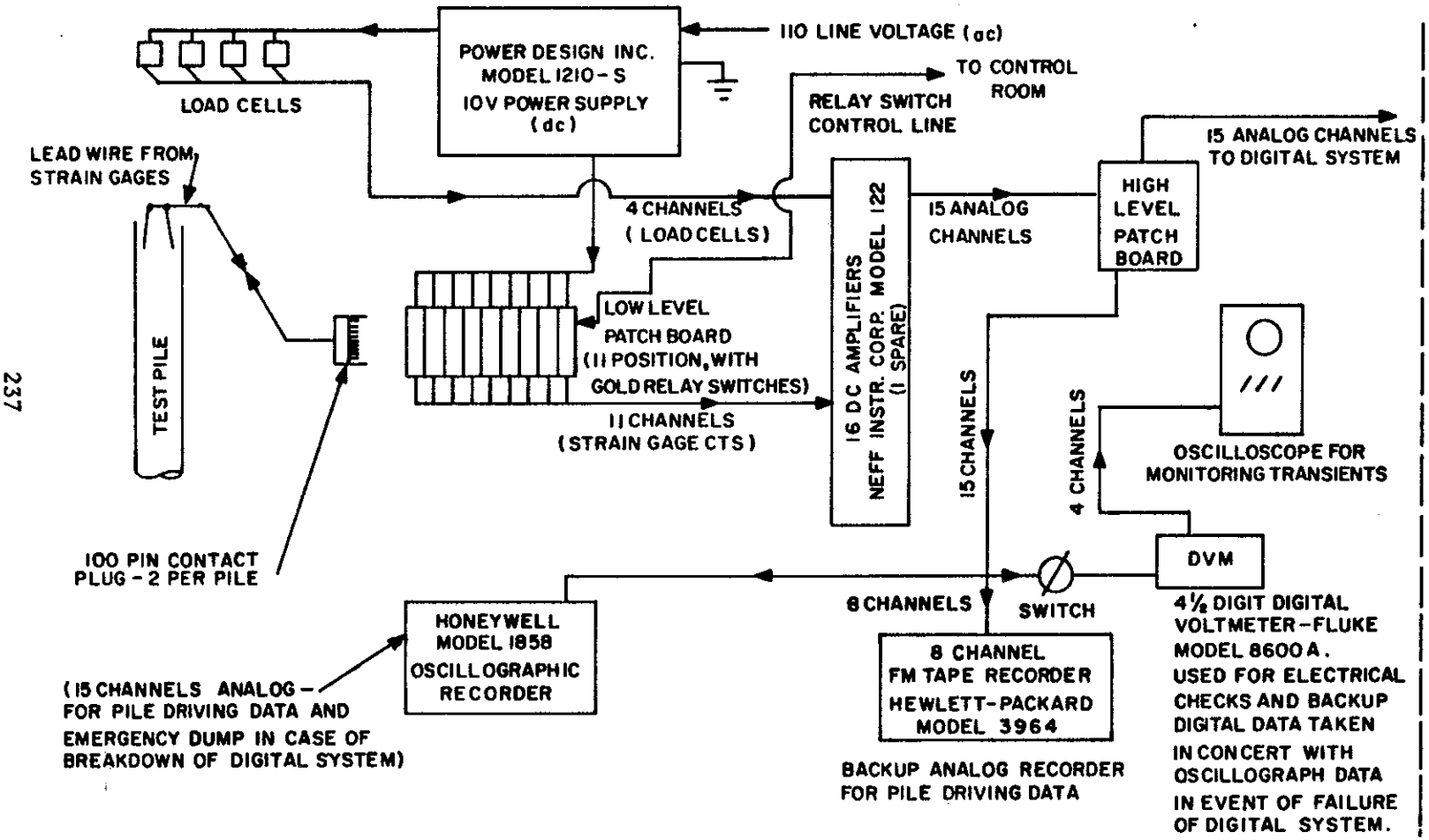

FIGURE 5.27. ANALOG PORTION OF ELECTRONIC DATA ACQUISITION SYSTEM (SCHEMATIC)

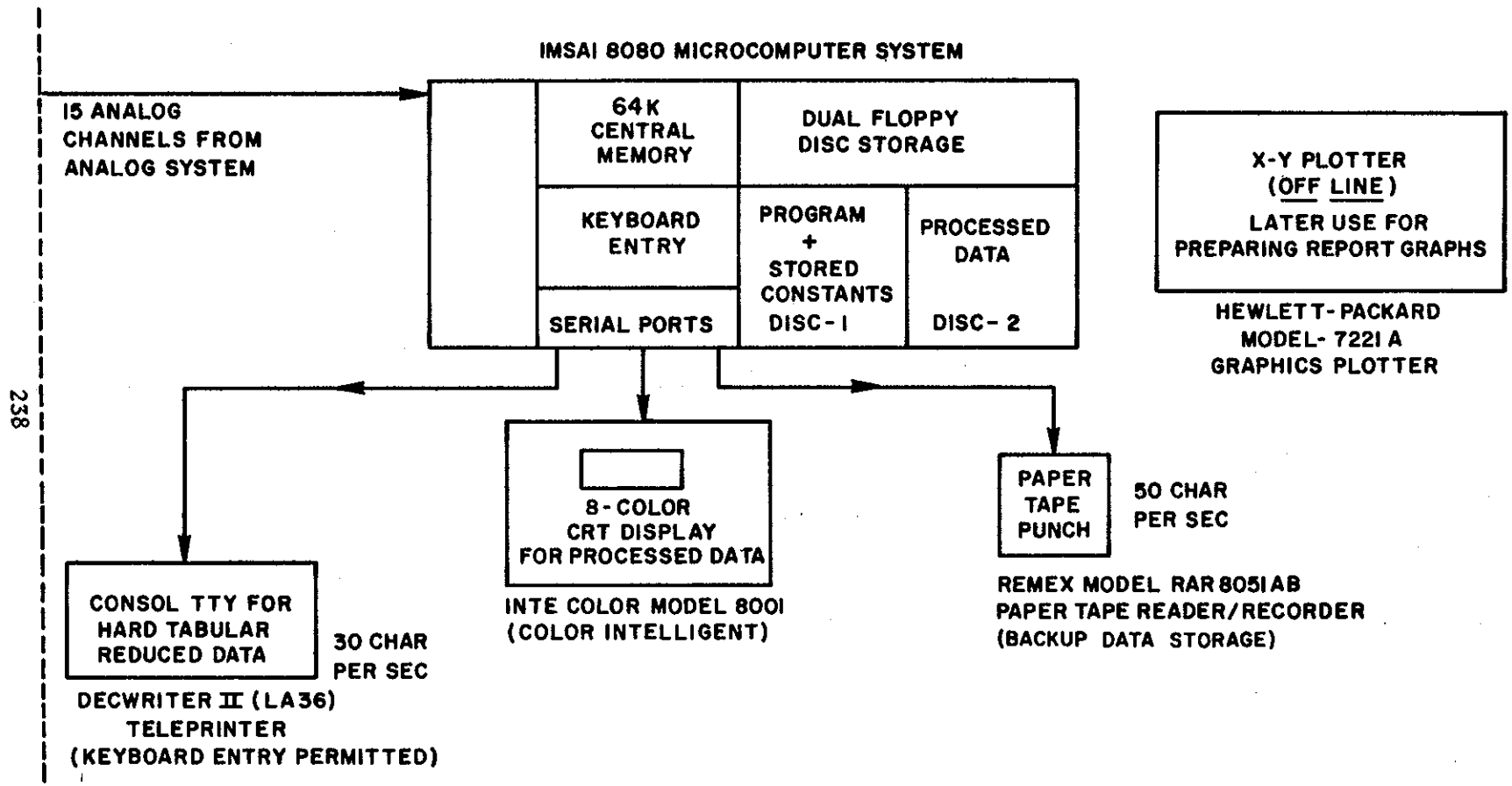

FIGURE 5.28. DIGITAL PORTION OF ELECTRONIC DATA ACQUISITION SYSTEM (SCHEMATIC)

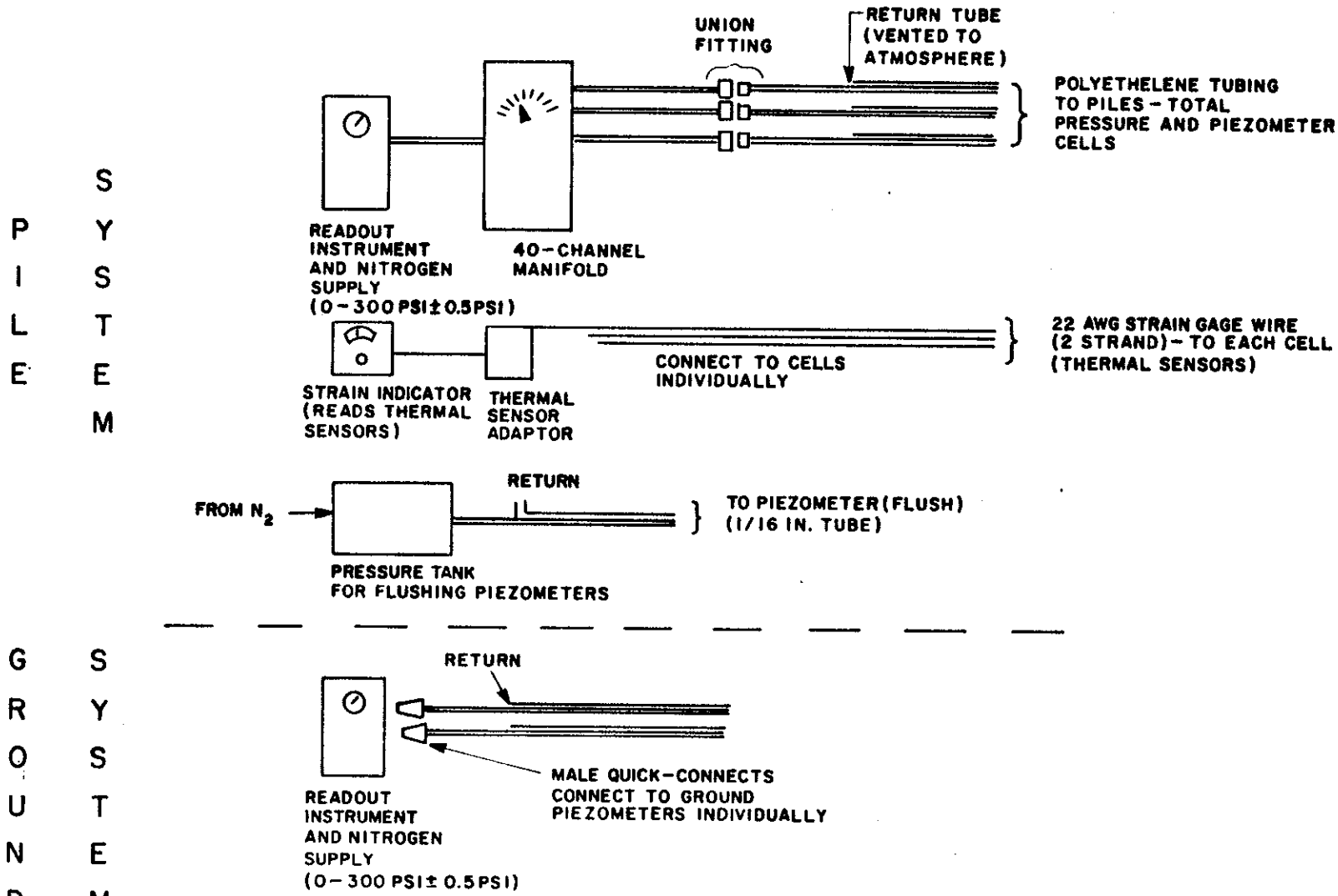

FIGURE 5.29. PNEUMATIC DATA ACQUISITION SYSTEMS (SCHEMATIC)
(1 psi = 6.89 kN/m^2)

wall of the Band Annex, and all lines from the piezometers to the manifold were buried approximately 12 inches (0.305 m) below the surface to prevent accidental damage. The ground piezometer readout system was separate from the pile piezometer and total pressure readout system, described later. All data were recorded manually.

(3) Surface and depth vertical movement ("settlement") points. These devices are installed as indicated in Fig. 5.12. Depth points were Borros-type heave-settlement points, with self-activating anchors obtained from Slope Indicator Co. Surface points were straight rods. All points were placed at least 12 inches (0.305 m) into undisturbed soil. Access holes were made by pushing static cone rod and then inserting the casing and then the Borros points - telltale rod assembly as a single unit.

Data acquisition for vertical movement points is described in the section on sequence of field operations. All data were recorded manually.

b. Pile Instruments

The following is a description of the pile instrumentation. Detailed descriptions of the calibration procedure and performance of the various instruments (including ground instruments) are given in Appendix E.

(1) Strain gages. Electrical resistance strain gage circuits were installed on the interior of the eleven test piles at locations shown in Figs. 5.13 - 5.18. A detail of each circuit is shown in Fig. 5.24. The interior location was chosen to afford maximum mechanical protection and to permit flushing of the ambient air with dry nitrogen, depicted in Fig. 5.13, in order to minimize build-up of moisture on the gage elements, thereby enhancing the long-term stability. All gages were Micromeasurements, Inc., EA-06-250BF-350-W encapsulated, single element gages. Full bridge arrangement was used to minimize drift due to temperature variations in the pile material and to cancel the effects of bending. The dummy, temperature compensating gages were bonded to relatively unstrained tabs rather than to the pile wall to minimize the effects of differences in hoop stresses in the piles that occured between

the calibration condition and the in-situ condition. Leads were continuous, shielded ribbon wire, three strands per half bridge, terminating in a high-quality contact plug at the top of the pile. The length of the cable exceeded the length of the pile by about twelve feet (4 m) to permit plugging of the circuits into access cables to the data acquisition system free of the pile heads.

In addition to the strain gage instrumentation for load transfer measurements detailed in Fig. 5.24, single element strain gages were also installed in the interior of Piles 1, 2, 4, and 5 at locations described on Fig. 5.13. These longitudinally mounted gages were essentially identical to the active gages shown on Fig. 5.24 but were wired separate from that system and were placed in a full bridge in which the completion gages were on the surface. These single element gages were used exclusively to assess the attenuation of the stress wave produced by the hammer as a means of checking wave equation parameters for reference and group piles. These gages were powered by a 10-volt power supply and amplified as indicated in Fig. 5.27. This system of "dynamic" strain gages was read on each of the four indicated piles for several blows of the hammer at various penetrations by means of the oscillograph (Fig. 5.27). Back-up readings were made on a multi-track FM tape recorder. The data acquisition equipment was run continuously during installation of these four test piles.

Accelerometers of the piezoelectric type were also placed adjacent to the dynamic strain gages at the locations indicated on Fig. 5.13. These emplacements were made by University of Houston personnel at no cost to the FHWA as an experiment to assess the attenuation of driving energy along each of the four piles with dynamic instrumentation. No discussion of data for these accelorometers is presented in this report or in the Final Report.

(2) Strain gage data acquisition system. The high quality contact plugs from each half of the strain gage circuits were plugged, two per pile, into a low level patch board situated adjacent to the test piles. The full Wheatstone bridges at all levels were completed within this patch board. See Fig. 5.27. Once the plugs from all piles to be read during a test had been plugged into the patchboard, switching from pile to pile was accomplished through gold coated (T-Bar)

electrical switching units. In the event of gage outages, this system permitted reading of half bridges. The electronic data acquisition system shown schematically in Figs. 5.27 and 5.28 had the capacity of acquiring 16 independent channels of data simultaneously with relative long-term stability. The channels included eleven channels for the eleven strain gage circuits in the group piles, four channels for the group load cells, and one spare channel in case of a malfunction of an amplifier. The switching unit allowed acquisition of 103 channels of electronic data (not simultaneously) during a test on the group.

The various components of the system, with model numbers, manufacturers, and functions (where not obvious) are shown in Figs. 5.27 and 5.28. Primary raw data storage was on a punched paper tape record. Raw data included load (read from load cells), settlement (read from dial gages and entered manually from the keyboard), and pile and strain gage number and digital output voltage. An IMSAI 8080 microcomputer system was used to process the data in real time. A computer program unique to the IMSAI 8080 machine was developed to convert all strain circuit outputs to load using calibration curves obtained prior to the tests. Load as a function of depth in a given pile was displayed in bar chart form under control of the program on a color CRT display for immediate inspection during a test. The computer program then performed numerical differentiation (using least squares curve fitting) and integration on the load versus depth data to obtain numerical values of f versus z at prescribed depths. Zero values for loads were considered to be both the pre-driving and pre-test zero values. Use of the pre-driving values was included to attempt the direct inclusion of residual stress effects. Tabular values of f versus z for each zero and for each load on each pile were printed immediately by a teletype. The teletype output was the mode of storing the reduced data output. Raw data were also printed by the teletype. Each table so obtained also displayed the load and settlement at the butt of the pile and appropriate identification.

Load data for a given pile were not stored in the microcomputer once the readings on that pile were made. In the group test, when the next pile was to be read, the gold contact switching unit was employed to switch to the eleven-gage plugs for the next pile. No plugging-

unplugging was done once a test started. Readings then continued until all piles were read. A full set of strain gage readings on a pile required a time of about 10 seconds (including switching time). Group loads, as indicated by the sum of the load cell readings, and corresponding group settlements, as indicated by the average settlements for the individual piles, were retained in central memory. The partial load-settlement curve was displayed on the CRT at any time desired by the investigator under control of the computer program.

The following relevant specifications for the components of the data acquisition system, all of which are owned by the Department of Civil Engineering at the University of Houston, except where noted, are given:

(a) Electronic Power Supply

0-15 volts
0-10 amps
Regulation: 0.01% + 2 millivolts
RMS ripple: 500 microvolts

(b) DC Amplifiers (12 owned by UH, 4 purchased for this study by FHWA funds)

Gain: 1 to 2500 (in steps)
Accuracy: 0.01%
Stability: 0.005%
Input Impedence: 100 megohms
Output: 10 volts, 100 milliamps

(c) Oscillograph Recorder

Sensitivity: 100 microvolts
Capacity: 18 channels
Response: 5 kHz at 7.2 inch (18.3 cm) trace amplitude; greater at lower amplitudes

(d) FM Tape Recorder

Number of Channels: 8
Tape: ¼ inch (0.6 cm) wide, standard 7 inch (18 cm) plastic reel

(e) Microcomputer

Addressable memory: 65,536 words

Word size: 8 bits

Cycle time (machine): 0.5 microsecond

(f) Paper tape punch

Tape: 1 inch (2.5 cm) wide, unoiled, ANSI X 3.18, 1000 ft. (305 m) roll

Punch speed: 50 characters per second, standard

(g) Teletype (TTY)

Keyboard: Standard ASCII, 10 characters per inch, six lines per inch (approximately 2 lines per cm)

Print Speed: 30 characters per second maximum

(h) CRT Unit (color intelligent)

Screen: 19-inch (48 cm) diagonal, 4 x 3 aspect ratio

Number of colors: 8

The electronic data acquisition system was housed in a building immediately adjacent to the test site, as shown in Fig. 5.10, for reasons of security, convenience, and availability of line voltage. The leads connecting the low-level patchboard and the remainder of the system were buried to prevent differential heating and cooling.

(3) Lateral pressure cells. The lateral pressure cells were conceptually designed by University of Houston personnel. They were pneumatic and were specially constructed for this project by Petur Instrument Co. A detail of a cell is shown in Fig. 5.25. Both the total and pore water pressure components had a capacity of 300 psi (2 mN/m^2). The pore water portion was also be fitted with a flushing system to permit de-airing as shown schematically in Fig. 5.29. Both total and pore water pressures were sensed using patented Petur Model P-100 sensing elements that were protected from pile driving forces, as indicated, by potting them into protective steel piping. Positive pressure lines terminated with union fittings which were stored inside the extension portion of the pile when readings were not being made. During a test, the arrangement shown in Fig. 5.29 was used to connect the cells to the readout device.

The temperature-sensitive total pressure instruments necessitated the development of a calibration curve for each cell giving indicated pressure as a function of indicated temperature obtained through a thermal sensor placed on the cell. The cells were also constructed in such a way that they did not register pressure at temperatures below about 16°C, which, prior to pile installation, was estimted to be the minimum ground temperature likely to occur at the site.

The backing plates for the cells, as constructed, were also slightly concave in longitudinal profile, so that they were placed into the pile with the bottom (pore pressure) end flush with the pile wall and the top end protuding approximately 3 mm. This protrusion was ground essentially flush with the pile surface. This still left the center of the total pressure plate recessed about 2 mm, while the shoulders of the plate protruded about 2 mm. Further details of this anomoly are presented in Appendix E, Final Report.

(4) Lateral pressure cell readout system. The lateral pressure readout system was similar to that used for the ground piezometers, except that an intermediate manifold was provided for connecting all the lines to the readout during a test. All data were recorded manually, and corrections to raw data readings were also made manually.

(5) Settlement, translation, and rotation. All displacement readings on the piles and cap were made with 0.001-inch (0.025 mm) accuracy dial gages. Details of the reference system for the various dial gages are shown in Figs. 5.30 and 5.31. Dial gage data were recorded manually. Back-up settlement readings on the cap were made by reading scales on cap with a microhead level, as indicated in the following section on sequence of field operations.

(6) Load. Load was measured through four (for group test) or one (for single pile test) precalibrated electronic load cells, as described in Chapter 4. For the single pile, backup load measurement was obtained from the uppermost level of strain gages. For the group tests, two levels of strain gages at or above the ground surface were provided to give two separate measurements of load on a given pile. All data were recorded using the electronic data acquisition system.

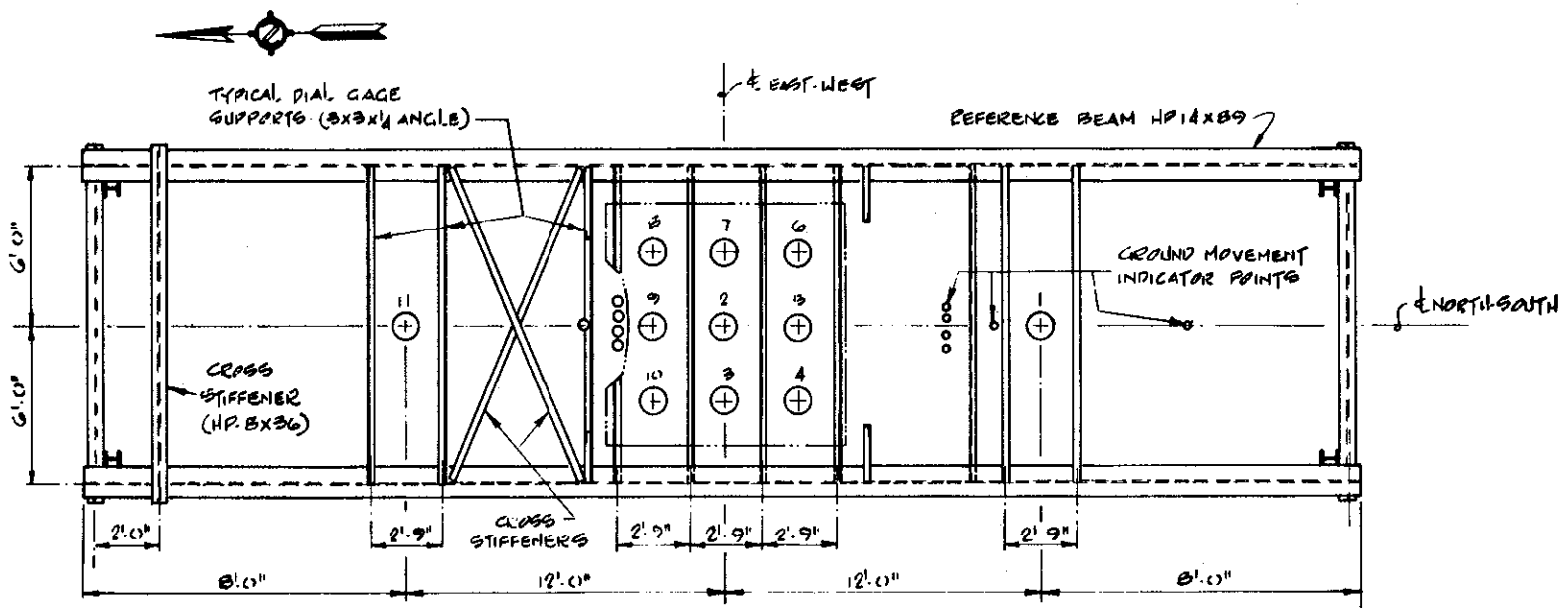

FIGURE 5.30. PLAN VIEW OF REFERENCE SYSTEM (1 ft = 0.305 m; 1 in = 25.4 mm)

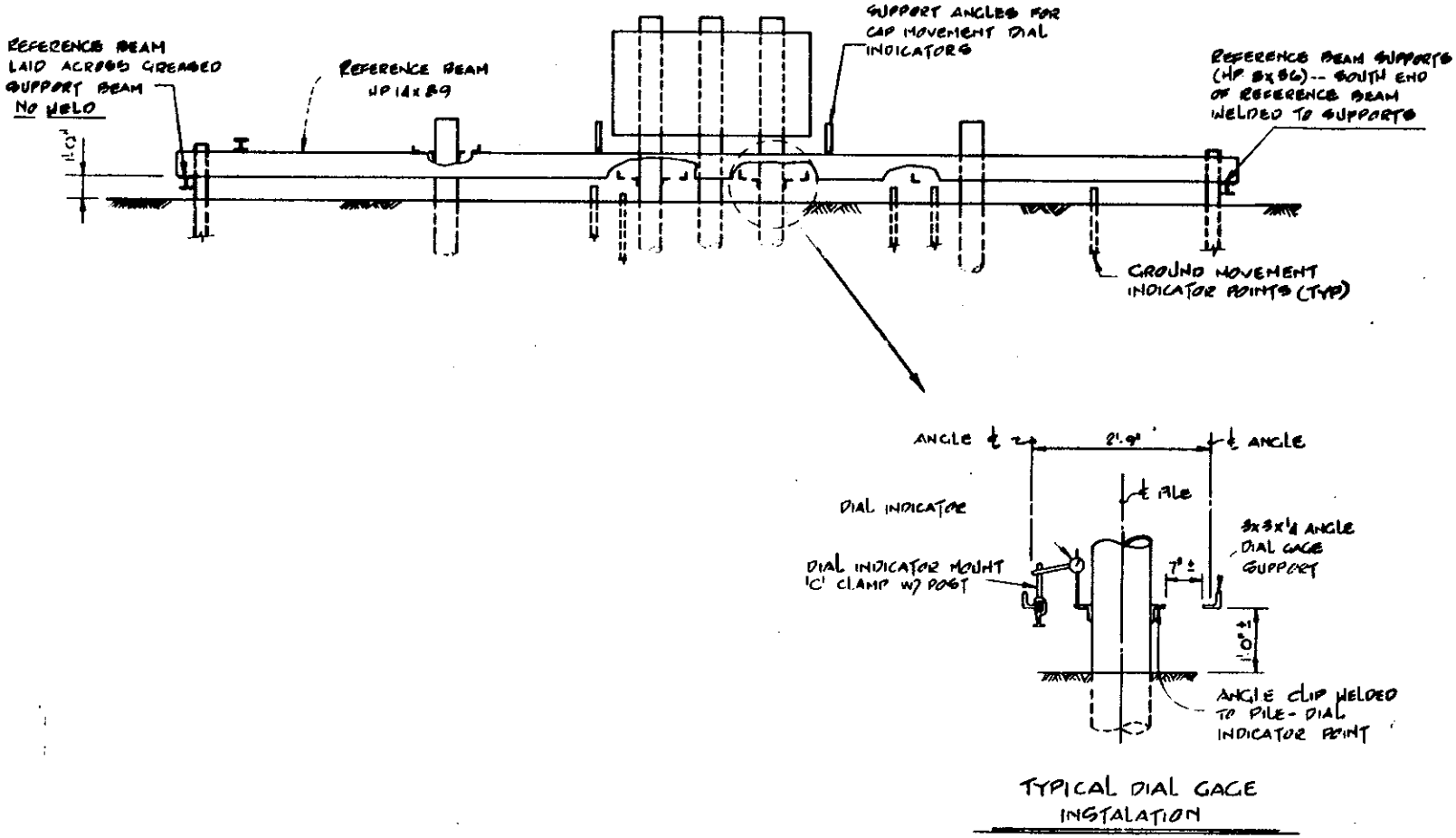

FIGURE 5.31. ELEVATION VIEW OF REFERENCE SYSTEM (1 ft = 0.305 m; 1 in = 25.4 mm)

(7) Axial foreshortening. Relative deformation between the top of every pile and points at various depths were made using a borehole extensometer system. This system also served as a backup for the strain gage system in that it permited hand calculation of the load transfer pattern in the event the electrical system failed. The following specifications were used:

System: Terrametrics multiple position extensometer system.

Reference heads: Terrametrics model 6-CSLT(R) with 6, 25 lb. per in. (4.4 N/mm) spring elements and stationary head, modified to maximum length = 26 in. (66 cm).

Method of Readout: Moveable dial gage.

Sensitivity of reading: 0.001 in. (0.025 mm)

Method of data recording: Manual

Measuring rod: 3/16-inch (5 mm) diameter 6061-T6 aluminum, continuous.

Anchors: Special hook anchors shown in Figs. 5.21 and 5.22.

See Fig. 5.23 for schematic of readout method.

(8) Inclinometers. Inclinometer readings were made electrically and recorded manually at two-foot (0.61 m) intervals from the top of each pile to the bottom in two perpendicular directions in order to ascertain horizontal departures from plumb alignment. The following are the specifications for the inclinometer:

Sensor: Slope Indicator Co. Model 50325 "microtilt" inclinometer.

Readout: Slope Indicator Co. Model 50306 digitilt indicator, battery operated.

Accuracy: 0.025 ft. per 100 ft. (0.8 cm per 30.5 m)

Wheel base: 24 inches (61 cm)

Inside diameter (not including wheels): 1.0 inch (2.54 cm)

(9) Internal pressure. Internal pressure in the piles was maintained at approximately 20 psi (140 kN/m^2) while readings are not being made by introducing dry nitrogen from pressurized bottles into the bottom of the piles. Periodic flushing was made from the top. A schematic of the sealing system is shown in Fig. 5.13. Bulkhead fittings were used to pass the nitrogen through the cover plate.

Schedule of Parts

The following is a schedule of parts for the ground and pile instrumentation systems. The symbol P after the the number of parts indicates that the parts were purchased with D.O.T. funds. The symbol R indicates that a portion of the parts were purchased with D.O.T. funds. Other items are owned by Raymond, Fugro, or the University of Houston.

a.	Lateral pressure cells (total and pore water) with integral leads	20	(P)
b.	Strain gages (static readings)	476	(P)
c.	Strain gage ribbon leads	22	(P)
d.	Male patch plugs	22	(P)
e.	Female patch plugs	22	(P)
f.	Power supply	1	
g.	DC amplifiers	16	(R)
h.	Oscillograph	1	
i.	FM tape recorder	1	
j.	Digital voltmeter	1	
k.	Oscilloscope	1	
l.	High level patch board	1	
m.	Microcomputer	1	
n.	CRT Unit	1	
o.	Teletype	1	
p.	Paper tape punch	1	
q.	X-Y plotter	1	
r.	Pneumatic pressure readout boxes	2	(R)
s.	Pneumatic pressure manifold	2	(P)
t.	Ground piezometers	14	(P)
u.	Depth settlement monuments	6	(P)
v.	Surface settlement monuments	9	(P)
w.	Extensometer heads	9	(P)
x.	Extensometer rods	66	(P)
y.	Extensometer anchors	66	(P)
z.	Dial gages (0.001 inch)	41	(R)

aa.	Load cells (rented)	4	
bb.	Microhead level and rod	1	
cc.	Gold contact switching system	1	(P)
dd.	Strain gages (dynamic readings)	16	(P)

The following is a schedule of subassemblies for the piles.

a.	Five-foot (1.5 m) segments with lateral pressure cells	15
b.	Five-foot (1.5 m) segments without lateral pressure cells	73
c.	Three-foot (1 m) bottom segments with lateral pressure cells	5
d.	Three-foot (1 m) bottom segments without lateral pressure cells	6
f.	10.75" (27.3 cm) closure plates	11
g.	8'3" (2.52 m) extension segments	9
h.	3'4" (1.02 m) extension segments	2
i.	Pressure seals (pile covers)	11
j.	Loading heads	2

Reaction and Loading System Details

The anchor and reaction frame details are shown Figs. 5.32 through 5.36. Note that anchorage for the compression tests on the group was provided by two very deep truncated sections of drilled piers to which Dywidag tension rods were attached. The soil mass in the vicinity of the test group was essentially unstressed by the anchors. Stress relief effects from drilling these piers were minimized by drilling and concreting the anchor piers under a drilling slurry. Furthermore, the unconcreted portions of the anchor pier holes were permanently lined with steel casing as soon as the drilling operation reached the level to which concrete was to be poured.

The main reaction beams (Fig. 5.34) were fully articulated, being held in place during a group compression test only by the flexible Dywidag bars. Each of the Dywidag bars was pretensioned to about one ton (98.9 kN) before each load test to affect a uniform pull on the bars. Because of slight imperfections in locations of the Dywidag

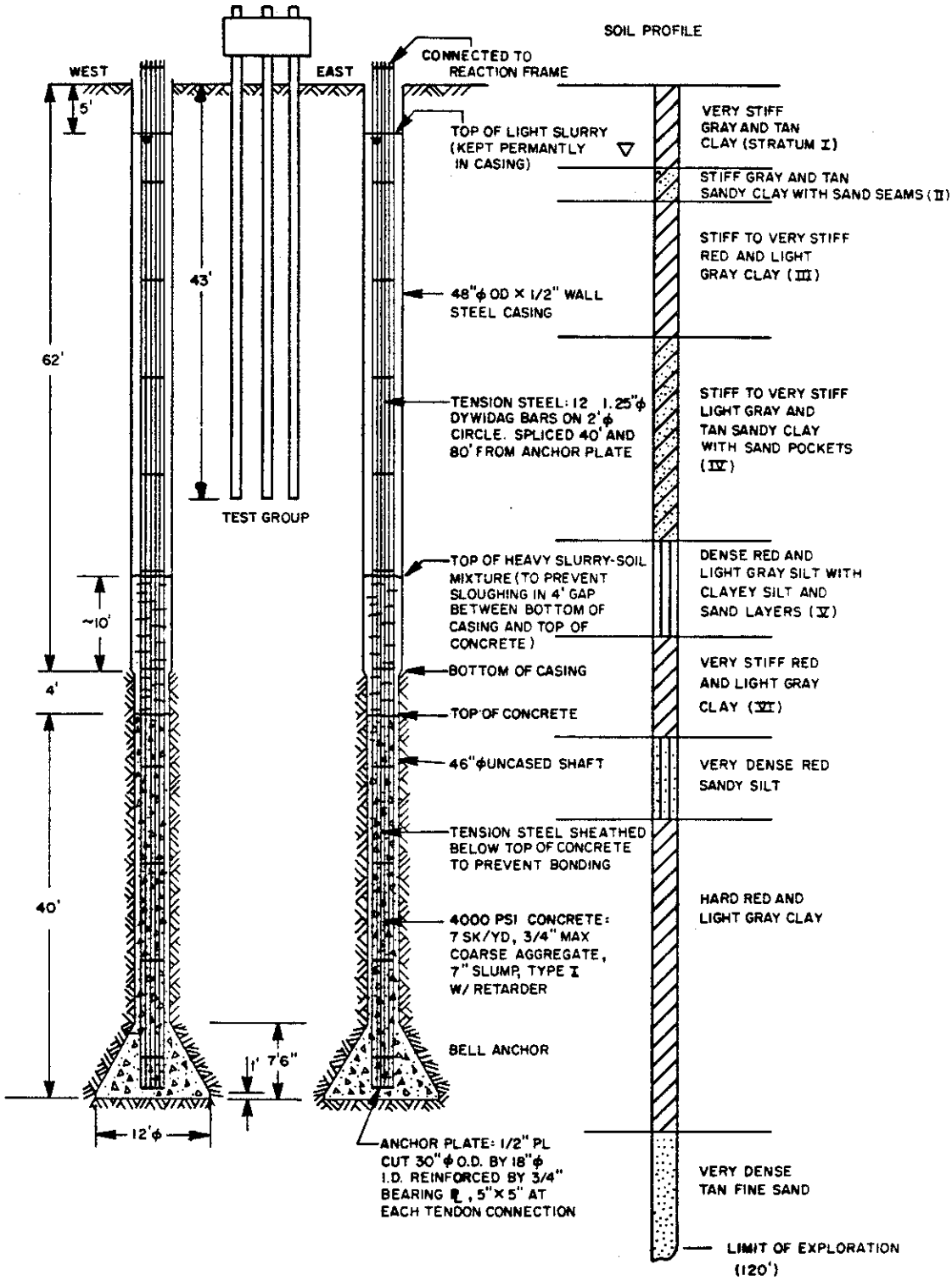

FIGURE 5.32. DRILLED PIER ANCHOR DETAIL (1 in = 25.4 mm; 1 ft = 0.305 m; 1 psi = 6.89 kN/m^2)

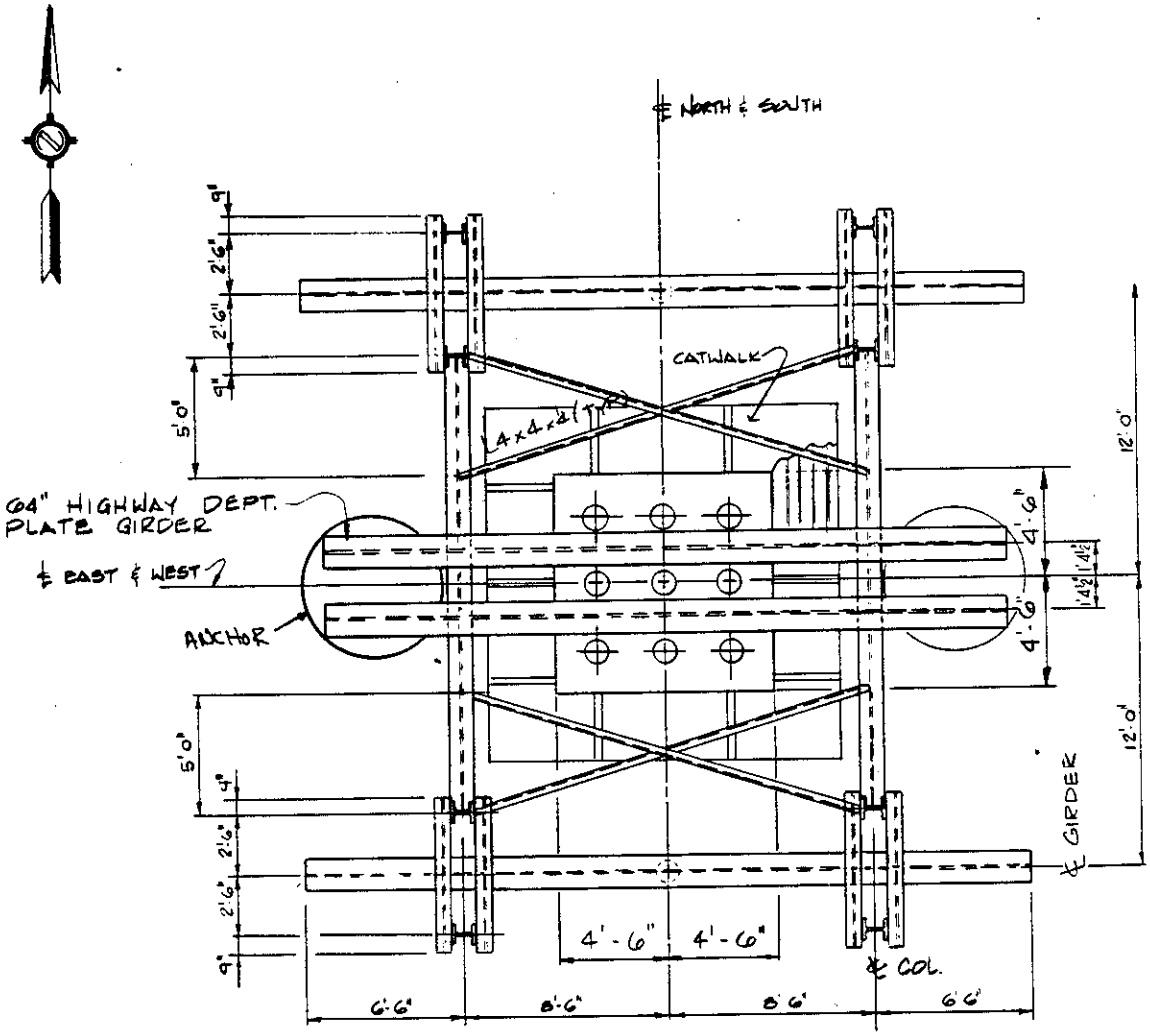

PLAN

FIGURE 5.33. REACTION STRUCTURE; PLAN VIEW (1 ft = 0.305 m; 1 in = 25.4 mm)

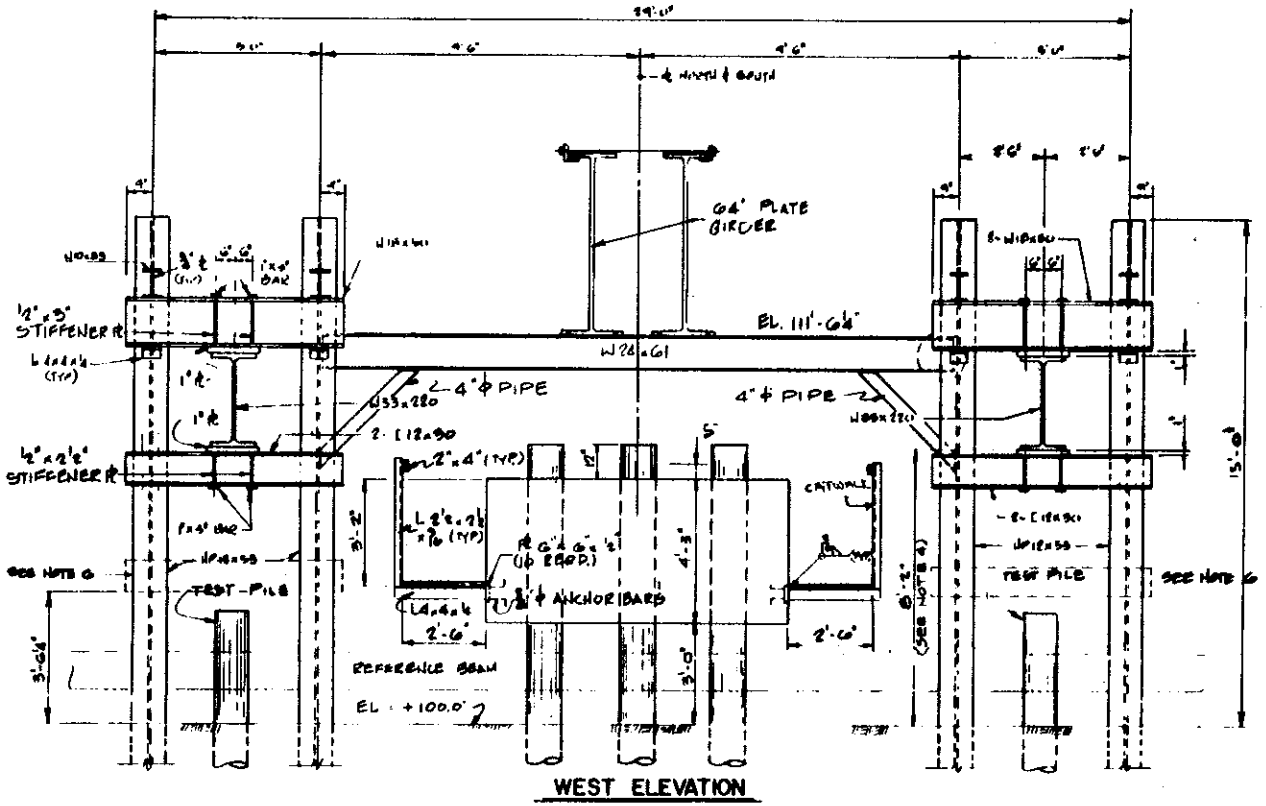

WEST ELEVATION

NOTES:

1. STRUCTURAL STEEL FRAME TO BE MADE OF A-36 STEEL
2. WELDING ELECTRODES TO BE USED: E70 xx
3. HP 12x53 PILES TO BE 40' LONG. DRIVEN PENETRATION: 25 FEET.
4. DIMENSION 8'-2" SHOWN SUBJECT TO CHANGE.
5. PLATES FOR WALKWAY SUPPORT TO BE CAST WITH THE CONCRETE CAP. (10 PLATES REQ'D)
6. C12.30 TO BE RELOCATED FOR TUNNEL TEST
7. NO WELDING, TORCH CUTTING OR HEAT TO BE APPLIED TO ANY DYWIDAG BAR.

FIGURE 5.34. REACTION STRUCTURE; WEST ELEVATION (1 ft = 0.305 m; 1 in = 25.4 mm)

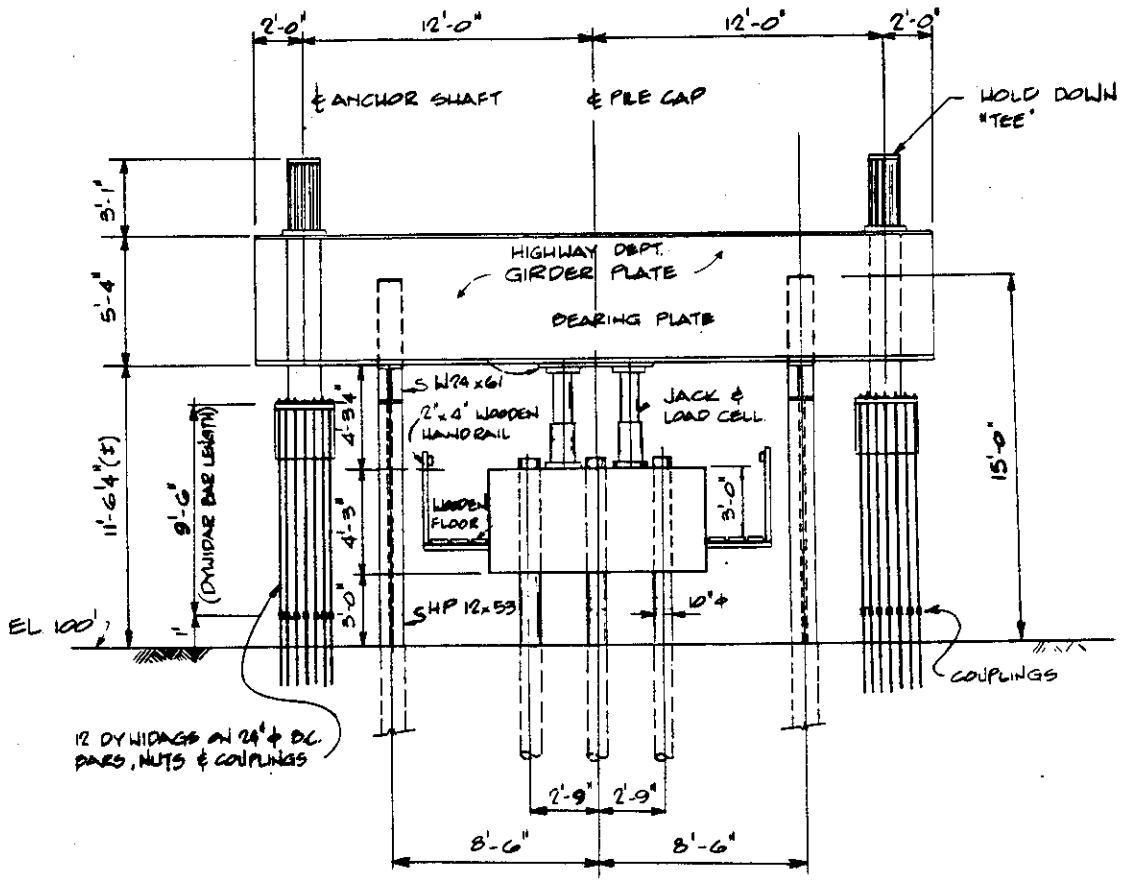

FIGURE 5.35. REACTION SYSTEM FOR GROUP, SHOWING CAP, JACKS, MAIN REACTION BEAMS AND LINKAGE TO ANCHORS
(1 ft = 0,305 m; 1 in = 25,4 mm)

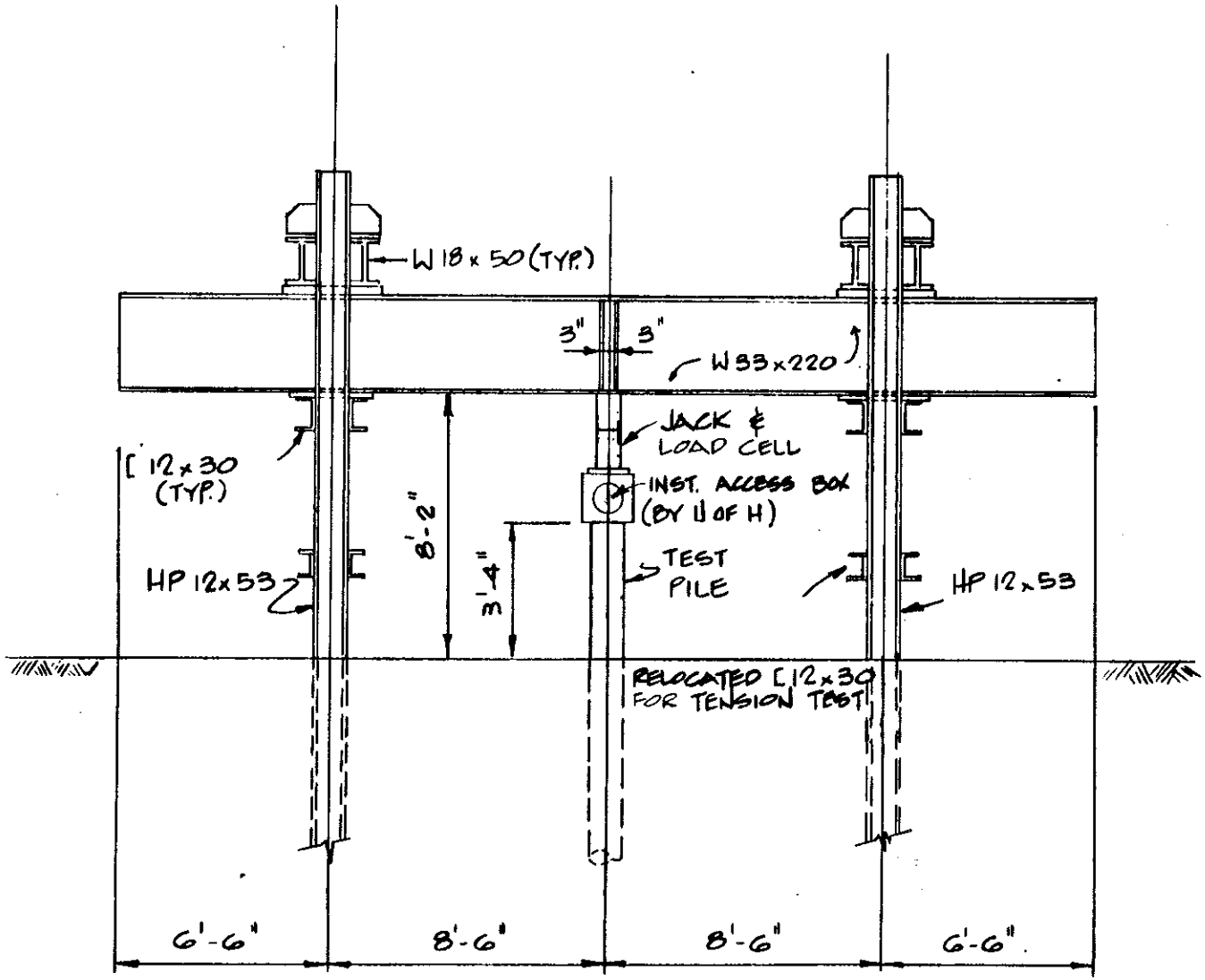

FIGURE 5.36. REACTION SYSTEM FOR REFERENCE PILES; SOUTH ELEVATION
(1 ft = 0.305 m; 1 in = 25.4 mm)

anchors at the bases of the drilled piers, the bars were very slightly inclined so that when the load was applied, the main reaction beams tended to translate slightly to the north during the first nine-pile group test. In order to prevent this translation from occurring in the second nine-pile group test and subsequent tests, knee braces, which provided no resistance to vertical beam movement, were installed on the north-south beams that supported the main reaction beams when not testing after the first test to block the main reaction beams against north-south translation. These braces were not shown in Figs. 5.33-5.36.

Anchorage for each reference test pile was provided by four H-piles driven to a depth of 25 feet (7.8 m) at the locations shown in Fig. 5.33. These piles also served as compression reactions for all six tension tests.

The details of the pile cap are shown in Fig. 5.37, and the jacking system for the compression tests on the group is shown in Fig. 5.38. The jacking system for the reference pile tests was similar to this system, except that only one jack was employed. That jack was pumped by means of a high volume electrical pump so that load increments could be applied rapidly.

The arrangement and details of the tension (uplift) test system are shown in Figs. 5.39 and 5.40.

Sequence of Field Observations

The field observations were made in the following sequence, with the indicated detail.

a. Install anchor piers.

b. Install all ground instruments. Take a minimum of five sets of readings on all ground instruments between the time of instrument installation and the time of installation of the first test pile to assure accurate baseline readings of piezometric pressures and settlement point elevations.

All settlement points were monitored with the use of a microhead level and a portable rod with micrometer target, and all readings were referenced to a temporary bench mark in the grade beam of an adjacent building.

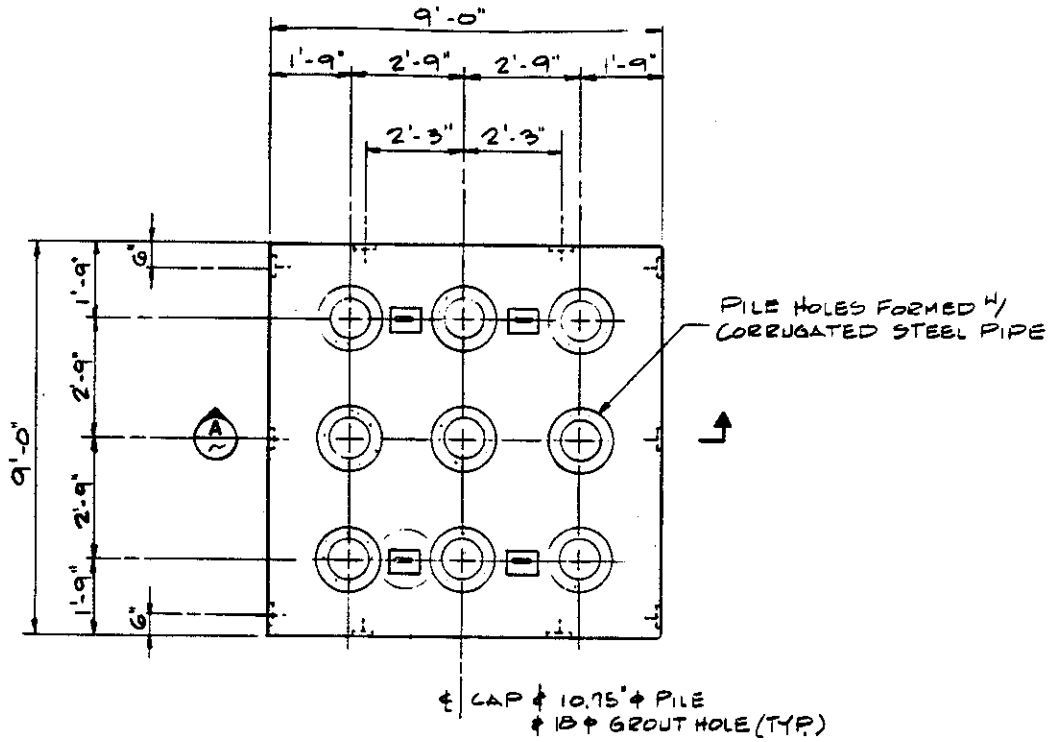

PLAN

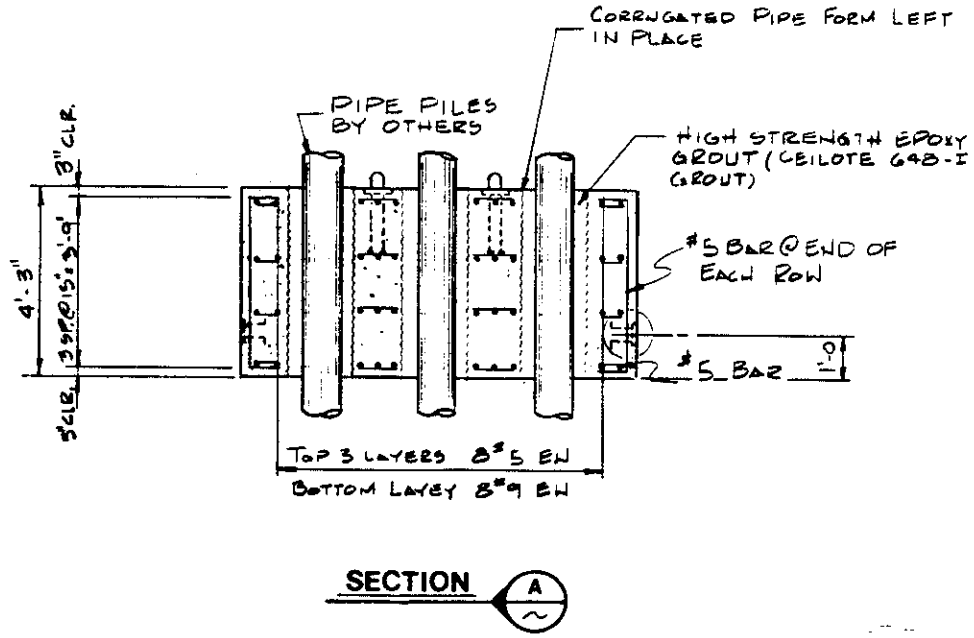

SECTION A

FIGURE 5.37. CAP DETAIL (1 ft = 0.305 m; 1 in = 25.4 mm)

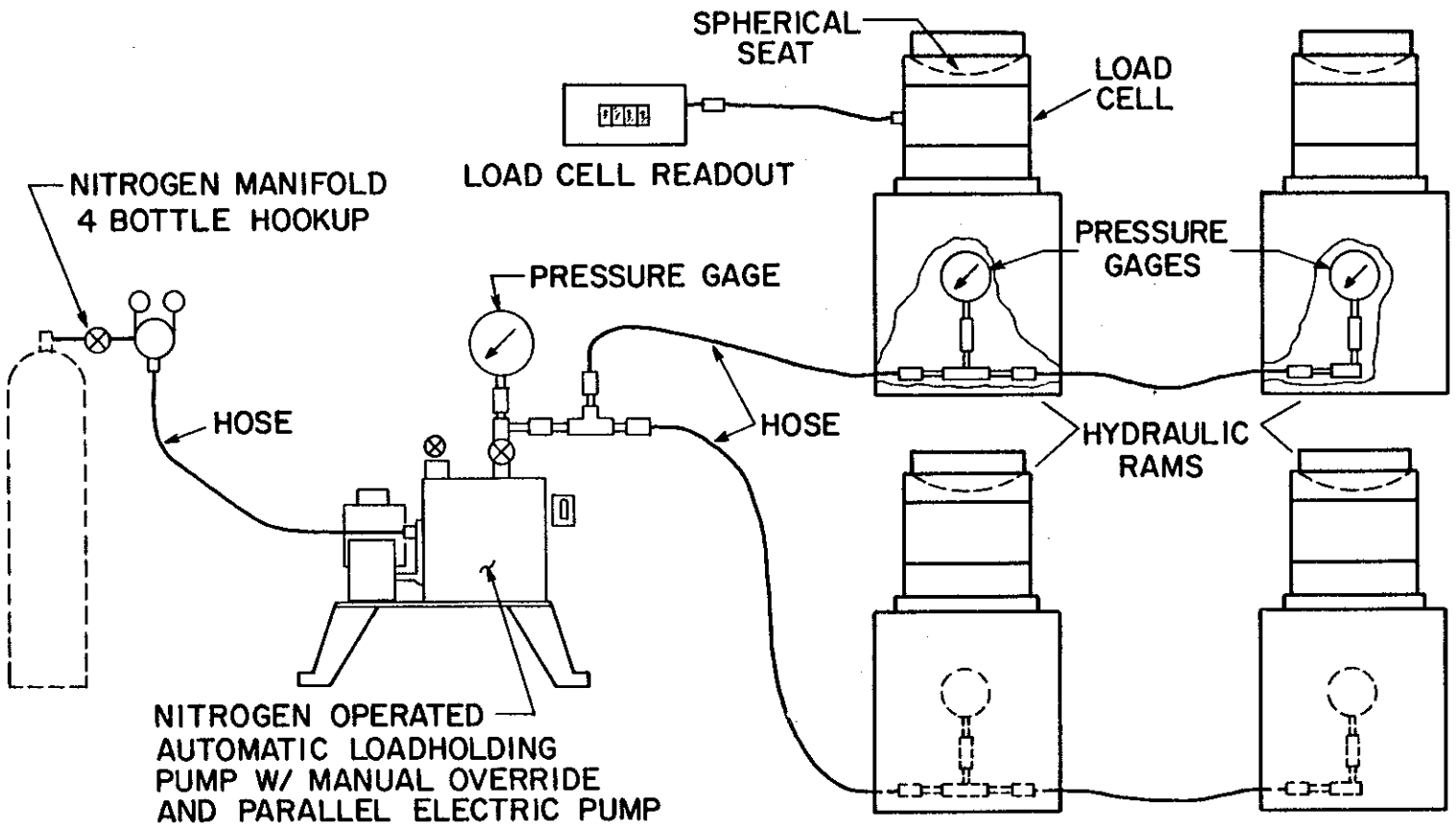

FIGURE 5.38. JACKING SYSTEM FOR GROUP COMPRESSION TESTS (SCHEMATIC)

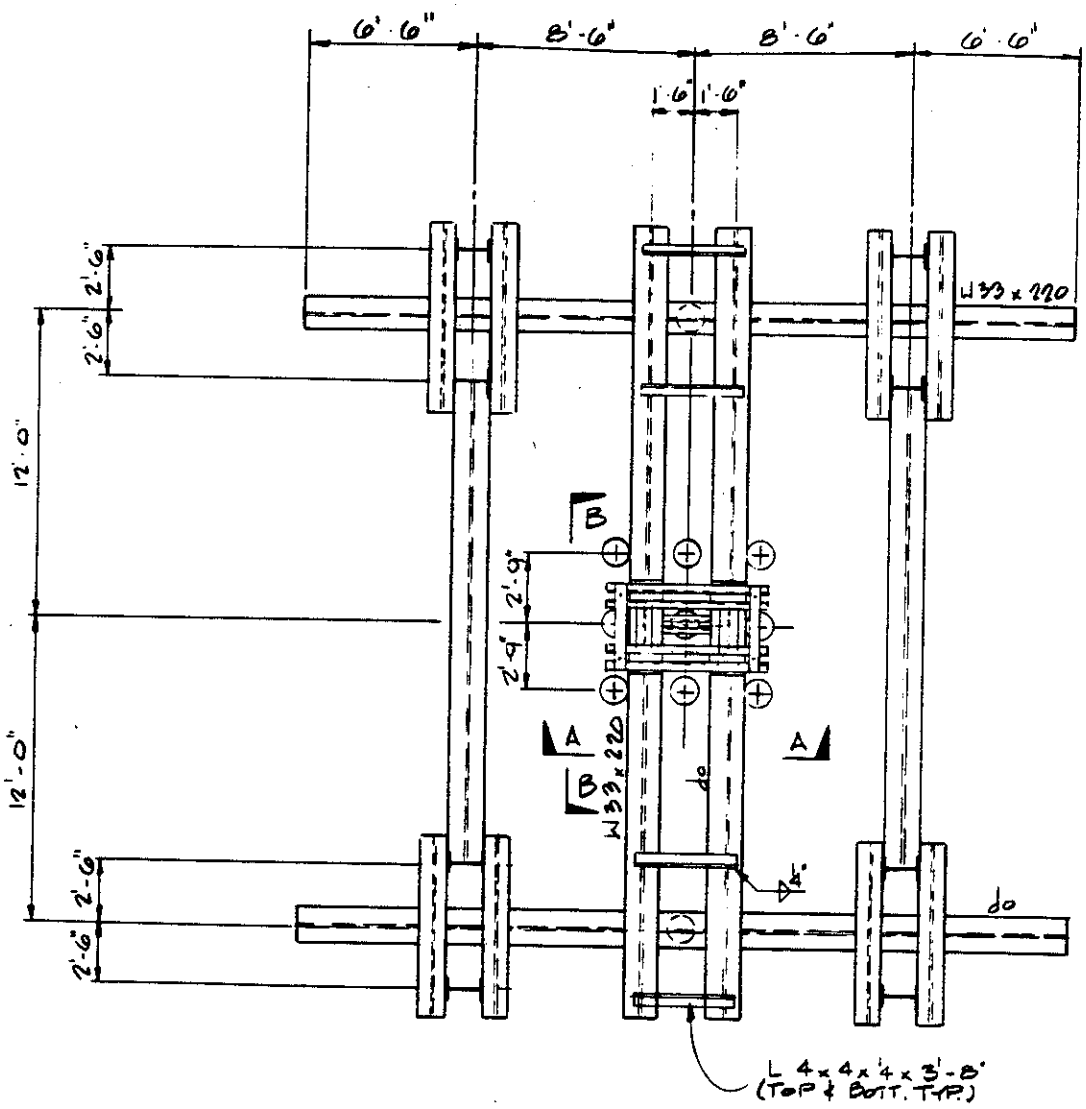

FIGURE 5.39. PLAN VIEW OF UPLIFT TEST ARRANGEMENT (SINGLE PILE)
(1 ft = 0.305 m; 1 in = 25.4 mm)

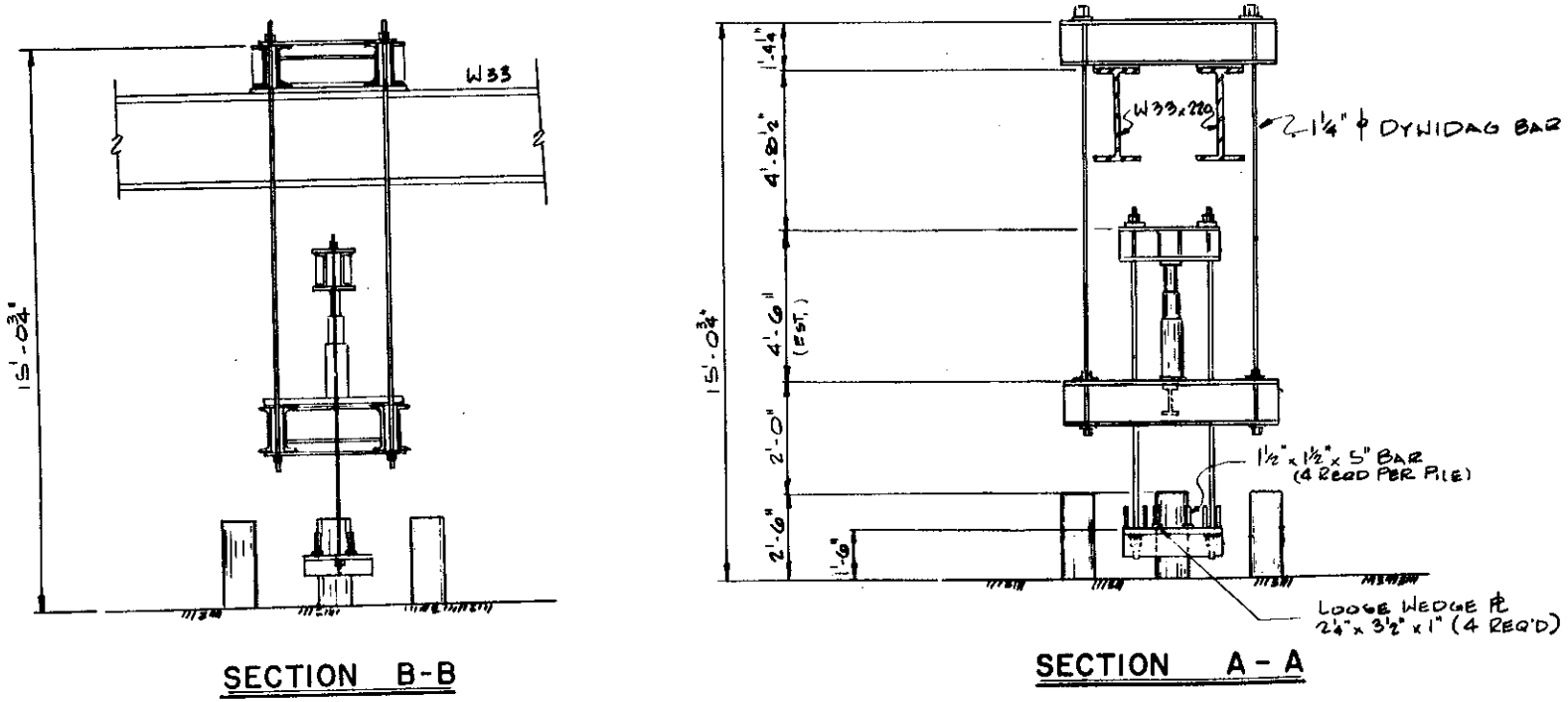

FIGURE 5.40. ELEVATION VIEW OF UPLIFT TEST ARRANGEMENT (SINGLE PILE)
(1 ft = 0.305 m; 1 in = 25.4 mm)

c. Exercise and calibrate the strain gage circuits. Transport piles to test site.

d. Drive the reaction H-piles and the test piles. Stop test piles 1, 2, 4, 8, and 11 6 inches (15 cm) short of full penetration. Record blow counts on all piles. Record strain and acceleration vs. time for gages in segments A, F, and I or J for several blows on Piles 1, 2, 4, and 5 at full penetration to obtain an indication of the variation in damping during driving within piles in the group.

(1) Before each pile was driven, obtain zero strain gage circuit readings with the pile lying level on the ground. Flush-saturate all lateral pressure cell piezometers.

(2) Upon completion of driving a pile, read

(a) All ground piezometers and all lateral pressure cells on the pile just driven.

(b) All strain gage circuits on the pile just driven.

(3) Within approximately 30 minutes of the completion of the readings outlined above, read

(a) All lateral pressure cells on all other piles in place.

(b) All surface and depth settlement points, using microhead level and rod with micrometer target.

(c) All strain gage circuits on other representative piles already in place.

(d) Pile-head elevation on all piles (using microhead level).

(4) After all piles have been driven

(a) Obtain site coordinates and elevations of the tops of all piles.

(b) Retap Piles. Piles 1, 2, 4, 8, and 11, which were stopped slightly short of full penetration, were retapped to full penetration following a time delay in order to develop an indirect assessment of short-term set-up. (Any other piles that had heaved in excess of 0.25 inch (0.7 cm) were also to be retapped to their original penetrations. None heaved this amount.)

(c) Place precast pile cap over group piles and grout to piles.

(d) Obtain the horizontal departure (batter) of all piles along their lengths with inclinometer.

(e) Install extensometer system and make full set of readings.

(f) Apply nitrogen pressure to all piles.

(g) Erect reaction and reference frames.

(h) Read all pile and ground piezometers and pile total lateral pressure cells periodically until the initial compression test was conducted.

e. Conduct the initial compression tests:

(1) Pile No. 1 and Pile No. 11, simultaneously, approximately 16 days after driving Pile No. 11.

(2) Four-day lapse period before group test.

(3) Nine-pile group test, four days after testing reference piles (1 and 11).

f. During each test, the following instruments and monuments were read for every load applied, including initial and final zero.

(1) Lateral pressure cells in all piles (only on pile being loaded in the case of the single pile tests).

(2) Surface settlement points. All points immediately adjacent to the reference beams (SSP1, SSP2, SSP3, SSP6) were read with 0.001-inch (0.025 mm) division dial gages suspended from the reference beams. The remaining points were read during the group tests with a microhead level, using the procedure that was employed during driving. SSP1, SSP2 and SSP3 were read during the isolated pile test on Pile No. 1. The other surface points were not read during the single pile tests.

(3) Depth settlement points. All points were monitored with 0.001-inch (0.025 mm) division dial gages suspended from the reference beams.

(4) Reference beam supports and reference points along the reference beams. These were monitored for settlement using the micro-head level and referenced to a vertical reference point to assure proper vertical control.

(5) Ground piezometers (only P195, P345, and P503 during reference pile tests).

(6) Mechanical extensometers (only on the pile being loaded in the case of the single pile tests).

(7) Strain gage circuits (only on the pile being loaded in the case of the single pile tests).

(8) Group or single pile load as indicated by load cells. Load was monitored as the load was being increased within an increment of loading, as a means of assuring that failure load could be accurately detected.

(9) Group settlement, rotation, and horizontal translation, as indicated by 0.001-inch (0.025 mm) division dial gages suspended from the reference beams and resting on the cap (mounted at corners in three orthogonal directions) and by using microhead level and scale, with readings referenced to the vertical reference point (only on group tests).

(10) Individual pile settlements for every pile being loaded as indicated by pairs of diametrically opposite dial gages suspended from the reference system. All group piles had dial gage pairs during group tests. During single pile tests only those piles being tested had dial gages. Settlement was also monitored by the microhead level for the single pile tests.

g. Readings under Item f were made at the frequencies indicated in Table 5.2.

h. Loads were applied in increments of 10 tons (89 kN) to the reference piles every 60 minutes until failure occurred. However, the first test on Pile 11 was conducted with loading time increments of 2.5 minutes (i.e., "quick," or modified constant-rate-of-penetration test). This test was conducted completely during the 20-ton (180 kN) load on Pile No. 1. Readings taken for each increment of load in the quick test on Pile 11 are indicated in Table 5.3. In both types of tests, when failure occurred under a given load increment, load was reduced to the next lowest load that was a multiple of 25 tons (223 kN), that load was held for 60 minutes (2.5 minutes for quick test), and the load was then removed in 25-ton (223 kN) decrements using the same time increments used during loading. The same loading procedure was used on the group, except that no quick tests were run and that 100-ton (890 kN) load increments and 250-ton (2230 kN) load decrements were employed.

TABLE 5.2. FREQUENCIES OF READINGS DURING A STANDARD COMPRESSION TEST

Time After Applying Or Removing Load Increment (min.)	Reading[a] (Refer to text Item f)	Responsibility[b]
1	1,6,7,8	U
	2,3,5	F
	4,8,9,10	R
15	6(bottom points only), 8	U
	8,9,10	R
30	1,6,7,8	U
	2,3,5	F
	4,8,9,10	R
55	6 (bottom points only),8	U
	8,9,10	R
60	Apply next increment/ decrement	

a Delete where not applicable
b U - University of Houston personnel
F - Fugro - Gulf personnel
R - Raymond personnel

Note: Omit Item 6 in Detached Piles in Subgroup Tests.

TABLE 5.3. FREQUENCIES OF READINGS DURING QUICK TEST (PILE 11)

Time After Applying Or Removing Load Increment	Reading (Refer to text Item f)	Responsibility
30 sec.	6,7,8	U
	8,10	R

Where pluging failure was observed while attempting to develop a certain load only readings 8 and 10 were made as pumping continued. Immediately after these readings were made, load was released to the highest possible multiple of the unloading decrement, and the normal unloading process was then followed.

i. Discontinue testing for approximately sixty days.

j. Conduct a second series of compression tests on Pile 1, the nine-pile group, and Pile 11 in order to assess the effects of soil set-up. The same procedures as for the initial series of compression tests were followed except that Pile 11 was tested using the standard (not quick) test procedure simultaneously with Pile 1.

k. Discontinue testing for approximately thirty days.

l. Conduct a third series of compression tests on Pile 1, the nine-pile group, and Pile 11 as in Item j in order to further assess the effects of set-up. Follow the same procedures as for the second series of compression tests.

m. Immediately following Step l, cut off Piles 4, 6, 8, and 10 below the pile cap and recap and repressurize these piles. Note that the upper strain gage level in these piles was cut away in this process, but one level remained at the ground surface.

n. Conduct a subgroup compression test on the subgroup consisting of Piles 2, 3, 5, 7, and 9. Make readings as per the initial compression test on the group, including readings on the piles cut away from the group. Use 50-ton (445 kN) loading increments and 150-ton (1340 kN) unloading decrements.

o. Immediately following Step n, cut away Pile 2 per Step m.

p. Conduct a subgroup compression test on the subgroup consisting of Piles 3, 5, 7, and 9 as per Step n.

q. Remove the cap from the group.

r. Take a full set of readings on all instruments.

s. Adapt piles and reaction system to uplift tests.

t. Conduct uplift tests on Piles 1, 2, 4, 5, 9, and 11 in order to obtain an independent check on side resistance. During the uplift tests, read only the instruments on the pile being pulled and omit all ground instrument readings. Otherwise, take readings as for single pile compression tests.

u. Make final set of cone soundings adjacent to test piles and in free field to assess soil disturbance.

In the uplift tests load was applied in the same increments as in the single pile compression tests. Only readings 1, 7, 8, and 10 (Item f) were made during the uplift tests. Once failure was observed, the load was reduced to zero and a final set of readings was acquired. Reading frequency was as indicated in Table 5.2.

v. Testing Completed.

Data were reduced and analyzed partially during the period of time covered from Step b to Step u so that adjustments to test procedures could be made where desirable.

ACKNOWLEDGEMENTS

The author gratefully acknowledges the assistance of the following individuals, who contributed materially to the contents of this report: J. G. Badgett, Biswas Datta, Chester Drash, H. B. Ha, Hidayet Sarac, Shalom Shamooelian, and T. C. Yin of the University of Houston, who performed the analyses described in Chapters 2-4; R. M. Armstrong and Richard Hawkins of Raymond International, who played an integral part in developing the research plan contained in this report; and W. B. Ingram and Larry Mahar of Fugro Gulf, who played an integral part in developing the plans for the site investigation, ground instrumentation, and laboratory studies.

REFERENCES

1. American Petroleum Institute, Recommended Practice for Planning, Designing and Constructing Fixed Offshore Platforms, 1976.

2. American Railway Engineering Association, Committee 8, "Steel and Timber Pile Texts - West Atchafalaya Floodway - New Orleans, Texas, and Mexico Railway," Bulletin No. 489, Sept-Oct., 1950, pp. 149-202.

3. Aschenbrenner, R., "Three Dimensional Analysis of Pile Foundations," Journal of the Structural Division, A.S.C.E., Vol. 93, No. ST1, Feb. 1967, pp. 201-219.

4. Awoshika, K., and L. C. Reese, "Analysis of Foundation with Widely Spaced Batter Piles," Research Report 117-3F, Center for Highway Research, The University of Texas at Austin, Feb. 1971.

5. Banerjee, P. K., and T. G. Davies, "Analysis of Pile Groups Embedded in Gibson Soil," Proceedings, Ninth International Conference on Soil Mechanics and Foundation Engineering, Vol. 1, Tokyo, 1977, pp. 381-386.

6. Banerjee, P. K., and R. M. Driscoll, "Three-Dimensional Analysis of Raked Pile Groups," Proceedings of the Institution of Civil Engineers, London, Part 2, Vol. 61, Dec., 1976, pp. 653-671.

7. Berezantzev, V. G., V. S. Khristoforov, and V. N. Golubkov, "Load Bearing Capacity of Piled Foundations," Proceedings, Fifth International Conference on Soil Mechanics and Foundation Engineering, Paris, 1961, Vol. II, pp. 11-15.

8. Brand, E. W., C. Muktabhant, and A. Taechathummarak, "Load Tests on Small Foundations in Soft Clay," Proceedings, A.S.C.E. Specialty Conference on Performance of Earth and Earth-Supported Structures, 1972, Vol. I, Part 2, pp. 903-928.

9. Brod, E. J., J. N. Fowler, and L. A. Boston, "A Unified Technique for the Analysis of Structure-Soil-Pile Systems," Proceedings, Seventh Annual Offshore Technology Conference, Paper No. OTC 2262, May 1975.

10. Broms, B. B., "Settlement of Pile Groups," Proceedings, A.S.C.E. Specialty Conference on Performance of Earth and Earth-Supported Structures, Vol. III, 1972, pp. 181-199.

11. Bryant, L. M., and H. Matlock, "Three-Dimensional Analysis of Framed Structures with Nonlinear Pile Foundations," Proceedings, Ninth Annual Offshore Technology Conference, Paper No. OTC 2955, May 1977.

12. Butterfield, R., and P. K. Banerjee, "The Elastic Analysis of Compressible Piles and Pile Groups," Geotechnique, Vol. 21, No. 1, March 1971, pp. 43-60.

13. Butterfield, R., and P. K. Banerjee, "The Problem of Pile Group-Pile Cap Interaction," Geotechnique, Vol. 21, No. 2, June, 1971, pp. 135-142.

14. Cooke, R. W., and G. Price, "Strains and Displacements Around Friction Piles," Building Research Establishment Current Paper 28/73, Garston, England, Oct., 1973.

15. Cooke, R. W., G. Price, and K. J. Tarr, "Jacked Piles in Lonon Clay: A Study of Load Transfer and Settlement Under Working Conditions," Geotechnique, Vol. XXIX, No. 2, June, 1979.

16. Coyle, H. M., and L. C. Reese, "Load Transfer for Axially Loaded Piles in Clay," Journal of the Soil Mechanics and Foundations Division, A.S.C.E., Vol. 92, No. SM2, March 1966, pp. 1-26.

17. Coyle, H. M., and I. H. Sulaiman, "Skin Friction for Steel Piles in Sand," Journal of the Soil Mechanics and Foundations Division, A.S.C.E., Vol. 93, No. SM6, Nov. 1967, pp. 261-296.

18. Davis, E. H., and H. G. Poulos, "The Analysis of Pile-Raft Systems," Australian Geomechanics Journal," Vol. 62, No. 1, 1972, pp. 21-27.

19. Desai, C. S., L. D. Johnson, and C. M. Hargett, "Finite Element Analysis of the Columbia Lock Pile Foundation System," U.S.A.E. Waterways Experiment Station Technical Report S-74-6, July, 1974, 31 pp.

20. Ellison, R. D., E. D'Appolonia, and G. Thiers, "Load-Deformation Mechanism for Bored Piles," Journal of the Soil Mechanics and Foundations Division, A.S.C.E., Vol. 97, No. SM4, April 1971, pp. 661-678.

21. Esrig, M. I., R. C. Kirby, R. G. Bea, and B. S. Murphy, "Initial Development of a General Effective Stress Method for the Prediction of Axial Capacity for Driven Piles in Clay," Proceedings, Ninth Offshore Technology Conference, Vol. III, Paper No. OTC 2943, May, 1977.

22. Feld, J., Discussion of "Timber Friction Pile Foundations," Transactions, A.S.C.E., Vol. 108, 1943, pp. 143-144.

23. Fellenius, B. H., "Test Loading of Piles and New Proof Testing Procedure," Journal of the Geotechnical Engineering Division, A.S.C.E., Vol. 101, No. GT9, Sept. 1975, pp. 855-869.

24. Flaate, Kaare, "Effects of Pile Driving in Clays," Canadian Geotechnical Journal, Vol. 9, No. 1, Feb. 1973, pp. 81-88.

25. Focht, J. A., Jr., and K. J. Koch, "Rational Analysis of the Lateral Performance of Offshore Pile Groups," Preprint, Fifth Offshore Technology Conference, Paper No. OTC 1896, May 1973.

26. Francis, A. J., "Analysis of Pile Groups with Flexural Resistance," Journal of the Soil Mechanics and Foundations Division, A.S.C.E., Vol. 90, No. SM3, May 1964, pp. 1-32.

27. Fuller, F. M., and H. E. Hoy, "Pile Load Tests, Including Quick-Load Test Method, Conventional Methods, and Interpretations," Highway Research Record 333, Highway Research Board, 1970, pp. 74-86.

28. Hagerty, D. J., and J. E. Garlinger, "Consolidation Effects Around Driven Piles," Proceedings, A.S.C.E. Specialty Conference on Performance of Earth and Earth-Supported Steuctures," Vol. I, Part 2, 1972, pp. 1207-1221.

29. Holloway, D. M., G. W. Clough, and A. S. Vesić, "The Effects of Residual Driving Stresses on Pile Performance Under Axial Load," Proceedings, Tenth Offshore Technology Conference, Paper No. OTC 3306, May 1978.

30. Holmquist, D. V., and H. Matlock, "Resistance-Displacement Relationships for Axially Loaded Piles in Soft Clay," Proceedings, Eighth Offshore Technology Conference, Paper No. OTC 2474, May 1976.

31. Hrennikoff, A., "Analysis of Pile Foundations with Batter Piles," Transactions, A.S.C.E., Vol. 115, Paper No. 2401, 1950.

32. Hunter, A. H., and M. T. Davisson, "Measurements of Pile Load Transfer," Performance of Deep Foundations, A.S.T.M S.T.P 444, 1969, pp. 106-111.

33. Kézdi, A., "Bearing Capacity of Piles and Pile Groups," Proceedings, Fourth International Conference on Soil Mechanics and Foundation Engineering," Vol. II, London, 1957, pp. 46-51.

34. Kim, J. B., R. J. Brungraber, and C. H. Kindig, "Lateral Load Tests on Full-Scale Pile Groups," Proceedings, A.S.C.E. Specialty Conference on Performance of Earth and Earth-Supported Structures, 1972, Vol. I, Part 2, pp. 1105-1133.

35. Kim, J. B., R. J. Brungraber, C. H. Kindig, J. L. Goodman, and L. P. Singh, "Pile Group Foundations, Analysis and Full-Scale Load Tests," Final Report, Civil Engineering Department, Bucknell University, Lewisburg, Pa., July 1973.

36. Kim, J. B., and R. J. Brungraber, "Full-Scale Lateral Load Tests of Pile Groups," Journal of the Geotechnical Engineering Division, A.S.C.E., Vol. 102, No. SM1, Jan. 1976, pp. 87-105.

37. Kishida, H., "Ultimate Bearing Capacity of Piles Driven into Loose Sand," Soil and Foundation, Vol. VII, No. 3, September, 1967, pp. 20-29.

38. Koizumi, Y., and K. Ito, "Field Tests with Regard to Pile Driving and Bearing Capacity of Piled Foundations," Soil and Foundation, Vol. VII, No. 3, Aug. 1967, pp. 30-53.

39. Ladd, C. C., "Stress-Strain Modulus of Clay in Undrained Shear," Journal of the Soil Mechanics and Foundations Division, A.S.C.E., Vol. 90, No. SM5, Sept. 1964, pp. 103-132.

40. Marsland, A., "Laboratory and In-situ Measurements of the Deformation Moduli of London Clay," Building Research Establishment Current Paper 24/73, Garston, England, Sept. 1973.

41. Masters, F. M., "Timber Friction Pile Foundations," Transactions, A.S.C.E., Vol. 108, 1943, pp. 115-140.

42. Mattes, N. S., and H. G. Poulos, "Settlement of Single Compressible Pile," Journal of the Soil Mechanics and Foundations Division, A.S.C.E., Vol. 95, No. SM1, Jan. 1969, pp. 189-207.

43. McClelland, B., "Design and Performance of Deep Foundations," Proceedings, A.S.C.E. Specialty Conference on Performance of Earth and Earth-Supported Structures, Vol. II, 1972, pp. 111-144.

44. Meyerhof, G. G., "Bearing Capacity and Settlement of Pile Foundations," Journal of the Geotechnical Engineering Division, A.S.C.E., Vol. 102, No. GT3, March, 1976, pp. 197-228.

45. Moorhouse, D. C., and J. V. Sheehan, "Predicting Safe Capacity of Pile Groups," Civil Engineering, A.S.C.E., Oct. 1968, pp. 44-48.

46. Nair, K., H. Gray, and N. C. Donovan, "Analysis of Pile Group Behavior," Performance of Deep Foundations, A.S.T.M, S.T.P. 444, 1969.

47. Novak, M., and R. F. Grigg, "Dynamic Experiments with Small Pile Foundations," Canadian Geotechnical Journal, Vol. 13, No. 4, Nov. 1976, pp. 372-385.

48. Ollila, M., "Elasto-Plastic Analysis of Pile Foundations," Unpublished paper, Helsinki, Finland, 1977.

49. O'Neill, M. W., O. I. Ghazzaly, and H. B. Ha, "Analyses of Three-Dimensional Pile Groups with Nonlinear Soil Response and Pile-Soil-Pile Interaction," Proceedings, Ninth Annual Offshore Technology Conference, Paper No. OTC 2838, May 1977.

50. O'Neill, M. W., H. B. Ha, and O. I. Ghazzaly, "Assessment of Hybrid Model for Pile Groups," Paper presented to Transportation Research Board," Washington, D.C., Jan., 1979.

51. O'Neill, M. W., and L. C. Reese, "Behavior of Bored Piles in Beaumont Clay," Journal of the Soil Mechanics and Foundation Division, A.S.C.E, Vol. 98, No. SM2, Feb. 1972, pp. 195-213.

52. O'Neill, M. W., and L. C. Reese, "Load Transfer in a Slender Drilled Pier in Sand," Paper Presented to A.S.C.E. Spring Convention, Pittsburgh, Pa., Paper No. 3141, April, 1978.

53. Ottaviani, M., "Three-Dimensional Finite Element Analysis of Vertically Loaded Pile Groups," Geotechnique, Vol. 25, No. 2, June, 1975, pp. 159-174.

54. Poulos, H. G., "Analysis of the Settlement of Pile Groups," Geotechnique, Vol. XVIII, No. 4, Dec. 1968, pp. 449-471.

55. Poulos, H. G., "Load-Settlement Prediction for Piles and Piers," Journal of the Soil Mechanics and Foundations Division, A.S.C.E, Vol. 98, No. SM9, Sept. 1972, pp. 879-897.

56. Poulos, H. G., and E. H. Davis, "The Settlement of Single Axially-Loaded Incompressible Piles and Piers," Geotechnique, Vol. XVIII, No. 3, Sept. 1968, pp. 351-371.

57. Poulos, H. G., and E. H. Davis, Pile Analysis and Design, New York: John Wiley and Sons, 1979 (in press).

58. Poulos, H. G., and N. S. Mattes, "Settlement and Load Distribution Analysis of Pile Group," Australian Geomechanics Journal, Vol. G1, No. 1, 1971, pp. 18-28.

59. Poulos, H. G., and N. S. Mattes, "Displacements in a Soil Mass Due to Pile Groups," Australian Geomechanics Journal, Vol. G2, No. 1, 1971, pp. 29-35.

60. Poulos, H. G., and N. S. Mattes, "Settlement of Pile Groups Bearing on Stiffer Strata," Journal of the Geotechnical Engineering Division, A.S.C.E, Vol. 100, No. GT2, Feb. 1974, pp. 185-180.

61. Price, G., "Field Tests on Vertical Piles Under Static and Cyclic Horizontal Loading in Overconsolidated Clay," Paper presented to A.S.T.M Symposium on Deep Foundations, Boston, Mass., June, 1978, 41 pp.

62. Radosavljević, Z., "Calcul et Essais des Pieux en Groupe," Proceedings, Fourth International Conference on Soil Mechanics and Foundation Engineering, Vol. II, London, 1957, pp. 56-60.

63. Saul, W. E., "Static and Dynamic Analysis of Pile Foundations," Journal of the Structural Division, A.S.C.E., Vol. 94, No. ST5, May, 1968, pp. 1077-1100.

64. Schlitt, H. G., "Steel Pile Tests, Q Street Viaduct, Omaha, Neb.," Dept. of Roads and Irrigation, Bridge Design Section, Lincoln, Neb., 1950.

65. Schlitt, H. G., "Group Pile Loads in Plastic Soils," Proceedings, Highway Research Board, Vol. 31, 1952, pp. 62-81.

66. Singh, J. P., N. C. Donovan, and A. C. Jobsis, "Design of Machine Foundation on Piles," Journal of the Geotechnical Engineering Division, A.S.C.E., Vol. 103, No. GT8, Aug. 1977, pp. 863-877.

67. Skempton, A. W., "Discussion: Piles and Pile Foundations," Proceedings, Third International Conference on Soil Mechanics and Foundation Engineering, Vol. 3, Zurich, 1953, p. 172.

68. Soderberg, L. O., "Consolidation Theory Applied to Foundation Pile Time Effects," Geotechnique, Vol. XII, No. 3, Sept., 1962, pp. 217-225.

69. Sowers, G. F., C. B. Martin, L. L. Wilson, and M. Fausold, "The Bearing Capacity of Friction Pile Groups in Homogeneous Clay from Model Studies," Proceedings, Fifth International Conference on Soil Mechanics and Foundation Engineering, Paris, Vol. II, Paris, 1961, pp. 155-159.

70. Stevens, J., "Prediction of Pile Response to Vibratory Loads," Proceedings, Tenth Offshore Technology Conference, Vol. IV, May, 1978.

71. Terzaghi, K., and R. B. Peck, Soil Mechanics in Engineering Practice, Second Ed., New York: John Wiley and Sons, pp. 537-539.

72. Tomlinson, M. J., Foundation Design and Construction, Second Ed., New York: Wiley Interscience, 1969, Chapter 7.

73. Vesić, A. S., "Bearing Capacity of Deep Foundations in Sand," Highway Research Record No. 39, 1963, pp. 112-153.

74. Vesić, A. S., "Ultimate Loads and Settlements of Deep Foundations in Sand," Proceedings, Symposium on Bearing Capacity and Settlement of Foundations, Duke University, 1967, pp. 53-68.

75. Vesić. A. S., "A Study of Bearing Capacity of Deep Foundations," Final Report, Project B-189, Georgia Institute of Technology, 1967, 264 pp.

76. Vesić, A. S., "Experiments with Instrumented Pile Groups in Sand," Performance of Deep Foundations, A.S.T.M. S.T.P. 444, 1969, pp. 177-222.

77. Vesić, A. S., "Expansion of Cavities in Infinite Soil Mass," Journal of the Soil Mechanics and Foundations Division, A.S.C.E., Vol. 98, No. SM2, Feb. 1972, pp. 265-290.

78. Vesić, A. S., "Problems of Development of a Mathematical Model to Predict the Performance of a Pile Group," Paper presented to Federal Highway Administration FCP Review Conference, Oct. 1977, 28 pp.

79. Vesić, A. S., "Design of Pile Foundations," N.C.H.R.P. Synthesis of Highway Practice No. 42, Transportation Research Board, Washington, D.C., 1977, 68 pp.

80. Vijayverqiya, V. N., "Load-Movement Characteristics of Piles," Proceedings, Ports '77 Conference, Long Beach, Cal., March, 1977, 16 pp.

81. Whitaker, T., "Experiments with Model Piles in Groups," Geotechnique, Vol. VII, No. 4, Dec. 1957, pp. 147-167.

82. Wolf, J. P., and G. A. von Arx, "Impedence Function of a Group of Vertically Loaded Piles," Proceedings, A.S.C.E. Specialty Conference on Earthquake Engineering and Soil Dynamics, Vol. II, June, 1978, pp. 1024-1041.